# Teorías efectivas aplicadas a la física más allá del Modelo Estándar

Pablo Olgoso Ruiz

Director: José Santiago Pérez
Codirector: Adrián Carmona Bermúdez

UNIVERSIDAD DE GRANADA

Programa de Doctorado en
Física y Ciencias del Espacio

Departamento de Física
Teórica y del Cosmos

Junio, 2023

Editor: Universidad de Granada. Tesis Doctorales
Autor: Pablo Olgoso Ruiz
ISBN: 978-84-1195-057-2
URI: https://hdl.handle.net/10481/85067

# Agradecimientos

Han sido muchas las personas que, durante estos años, han hecho posible que hoy me encuentre escribiendo estas líneas o me han hecho este duro camino un poco más fácil. Este es un intento de agradecéroslo como os merecéis.

En primer lugar quiero agradecer a mis tutores: Adrián Carmona, por la dimensión de lo que me ha enseñado y sus mil recomendaciones, y José Santiago, por siempre apostar por mí, hacérmelo todo más fácil y haberme transmitido tu forma de pensar ante un problema. Esta tesis no hubiera sido posible sin ti.

También quiero agradecer a los miembros de mi departamento por propiciar un clima tan agradable, en especial a Supratim das Bakshi, por todo lo que has compartido conmigo, Renato Fonseca, por toda tu ayuda con teoría de grupos, y Javier Fuentes-Martín, por todo lo que he aprendido de ti.

Gracias también a todas las personas que han pasado por el despacho y con quienes he compartido muchas horas y comidas, como Alejandro Jiménez, José María Pérez, Marina Bravo, Luis Pelegrina, Alejandro Sánchez, Paolo Figueira y Álvaro Díaz Carmona. Dos de ellos, además, me han acompañado desde mis inicios en el grado de Física: Pablo Canca, gracias por todas nuestras conversaciones, lo que me has enseñado y ser tan buen amigo, y Francisco Javier Nicolás (Fran), por estar (literalmente) a mi lado todos estos años y todos los momentos que hemos compartido. Habéis sido un gran apoyo y espero conservaros muchos años más.

Merecen una mención especial mis portugueses: António Torres, por nuestros ratos de escalada y ser un ejemplo de constancia y esfuerzo, María Ramos, por preocuparte siempre por mí y la pasión que me transmites cuando hablas de física, y Guilherme Guedes, quien quizá sea la persona más influyente en mi tesis, por formar tan buen equipo conmigo y enseñarme tantas cosas dentro y fuera del trabajo. Gracias por todos los buenos momentos y por ser tan buenos amigos.

Quiero también dar las gracias a todos los amigos que he hecho en Benasque, Cargèse y Florencia por haberme enriquecido con tantas experiencias y discusiones, y a Atala Jacobo, por toda la ayuda que me ha brindado y la claridad que siempre me aporta.

No podría olvidarme de mis amigos de toda la vida, que son un constante apoyo y con quienes he compartido muchas aventuras. Gracias, Ángela Castañeda, por las historias que nos cuentas, Ahmad Hamod, por ser tan especial en tantos sentidos, Ángela Macías, por ser mi prima adoptiva, Ana Jiménez, por nuestros paseos y tus constantes visitas, Rocío Padial, por aguantar siempre animada hasta el final, Pedro Padial, por ser tan espontáneo y natural, Jesús Herranz, por motivarme a superarte escalando, Julia Serrano, por nuestras noches tan random y vigilar que no me distraiga, Sergio García, por ser tan atento, cariñoso y payaso, Irene Barranco, por cuidarme como una madre, y Pablo Sabino, por no rendirte nunca conmigo incluso cuando yo mismo lo he hecho. No dejéis nunca de ser tan disaster.

Finalmente quiero agradecer a toda mi familia, acordándome mucho de todos mis primos y nuestras fiestas, y en especial a mi padre, mi madre y mi hermano, por estar incondicionalmente a mi lado, apoyarme en todos los sentidos y aguantarme tanto tiempo (y espero que mucho más). Esta tesis es gracias a vosotros.

# Resumen

El Modelo Estándar es la teoría que engloba nuestro conocimiento actual sobre las interacciones fundamentales, pero tenemos numerosas razones, tanto teóricas como experimentales, para creer que la historia no acaba aquí y debe haber física más allá.

Sin embargo, pese a décadas de búsqueda en un amplio rango de energías, todavía no hemos encontrado señales claras de nueva física. Esto motiva el uso de Teorías de Campos Efectivas como una manera muy eficiente de realizar la búsqueda, ya que permite dividir el problema en dos partes independientes: una parametrización agnóstica de las posibles desviaciones del Modelo Estándar y la conexión entre estas desviaciones y modelos concretos de nueva física.

Esta traducción se puede realizar a varios niveles en un desarrollo perturbativo, y tanto la creciente precisión de los experimentos como la necesidad de capturar algunos efectos de lo contrario ausentes requiere su realización a nivel lazo. El hecho de ser dependiente del modelo hace que calcularlo para el vasto número de posibles modelos que nos podrían interesar sea complejo y propenso a errores. La automatización de esta tarea sería por tanto muy útil a la hora de simplificar esta conexión entre nuestras teorías y sus consecuencias experimentales y es un problema que se aborda en esta tesis.

Además de por su eficiencia, las Teorías de Campos Efectivas nos proporcionan un mecanismo para ordenar las mencionadas desviaciones por su tamaño, de forma que solo un conjunto de las mismas es observable a una precisión finita. Esto nos permite clasificar, de forma bidireccional, todos los posibles modelos de nueva física y todos los efectos que generan, construyendo así un diccionario Infrarrojo/Ultravioleta. En esta tesis calculamos parcialmente este diccionario a un lazo para el caso del Modelo Estándar.

Finalmente, usamos las herramientas previamente desarrolladas para su aplicación a un caso fenomenológicamente relevante, en concreto sobre la tensión observada en el momento magnético del muón. Proponemos no solo una nueva clase de modelos para explicar esta tensión sino también un modelo específico como ejemplo para explicar también otras anomalías.

# Abstract

The Standard Model is the theory that comprises our current understanding of fundamental interactions, but we have several reasons, both theoretical and experimental, to believe that it cannot be the end of the story and there must be new physics beyond it.

However, despite decades of search over a long range of energies, we still do not have clear signatures of new physics. This motivates the use of Effective Field Theories as an efficient way of performing the search, because it allows to split the problem in two steps: an agnostic parametrization of the possible deviations of the Standard Model and the connection between these deviations and models of new physics.

This translation can be done at various levels in a perturbative expansion, and both the increasing precision in experiments and the necessity of capturing some otherwise missing effects require performing it at one loop. Being a model-dependent process makes it cumbersome and prone to errors to do it for the large number of possible models that we could be interested in. The automatization of this task would be therefore very useful to simplify the connection between theories and experimental consequences and it is a problem we address in this thesis.

Besides its efficiency, Effective Field Theories provide us the mechanism to order the mentioned deviations by their size, so that only a number of them are observable at a finite experimental precision. This allows us to classify bidirectionally all possible models of new physics and all the effects they generate, thus constructing an Infrared/Ultraviolet dictionary. In this thesis we partially compute this dictionary at one loop for the case of the Standard Model.

Finally, we apply the tools previously developed to perform a phenomenologically relevant analysis, in particular concerning the observed tension in the magnetic moment of the muon. We propose a new class of models to account for this tension and a specific example of a model addressing other anomalies as well.

# Table of Contents

# 1

# Introduction

The history of particle physics is one of a quest for the most fundamental description of nature. Over the course of the past century, this quest has changed the way we look at the universe. We have explored a wide range of energies and not only discovered several particles, but learned to describe how they behave. We even developed the very notion of a fundamental description, based on a few principles and symmetries, as what we aim for in this quest. Nowadays people think of the Standard Model (SM) as the first culmination of this pursuit. Its simplicity, together with the never-ending list of experimental tests to which it has been successfully subjected, make it the best description of nature we have... yet.

Even though the ultimate experimental confirmation only came in 2012 with the discovery of the Higgs boson, it has been decades since we have reasons to believe that there must be physics beyond the Standard Model (BSM). First, we have experimental evidences that hint to new physics that the SM should be extended to accommodate, like neutrino oscillations, dark matter, matter-antimatter asymmetry, etc. The second type of reasons are theoretical problems with the SM. These include the lack of a quantum description of gravity, the Hierarchy problem, flavor puzzle, the Strong CP problem, etc.

All these problems have motivated an active search for a theory more fundamental that the SM, designed to overcome its shortcomings. Given the vast number of possible models, this search has been traditionally guided by the compass of these theoretical arguments, mainly naturalness, to favor some models against others. However, despite expanding the energy range of search about an order of magnitude above the electroweak scale, nothing has been observed yet. Arguments of naturalness have weakened over the years – some do not even acknowledge it as a problem – and there is currently no clear criteria to choose the candidate to surpass the SM.

The fact that the new physics is hiding behind the observed energy gap makes the SM an effective description, at low energies, of the theory we want to discover, whatever it is. The idea that any dynamics happening at an inaccessible scale can be traded by an effective description at low energy opens up the possibility to perform the search in more unprejudiced, agnostic way. The formalism of Effective Field Theories (EFTs) allows us to classify all possible effects of new physics in terms of the Wilson Coefficients (WCs) of some operators, and order them by their size in a double perturbative expansion in mass dimension and loops. Thus, given a certain precision, only a finite number of coefficients will actually contribute and have to be considered. Through the bottom-up approach, we can use global fits to interpret what the experimental data are telling us, and parametrize deviations from SM while being agnostic about their UV origin.

However, this would be just a parametrization of the data unless we extract information about the structure of new physics. There needs to be a connection between the pattern of WCs that we measure (or constrain) and how different models leave their imprints on them. This is precisely the top-down approach, in which we use the matching procedure to translate the parameters of a model of heavy new physics into Wilson Coefficients. Performing the matching at leading order (tree level) is straightforward and there is only a finite number of relevant completions (under certain assumptions).

Nevertheless, the increasing precision in experimental data, together with the fact that some effects only appear at one loop, makes it necessary to consider loop effects to perform a competitive analysis. This makes the process tedious, prone to errors, and loses some of the power of EFTs due to the need of repeating this task for any interesting model. The automatization of the process of matching at one loop is therefore crucial in the efficiency of this comparison between models and experiments.

A natural consequence arising from the need of this translation between experimental data and models of new physics, eased by the automation of the matching process, is the utility of IR/UV dictionaries. The idea behind this is to be able to connect a set of WCs with specific extensions of the SM in two directions. One should be able to, first, read the list of possible models that contribute to a particular WC and, second, extract the list of WCs that a particular model generates. The ordering principle of which we dispose in EFTs ensures that at a certain precision, any observable new physics extending the SM, whatever it is, is already included in that list.

The research done during this PhD, which constitutes the main body of this thesis, was oriented to fill this gap between proposing models of new physics and comparing efficiently with experimental data, and apply the results to the study of some phenomenologically relevant examples.

The rest of the thesis is structured as follows. In Chapter 2 we will review the formalism of Effective Field Theories, making emphasis on the concepts that will be used thereafter and putting several examples. Next, Chapter 3 introduces `Matchmakereft`, an automated tool to perform the matching at tree level and one loop between two general theories and compute one-loop beta functions. Chapter 4 is devoted to present the partial UV/IR dictionary for the SMEFT at dimension six and one loop, encoded in the `Mathematica` package `SOLD`. Finally, in Chapter 5, we will make use of this dictionary to propose a whole new class of models to explain the g-2 anomaly, and study the one-loop phenomenology of an specific model able to explain, in addition, the neutral B anomalies and the Cabibbo angle anomaly.

# 2

# Effective Field Theories

The Standard Model is the best theory of nature that we have at the moment, and works even better than some physicists wish, but it still has some shortcomings. Motivated by the energy gap observed in experiments, the formalism Effective Field Theories seems the ideal candidate to perform an agnostic, exhaustive search for new physics.

In this chapter, we will first briefly introduce the Standard Model, since it will be our starting point for any new physics extension, which constitutes our main object of study. Next, we will review the basics of EFTs, beginning by establishing its basic principles in Section 2.2 to then go over all the steps involved in a realistic calculation. This include the concept and construction of a basis, in Section 2.3, the treatment of evanescent structures (Section 2.4), and one-loop matching and running (Sections 2.5, 2.6). Finally, we include in Section 2.7 a review of the current status of how a phenomenology study within the EFT framework is streamlined in the literature, motivating the work presented in next chapters.

## 2.1 The Standard Model of Particle Physics

The Standard Model is the theory that encapsulates our current description of strong and electroweak (EW) interactions. The history of its development shows a tremendous collective effort to overcome several challenges along the way, both theoretical and experimental, that culminated in an unprecedentedly successful theory. It is constructed under the assumption of invariance under the Lorentz symmetry and the Standard Model gauge group $\mathcal{G}_{\mathrm{SM}} \equiv \mathrm{SU}(3)_{\mathrm{c}} \otimes \mathrm{SU}(2)_{\mathrm{L}} \otimes \mathrm{U}(1)_{\mathrm{Y}}$.

The particle content of the theory comprises all elementary particles currently observed. It consists of three sectors: gauge bosons associated with each symmetry group, fermions, that can be further divided up to quarks and leptons, depending on whether they are charged under strong interactions, and the Higgs doublet, responsible of the mechanism that provides mass to the particles. In the case of fermions, there are three copies (with the same quantum numbers) of each of them, called flavors or families. The matter fields are collected in Table 2.1, along with their representations under the gauge group. This already reveals the chiral structure of the theory, in which different chiralities belong to different representations of the gauge group.

| Field | $\mathrm{SU}(3)_\mathrm{c} \otimes \mathrm{SU}(2)_\mathrm{L} \otimes \mathrm{U}(1)_\mathrm{Y}$ |
|---|---|
| $q_L$ | $(3, 2, 1/6)$ |
| $u_R$ | $(3, 1, 2/3)$ |
| $d_R$ | $(3, 1, -1/3)$ |
| $\ell_L$ | $(1, 2, -1/2)$ |
| $e_R$ | $(1, 1, -1)$ |
| $H$ | $(1, 2, 1/2)$ |

**Table 2.1:** Matter content of the Standard Model.

Once all the fields are specified, the SM Lagrangian is given by the set of all possible renormalizable interactions among all these particle respecting the aforementioned symmetries:

$$\begin{aligned}\mathcal{L}_\mathrm{SM} &= \mathrm{i}[\bar{\ell}\not{D}\ell + \bar{e}\not{D}e + \bar{q}\not{D}q + \bar{u}\not{D}u + \bar{d}\not{D}d] - [\bar{\ell}Y_e eH + \bar{q}Y_u u\tilde{H} + \bar{q}Y_d dH + \mathrm{h.c.}] \\ &+ -\frac{1}{4}G^A_{\mu\nu}G^{A\,\mu\nu} - \frac{1}{4}W^I_{\mu\nu}W^{I\,\mu\nu} - \frac{1}{4}B_{\mu\nu}B^{\mu\nu} + \mathcal{L}_\mathrm{g.f.} + \mathcal{L}_\mathrm{gh} \\ &+ (D_\mu H)^\dagger D^\mu H - m^2 H^\dagger H - \lambda(H^\dagger H)^2\ ,\end{aligned} \tag{2.1}$$

with $\tilde{H} \equiv \mathrm{i}\sigma_2 H^*$, and gauge and flavor indices omitted. The first line is the fermionic sector, which includes both gauge and Yukawa interactions for fermions. The second line is called the Yang-Mills lagrangian, and includes the kinetic terms for the gauge bosons and the gauge fixing, $\mathcal{L}_\mathrm{g.f.}$, and ghost, $\mathcal{L}_\mathrm{gh}$, terms necessary for their consistent quantization.

Finally, the last line is the scalar sector, including the Higgs kinetic term and the scalar potential. For $m^2 > 0$ and $\lambda > 0$, the minimum of the potential occurs at $H = 0$. However, for $m^2 < 0$, this potential has its minimum at a non-trivial vacuum expectation value (vev) of the Higgs doublet:

$$\langle H \rangle = \sqrt{\frac{-m^2}{2\lambda}} \equiv \frac{v}{\sqrt{2}} \tag{2.2}$$

This leads to the spontaneous symmetry breaking (SSB) of the SM gauge symmetry when Eq. (2.1) is parametrized with the actual quantum, propagating Higgs field.

The pattern of symmetry breaking is the following:

$$\mathrm{SU}(3)_\mathrm{c} \otimes \mathrm{SU}(2)_\mathrm{L} \otimes \mathrm{U}(1)_\mathrm{Y} \longrightarrow \mathrm{SU}(3)_\mathrm{c} \otimes \mathrm{U}(1)_\mathrm{em}, \tag{2.3}$$

so that there are 3 broken generators. The Goldstone theorem then implies that there are three degrees of freedom, the Goldstone bosons, that remain massless. These are “eaten up” by the $W^\pm, Z$ bosons, by the so-called Higgs mechanism, becoming their longitudinal polarizations, as they acquire a mass. The only remaining physical field in the Higgs doublet is the Higgs boson, that also acquires a mass after the breaking.

The Yukawa interactions, on their side, generate a mass matrix for quarks and leptons, proportional to the Yukawa matrices $Y_{u,d,e}$. The texture of these matrices is (a priori) arbitrary and ultimately determines the value of the masses. The chiral arrangement of the fermions, in which the two chiralities belong to different representations of $\mathcal{G}_\mathrm{SM}$, makes the diagonalization of the quark mass matrices introduce flavor changing processes in the charged currents, through the famous Cabbibo-Kobayashi-Maskawa (CKM) matrix. The same would happen in the leptonic sector in the (realistic, but BSM) scenario in which neutrinos have masses and diagonalization of the mass matrix introduces the Pontecorvo-Maki-Nakagawa-Sakata (PMNS) matrix.

Besides the SM gauge symmetry, Eq. (2.1) exhibits some global, accidental symmetries. They are called accidental because they are not imposed or neccessary in the construction in the theory but "happen" to be there and are observed experimentally. These include the baryon ($B$) and lepton ($L$) number U(1) symmetries, associated to the baryon and lepton "charge" carried by a field. Despite being accidental, the scale in which new physics can violate them is very constrained. Bounds on $|\Delta B| \neq 0$ nucleon decay [1–3] constrain the scale in which $B$ can be violated to be around $10^{14-16}$ GeV. The situation for $L$ is a bit different, because it may be violated by neutrino masses, but a naive estimation also sets the scale to $\sim 10^{14}$ GeV. This will be important in the construction of an EFT for the Standard Model, in which the assumption of symmetries plays a defining role.

It is worth stressing at this point that the huge separation of scales already present in the SM and provided us with an historic example of how heavy physics decouples and an effective description can pave the way to a deeper understanding of phenomena. The first realistic quantum field theory was developed to describe Quantum Electro-Dynamics (QED), which already *was* and effective field theory. In fact, QED is the limit of Eq. (2.1) in which everything but the electron is integrated out (ignoring the strong sector). When weak interactions were first studied, it was observed that they could be parametrized at low energies by adding an effective operator describing a point-like interaction between four fermions (today known as Fermi theory). As experiments grew in energy, it was eventually possible to resolve the structure in this interaction and verify that it was mediated by the weak bosons, but it was the study of these effective interactions (why some of them were present and some others were not, their relative values, etc.) which allowed to understand the characteristics of weak interactions.

The Standard Model meant a huge success in the history of physics. It has been experimentally tested with an unprecedented degree of agreement with observations. During decades, experiments seemed to discover things right were the SM predicted them to be. Thus far, even when some deviations seemed to be observed, the SM ended up being correct. But, besides being experimentally unparalleled, it also set some significant theoretical milestones, among which the following, at least, are worth stressing:

- **Simplicity**. Its simple formulation, solely in terms of invariance under a gauge group, is enough to explain the vast majority of phenomenology observed during the last hundred years.

- **Origin of the mass**. The description of the weak interactions based on isospin symmetry was initially hard to reconcile with the observation of mass for weak bosons (and fermions). The Higgs mechanism for the electroweak symmetry breaking (EWSB) solved this problem and set our current paradigm of the generation of mass.

- **Electroweak unification**. The electromagnetic and weak interactions, with very different properties, were understood to be the low energy manifestation of the SM gauge group after EWSB. The idea of a larger unification has fueled many endeavors in the search for an ultimate theory.

- **Asymptotic freedom and confinement**. These two features of the strong interactions were explained as the result of the dynamics of a strongly coupled sector with a non-abelian gauge symmetry. This idea has also inspired many models ever since.

However, despite the fact that the ultimate confirmation of the Standard Model was only recently discovered with the measure of the Higgs boson, there have been indications of its insufficiencies since a long time ago. The reasons can be classified in two groups, according to their nature.

In the first place we have experimental observations of physics that cannot be explained within the Standard Model. For instance, the observation of neutrino oscillations implies that there must be at least two massive states in the neutrino sector, that are not a feature of the SM in its minimal setup. We also know that the matter content in the universe is greater than what baryonic matter can account for, so it is highly possible that another type of (dark) matter also exists. Moreover, the fact that we are made of matter and not antimatter can only be explained by an additional source of CP violation besides the one in the SM. There are also some tensions with the SM predictions in different observables which, in the case of persisting, would be signs of new physics. These include the B anomalies, the anomalous magnetic moment of the muon, the Cabibbo angle anomaly, etc.

On the other hand, there are several theoretical arguments to search for a more complete, fundamental theory. First, the SM does not include a quantum description of gravity, so we know it must be extended, even if we do not know how. Likewise, our eagerness for simplicity, together with the running of gauge coupling constants, invites us to think that $\mathcal{G}_{\rm SM}$ could be a subgroup of a larger gauge group broken at a high scale, motivating models of Grand Unification. Furthermore, the mass of the Higgs is not protected from contributions of the new physics that we know is present at a very high scale, and this large hierarchy makes its actual value seem extremely fine-tuned. This is known as Hierarchy problem. Another intriguing feature of the SM is the presence of three flavors of fermions and the huge hierarchy among their masses, which could point to a more fundamental description (flavor puzzle). The fine-tuning of the QCD $\theta$ angle, stringently constrained by bounds on the neutron electric dipole moment, is also not yet explained and known as the Strong CP problem.

Altogether, all these reasons strongly suggest the presence of new, undiscovered physics. The experimental indication of a mass gap between the EW scale and the scale in which this physics hides (hinted by the absence of resonances or any significant deviations) makes the Effective Field Theories framework a very efficient tool for its search. In the next section, we will see what the idea behind EFTs is and what does it make them so useful.

## 2.2 The use of EFTs for BSM

An effective field theory is just a simplified, effective description of another theory in which there is a separation of scales. In the context of physics beyond the Standard Model this will apply to energy scales, but the concept is more general and can be applied as long as a power-counting parameter can be identified. The idea is to make use of this separation to perform an perturbative expansion in inverse powers of the heavy masses to obtain a simpler theory, with less degrees of freedom, which will reproduce the results of the complete theory in the regime where this energy expansion is meaningful.

A priori, the reason to use an effective field theory when the complete one is known is not only that it makes calculations easier, but also that it improves the convergence of perturbation theory, and can be crucial in cases with a large separation of scales. But its actual applicability goes much beyond that.

From now on, we will refer as full or ultraviolet (UV) theory to the complete theory with a light sector of fields, denoted collectively as $\phi$, and a sector of heavy fields $\Phi$ of masses of order $\Lambda$. This is a simplification, and a realistic case would typically be a multiscale problem, but the same ideas can be applied to one scale at a time. Note that, in principle, integration of momentum in loop diagrams makes results sensitive to physics happening at all scales, so it is not straight-forward that we can construct a simplified theory forgetting about the details in the UV. The reason why we are, in fact, allowed to use EFTs relies on two facts. The first one is that heavy physics decouples: Appelquist and Carazzone proved in [4] the decoupling theorem in which they stated that amplitudes with (virtual) propagation of heavy states vanish in the limit of very high masses. The second one is that the effects of this propagation, when seen from low energies, are local.

Thus, we can perform an expansion in powers of the heavy masses and obtain an effective description in terms of local operators. This description would be of course only valid when performing experiments at energies $E << \Lambda$. Formally, constructing the effective theory consists of “integrating-out” the heavy degrees of freedom in the path integral:

$$\int d\phi \, d\Phi \, e^{iS[\phi,\Phi]} = \int d\phi \, e^{iS_{\text{eff}}[\phi]}. \tag{2.4}$$

This integration trades out the virtual effects of heavy particles for a (formally infinite) set of operators suppressed by the heavy scale $\Lambda$:

$$\mathcal{L}_{\text{eff}} = \mathcal{L}_{d\leq 4} + \sum_{n,i} \frac{c_i^{(n)}}{\Lambda^{n-4}} \mathcal{O}_i^{(n)}, \tag{2.5}$$

where $\mathcal{L}_{d\leq 4}$ comprises (renormalizable) operators of mass dimension less or equal to four, that also receive contributions, and $\mathcal{O}_i^{(n)}$ are local operators of dimension $n$. The coefficients of these operators, $c_i^{(n)}$, are called Wilson Coefficients, and encode the effects of heavy physics[1]. Insertions of these operators in amplitudes for a certain process are suppressed by the heavy energy scale $\Lambda$, and increasingly suppressed the higher their dimension is. Therefore, working at a certain precision level, we can truncate this expansion and consider only a finite set of operators. In mass independent renormalization schemes this also happens at loop order, which is crucial to keep both the operator and loop expansion meaningful.

This is where the power of EFTs in the search for new physics comes in, because the problem can be then split in two independent steps. Even if we do not know about the UV theory, this construction allows us to be completely agnostic about its details. All we need is

[1] The definition of Wilson Coefficients typically includes also the heavy scale $\Lambda$. We will talk indistinctly about the two unless there could be a source of confusion.

to parametrize the set of all possible observable effects of UV physics, at a certain precision, in terms of a set of local operators with (unknown) Wilson Coefficients. When comparing with experiments, performed at low energies, we can measure or constrain the value of these coefficients by computing observables in terms of the parameters of the effective theory. The key advantage is that this calculation can be done just once (for each order in the loop and mass dimension expansion) and will remain valid no matter what the actual UV theory is. This is known as the bottom-up approach.

However, pursuing the idea of learning about the physics at the UV scale, we do not want to stick to an effective description. In the end, as agnostic as it is, it is just a parametrization of the effects of physics at high scales. This physics is encoded in the values of the Wilson Coefficients, so to obtain information about it, we need to abandon the agnosticism and compute the implications of the candidate theories to be able to distinguish between them. This constitutes the top-down approach, and implies a process of translation between the parameters of the effective theory, that we are able to extract from experiment, and the parameters of the UV theory, whose effect at low energies is imprinted in the former. This translation is the process known as matching.

Furthermore, the use of the effective field theory formalism is not only justified, but inevitable in some sense. Since there is physics beyond the Standard Model, at the very least because gravity exists, the Standard Model *is* an effective field theory, irrespective of how well it works at the renormalizable level. It is just the $d \leq 4$ part of an effective Lagrangian called Standard Model Effective Theory (SMEFT).

Since the topic of this thesis is the application of effective field theories to physics beyond the Standard Model, in the rest of this chapter we will review the fundamental concepts of this formalism directly in the context of SMEFT. See [5–9] for extensive reviews on the topic.

## 2.3 Construction of an EFT

In the bottom-up approach, we are completely agnostic about what is the theory that extends, in our case, the Standard Model. To construct an effective field theory, we need to be completely general using the information that we have from low energy experiments. The purpose of this section is to review the procedure for such a construction and specify for the case of the SMEFT.

The first step is to identify the degrees of freedom that propagate, or can be excited, at low energies. These will be the fields upon which we construct our Lagrangian. In the case of the SM, we will use the fields described in Section 2.1. Different assumptions for the content of light fields define different EFTs, and subsequently lead to a different interpretation of experimental data. For this reason, although the SMEFT is the most broadly used by the community, there are also some other EFTs extending the SMEFT with another light particle that, even not being observed, is theoretically motivated. This is the case of the axion-like particle (ALP) EFT [10–12], extending the SM content with an ALP, or the $\nu$SMEFT [13–17], that includes a right-handed neutrino. Likewise, in order to compare the implications of a model with precision experiments are low energies, it is convenient to use an effective theory in which the heaviest particles of the SM are also integrated out. This is called Low-energy Effective Field Theory (LEFT).

The next ingredient is the symmetry to be imposed on the Lagrangian. Experimentally, we know that the SM gauge symmetry is a very accurate description at low energies, and any other symmetry extending the SM one must be in principle broken at sufficiently high energy. We want therefore to construct the SMEFT imposing the SM gauge symmetry.

In the case of the SM and the SMEFT, an extra assumption is made concerning the Higgs boson. In Section 2.1, we have introduced a Higgs doublet which contained four degrees of freedom transforming linearly under SU(2): one scalar singlet (the physical Higgs boson) and three Goldstone bosons that became the longitudinal polarizations of the weak bosons after EWSB. However, this does not necessarily have to be the case; if the symmetry is not linearly realized, the Higgs and the Goldstone bosons do not have to form a single SU(2) multiplet and can transform independently. This is the case, for instance, of Composite-Higgs models. The more general EFT constructed upon the SM fields but relaxing this assumption is called Higgs Effective Field Theory or HEFT (see [18–20] for recent reviews on the topic).

The last step is to build all possible kinematic structures allowed by Lorentz and gauge symmetry that could be generated by UV physics effects, and, as such, that can be encoded in local operators. As we will see in the next section, the process of matching can be performed at any order in the mass and loop expansion. To do such calculations involving loops, we use dimensional regularization, for which we need to regularize our action extending it to $d = 4-2\epsilon$ dimensions. We also do not employ any on-shell relations for the kinematic quantities. This leads us to the concept of *Green's basis*: a set of all independent operators (up to a certain mass dimension) off-shell and in $d$ space-time dimensions.

However, it is clear that among the most general set of Lorentz and gauge invariant operators, we will find that not all of them are independent. We need to find relations to express some of them in terms of others, the choice of which operators conform the basis being not unique. In general, there are three types of identities that we can use to select a Green's basis out of this set:

(i) **Integration by parts**. Considering the set of SMEFT operators with a fermionic tensor current, a Higgs and two derivates, we could in principle write the three following combinations:

$$\begin{aligned}
\mathcal{O}_1 &= D_\mu \overline{\psi_L} \sigma^{\mu\nu} D_\nu \psi_R H, \\
\mathcal{O}_2 &= \overline{\psi_L} \sigma^{\mu\nu} D_\nu \psi_R D_\mu H, \\
\mathcal{O}_3 &= D_\mu \overline{\psi_L} \sigma^{\mu\nu} \psi_R D_\nu H,
\end{aligned} \tag{2.6}$$

where $\sigma^{\mu\nu} \equiv \frac{i}{2}[\gamma^\mu, \gamma^\nu]$ and gauge and flavor indices are omitted. There are no more combinations with the same components because two derivatives acting on the same field could always be traded by a field-strength tensor $X_{\mu\nu}$. However, we can integrate by parts to realize that in fact:

$$\begin{aligned}
\mathcal{O}_1 &= -\mathcal{O}_2 + X_{\mu\nu}\,[\ldots], \\
\mathcal{O}_3 &= \mathcal{O}_2 + X_{\mu\nu}\,[\ldots],
\end{aligned} \tag{2.7}$$

so there is actually only two independent operators in this sector.

(ii) **Group theory identities**. There are cases in which we can find several independent gauge invariant tensors to contract the same Lorentz structure. For instance, considering four fermion operators with vector currents of SM lepton doublets, we could write in principle the following possibilities:

$$\begin{aligned}
\mathcal{O}'_1 &= \delta_{ab}\,\delta_{cd}\,\overline{\ell_{La}}\gamma_\mu\ell_{Lb}\,\overline{\ell_{Lc}}\gamma^\mu\ell_{Ld}\\
\mathcal{O}'_2 &= \delta_{ad}\,\delta_{bc}\,\overline{\ell_{La}}\gamma_\mu\ell_{Lb}\,\overline{\ell_{Lc}}\gamma^\mu\ell_{Ld}\\
\mathcal{O}'_3 &= \sigma^I_{ab}\,\sigma^I_{cd}\,\overline{\ell_{La}}\gamma_\mu\ell_{Lb}\,\overline{\ell_{Lc}}\gamma^\mu\ell_{Ld}\\
\mathcal{O}'_4 &= \sigma^I_{ad}\,\sigma^I_{cb}\,\overline{\ell_{La}}\gamma_\mu\ell_{Lb}\,\overline{\ell_{Lc}}\gamma^\mu\ell_{Ld}\\
\mathcal{O}'_5 &= \epsilon_{ac}\,\epsilon_{bd}\,\overline{\ell_{La}}\gamma_\mu\ell_{Lb}\,\overline{\ell_{Lc}}\gamma^\mu\ell_{Ld}
\end{aligned} \tag{2.8}$$

where $\sigma^I$ are the Pauli matrices and $\epsilon \equiv \mathrm{i}\sigma^2$. Latin letters a,b,... denote SU(2) indices and flavor indices are omitted. But using the SU(2) Fierz identity and the property of the Levi-Civita tensor:

$$\sigma^I_{ab}\sigma^I_{cd} = 2\delta_{ad}\delta_{cb} - \delta_{ab}\delta_{cd}, \tag{2.9}$$

$$\epsilon_{ab}\epsilon_{cd} = \delta_{ac}\delta_{bd} - \delta_{ad}\delta_{bc}, \tag{2.10}$$

it is easy to show that:

$$\mathcal{O}'_2 = \frac{1}{2}\mathcal{O}'_1 + \frac{1}{2}\mathcal{O}'_3, \tag{2.11}$$

$$\mathcal{O}'_4 = 2\mathcal{O}'_3 - \mathcal{O}'_2 = \frac{1}{2}\mathcal{O}'_3 - \frac{1}{2}\mathcal{O}'_1, \tag{2.12}$$

$$\mathcal{O}'_5 = \mathcal{O}'_1 - \mathcal{O}'_2 = \frac{1}{2}\mathcal{O}'_1 - \frac{1}{2}\mathcal{O}'_3. \tag{2.13}$$

(iii) **Algebraic identities**. Considering this time four fermion operators with charge conjugation, even after applying group theory identities, we are left in principle with two independent combinations for the product of two scalar currents of lepton doublets:

$$\tilde{\mathcal{O}}_1 = \overline{\ell_{La}}\ell^c_{Lb}\,\overline{\ell^c_{La}}\ell_{Lb} \tag{2.14}$$

$$\tilde{\mathcal{O}}_2 = \overline{\ell_{La}}\ell^c_{Lb}\,\overline{\ell^c_{Lb}}\ell_{La} \tag{2.15}$$

where $\ell^c \equiv \mathcal{C}\overline{\ell}^T$ and $\mathcal{C}$ is the charge conjugation matrix. Flavor indices are again omitted. However, since $\overline{\ell_1}\ell^c_2 = \overline{\ell_2}\ell^c_1$, it is straight-forward to show that:

$$\tilde{\mathcal{O}}_1 = \tilde{\mathcal{O}}_2. \tag{2.16}$$

To put another example, one can construct a Green's basis for SMEFT at operator dimension five using very simple schematic arguments. It turns out that the Lorentz and gauge invariance are so restrictive at dimension five that there is only one independent operator (ignoring flavor). First, we cannot have $H^5$ because that can never be invariant under SU(2). Any operator built with Higges and derivatives would need to have an even number of both, so there is none at dimension 5. For operators with two fermions, one cannot add two derivates because it is always forbidden by gauge symmetry. Adding one Higgs and one derivative is not possible either because this would force us to form a vector current, which cannot couple to a gauge singlet with the Higgs. Finally, the only possibility is to have an scalar current of two fermions and two higgses. However, a combination in the form $\overline{\psi}\psi$ could never be gauge invariant, so there can only be an operator of the form $\overline{\psi^c}\psi$, among which we find that the only gauge invariant one is formed of two lepton doublets. We can still find three different gauge structures, but there is only one independent:

$$\mathcal{O}_W = \epsilon_{ab}\,\epsilon_{cd}\,\overline{\ell^c_{Lb}}\,\ell_{Ld}\,H_a\,H_c, \tag{2.17}$$

which is called the Weinberg operator [21] and has been extensively studied because it generates a Majorana mass for left-handed neutrinos after EWSB [22–24].

The same procedure can be applied at dimension six, which will be our main case of interest for the rest of the thesis. The operators conforming a Green's Basis for the SMEFT are listed in Tables B.1-B.9 of Appendix B.

Nevertheless, constructing a Green's basis is not the end of the story. When computing observables, we compute on-shell quantities and project results into four space-time dimensions. It is easy then to imagine how our construction of a basis in $d$ dimensions will contain some degree of redundancy among its operators, which could be further related using properties that only hold on four dimensions. The use of these properties implicitly defines an operator – the difference between the ones that are related – that vanishes in four dimensions, but that when inserted in divergent loop diagrams during the calculations in the EFT, can give a finite result. These are called *evanescent* operators and will be explored in greater detail in Section 2.4.

Moreover, even if it is not wrong to compute on-shell quantities with this basis, it could be simplified having in mind that the ultimate goal is to compute physical quantities, and this would make the computation easier. This can be achieved recalling that the LSZ formula states that the S matrix elements can be computed using any interpolating field. This implies that we can perform field redefinitions to our theory and still obtain the same physical results. The operators in a Green's basis that are reduced to others using field redefinitions are called *redundant*.

This field redefinitions can be shown to be equivalent to applying the Equations of Motion (EOMs) for the fields in the operator to be reduced, but only at the first order [25, 26]. This process is usually referred to as using equations of motion in the literature, but the correct way to proceed when you have a basis spanning over more than one operator dimension is indeed using field redefinitions.

Let us put an example to illustrate what this difference is. Consider an EFT with a fermion $\psi$ and a real scalar $\phi$:

$$\mathcal{L} = \overline{\psi}i\not{D}\psi + y\,\overline{\psi}\psi\phi + \frac{c_5}{\Lambda}\,\overline{\psi}\psi\phi^2 + \frac{r_5}{\Lambda}\,\overline{\psi}i\not{D}\psi\phi + \text{h.c.}, \tag{2.18}$$

where $y, c_5 \in \mathbb{R}$, $r_5 \in \mathbb{C}$, and we are writing explicitly the suppresion by a mass scale $\Lambda$. The equation of motion for the fermion reads:

$$i\not{D}\psi = -y\psi\phi. \tag{2.19}$$

Substituting this expression back in Eq. (2.18), we obtain:

$$\mathcal{L}_{\text{EOM}} \supset \left(\frac{c_5}{\Lambda} - y\frac{r_5}{\Lambda} - y\frac{r_5^*}{\Lambda}\right)\overline{\psi}\psi\phi^2 + \mathcal{O}(\frac{1}{\Lambda^2}). \tag{2.20}$$

We see that we have eliminated the operator $\overline{\psi}i\not{D}\psi\phi$ in favour of $\overline{\psi}\psi\phi^2$, so the former is redundant. The same can be achieved by performing the following field redefinition:

$$\psi \to \frac{r_5^*}{\Lambda}\,\psi\phi, \tag{2.21}$$

after which we obtain:

$$\begin{aligned}\mathcal{L} \to \mathcal{L}_{\text{F.R.}} &= \mathcal{L} - \frac{r_5}{\Lambda}\overline{\psi}\Big(i\not{D}\psi + y\phi\psi\Big)\phi + \text{h.c.} + \mathcal{O}(\frac{1}{\Lambda^2}) = \\ &= \overline{\psi}i\not{D}\psi + y\,\overline{\psi}\psi\phi + \left(\frac{c_5}{\Lambda} - y\frac{r_5}{\Lambda} - y\frac{r_5^*}{\Lambda}\right)\overline{\psi}\psi\phi^2 + \mathcal{O}(\frac{1}{\Lambda^2}).\end{aligned} \tag{2.22}$$

Notice that the term in parenthesis in the first line of Eq. (2.22) is, in fact, proportional to the equation of motion in Eq. (2.19), so we obtain the same result with both approaches at this first order in the expansion. However, inspecting the terms at dimension six quadratic in the field redefinition, we find a term:

$$\mathcal{L}_{\text{F.R.}} \supset \frac{y\,r_5\,r_5^*}{\Lambda^2}\,\overline{\psi}\psi\phi^3 \tag{2.23}$$

that can never be recovered using equations of motion. In fact, such a term could only come from applying EOMs in an operator of the type $\overline{\psi}i\not{D}\psi\phi^2$, but it would be proportional to a dimension six Wilson Coefficient, and not the combination $r_5\,r_5^*$. For this reason, the correct procedure to eliminate redundant operators is to use field redefinitions.

This reduction leads us to define the concept of a physical basis for an EFT: it is the minimal set of operators that are independent on-shell and four space-time dimensions. As it happened for the Green's basis, the choice is not unique. In the case of the SMEFT at dimension six, the most popular one is the Warsaw basis [27], broadly adopted by the community, which will be used in the rest of the thesis.

In Tables B.1–B.9, the operators are classified in three sectors. We use the notation $\mathcal{O}_{xxx}$ for the operators that conform a physical basis (the Warsaw basis). $\mathcal{R}_{xxx}$ is reserved for redundant operators, that can be written as a combination of physical operators using field redefinitions. Lastly, we use $\mathcal{E}_{xxx}$ for redundant operators that implicitly define evanescent structures in their reduction, and call them evanescent in a little abuse of notation. Their corresponding coefficients will be denoted by $\alpha_{xxx}$, $\beta_{xxx}$ and $\gamma_{xxx}$, respectively.

As mentioned above, the SM exhibits some global, accidental symmetries like baryon or lepton number conservation. As these are not necessary in the construction of the SM, they could in principle be violated at high energies, so the most general version of SMEFT should capture these effects. Indeed, the Weinberg operator violates lepton number in two units, and there is a whole sector of B-violating operators at dimension six. We will, however, restrict ourselves to the basis in Appendix B, that does not include B-violating effects.

The B-preserving sector of SMEFT at dimension six includes 59 operators (2499 independent coefficients counting flavor). To simplify the analysis of data in terms of these coefficients, sometimes extra theoretical assumptions (concerning flavor) are taken into account, so that the number of independent coefficients can be severely reduced. These include flavor universality with an $\mathrm{U}(3)^5$ symmetry, only third generation flavor, Minimal Flavor Violation [28]... See [29–32] for some studies along this line.

## 2.4 Evanescent operators

The process of matching beyond leading order entails calculations in $d$ dimensions. In order to "prepare" the EFT to receive all possible contributions from UV physics, we therefore have to parametrize all independent operators in $d$ dimensions. When reducing them to a physical basis, we are implicitly defining a prescription to project a set of $d$-dimensional structures into a physical and evanescent part. However, this evanescent part, when inserted in divergent loop diagrams in the EFT, can give a finite contribution that has to be taken into account. In this section we will review the prescription detailed in [33] to deal with evanescent operators, which we will adopt in the following.

For instance, let us consider the following SMEFT operators:

$$\mathcal{E}^c_{\ell e} = \overline{\ell^c}\gamma^\mu e\, \bar{e}\gamma_\mu \ell^c, \tag{2.24}$$

$$\mathcal{O}_{le} = \bar{\ell}\gamma^\mu \ell\, \bar{e}\gamma_\mu e. \tag{2.25}$$

Both operators are related, in four dimensions, by the following Fierz identity:

$$\mathcal{E}^c_{\ell e} = -\mathcal{O}_{le}. \tag{2.26}$$

This identity is only true in four dimensions, so by making the substitution above, we are implicitly defining an evanescent operator:

$$E_{le} \equiv \mathcal{E}^c_{\ell e} + \mathcal{O}_{le}, \tag{2.27}$$

which is formally $\mathcal{O}(\epsilon)$. This operator can contribute, for instance, in the dipole amplitude between $\ell, e, H$ and $W^\mu$. The relevant diagrams are depicted in Figure 2.1. The divergences in these loops can be compensated by the insertion of $E_{le}$ and yield a finite contribution. In order to take this contribution into account, one can either keep track of these evanescent operators and insert them in the calculations in the EFT, or absorb this effect by a shift in the Wilson Coefficients of the operators in the physical basis, in a so-called evanescence-free renormalization scheme [33].

In order to do so, we have to compute the finite part of all insertions of $E_{le}$ in the EFT loop amplitudes. For concreteness we will focus on the process depicted in Figure 2.1. Since we are interested in the UV divergence of the amplitude, we can expand the integrand in a

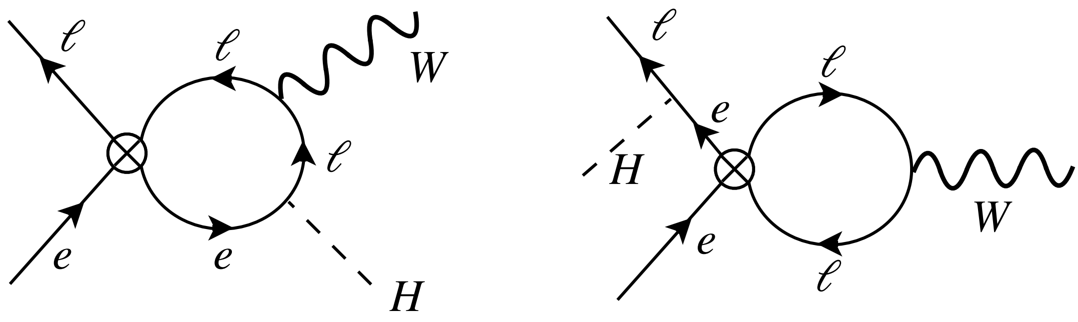


**Figure 2.1:** One loop diagrams with an insertion of $E_{le}$ (denoted by the crossed circle) that contribute to the dipole amplitude.

(hard) region in which $k >> p$, with $k$ being the loop momentum and $p$ any of the external momenta. Moreover, since we will absorb this contribution by a shift in the physical basis, we can perform the calculation on-shell. Using the conventions stated in Appendix A, we obtain the following,:

$$i\mathcal{M}_{(e_j W_\mu \to H\ell_i)} = -ig_2[Y_e]_{kl}\,[\gamma^c_{le}]_{kjli}\,\overline{u_\ell}\sigma_{\mu\nu}P_R u_e\; q^\mu \epsilon^\nu \epsilon \int \frac{d^dk}{(2\pi)^d}\frac{1}{k^4}, \tag{2.28}$$

where gauge structure is omitted, $\gamma^c_{le}$ denotes the Wilson Coefficient of $\mathcal{E}^c_{\ell e}$, $u_{\ell,e}$ are external spinors, $\epsilon^\nu$ is the $W$'s polarization vector and $q$ is its four-momentum. As anticipated, the Dirac algebra from the insertion of $E_{le}$ yields an $\epsilon$ factor that will extract the pole of the divergent integral.

The only operator in the physical basis contributing to this amplitude is the dipole operator:

$$[\mathcal{O}_{eW}]_{ij} = (\bar{\ell}_i\sigma^{\mu\nu}e_j)\sigma^I H W^I_{\mu\nu}, \tag{2.29}$$

so we can absorb the contribution in Eq. [2.28] by a shift in its Wilson Coefficient:

$$[\alpha_{eW}]_{ij} \longrightarrow [\alpha_{eW}]_{ij} - \frac{1}{32\pi^2}g_2[Y_e]_{kl}\,[\gamma^c_{le}]_{kjli}. \tag{2.30}$$

Besides the Fierz identities, the other source of evanescence structures that will be relevant in our analysis is the reduction of Dirac structures. In four dimensions, any four-fermion structure can be expressed as a combination of elements in this basis:

$$\begin{aligned}\left\{\Gamma^i_1\otimes\Gamma^i_2\right\} = \Big\{&P_L\otimes P_L, P_R\otimes P_R, P_L\otimes P_R, P_R\otimes P_L, P_R\gamma^\mu P_L\otimes P_R\gamma_\mu P_L,\\ &P_L\gamma^\mu P_R\otimes P_L\gamma_\mu P_R, P_R\gamma^\mu P_L\otimes P_L\gamma_\mu P_R, P_L\gamma^\mu P_R\otimes P_R\gamma_\mu P_L,\\ &P_L\sigma^{\mu\nu}P_L\otimes P_L\sigma_{\mu\nu}P_L, P_R\sigma^{\mu\nu}P_R\otimes P_R\sigma_{\mu\nu}P_R\Big\}.\end{aligned} \tag{2.31}$$

In $d$ dimensions, however, we can encounter additional gamma structures that have to be projected onto this basis up to an $\mathcal{O}(\epsilon)$ structure that will define our evanescent operators [33]:

$$A_1\otimes A_2 = \sum_i a_i(A_1,A_2)\Gamma^i_1\otimes\Gamma^i_2 + E(A_1,A_2). \tag{2.32}$$

In order to obtain the $a_i$ coefficients, we can contract both sides of the equation with all the basis elements and take the ($d$-dimensional) trace:

$$\mathrm{Tr}[A_1\Gamma_1^j A_2\Gamma_2^j] = \sum_i a_i\,\mathrm{Tr}[\Gamma_1^j\Gamma_1^i\Gamma_2^j\Gamma_2^i] \tag{2.33}$$

defining a system of 10 equations in which we can solve for $a_i$. These coefficients are fixed once a choice for the basis and a prescription for $\gamma_5$ is made. Different choices for the basis or the treatment of $\gamma_5$ involve other evanescent structures or give different coefficients at order $\epsilon$ and simply define other renormalization/$\gamma_5$ schemes, as the shift (or counterterms) needed to compensate the evanescent contributions will be different. For the evaluation of these traces, as in the rest of calculations, we will use a Naive Dimensional Regularization (NDR) prescription for $\gamma_5$, i.e., anticommuting $\gamma_5$.

The matrix $M_{ij} \equiv \mathrm{Tr}[\Gamma_1^i\Gamma_1^j\Gamma_2^i\Gamma_2^j]$ only depends on the choice of elements of the basis. For the basis in Eq. (2.31), we obtain the following:

$$M_{ij} = \begin{pmatrix} 2 & 0 & 0 & 0 & 0 & 0 & 0 & 0 & 24-28\epsilon & 0 \\ 0 & 2 & 0 & 0 & 0 & 0 & 0 & 0 & 0 & 24-28\epsilon \\ 0 & 0 & 0 & 0 & 0 & 0 & 8-4\epsilon & 0 & 0 & 0 \\ 0 & 0 & 0 & 0 & 0 & 0 & 0 & 8-4\epsilon & 0 & 0 \\ 0 & 0 & 0 & 0 & 0 & 24\epsilon-16 & 0 & 0 & 0 & 0 \\ 0 & 0 & 0 & 0 & 24\epsilon-16 & 0 & 0 & 0 & 0 & 0 \\ 0 & 0 & 0 & 8-4\epsilon & 0 & 0 & 0 & 0 & 0 & 0 \\ 0 & 0 & 8-4\epsilon & 0 & 0 & 0 & 0 & 0 & 0 & 0 \\ 24-28\epsilon & 0 & 0 & 0 & 0 & 0 & 0 & 0 & 72-180\epsilon & 0 \\ 0 & 24-28\epsilon & 0 & 0 & 0 & 0 & 0 & 0 & 0 & 72-180\epsilon \end{pmatrix} \tag{2.34}$$

Therefore, given any Dirac structure, for instance $P_L\gamma_\mu\gamma_\nu P_L \otimes P_R\gamma^\mu\gamma^\nu P_R$, we can compute the left-hand side of Eq. (2.33):

$$\mathrm{Tr}[P_L\gamma_\mu\gamma_\nu P_L\Gamma_1^i P_R\gamma_\mu\gamma_\nu P_R\Gamma_2^i] = \begin{cases} -8d+12d^2-2d^3 & i=7 \\ 0 & \text{otherwise} \end{cases}, \tag{2.35}$$

and solve for $a_i$. Considering structures with at most three gamma matrices, we obtain the following:

$$P_L\gamma^{\mu\nu}P_L \otimes P_L\gamma_{\mu\nu}P_L = (4-2\epsilon)P_L\otimes P_L - P_L\sigma^{\mu\nu}P_L\otimes P_L\sigma_{\mu\nu}P_L, \tag{2.36}$$
$$P_R\gamma^{\mu\nu}P_R \otimes P_R\gamma_{\mu\nu}P_R = (4-2\epsilon)P_R\otimes P_R - P_R\sigma^{\mu\nu}P_R\otimes P_R\sigma_{\mu\nu}P_R, \tag{2.37}$$
$$P_L\gamma^{\mu\nu}P_L \otimes P_R\gamma_{\mu\nu}P_R = 4(1+\epsilon)P_L\otimes P_R + E_{LR}^{(2)}, \tag{2.38}$$
$$P_R\gamma^{\mu\nu}P_R \otimes P_L\gamma_{\mu\nu}P_L = 4(1+\epsilon)P_R\otimes P_L + E_{RL}^{(2)}, \tag{2.39}$$
$$P_R\gamma^{\mu\nu\lambda}P_L \otimes P_R\gamma_{\mu\nu\lambda}P_L = 4(4-\epsilon)P_R\gamma^\mu P_L\otimes P_R\gamma_\mu P_L + E_{LL}^{(3)}, \tag{2.40}$$
$$P_L\gamma^{\mu\nu\lambda}P_R \otimes P_L\gamma_{\mu\nu\lambda}P_R = 4(4-\epsilon)P_L\gamma^\mu P_R\otimes P_L\gamma_\mu P_R + E_{RR}^{(3)}, \tag{2.41}$$
$$P_R\gamma^{\mu\nu\lambda}P_L \otimes P_L\gamma_{\mu\nu\lambda}P_R = 4(1+\epsilon)P_R\gamma^\mu P_L\otimes P_L\gamma_\mu P_R + E_{LR}^{(3)}, \tag{2.42}$$
$$P_L\gamma^{\mu\nu\lambda}P_R \otimes P_R\gamma_{\mu\nu\lambda}P_L = 4(1+\epsilon)P_L\gamma^\mu P_R\otimes P_R\gamma_\mu P_L + E_{RL}^{(3)}, \tag{2.43}$$

As it happened with the Fierz relations, these evanescent structures receive contributions that can be compensated by a shift in the coefficients of the physical operators. Since we are interested in matching at one loop, this shift will only be relevant in theories that generate tree level coefficients for the evanescent operators. For this reason, although there is formally an infinite number of evanescent structures, we only have to keep track of the shifts produced by the few that can be generated at tree level by renormalizable UV theories. We will use the results provided in [33] for the shift of the coefficients in the Warsaw basis.

## 2.5 Matching

The bottom-up approach to the use of EFTs provides an agnostic way of parametrizing and classifying all new heavy physics effects that we can observe at low energies. However, our ultimate goal is to learn about the physics at very high energies, so as mentioned above, we need to be able to translate between the parameters (WCs) of the effective theory and those of our UV "candidate" model. This is known as the top-down approach, which complements the former one and rounds up the EFT strategy in the search for new physics. This section will be devoted to review this process of translation, called matching.

In quantum field theory, we aim to compare with observables by computing the matrix element of some process that we can measure at a certain energy. In weakly coupled UV theories, which will be our focus of study, calculations are performed in a perturbative expansion. The requirement that the effective theory naturally has to fulfill is to reproduce the amplitudes of the UV model at low energies, in which its heavy modes are not excited, up to a certain order in the loop expansion. In this section, as well as in all the calculations in this thesis, we will work up to one-loop order. Therefore, the basic idea behind matching will be to identify the effective theory with a UV theory expanded in powers of the heavy masses and somehow solve for the Wilson Coefficients.

In order to do so, one can basically follow two strategies. We will briefly introduce the functional approach to matching and then review the diagrammatic approach, which will be used in the rest of the thesis. We will use a UV theory consisting of an extension of the SM with a heavy, zero-hypercharged fermion singlet $N$ as an example to illustrate how the matching procedure works. Since $N$ is real, we can give it a Majorana mass $M$ and a Yukawa-like interaction with the SM Higgs. The Lagrangian of the theory is the following:

$$\mathcal{L}_{\text{UV}} = \mathcal{L}_{\text{SM}} + \frac{1}{2}\,\overline{N}(i\partial\!\!\!/ - M)N + \left(y_N^i\,\overline{\ell_{a,i}}\,N H_b^* \epsilon_{ab} + \text{h.c.}\right), \tag{2.44}$$

where $\epsilon = \mathrm{i}\sigma_2$ and we only consider one generation for the heavy fermion for simplicity.

### 2.5.1 Functional methods

As mentioned in Section 2.2, the matching procedure formally consists of integrating-out the heavy degrees of freedom from the path integral [34, 35]. To consider quantum effects we need to obtain the one-loop effective action $\Gamma$, for which we split the fields $\phi$ in our theory into a classical background $\widehat{\phi}$ (satisfying the equations of motion), and a quantum fluctuation:

$\phi \to \widehat{\phi} + \phi$. The effective action is then given by:

$$e^{i\Gamma[\hat{\phi}]} = \int d\phi \; e^{iS[\phi+\hat{\phi}]}. \tag{2.45}$$

We can then formally expand the Lagrangian around the background configurations:

$$\mathcal{L}[\phi+\hat{\phi}] = \mathcal{L}[\hat{\phi}] + \frac{1}{2}\,\overline{\phi}\,\frac{\delta^2\mathcal{L}}{\delta\overline{\phi}\,\delta\phi}\Big|_{\phi=\hat{\phi}}\,\phi + \mathcal{O}(\phi^3), \tag{2.46}$$

where the linear term in the expansion is not present because it is proportional to the equations of motion and higher order terms are not needed because they will not contribute at one loop. We can then expand the equations of motion of the heavy fields $\widehat{\phi}_H$ in powers of the heavy masses to express them in terms of the light fields $\widehat{\phi}_L$, and truncate at the desired order. This reproduces exactly what we wanted: an action where the heavy fields are no longer dynamic and constitutes the low energy limit of the UV theory. At leading order, the tree level EFT action is then given by:

$$\Gamma^{(0)}_{\mathrm{EFT}}[\hat{\phi}] \equiv S^{(0)}[\widehat{\phi}_L, \widehat{\phi}_H(\widehat{\phi}_L)]. \tag{2.47}$$

In our example, the equation of motion for the heavy fermion reads:

$$(i\partial\!\!\!/ - M)N = -y_N \ell^c \epsilon H^* + y_N^* H^T \epsilon \ell, \tag{2.48}$$

where gauge and flavor indices are omitted for simpliticy. Expanding in powers of $M^{-1}$:

$$N = -\frac{1}{M}(1 + \frac{i\partial\!\!\!/}{M} + ...)(-y_N \ell^c \epsilon H^* + y_N^* H^T \epsilon \ell). \tag{2.49}$$

Substituting Eq. (2.49) back in Eq. (2.44), we obtain:

$$\begin{aligned}
\mathcal{L}^{(0)}_{\mathrm{EFT}} &= \Big(-\frac{1}{2M} y_N^i y_N^j \overline{\ell}_i \epsilon H^* \ell_j^c \epsilon H^* + \mathrm{h.c}\Big) - \frac{1}{M^2} y_N^i y_N^{*j} (\overline{\ell}_i \epsilon H^*) i\partial\!\!\!/ (H^T \epsilon \ell_j) \\
&\equiv \Big(\frac{1}{2M} y_N^{*i} y_N^{*j} [\mathcal{O}_W]_{ij} + \mathrm{h.c}\Big) - \frac{1}{M^2} y_N^i y_N^{*j} [\mathcal{O}^{1,3}_{H\ell}]_{ij},
\end{aligned} \tag{2.50}$$

where $\mathcal{O}_W$ is the Weinberg operator in Eq. (2.17) and we have defined the operator $\mathcal{O}^{1,3}_{H\ell}$, that can be written as a combination of two operators in the Warsaw basis:

$$\mathcal{O}^{1,3}_{H\ell} = \frac{1}{4}[\mathcal{O}^{(3)}_{H\ell} - \mathcal{O}^{(1)}_{H\ell}]. \tag{2.51}$$

Back to the functional matching at one-loop order, It is common to define the fluctuation operator [34]:

$$\mathcal{O}_{ij} \equiv \frac{\delta^2\mathcal{L}}{\delta\overline{\phi_i}\,\delta\phi_j}\Big|_{\phi=\hat{\phi}} = \delta_{ij}\Delta^{-1}_{(i)} - X_{ij}, \tag{2.52}$$

where $\Delta_i$ is the propagator of the field $\phi_i$ and $X_{ij}$ encodes the interaction terms. At one-loop, we are left with the following integral:

$$e^{i\Gamma^{(1)}[\hat{\phi}]} = \int d\phi \, \exp\Big[i\int dx^d \, \frac{1}{2}\overline{\phi}_i \mathcal{O}_{ij}\phi_j\Big], \tag{2.53}$$

which can be done analytically since it is a Gaussian integral. The formal solution is:

$$\Gamma^{(1)} = \frac{i}{2}\,\mathrm{STr}\ln\mathcal{O} = \frac{i}{2}\,\mathrm{STr}\ln[\Delta^{-1}] + \frac{i}{2}\,\mathrm{STr}\ln[1-\Delta X], \tag{2.54}$$

where the supertrace STr is a generalization of the usual trace to accommodate fermionic and bosonic indices. However, this effective action still includes EFT loops with insertions of tree level coefficients from $\Gamma^{(0)}_{\mathrm{EFT}}$, that we do not want to include in the definition of the one-loop coefficients of the EFT action. For that reason, we will actually extract the *hard region* of the effective action:

$$S^{(1)}_{\mathrm{EFT}} \equiv \Gamma^{(1)}\big|_{\mathrm{hard}}. \tag{2.55}$$

We will see what this hard region means precisely in the next subsections. For the moment, let us anticipate that $\Delta X \sim \Lambda^{-1}$ so we can Taylor expand the second term in Eq. (2.54) up to the desired order in the mass expansion:

$$S^{(1)}_{\mathrm{EFT}} = \frac{i}{2}\,\mathrm{STr}\ln[\Delta^{-1}]\big|_{\mathrm{hard}} - \frac{i}{2}\sum_n \frac{1}{n}\,\mathrm{STr}[(\Delta X)^n]\big|_{\mathrm{hard}}. \tag{2.56}$$

There are two terms in this formula for the one-loop matching, known as log-type and power-type supertraces. The first one only depends on the number and type of heavy propagators and is therefore universal: it can be computed once and for all and only changes depending on the particle content of the UV theory. The second type depends on the interactions between heavy and light particles, and has to be computed specifically for the theory that is to be matched. There are currently two publicly available tools to compute these supertraces automatically given the $X$ interaction terms (`Supertracer` [36], `STrEAM` [37]).

The evaluation of these supertraces is based on the Covariant Derivative Expansion (CDE) method [38–40], developed in the 1980s, but these methods have only experienced a revival in the last years, specially since Ref. [41] presented some universal results and the calculation in [42] of the Universal One-Loop Effective Action (UOLEA).

The beauty of this functional matching is that we do not need any details, a priori, about the effective field theory; integration of heavy modes yields directly effective operators that are generated up to the ordered considered in the expansion. However, the ($d$-dimensional) action recovered by this procedure does not in general conform even a Green's basis, so in practice one still needs to perform a reduction either to a Green's or a physical basis to interpret the results. There are also some public codes to perform this functional matching automatically at tree level (`MatchingTools` [43]) and one loop (`CoDEx` [44], `Matchete` [45]).

### 2.5.2 Diagrammatic approach

The other equivalent way to perform matching is to impose that all scattering amplitudes (between light external states) in the EFT reproduce the result of those in the UV theory up to a certain order in the mass and loop expansion. In this diagrammatic approach one logically needs to know before-hand the basis of operators, since the processes have to be computed also in the EFT.

This equivalence between amplitudes can be enforced at two different levels. The strongest requirement is to enforce the equality at the level of generating functionals of (connected)

Green functions, i.e., equating all the off-shell Green functions of the two theories. Since we are only interested in correlation functions of light external states, we can turn off the source for the heavy fields:

$$\mathcal{W}_{\rm EFT}[J_\phi] = \mathcal{W}_{\rm UV}[J_\phi, 0], \tag{2.57}$$

where $J_\phi$ is the source for light fields. This equality has to be understood as holding up to some order in the mass expansion. Applying a Legendre transformation returns:

$$\Gamma_{\rm EFT}[\hat{\phi}] = \Gamma_{\rm UV}[\hat{\phi}, \hat{\Phi}[\hat{\phi}]]. \tag{2.58}$$

In this approach the goal is therefore to compute $\Gamma_{\rm UV}[\hat{\phi}, \hat{\Phi}[\hat{\phi}]]$, which is an effective action of one-light-particle-irreducible (1lPI) vertices. To compute this object, it is sufficient to compute all the 1lPI diagrams contributing to all the amplitudes (between light states) of the theory. This means that light fields can only run in loops and heavy bridges have to be included. The reason is that diagrams with light bridges can be recovered joining vertices from $\Gamma_{\rm UV}[\hat{\phi}, \hat{\Phi}[\hat{\phi}]]$, and heavy bridges account for external heavy particles $\hat{\Phi}[\hat{\phi}]$ fulfilling equations of motion.

Since this calculation is done in $d$ dimensions and off-shell, we have to use a Green's basis for the EFT. After solving for the Wilson Coefficients, it is convenient to reduce the results, as explained in Section 2.3, to a physical basis. These will be the approach used in the example below as well as in the rest of the matching results presented in this thesis.

The alternative is to equate all the on-shell matrix elements of the two theories. In this case, it is enough to use a physical basis of operators in the EFT, since they are, by construction, a set of all independent structures on-shell. However, one has to include all connected diagrams in the UV theory, including the ones with light bridges, since these light bridges account for the field redefinitions performed in the EFT to obtain the physical basis. This method has the advantage of a simpler calculation, because there are less operators in the EFT and on-shell kinematic configurations can be used, but the disadvantage that the number of diagrams with light bridges rapidly blows up at one loop, which makes it computationally more expensive. Moreover, non-local terms coming from light bridges have to be cancelled between the EFT and UV theory and need to be handled with care.

Let us revisit our example to illustrate its matching up to dimension six, this time both at tree level and one loop. Our convention in the following calculations will be to take all momenta incoming, and all indices identified by a numeric tag of the particle. We will adopt, once again, the conventions in Appendix A and use $v, u$ for the external spinors.

At tree level, the only processes allowed in the UV theory are the amplitudes $\langle \ell_1\, \ell_2\, H_3\, H_4 \rangle$ and $\langle \bar{\ell}_1\, \ell_2\, H_3\, H_4^* \rangle$ (omitting gauge and flavor indices). For the first one, there is only one dimension five operator, the Weinberg operator, contributing to the amplitude, so the matching is particularly simple. The diagrams contributing to the process are depicted in Figure 2.2.

The first amplitude then reads:

$$i\mathcal{M}^{\rm (EFT)}_{\ell_1\ell_2 H_3 H_4} = 2i\alpha_W (\varepsilon_{41}\varepsilon_{32} + \varepsilon_{42}\varepsilon_{31})\, \overline{v}_1 P_L u_2, \tag{2.59}$$

$$\begin{aligned} i\mathcal{M}^{\rm (UV)}_{\ell_1\ell_2 H_3 H_4} &= -\frac{i y_N^* y_N^*}{(p_1+p_3)^2 - M^2} (\varepsilon_{42}\varepsilon_{31})\, \overline{v}_1 P_L (\not{p}_1 + \not{p}_3 + M) P_L u_2 + (3 \leftrightarrow 4) \\ &= \frac{i y_N^* y_N^*}{M} (\varepsilon_{41}\varepsilon_{32} + \varepsilon_{42}\varepsilon_{31})\, \overline{v}_1 P_L u_2 + \mathcal{O}(M^{-3}), \end{aligned} \tag{2.60}$$

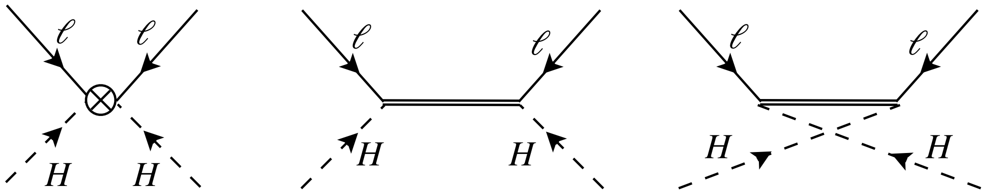


**(a)** **(b)**

**Figure 2.2:** Diagrams contributing at tree level to the process $\langle \ell\, \ell\, H\, H \rangle$ in the (a) effective theory and (b) UV theory. The double line denotes the heavy fermion $N$, that we represent without an arrow since, being a Majorana fermion, does not carry a fermion flow.

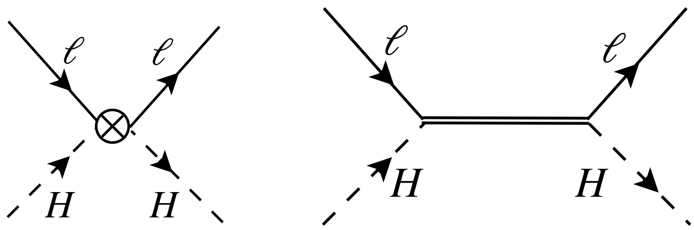


**(a)** **(b)**

**Figure 2.3:** Diagrams contributing at tree level to the process $\langle \bar{\ell}\, \ell\, H\, H^* \rangle$ in the (a) effective theory and (b) UV theory. The double line denotes the heavy fermion $N$, that we represent without an arrow since, being a Majorana fermion, does not carry a fermion flow.

where we have expanded the propagator in powers of the heavy mass $M$ in the last line. Comparing both equations, it is straight-forward to extract the value for the Wilson Coefficient imposing the matching condition $i\mathcal{M}^{(\mathrm{EFT})} = i\mathcal{M}^{(\mathrm{UV})}$:

$$[\alpha_W]_{ij} = \frac{y_N^{*i} y_N^{*j}}{2M}. \tag{2.61}$$

For the second amplitude, $\langle \bar{\ell}_1\, \ell_2\, H_3\, H_4^* \rangle$, there are several operators contributing in the EFT, collected in Table B.2. The diagrams contributing to the process, both in the EFT and the UV, are depicted in Figure 2.3. Using the simplified notation $\alpha_{1,3}$, $\beta'_{1,3}$, $\beta''_{1,3}$ for the coefficients of $\mathcal{O}_{H\ell}^{(1),(3)}$, $\mathcal{R}_{H\ell}^{\prime(1),(3)}$ and $\mathcal{R}_{H\ell}^{\prime\prime(1),(3)}$, respectively, we obtain the following expression:

$$\begin{aligned} i\mathcal{M}^{(\mathrm{EFT})}_{\bar{\ell}_1\, \ell_2\, H_3\, H_4^*} = &- i \Big( 2\bar{v}_1 \not{p}_2 P_L u_2 (\beta'_1 \delta_{12}\delta_{34} + \beta'_3 \sigma_{12}\sigma_{43}) \\ &+ \bar{v}_1 \not{p}_3 P_L u_2 (\delta_{12}\delta_{34}(\alpha_1 + \beta'_1 - i\beta''_1) + \sigma_{12}\sigma_{43}(\alpha_3 + \beta'_3 - i\beta''_3)) \\ &- \bar{v}_1 \not{p}_4 P_L u_2 (\delta_{12}\delta_{34}(\alpha_1 - \beta'_1 + i\beta''_1) + \sigma_{12}\sigma_{43}(\alpha_3 - \beta'_3 + i\beta''_3)) \,\Big) \end{aligned} \tag{2.62}$$

We can see here that the structure of the EFT amplitude at tree level, which will be a general feature, is a sum over all independent kinematic structures multiplying a combination of gauge tensors "weighted" by all the WCs that can generate that particular structure. This, by construction, is a basis of all possible kinematic and gauge structures allowed between these external fields, and the WCs have to be fixed so that they reproduce the value of each particular term in the UV theory. Therefore, equating the coefficient of each kinematic structure both in the EFT and the UV theory gives us a system of equations:

$$\begin{aligned}
&2i\,\beta_1'\,\delta_{12}\,\delta_{34} + 2i\,\beta_3'\,\sigma_{12}\,\sigma_{43} = \frac{i\,y_N\,y_N^*}{2M^2}(\delta_{12}\,\delta_{43}\ -\sigma_{12}\,\sigma_{43}) \\
&(-i\,\alpha_1 + i\,\beta_1' + \beta_1'')\delta_{12}\,\delta_{34} + (-i\,\alpha_3 + i\,\beta_3' + \beta_3'')\sigma_{12}\,\sigma_{43} = 0 \\
&(i\,\alpha_1 + i\,\beta_1' + \beta_1'')\delta_{12}\,\delta_{34} + \sigma_{12}\,\sigma_{43}(i\,\alpha_3 + i\,\beta_3' + \beta_3'') = \frac{i\,y_N\,y_N^*}{2M^2}(\delta_{12}\,\delta_{43}\ -\sigma_{12}\,\sigma_{43})
\end{aligned} \tag{2.63}$$

that we can solve to obtain the Wilson Coefficients:

$$[\alpha_1]_{ij} = -[\alpha_3]_{ij} = \frac{y_N^i y_N^{*j}}{4M^2} \tag{2.64}$$

$$[\beta_1']_{ij} = -[\beta_3']_{ij} = \frac{y_N^i y_N^{*j}}{4M^2} \tag{2.65}$$

$$[\beta_1'']_{ij} = [\beta_3'']_{ij} = 0 \tag{2.66}$$

There is a more efficient way of solving this system of equations in general. Let us denote by $K = \{K_i\}$ the set of all possible kinematic structures allowed in a certain process. The tree level amplitude in the EFT will be a sum over this set, where each element will be multiplied by some linear combination of gauge tensors $g_j$ and a sum of Wilson Coefficients $C_{ij}$. The matching condition can then be expressed as follows:

$$\sum_{ij} K_i g_j C_{ij} = \sum_{ij} K_i g_j' Y_{ij}, \tag{2.67}$$

where $g_j'$ are a set of different (in principle) gauge tensors (that can be expressed as a linear combination of $g_i$) and $Y_{ij}$ are functions of the couplings and masses in the UV theory.

Performing the matching between two theories amounts to solve this equation for particular values of $g^{(\prime)}$, $C$, $Y$ (with enough amplitudes to fix all the WCs). However, given an EFT, the left-hand side of Eq. (2.67) is determined, so we can formally solve this equation without knowing any details about the actual values of $g_i'$ and $Y_{ij}$. Matching to a particular UV theory is then just identifying $g_j' Y_{ij}$ for the relevant amplitudes and substitute their values in the solution of Eq. (2.67). This is particularly efficient for EFTs susceptible of being matched with several different UV theories, as it is the case of the SMEFT.

For concreteness, in our example we identify the gauge structures $g_1 = \delta_{12}\,\delta_{34}$ and $g_2 = \sigma_{12}\,\sigma_{43}$, which leave us with the following combination of Wilson Coefficients:

$$C = \begin{pmatrix} 2i\beta_1' & 2i\beta_3' \\ -i\,\alpha_1 + i\,\beta_1' + \beta_1'' & -i\,\alpha_3 + i\,\beta_3' + \beta_3'' \\ i\,\alpha_1 + i\,\beta_1' + \beta_1'' & i\,\alpha_3 + i\,\beta_3' + \beta_3'' \end{pmatrix}. \tag{2.68}$$

Then, for each kinematic structure $K_i$:

$$\sum_j g_j C_{ij} = \begin{pmatrix} \begin{pmatrix} C_{i1} + C_{i2} & 0 \\ 0 & C_{i1} - C_{i2} \end{pmatrix} & \begin{pmatrix} 0 & 0 \\ 2C_{i2} & 0 \end{pmatrix} \\ \begin{pmatrix} 0 & 2C_{i2} \\ 0 & 0 \end{pmatrix} & \begin{pmatrix} C_{i1} - C_{i2} & 0 \\ 0 & C_{i1} + C_{i2} \end{pmatrix} \end{pmatrix}, \tag{2.69}$$

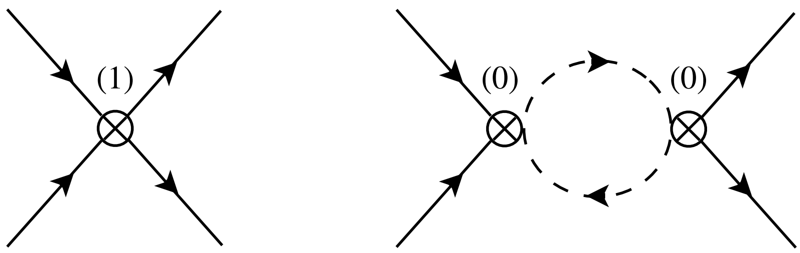

**Figure 2.4:** Diagrams contributing at one loop level to the process $\langle \bar{\ell}\,\ell\,\bar{\ell}\,\ell \rangle$ in the effective theory. The superscripts (0), (1) denote insertions of tree and one loop level operators, respectively.

so we are left with the following system of equations:

$$\begin{cases} 2i\beta_3' = \sum_j Y_{1j}[g_j']_{2112} \\ -i\,\alpha_3 + i\,\beta_3' + \beta_3'' = \sum_j Y_{2j}[g_j']_{2112} \\ i\,\alpha_3 + i\,\beta_3' + \beta_3'' = \sum_j Y_{3j}[g_j']_{2112} \\ 2i\beta_1' = C_{12} + \sum_j Y_{1j}[g_j']_{1122} \\ -i\,\alpha_1 + i\,\beta_1' + \beta_1'' = C_{22} + \sum_j Y_{2j}[g_j']_{1122} \\ i\,\alpha_1 + i\,\beta_1' + \beta_1'' = C_{32} + \sum_j Y_{3j}[g_j']_{1122} \end{cases} \tag{2.70}$$

that allows us to obtain a symbolic expression for all the Wilson Coefficients.

There is one last advantage of formulating the matching as this system of equations. We have seen in Section 2.3 how constructing a basis of operators and reducing it to an independent set in $d$ dimensions can be in general a cumbersome task. By constructing this system of equations we have a powerful cross-check at hand: if the rank of the system (with vanishing UV amplitudes) is smaller than the number of Wilson Coefficients, it means that they are not linearly independent. Moreover, solving this system can give us the relations between them, without the necessity of working out any operator relations.

### 2.5.3 One-loop matching

At one loop the idea is exactly the same, but there are many more coefficients generated. We will match the amplitude $\langle \bar{\ell}_1\,\ell_2\,\bar{\ell}_3\,\ell_4 \rangle$ as an example. With the purpose of keeping it simple, we will set to zero all couplings in the UV theory of Eq. (2.44) except for $y_N$. The diagrams contributing to this process at one-loop in the EFT and the UV theory in this approximation are depicted in Figures 2.4 and 2.5, respectively.

Before computing anything, we can apply some simplifications only by looking at the diagrams. First, the class of four-fermion operators at dimension six that contribute at tree level in Figure 2.4 does not produce matrix elements proportional to external momenta. For this reason, we can set to zero all external momenta in our ensuing calculations. We can also see that no structures with three gammas can be generated only by one propagator in each fermionic current. Therefore, the operators $\mathcal{E}_{\ell\ell}^{c[2]}$, $\mathcal{E}_{\ell\ell}^{[3]}$ and $\mathcal{E}_{\ell\ell}^{[3](3)}$ can be ignored in this particular calculation.

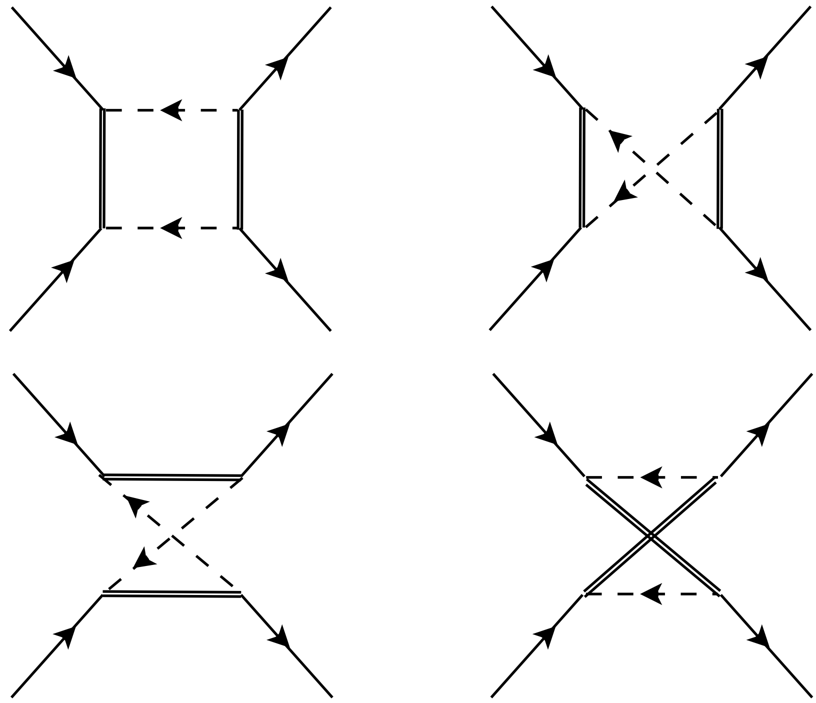

**Figure 2.5:** Diagrams contributing at one loop level to the process $\langle \bar{\ell}\,\ell\,\bar{\ell}\,\ell \rangle$ in the UV theory.

For simplicity, we will divide the amplitude in two parts: the set of diagrams proportional to (a) scalar currents $P_R \otimes P_L$ and (b) the ones proportional to vector-axial currents $\gamma^\mu P_L \otimes \gamma_\mu P_L$. The first part of the amplitude in the EFT, under the considerations mentioned above, reads:

$$\begin{aligned} i\mathcal{M}^{(\mathrm{EFT})\,(a)}_{\bar{\ell}_1\,\ell_2\,\bar{\ell}_3\,\ell_4} &= \overline{v}_1 P_R u_3\, \overline{v}_2 P_L u_4\, (\delta_{23}\delta_{14} + \delta_{34}\delta_{12})\, 2i[\gamma^c_{\ell\ell}]_{1324} \\ &\quad + 4\overline{v}_1 P_R u_3\, \overline{v}_2 P_L u_4 [\alpha_W]_{24} [\alpha^*_W]_{13}\, (\delta_{23}\delta_{14} + \delta_{34}\delta_{12})\, I_{\mathrm{EFT}}, \end{aligned} \tag{2.71}$$

whereas the same process in the UV has the following expression:

$$i\mathcal{M}^{(\mathrm{UV})\,(a)}_{\bar{\ell}_1\,\ell_2\,\bar{\ell}_3\,\ell_4} = \overline{v}_1 P_R u_3\, \overline{v}_2 P_L u_4\, (\delta_{23}\delta_{14} + \delta_{34}\delta_{12})\, y^3_N y^1_N y^{*4}_N y^{*2}_N I_{\mathrm{UV}}, \tag{2.72}$$

where we have defined the following integrals:

$$I_{\mathrm{EFT}} = \mu^{2\epsilon} \int \frac{d^d k}{(2\pi)^d} \frac{1}{(k^2 - m^2)^2} = \frac{i}{16\pi^2} \left( \frac{1}{\epsilon} - \log\left[\frac{m^2}{\mu^2}\right] \right), \tag{2.73}$$

$$\begin{aligned} I_{\mathrm{UV}} &= \mu^{2\epsilon} \int \frac{d^d k}{(2\pi)^d} \frac{M^2}{(k^2 - m^2)^2 (k^2 - M^2)^2} = \\ &= \frac{i}{16\pi^2} \frac{M^2}{(M^2 - m^2)^2} \left( -2 + \frac{M^2 + m^2}{M^2 - m^2} \log\left[\frac{M^2}{m^2}\right] \right). \end{aligned} \tag{2.74}$$

In a little abuse of notation, we will use the minimal substraction scheme ($\overline{\mathrm{MS}}$) writing the scale $\mu$ inside the logarithms instead of the $\overline{\mathrm{MS}}$ scale $\overline{\mu}^2 = 4\pi e^{-\gamma_E}\mu^2$, with $\gamma_E$ the Euler-Mascheroni constant, so that we can remove the terms proportional to $\epsilon$ (equivalently, one could send $1/\epsilon \to 1/\overline{\epsilon} \equiv 1/\epsilon + \gamma_E - \mathrm{Log}(4\pi)$ in our equations).

Substituting the value of the tree level coefficient for $\alpha_W$ in Eq. (2.61) and expanding in powers of $M^{-1}$, we obtain:

$$[\gamma^c_{\ell\ell}]_{ijkl} = -\frac{y_N^i y_N^k y_N^{*j} y_N^{*l}}{32\pi^2 M^2}\left(2 + \frac{1}{\epsilon} - \log\left[\frac{M^2}{\mu^2}\right]\right). \tag{2.75}$$

This operator does not belong to our physical basis, so we can reduce it by means of the following Fierz identity:

$$[\mathcal{E}^c_{\ell\ell}]_{ijkl} = \frac{1}{2}[\mathcal{O}]_{likj} \tag{2.76}$$

As mentioned above, this identity is only valid in four dimensions, so we are implicitly defining an evanescent operator, $E^c_{\ell\ell} \equiv [\mathcal{E}^c_{\ell\ell}]_{ijkl} - \frac{1}{2}[\mathcal{O}]_{likj}$. However, since this operator is only generated at one loop, its physical effect, only obtained when inserted in divergent loops, is at least two loops order, and can therefore be disregarded.

The second part of the amplitude has the following expression, both for the EFT and UV theories:

$$\begin{aligned} i\mathcal{M}^{\text{(EFT) (b)}}_{\bar\ell_1\,\ell_2\,\bar\ell_3\,\ell_4} =& 2i\,\bar v_1\gamma^\mu P_L u_2\,\bar v_3\gamma_\mu P_L u_4\big([\alpha_{\ell\ell}]_{1234}\delta_{12}\delta_{34} + [\gamma^{(3)}_{\ell\ell}]_{1234}\sigma_{12}\sigma_{34}\big) \qquad (2.77)\\ &+ 2i\,\bar v_1\gamma^\mu P_L u_4\,\bar v_3\gamma^\mu P_L u_2\big([\alpha_{\ell\ell}]_{1432}\delta_{14}\delta_{32} + [\gamma^{(3)}_{\ell\ell}]_{1432}\sigma_{14}\sigma_{32}\big)\\ i\mathcal{M}^{\text{(UV) (b)}}_{\bar\ell_1\,\ell_2\,\bar\ell_3\,\ell_4} =& \big(\bar v_1\gamma^\mu P_L u_2\,\bar v_3\gamma_\mu P_L u_4\;\delta_{23}\delta_{14} \qquad (2.78)\\ &+ \bar v_1\gamma^\mu P_L u_4\,\bar v_3\gamma_\mu P_L u_2\;\delta_{34}\delta_{12}\big)\; y_N^3 y_N^1 y_N^{*4} y_N^{*2}\; I^{(b)}_{\text{UV}}, \end{aligned}$$

where we have defined the integral:

$$\begin{aligned} I^{(b)}_{\text{UV}} &= \mu^{2\epsilon}\int \frac{d^dk}{(2\pi)^d}\frac{k^2/d}{(k^2-m^2)^2(k^2-M^2)^2} = \\ &= \frac{i}{64\pi^2(M^2-m^2)^3}\left(m^4 - M^4 + 2M^2m^2\log\left[\frac{M^2}{m^2}\right]\right). \end{aligned} \tag{2.79}$$

Expanding $I^{(b)}_{\text{UV}}$ in powers of $M^{-1}$ and solving the system of equations, we obtain the following values for the coefficients:

$$[\alpha_{\ell\ell}]_{ijkl} = -[\gamma^{(3)}_{\ell\ell}]_{ijkl} = -\frac{y_N^i y_N^j y_N^{*k} y_N^{*l}}{256\pi^2 M^2}. \tag{2.80}$$

Using, again, Fierz identities to reduce the result to the physical basis:

$$[\mathcal{E}^{(3)}_{\ell\ell}]_{ijkl} = 2[\mathcal{O}_{\ell\ell}]_{ilkj} - [\mathcal{O}_{\ell\ell}]_{ijkl}, \tag{2.81}$$

we obtain the final result:

$$[\alpha_{\ell\ell}]_{ijkl} = -\frac{y_N^i y_N^j y_N^{*k} y_N^{*l}}{16\pi^2 M^2}\left(\frac{5}{8} - \frac{1}{4\epsilon} + \frac{1}{4}\log\left[\frac{M^2}{\mu^2}\right]\right). \tag{2.82}$$

Finally, when matching at one loop (or more), there is one last problem to take into account. The propagator of the light fields can also receive contributions in the matching, and that would leave an effective theory with a non-canonical kinetic term. This can be avoided by performing a canonical normalization of the kinetic terms in the EFT, which consists of performing a field redefinition to get rid of the one-loop contribution to the kinetic term. Consequently, the one-loop coefficients of the operators generated at tree level experience a shift proportional to its tree-level coefficient. Taking again our example, we would have:

$$\mathcal{L}_{\text{EFT}} \supset [1+\alpha^{(1)}_{K\ell}]_{ij}\, \bar{\ell}_i\, i\not{D}\ell_j + [\alpha_W]_{ij}[\mathcal{O}_W]_{ij} + ..., \tag{2.83}$$

where the superscript $^{(1)}$ indicates that is a one-loop order correction. We can perform the field redefinition:

$$\ell \to \ell_i - \frac{1}{2}[\alpha^{(1)}_{K\ell}]_{ij}\ell_j, \tag{2.84}$$

after which we would end up with the following Lagrangian:

$$\mathcal{L}_{\text{EFT}} \supset \bar{\ell}\, i\not{D}\ell + [\widetilde{\alpha_W}]_{ij}[\mathcal{O}_W]_{ij} + \mathcal{O}(\frac{1}{(16\pi^2)^2}), \tag{2.85}$$

where the Wilson Coefficient $[\alpha_W]_{ij}$ is shifted by:

$$[\widetilde{\alpha_W}]_{ij} = [\alpha_W]_{ij} - \frac{1}{2}[\alpha^{(0)}_W]_{mj}[\alpha^{(1)}_{K\ell}]_{mi} - \frac{1}{2}[\alpha^{(0)}_W]_{im}[\alpha^{(1)}_{K\ell}]_{mj}. \tag{2.86}$$

### 2.5.4 Expansion by regions

At this point, one could wonder how efficient, or useful, could an effective field theory calculation be if we need to compute not only loop amplitudes in the EFT, but also the full UV calculation, to perform the matching. The reason why we are able to get away with it, and one of the core reasons of the usefulness of EFTs, is the idea of expansion by regions [46].

Let us take again the integral in our example:

$$\begin{aligned} I_{\text{UV}} &= \mu^{2\epsilon}\int \frac{d^dk}{(2\pi)^d}\frac{M^2}{(k^2-m^2)^2(k^2-M^2)^2} = \\ &= \frac{i}{16\pi^2 M^4}\Big[-2(2m^2+M^2) + (4m^2+M^2)\log\Big[\frac{M^2}{m^2}\Big]\Big] + \mathcal{O}(M^{-6}), \end{aligned} \tag{2.87}$$

where this time we have retained terms up to dimension eight in the expansion to better illustrate our point. The first observation is that the $I_{\text{EFT}}$ integral in Eq. (2.73) corresponds (up to factors that we left out of its definition) to the expansion of $I_{\text{UV}}$ in powers of $M^{-1}$:

$$\begin{aligned} &\mu^{2\epsilon}\int \frac{d^dk}{(2\pi)^d}\frac{M^2}{(k^2-m^2)^2(k^2-M^2)^2} \simeq \mu^{2\epsilon}\int \frac{d^dk}{(2\pi)^d}\frac{1}{(k^2-m^2)^2}\frac{1}{M^2}\Big[1+2\frac{k^2}{M^2}+...\Big] = \\ &= \frac{i}{16\pi^2M^4}\Big[2m^2 + (4m^2+M^2)\frac{1}{\epsilon} - (4m^2+M^2)\log\Big[\frac{m^2}{\mu^2}\Big]\Big] + \mathcal{O}(M^{-6}), \end{aligned} \tag{2.88}$$

with the difference that here we are retaining terms up to dimension eight. This happened by construction of the EFT; the expansion of the heavy propagator is encoded in the insertion of the Wilson Coefficients, pictorially equivalent to “shrink” the line into a point. This expansion corresponds to integrating in a *soft* region in which $k^2 \sim m^2, p^2 << M^2$.

Looking at our results, integrating and then expanding is therefore not the same as expanding an then integrating, but the commutation gives us precisely the integral of the matching condition:

$$I_M = I_{\text{UV}} - I_{\text{EFT}}. \tag{2.89}$$

The second observation is that integrating around the other scale in the integral, i.e., $k^2 \sim M^2 >> m^2, p^2$, known as the *hard* region expansion, we obtain:

$$\begin{aligned} I_{\text{UV}}^{(h)} &= \mu^{2\epsilon} \int \frac{d^d k}{(2\pi)^d} \frac{M^2}{(k^2 - M^2)^2 k^4} \left[ 1 + \frac{m^2}{k^2} + ... \right] = \\ &= \frac{i}{16\pi^2 M^4} \big[ -6m^2 - 2M^2 - (4m^2 + M^2) \frac{1}{\epsilon} + (4m^2 + M^2) \log \left[ \frac{M^2}{\mu^2} \right] \big]. \end{aligned} \tag{2.90}$$

We can check that splitting the integration in the soft and hard region and adding them up recovers the full result, not twice the result, as one could naively expect:

$$I_{\text{UV}} = I_{\text{UV}}^{(h)} + I_{\text{UV}}^{(s)}. \tag{2.91}$$

This does not only apply to this particular example, it is a general feature of dimensional regularization and does not happen with other regulators. In the case of the EFT integral:

$$\begin{aligned} I_{\text{EFT}}^{(s)} \equiv I_{\text{EFT}} &= \mu^{2\epsilon} \int \frac{d^d k}{(2\pi)^d} \frac{1}{(k^2 - m^2)^2} \frac{1}{M^2} \left[ 1 + 2\frac{k^2}{M^2} + ... \right] = \\ &= \frac{i}{16\pi^2 M^4} \left[ 2m^2 + (4m^2 + M^2) \frac{1}{\epsilon} - (4m^2 + M^2) \log \left[ \frac{m^2}{\mu^2} \right] \right], \end{aligned} \tag{2.92}$$

$$I_{\text{EFT}}^{(h)} = \mu^{2\epsilon} \int \frac{d^d k}{(2\pi)^d} \frac{1}{k^4} \left[ 1 + \frac{2m^2}{k^2} + \frac{3m^4}{k^4} + ... \right] \frac{1}{M^2} \left[ 1 + 2\frac{k^2}{M^2} + ... \right] = 0. \tag{2.93}$$

We can see that the soft part of the EFT integral is the EFT integral itself, since heavy scales had been already expanded out by definition, and the hard region has all scales expanded out and is therefore scaleless (and vanishing in dimensional regularization). Consequently, we have for the matching condition:

$$I_{\text{M}} = I_{\text{UV}} - I_{\text{EFT}} = I_{\text{UV}}^{(h)} + I_{\text{UV}}^{(s)} - I_{\text{EFT}}^{(h)} - I_{\text{EFT}}^{(s)} = I_{\text{UV}}^{(h)}. \tag{2.94}$$

Both $I_{\text{UV}}$ and $I_{\text{EFT}}$ exhibit non-analyticities in the light scales ($m$), but they drop out in the difference $I_{\text{M}}$, rendering it analytic. This allows us to compute it by expanding in the hard region, obtaining the result in Eq. (2.94). This powerful relation tells us that we can extract the one-loop matching condition only by computing the hard region of the amplitude in the UV. Equating this to the tree level amplitude in the EFT is enough to compute the Wilson Coefficients at one loop.

## 2.6 Renormalization and Running

When doing loop calculations in quantum field theory, one often finds divergent integrals. In order to make sense of the calculation, and be able to compare with observables, one needs to use a regularization and renormalization procedure. This leads to physical effects such as the running of couplings constants of the theory. In this section we will review the process of renormalization in the context of effective field theories.

But before talking about renormalization, let us see how divergences appear in a loop calculation. A generic loop integral in the EFT, that could possibly have a non-polynomial dependence on external momenta $p$, could look like:

$$I(p) = \int \frac{d^4k}{(2\pi)^4} \frac{1}{(k+p)^2} \sim \int_0^\infty dk \frac{k^3}{k^2 + p^2 + 2c\, k.p} \tag{2.95}$$

This is a divergent integral, with superficial degree of divergence +2. We can take as many derivatives with respect to $p$ as necessary to reduce its degree of divergence until the integral is convergent. In this case it is enough with taking three derivatives:

$$I'''(p) = \frac{2 - 8c^2}{p} \tag{2.96}$$

Integrating then thrice in $p$, we have:

$$I(p) = \frac{1}{2} p \left( p \left( A_1 + 12c^2 - 3 \right) + 2A_2 + \left( 2 - 8c^2 \right) p \log(p) \right) + A_3, \tag{2.97}$$

with unknown integration constants $A_{1,2,3}$. Since the original integral was divergent, the divergences can only be in the integration constants, and therefore be a polynomial in external momenta. Consequently, after subdivergences have been substracted, we can absorb all the divergences in the Wilson Coefficients of local operators in our EFT.

Effective field theories are however often called non-renormalizable, because all divergences in the theory cannot be removed by a finite set of counterterms. Although this is in fact the case, as long as we work at a fixed order in the mass expansion we can remove divergences order by order so that the ones still present are formally subleading.

The key idea of renormalization is that objects in the Lagrangian are not observables, so they can formally be infinite. It is only after following a prescription to remove the infinite part that we can compare with experiment and fix the value of the (renormalized) parameters of the theory. We will follow dimensional regularization, for which we extend the action to a $d$-dimensional object, and $\overline{\text{MS}}$ prescription, in which we only eliminate the $1/\bar{\epsilon}$ UV divergences. The bare (original) fields ($\phi^{(0)}$) and WCs ($\alpha^{(0)}$) in the Lagrangian can be written in terms of the renormalized ones as:

$$\alpha_i^{(0)} = \mu^{n_i \epsilon} Z_i \alpha_i, \qquad \phi^{(0)} = \sqrt{Z_\phi} \phi, \tag{2.98}$$

where $\mu$ is a parameter with dimensions of mass that we introduce to parametrize the deviation from four dimensions, and $n_i$ is called the classical anomalous dimension of the operator $\mathcal{O}_i$.

The divergences of the theory can be absorbed in the Wilson Coefficients of the operators:

$$\hat{\mathcal{L}}_{\text{EFT}} = \hat{\alpha}_i \mathcal{O}_i, \tag{2.99}$$

and have to be canceled by the counterterms introduced in Eq. (2.98). Writing, at one loop:

$$Z_i = 1 + \frac{K_i}{\epsilon}, \tag{2.100}$$

and performing canonical normalization in Eq. (2.99), we end up with the condition:

$$K_i = -\frac{\hat{\alpha}_i}{\alpha_i}. \tag{2.101}$$

The original Lagrangian did not depend on the $\mu$ parameter, that we introduced artificially and has to be fixed to some value, so this implies a dependence of the renormalized Wilson Coefficients $\alpha_i$ on the value of this parameter. This dependence is encoded in the Renormalization Group Equation (RGE) of each Wilson Coefficient, that can be derived using the fact that $\alpha_i^{(0)}$ has to be $\mu$-independent. Defining:

$$\dot{X} \equiv \frac{dX}{d\log\mu}, \tag{2.102}$$

we can take this derivative in Eq. (2.98) to write:

$$0 = n_i\epsilon\mu^{n_i\epsilon} Z_i\alpha_i + \mu^{n_i\epsilon}\dot{Z}_i\alpha_i + \mu^{n_i\epsilon}Z_i\dot{\alpha}_i, \tag{2.103}$$

and we obtain:

$$\beta_i \equiv \dot{\alpha}_i = -n_i\epsilon\alpha_i - \frac{1}{\epsilon}\dot{K}_i\alpha_i, \tag{2.104}$$

that gives us the beta function for the Wilson Coefficient $\alpha_i$. Using this equation at tree level, we can derive the following expression for the one-loop beta function:

$$\dot{\alpha}_i^{(1)} = \alpha_i^{(0)} \sum_j \frac{\partial K_i}{\partial \alpha_j} n_j \alpha_j^{(0)}. \tag{2.105}$$

Coming back to our example, we can illustrate how the divergences of the amplitude $\langle \bar{\ell}_1\, \ell_2\, \bar{\ell}_3\, \ell_4\rangle$ are removed. Since we already computed the divergent part of the amplitude in $I_{\text{EFT}}$, we just have to match it to (minus) the tree level amplitude, i.e., the first line in Eq. (2.71). Directly in the physical basis, we obtain:

$$[\hat{\alpha_{\ell\ell}}]_{ijkl} = -\frac{[\alpha_W]_{jl}[\alpha_W^*]_{ik}}{16\pi^2\epsilon}, \tag{2.106}$$

and therefore:

$$\begin{aligned} \dot{\alpha}_{\ell\ell}^{(1)} &= -\frac{\alpha_{\ell\ell}}{16\pi^2}\left[\frac{\partial K_{\ell\ell}}{\partial \alpha_W} n_w\alpha_W + \frac{\partial K_{\ell\ell}}{\partial \alpha_W^*} n_w\alpha_W^* + \frac{\partial K_{\ell\ell}}{\partial \alpha_{\ell\ell}} n_{\ell\ell}\alpha_{\ell\ell}\right] = \\ &= -2\frac{\alpha_{\ell\ell}}{16\pi^2}\left[\frac{\alpha_W\alpha_W^*}{\alpha_{\ell\ell}} + \frac{\alpha_W\alpha_W^*}{\alpha_{\ell\ell}} - \frac{\alpha_W\alpha_W^*}{\alpha_{\ell\ell}^2}\alpha_{\ell\ell}\right] = \\ &= -\frac{\alpha_W\alpha_W^*}{8\pi^2} \end{aligned} \tag{2.107}$$

Equation (2.105) can be further simplified by considering the following[2]. The classical anomalous dimension for the coefficient $\alpha_i$ can be written as:

$$n_i\epsilon = [\mathcal{O}_i]^{(4)} - [\mathcal{O}_i]^{(d)} - 2\epsilon. \tag{2.108}$$

[2]We thank Renato Fonseca for this derivation.

We denote by $[X]^{(y)}$ the mass dimension of $X$ in $y$ dimensions. The difference $[\mathcal{O}_i]^{(4)} - [\mathcal{O}_i]^{(d)}$, proportional to $\epsilon$, will be the sum of the deviations from four dimensions for each of the fields, $\sum_j([\phi_j]^{(4)} - [\phi_j]^{(d)})$. This deviation is, however, universal for all type of fields, since it is dictated by the quadratic Lagrangian and we will extract the $\mathcal{O}(\epsilon)$ part, so it behaves like $[\phi_j]^{(d)} \sim \frac{d}{2} \sim -\epsilon$. Consequently, we can write:

$$n_i = N_i - 2, \tag{2.109}$$

with $N_i$ the number of fields in $\mathcal{O}_i$. On the other hand, in our diagrammatic approach, the divergent coefficients $\hat{\alpha_i}$ can be seen as originated by a sum of diagrams:

$$\hat{\alpha_i} = \sum_{\text{diagrams } \mathcal{D}} \hat{\alpha_i}^{(\mathcal{D})}. \tag{2.110}$$

Therefore, we have:

$$\begin{aligned} \dot{\alpha}_i^{(1)} &= \alpha_i^{(0)} \sum_j \frac{\partial K_i}{\partial \alpha_j} n_j \alpha_j^{(0)} = n_i \hat{\alpha}_i - \sum_j \frac{\partial \hat{\alpha}_i}{\partial \alpha_j} n_j \alpha_j = \\ &= \sum_{\substack{\text{diagrams} \\ \mathcal{D}}} \Big( n_i - \sum_j n_j \alpha_j \frac{\partial}{\partial \alpha_j} \Big) \hat{\alpha}_i^{(\mathcal{D})} = \sum_{\substack{\text{diagrams} \\ \mathcal{D}}} \Big( (N_i - 2) - \sum_{\substack{\text{vertices} \\ v \in \mathcal{D}}} (N_v - 2) \Big) \hat{\alpha}_i^{(\mathcal{D})} \end{aligned} \tag{2.111}$$

However, taking into account the topological relation between the number of legs $N$ of a a diagram, the number of loops $L$ and the number $V_k$ of vertices of $k$ legs:

$$N + 2L - 2 = \sum_k (k-2) V_k \equiv \sum_v (N_v - 2), \tag{2.112}$$

we see that it is equivalent to sum the number of legs of each vertex over the vertices of the diagram. Substituting this relation at one loop, we get:

$$\dot{\alpha}_i^{(1)} = \sum_{\substack{\text{diagrams} \\ \mathcal{D}}} \Big( (N_i - 2) - (N_i + 2L - 2) \Big) \hat{\alpha}_i^{(\mathcal{D})} = -2 \sum_{\substack{\text{diagrams} \\ \mathcal{D}}} \hat{\alpha}_i^{(\mathcal{D})} = -2\hat{\alpha}_i. \tag{2.113}$$

In fact, we can check that we would have obtained directly the result in Eq. (2.107) by taking the divergent part in Eq. (2.82).

The renormalization group evolution of couplings has remarkable physical consequences. First, the value of one coupling fixed by experiment at a certain energy will differ from its value at a different energy. This "running" of couplings can be computed integrating the renormalization group equation. In our example:

$$\int_{\mu_L}^{\mu_H} d\alpha_{\ell\ell} = -\int_{\mu_L}^{\mu_H} d\log\mu \, \frac{\alpha_W \alpha_W^*}{8\pi^2}. \tag{2.114}$$

Under the approximation that $\alpha_W$ does not run (is $\mu$-independent), we obtain:

$$\alpha_{\ell\ell}(\mu_L) = \alpha_{\ell\ell}(\mu_H) + \frac{\alpha_W \alpha_W^*}{8\pi^2} \log\left(\frac{\mu_H}{\mu_L}\right). \tag{2.115}$$

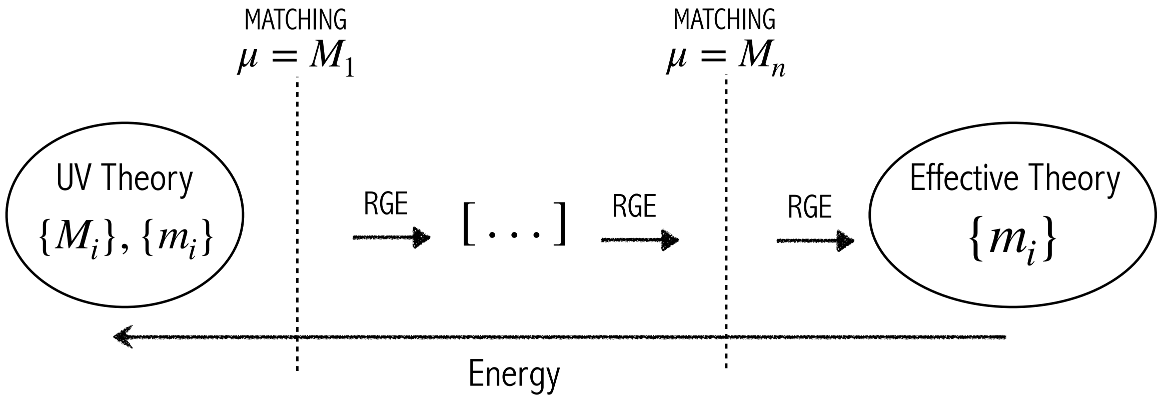


**Figure 2.6:** An outline for a complete EFT calculation. The original theory should be iteratively integrated-out and run down for each energy threshold, until the low energy scale in which experiments are performed is reached.

We can see how the value of $\alpha_{\ell\ell}$ differs between the two scales $\mu_{H,L}$. Moreover, this result also illustrates what is called *operator mixing*; even if our theory defined at a high scale $\mu_H$ has a vanishing coefficient $\alpha_{\ell\ell}$, it will be inevitably generated at low energies by the presence of $\alpha_W$.

Given that we perform experiments at low energies and want to probe, generically, physics at much higher scales, we need to run our coefficients down to the appropriate scale using RGEs. This, in turn, helps improve the convergence of the perturbative expansion in our calculations, since the RGE solution "resums" the large logarithms originated by the hierarchy of scales and we effectively work in a double expansion in $\alpha$ and $\alpha \log(\mu_H/\mu_L)$.

## 2.7 The streamlining of an EFT calculation

In this chapter, we reviewed the formalism of effective field theories, putting examples directly in the context of SMEFT. We used a toy version of a phenomenologically relevant model to illustrate isolatedly all the ingredients of a real calculation. However, the EFT recipe involves putting all those ingredients together in a (generically) multiscale problem. Thus, in a realistic scenario, comparing the predictions of a model with experiments can be much more complicated.

Let us suppose a UV theory with a set of heavy states, $\{M_i\}$, and light states, $\{m_i\}$, defined at the highest scale $M_1$. Let us also assume a separation of scales $M_i >> m_i$, making the situation suitable for the use of an effective field theory description. The procedure would be to match the UV theory to the EFT that is left when the heaviest state is integrated-out, run the Wilson Coefficients down to the next scale, $M_2$, and repeat for each energy threshold. Matching and running at each step have to be consistently performed at the same order in the mass and loop expansion to make sense of the final result. After $n$ iterations, we are left with an EFT where all heavy states are integrated out, and we finally need to run the coefficients down to the low energy scale in which our experiments are performed. Moreover, in the case of a hierarchy between the light masses, this process should be repeated to resum large logarithms. This process is depicted schematically in Figure 2.6.

The final result is an expression for your low energy observables in terms of the parameters (WCs) of the theory defined at a high scale. Examples of this type of calculation can be found in [47–49].

As mentioned in previous sections, in the bottom-up approach, calculations have to be done just once (at each order in the double expansion). There are many public tools to perform fits to the experimental data in the context of SMEFT [50–53], define or compute observables [54] or construct likelihood functions for the Wilson Coefficients [55].

In the top-down side of the story, we are intrinsically limited by the dependence on a UV model, and we just outlined how the process involves several steps. There are, however, some tasks that can also be done once and for all, and in which there have been significant advances in the last few years. For instance, starting by the basis construction, we have physical bases at several dimensions for SMEFT [27, 56–59], LEFT [60] and even $\nu$SMEFT/$\nu$LEFT [17]. Moreover, there are some automatic tools to generate physical operator bases compatible with a generic gauge symmetry [61, 62]. There are also Green's bases for SMEFT at dimension six [63, 64] and eight [65, 66].

Renormalization group equations at one loop are also known for LEFT [67] at dimension six and SMEFT at dimensions six [68–70] and eight (partially) [71, 72]. There are also some codes automatizing the running of Wilson Coefficients [73, 74]. Finally, the matching between SMEFT and LEFT is known up to one loop [75, 76].

And still, despite this significant effort described above, we are a one-loop matching away from comparing any possible model we could be interested in with experimental data. This process is not straightforward and completely model-dependent, so it has to be done on a case by case basis. Clearly, this task calls for automation. The next chapter is devoted to introducing `Matchmakereft`, an automatic tool designed to precisely fill this gap in the streamlining of an EFT calculation.

# 3

# Automatic one-loop matching: Matchmakereft

In Chapter 2, we motivated the use of Effective Field Theories as an efficient tool to compare experimental data with theoretical predictions. Splitting the problem in two independent steps allowed us to parametrize the effects of new physics in a model-independent way, in the bottom-up approach, to then sacrifice it in favor of model-discrimination through the top-down approach. This involved a complicated multiscale problem that, for searches of physics beyond the SM, is partially computed or automated (see Section 2.7). Thus, the only missing step towards a fully automated calculation of the phenomenological implications of new physics models is the calculation of the matching between arbitrary theories.

In this chapter, we introduce `matchmakereft`, a fully automated tool to perform tree-level and one-loop matching of arbitrary UV models onto arbitrary EFTs. `Matchmakereft` uses a diagrammatic approach to tree-level and one-loop matching, performed in the Background Field Method (BFM) when gauge theories are involved. The matching is done off-shell which, together with gauge invariance, provides a significant redundancy that results in a number of non-trivial cross-checks of the calculation. It has been designed with efficiency, generality and flexibility in mind, what allows a number of applications beyond the direct matching of UV models to EFTs. Current applications include the renormalization of arbitrary (effective) theories, the calculation of the RGEs of arbitrary (effective) theories, EFT basis translation and checks of (off-shell) linear independence of operators. All these calculations are done in a fully automated way.

This chapter is organised as follows. In Section 3.1, we describe how the tree-level and one-loop matching is performed in `matchmakereft`. Model creation in `matchmakereft` is explained in detail in Section 3.2. Section 3.3 compiles all the different commands available, and common pitfalls when using `matchmakereft` are described in Section 3.4. Some physical applications are given in Section 3.5, together with a minimal but complete example of the capabilities of `matchmakereft` in Section 3.6, and we conclude and provide some outlook in Section 3.7.

## 3.1 Matchmakereft in a nutshell

### 3.1.1 Types of models

The central objects in Matchmakereft are models, wich are classified according to two criteria. According to their field content they can be *light models*, if only light (but not necessarily massless) particles are present in the spectrum, or *heavy models*, when the spectrum includes at least one heavy particle. Depending on their role in the process of matching we also distinguish between *UV models*, which can be light or heavy under the former classification, and *EFTs*, which are necessarily light models. Models in matchmakereft are created using FeynRules [77], as described in detail in Section 3.2.

Matchmakereft performs the matching off-shell, in the BFM when gauge theories are involved, of a UV model onto an EFT. As explained in Chapter 2, this can be achieved by computing, in dimensional regularization in $d = 4 - 2\epsilon$ space-time dimensions, the hard region contribution to the one-light-particle-irreducible relevant amplitudes at tree and one-loop level in the UV theory and equating it to the tree level contribution in the EFT. In matchmakereft, we keep explicitly the $1/\bar{\epsilon}$ terms to allow for the automatic incorporation of evanescent operators and also to provide further information but, of course, the user should remove the $1/\bar{\epsilon}$ (denoted invepsilonbar in matchmakereft) terms explicitly from the renormalized Wilson coefficients in the physical basis. The list of amplitudes (only between external light particles) that are computed are fixed in an automated way by matchmakereft, but the user has flexibility on modifying it. All the relevant diagrams that contribute to the matching, both in the UV model and the EFT, are then automatically computed by QGRAF [78] and subsequently dressed by matchmakereft using the Feynman rules computed by FeynRules during the creation of the model.

### 3.1.2 Calculation of amplitudes

Matchmakereft can run in two different modes called RGEmaker and Matching modes, respectively. In RGEmaker mode, which is used to compute the RGEs of an arbitrary theory, the (light) UV model contains no heavy particles and matchmakereft computes the UV-divergent contribution of the corresponding one-particle-irreducible amplitudes necessary to absorb the divergences. In Matching mode, there are heavy particles in the spectrum and both the finite and divergent (both UV and IR) hard-region contributions to the corresponding one-light-particle-irreducible amplitudes are computed. The calculation of the hard region part of the amplitudes is performed using FORM [79] and proceeds as follows:

- **Hard region expansion**. As we saw in Section 2.5, the hard contribution is given by the expansion of the loop integrand in a region in which $k^2 \sim M^2 \gg p^2 \sim m^2$ where $k$ represents the loop momentum, $M$ a heavy mass, $p$ any of the external momenta and $m$

a light mass. This is achieved by iterating the following identities:

$$\begin{aligned}\frac{1}{(k+p)^2-M^2} &= \frac{1}{k^2-M^2}\left[1-\frac{p^2+2k\cdot p}{(k+p)^2-M^2}\right],\\ \frac{1}{(k+p)^2-m^2} &= \frac{1}{k^2}\left[1-\frac{p^2+2k\cdot p-m^2}{(k+p)^2-m^2}\right].\end{aligned} \tag{3.1}$$

These identities are iteratively applied to the amplitude until the power of light (IR) scales (external momenta or light masses) matches the maximum dimension of momenta produced by the operators appearing in the EFT, which is also automatically computed.

- **Tensor reduction**. This consists of applying the following identities:

$$k^{\mu_1}k^{\mu_2} = g^{\mu_1\mu_2}\frac{k^2}{d}, \tag{3.2}$$

$$k^{\mu_1}k^{\mu_2}k^{\mu_3}k^{\mu_4} = g^{\mu_1\mu_2\mu_3\mu_4}\frac{k^4}{d^2+2d}, \tag{3.3}$$

$$k^{\mu_1}\dots k^{\mu_6} = g^{\mu_1\cdots\mu_6}\frac{k^6}{d^3+6d^2+8d}, \tag{3.4}$$

$$k^{\mu_1}\dots k^{\mu_8} = g^{\mu_1\cdots\mu_8}\frac{k^8}{d^4+12d^3+44d^2+48d},\cdots \tag{3.5}$$

where $g^{\mu_1\cdots\mu_n}$ is the totally symmetric combination of metric tensors.

- **Dirac algebra**. Once the expression has been reduced to scalar integrals we proceed to perform the corresponding Dirac algebra. Since we are using dimensional regularization, this is done in $d$ dimensions in `Matching` mode. In `RGEmaker` mode, however, we are interested in extracting the divergences, so we can use the four-dimensional algebra (the difference will be finite or $\mathcal{O}(\epsilon)$). Version `1.1.0` of `matchmakereft` uses an anticommuting $\gamma^5$ prescription as discussed in Section 3.1.4. Our treatment of fermion number violating interactions follows the rules proposed in Ref. [80, 81].

- **Partial fractioning**. We use the following identity to separate propagators with different masses:

$$\frac{1}{(k^2-m_1^2)(k^2-m_2^2)} = \frac{1}{m_1^2-m_2^2}\left[\frac{1}{k^2-m_1^2}-\frac{1}{k^2-m_2^2}\right]. \tag{3.6}$$

This holds for light or heavy masses and one of them can be vanishing.

- **Reduction to tadpoles**. After partial fractioning, scaleless integrals are set to zero. In `RGEmaker` mode, however, the UV poles determine the anomalous dimensions and therefore they have to be kept by using:

$$\int \frac{d^dk}{(2\pi)^d}\frac{1}{k^4} = \frac{\mathrm{i}}{(4\pi)^2}\frac{1}{\epsilon}+\dots, \tag{3.7}$$

before setting the remaining scaleless integrals to zero. In `Matching` mode the following identity (that can be derived using integration by parts) is used to reduce the massive integrals (which are the only ones that can appear due to the hard-region expansion) to tadpoles:

$$\frac{1}{(k^2-m^2)^{n+1}} = \frac{d-2n}{2nm^2}\frac{1}{(k^2-m^2)^n}. \tag{3.8}$$

At this point we are only left with tadpole integrals:

$$a_0(m) = \int \frac{d^dk}{(2\pi)^d}\frac{1}{k^2-m^2} = \mathrm{i}\frac{m^2}{16\pi^2}\left[\frac{1}{\bar{\epsilon}} + 1 - \mathrm{Log}\left(\frac{m^2}{\mu^2}\right)\right] + \mathcal{O}(\epsilon), \tag{3.9}$$

where:

$$\frac{1}{\bar{\epsilon}} \equiv \frac{1}{\epsilon} + \gamma_E - \log(4\pi), \tag{3.10}$$

with $\gamma_E \approx 0.5772$ the Euler-Mascheroni constant.

### 3.1.3 EFT operator bases

In `matchmakereft`, no four-dimensional properties are used when running in `Matching` mode, with the purpose of ensuring maximum generality. This implies, in particular, that no Fierz relations or reduction of products of three or more gamma matrices are performed during the matching procedure. Therefore, all evanescent structures have to be explicitly defined as part of the Green basis to ensure a correct matching. These operators are then reduced to the physical basis by means of the redundancies of the EFT model (that have to be provided by the user). Moreover, the evanescent structures generated at tree level during this reduction, as explained in Section 2.4, have to be compensated by a shift of the coefficients in the physical basis given by their loop insertions in the EFT. `Matchmakereft` does not currently support this calculation in general but we include the shifts in the Warsaw basis as computed in [33]. We plan, however, to automatize this calculation in the future (see Section 3.7).

As an example, we provide the user with the complete Green's basis for the SMEFT at dimension 6 of Appendix B, that extends the basis of [63] with the operators that generate evanescent structures, as needed for the matching with `matchmakereft` of general theories with renormalizable couplings. Non-renormalizable theories can be matched also with `matchmakereft` but an extension of the basis with a larger number of gamma matrices in four-fermion operators would be needed. Similarly, if bosonic evanescent operators appear in the process of matching a specific UV model they would have to be included in the EFT basis.

### 3.1.4 Dealing with $\gamma_5$

It is well known that using dimensional regularization in chiral theories can lead to inconsistent results, due to $\gamma_5$ being a strictly four-dimensional object. In particular, traces of $\gamma_5$ and six or more gammas are ambiguous, in the sense that ciclycity of the trace is lost and different starting points would lead to different results at $\mathcal{O}(\epsilon)$. One approach to the problem is to give up the (anti)commutation relations of $\gamma_5$, which allows to have a consistent definition of $\gamma_5$ and recover ciclycity, in the so-called Breitenlohner-Maison/t'Hooft-Veltman (BMHV) scheme [82]. However, besides being computationally more involved, gauge invariance is broken and has to be recovered by the addition of some local counterterms [83, 84].

The other approach, called Naive Dimensional Regularization (NDR), consists of using a anti-commuting $\gamma_5$ at the cost of introducing finite ambiguous terms whenever one of the aforementioned traces rises in a divergent diagram. This is a problem, in particular, for the matching of extensions of the SM into the SMEFT, since these kind of traces can appear already at dimension six when computing amplitudes for the operators in classes $X^3, X^2H^2$.

Limiting ourselves, at first, to the matching or renormalizable UV models to the SMEFT at one loop, the problematic cases are, in practice, only a few. First, in order to have a trace at one loop, the diagram cannot have external fermions.x Moreover, the ambiguity is proportional to the fully antisymmetric $\epsilon_{\mu\nu\rho\sigma}$ tensor, so it can only contribute to one of the few CP violating bosonic operators of the SMEFT, with two or three field strength tensors. Therefore, we need two or three external gauge bosons. In order to have a trace with at least 6 $\gamma$-matrices there have to be four or three fermionic propagators, respectively. Consequently, we only need to worry about boxes contributing to $H^\dagger H X_{\mu\nu}\tilde{X}^{\mu\nu}$ type operators or triangles contributing to $X^\mu_\nu X^\nu_\rho \tilde{X}^\mu_\rho$. Triangle diagrams contributing to $X^\mu_\nu X^\nu_\rho \tilde{X}^\mu_\rho$, with heavy fermions running in the loop, are however non-ambiguous, because there are no $\gamma_5$'s involved in the vertices; all heavy fermions have to be vector-like. Triangle diagrams with only light particles are ambiguous, but they do not contribute to the matching. These ambiguities are fixed by the anomaly cancellation mechanism that we assume any EFT has built in.

Next, let us consider the box diagrams contributing to $H^\dagger H X_{\mu\nu}\tilde{X}^{\mu\nu}$. There are four internal fermionic propagators, of which at least one has to correspond to a heavy particle in the UV model. As mentioned above, these traces have ambiguous and non-ambiguous parts. The unambiguous part can be computed in any $\gamma_5$-scheme. The ambiguous part is proportional to $d-4$ and therefore only contributes if it multiplies the singularity of the integral. These singularities can be of two types: UV singularities emerging from the UV structure of the full theory, and IR (spurious) singularities that are generated by the hard region expansion. The latter coincide with the UV singularities of the EFT, as the soft region of the UV amplitude is, by definition, the EFT amplitude. Moreover, since we are assuming a renormalizable UV theory, the maximum possible number of $\gamma$-matrices in these diagrams is six, which means that the terms in the numerator of such integrals with mass insertions have a lower number of $\gamma$'s and are therefore unambiguous.

These box integrals have generically the following structure, ignoring couplings and group theory factors:

$$I^{\mu\nu} \sim \int_k T_{\mu_1\ldots\mu_4\mu\nu} \prod_{i=1}^{4} \frac{(k+q_i)^{\mu_i}}{(k+q_i)^2 - m_i^2}, \tag{3.11}$$

where $\int_k \equiv \int \frac{d^dk}{(2\pi)^d}$, and $T_{\mu_1\ldots\mu_4\mu\nu}$ denotes a trace with an odd number of $\gamma_5$ insertions and six $\gamma$'s, e.g.:

$$\mathrm{Tr}[\gamma_{\mu_1}\gamma_5\gamma_{\mu_2}\gamma_\mu\gamma_{\mu_3}\gamma_5\gamma_\nu\gamma_{\mu_4}\gamma_5]. \tag{3.12}$$

Expanding in the hard region expansion and performing tensor reduction we get:

$$
\begin{aligned}
I^{\mu\nu} \sim &\int_k T_{\mu_1\ldots\mu_4\mu\nu}\frac{1}{\prod_{i=1}^4(k^2-m_i^2)} \\
&\left(k^4\frac{g^{\mu_1\mu_2\mu_3\mu_4}}{d(d+2)}(1+\sum_i\frac{q_i^2}{k^2-m_i^2})+k^6\frac{g^{\mu_1\mu_2\mu_3\mu_4\rho\sigma}}{d(d+2)(d+4)}\sum_{i\leq j}\frac{4q_i^\rho q_j^\sigma}{(k^2-m_i^2)(k^2-m_j^2)}\right. \\
&\left.-2k^4\sum_{i,m}q_i^{\mu_i}q_m^\rho\frac{g^{\{\hat{\mu}_i\}\rho}}{d(d+2)}\frac{1}{k^2-m_m^2}+\sum_{i<j}k^2\frac{g^{\{\hat{\mu}_i,\hat{\mu}_j\}}}{d}q^{\mu_i}q^{\mu_j}\right) \\
\sim &\int_k T_{\mu_1\ldots\mu_4\mu\nu}\frac{g^{\mu_1\mu_2\mu_3\mu_4}}{d(d+2)}\frac{k^4}{\prod_{i=1}^4(k^2-m_i^2)}+\int_k T_{\mu_1\ldots\mu_4\mu\nu}\frac{k^2}{\prod_{i=1}^4(k^2-m_i^2)}\frac{1}{d(d+2)} \\
&\left(g^{\mu_1\mu_2\mu_3\mu_4}\sum_i q_i^2\left(1+\frac{m_i^2}{k^2-m_i^2}\right)+\frac{g^{\mu_1\mu_2\mu_3\mu_4\rho\sigma}}{(d+4)}\sum_{i\leq j}4q_i^\rho q_j^\sigma\prod_{l=i,j}\left(1+\frac{m_l^2}{(k^2-m_l^2)}\right)\right. \\
&\left.-2\sum_{i,m}q_i^{\mu_i}q_m^\rho g^{\{\hat{\mu}_i\}\rho}\left(1+\frac{m_m^2}{k^2-m_m^2}\right)+\sum_{i<j}(d+2)g^{\{\hat{\mu}_i,\hat{\mu}_j\}}q^{\mu_i}q^{\mu_j}\right),
\end{aligned}
\tag{3.13}
$$

where $\{\hat{\mu}_i\}=\mu_j\mu_k\mu_r$ with $j,k,r\neq i$, and $\{\hat{\mu}_i\hat{\mu}_j\}=\mu_k\mu_r$ with $k,r\neq i,j$.

The first term, of $\mathcal{O}(q^0)$, is UV divergent. However, it does not lead to ambiguities, since $g^{\mu_1\mu_2\mu_3\mu_4}$ makes the $\gamma_5$-dependent part of the trace vanish. The rest of the terms, of order $\mathcal{O}(q^2)$, are UV finite, but they could be IR singular depending on the number of heavy propagators. For two, three or four heavy propagators, there is no singularity, but for just one heavy propagator (and three light ones) we do have an IR singularity.

Therefore, we conclude that ambiguous contributions from $\gamma_5$-odd traces in box integrals can only be present in diagrams with one heavy and three light propagators. They appear as a product of the ambiguous $(d-4)$ coefficient of the trace multiplying a $1/\epsilon$ IR divergence resulting from the hard region expansion. Notice that, since these divergences correspond to the UV poles of the EFT, this ambiguous contribution will cancel during one-loop calculations in the EFT as long as the same reading point for the trace is used in the UV and the EFT. We would like however to remain within the naive anti-commuting $\gamma_5$ scheme, without fixing a reading point, when computing traces in `matchmakereft`. To this end, we would like to fix the ambiguous contributions of the $\gamma_5$-odd traces in box integrals with one heavy massive fermion a posteriori. Considering that the Wilson Coefficient we are trying to match must be real (all operators of the type $H^\dagger H X_{\mu\nu}\tilde{X}^{\mu\nu}$ are hermitian), any contribution from $\gamma_5$-odd traces, being imaginary, must be multiplied by a purely imaginary product of couplings of the full theory. But, in the case that leads to ambiguities, namely when the UV theory has Yukawa-like terms between the Higgs doublet, one heavy and one SM fermion, the corresponding Yukawa couplings in the amplitude are complex conjugates of each other, by virtue of the hermiticity of the UV Lagrangian. Consequently, the product of all couplings is real and, therefore, the $\gamma_5$-odd contributions are purely imaginary. They can be set to zero by hand, at the end of the computation. Note that this does not imply that the ambiguous contributions are zero: it is the sum of ambiguous and non-ambiguous traces that are set to zero.

This procedure also works if the effective theory is not the SMEFT. In such cases, more than one scalar field might be present, allowing for non-hermitian operators of the type $\phi_1^\dagger\phi_2 X_{\mu\nu}\tilde{X}^{\mu\nu}$. The constraint that the corresponding Wilson coefficient is real does not apply anymore, but in this case the Wilson Coefficient of this operator should equal the complex conjugate of the Wilson Coefficient of the hermitian conjugate operator $\phi_2^\dagger \phi_1 X_{\mu\nu} \tilde{X}^{\mu\nu}$. This is, again, enough to remove the ambiguities.

This ambiguity problem also appears when, following the prescription in [33], one computes EFT loops of evanescent operators in order to trade them for shifts of the physical basis coefficients. In this same work it is shown that it is consistent to apply NDR in this calculation as long as the same reading point is fixed for problematic traces in amplitudes of evanescent operators and one-loop amplitudes in the EFT. We adopt their convention and express our results, when there is a shift of the Warsaw basis coefficient, in terms of a reading point parameter `xRP`.

### 3.1.5 Matching results

After the calculation of the amplitudes, each output is written in two files, factorizing the gauge structure from the kinematic structures. Then, we match the tree level EFT amplitude to an arbitrary UV amplitude, solving for the Wilson Coefficients in terms of generic coefficients, as it was explained in Section 2.5. This process is performed the first time an EFT model is matched and the result is stored internally. Next, these generic coefficients are replaced by their specific values obtained from the tree and one-loop amplitudes of the UV model. This yields the first set of results provided by `matchmakereft`, the Wilson Coefficients of the Green's basis at tree level and one loop. Then we perform a canonical normalization of this basis, which conforms the second set of results. Finally, the matching is reduced to a physical basis as defined by the user (see Section 3.3 for details). Results at all three levels (Green's basis with non-canonical kinetic terms, canonically normalised Green's basis and physical basis) are reported by `matchmakereft` together with the corresponding renormalization of the gauge couplings as fixed by gauge boson renormalization in the BFM. If running in `RGEmaker` mode, `matchmakereft` automatically computes the beta functions for all the WCs of the EFT model.

Our use of the off-shell matching approach introduces a large degree of kinematic redundancy which, in addition to the explicit gauge redundancy in gauge theories due to the use BFM, provide a very powerful mechanism to cross-check the consistency of our results. `Matchmakereft` checks that all kinematic configurations and gauge directions are correctly matched, which in practice consists on checking whether the solution found is indeed a solution of the whole system of equations. If any of this checks is not fulfilled, `matchmakereft` will raise a warning and provide some extra information that can be useful to debug the problem (see Section 3.2).

## 3.2 Model creation

The creation of models in `matchmakereft` relies on the explicit input from the user. In the case of renormalizable theories with new fermions and scalars, it can be performed automatically by the `Mathematica` package `SOLD` (see Chapter 4). However, operators of mass dimension higher than four are not supported yet. Thus, effective theories have to be implemented with the greatest care, as this step is the most likely culprit in case of problems with the matching calculation.

### 3.2.1 Required files

`Matchmakereft` needs some different types of files with all the relevant information to create a model. The installation of `matchmakereft` comes with a number of sample models that can be obtained with the command `copy_models` (see Section 3.3), that the user can use to check more details on how to implement new models. `SOLD` can also be used to create most of these files automatically for renormalizable theories. The different types of files are the following:

- Model files (compulsory): one or more files `modfile1.fr, ..., modfilen.fr` that define the model in `FeynRules` format. The last one of the list during the creation of the model (see below) will determine the name of the `matchmakereft` model, which is defined as `modelfilen_MM`, and all the extra files need to have this same name. The Lagrangian has to be defined as `Ltot`. Otherwise, the model will not be created.

- Gauge information file (compulsory only if gauge groups are present): a file called `modfilen.gauge` with the definition of all the gauge functions, including structure constants, group generators in different representations and Clebsch-Gordan coefficients, appearing in the model (see below for more information). The user can choose any gauge basis of interest but they are responsible for the consistency of the chosen basis. The use of `SOLD` to generate this file is particularly efficient, specially in the case of exotic gauge representations.

- Symmetry file (optional): a file called `modfilen.symm` that indicates possible flavor symmetries in the parameters of the model. This is compulsory in the EFT model if flavor symmetries are present. This file has to include a `Mathematica` list called `listareplacesymmetry` in which the symmetries are given in the form of replacement rules. As an example we show the case of the symmmetries of the Wilson coefficient of the Weinberg operator (denoted by `alphaWeinberg[i,j]=alphaWeinberg[j,i]`) and the four-lepton operator $\mathcal{O}_{\ell\ell} = \bar{\ell}_i \gamma^\mu \ell_j \bar{\ell}_k \gamma_\mu \ell_l$ (denoted by `alphaOll[i,j,k,l]= alphaOll[k,l,i,j]`):

```
listareplacesymmetry=
    {
    alphaWeinberg[i_, j_] -> alphaWeinberg[j, i],
    alphaOll[i_, j_, k_, l_] -> alphaOll[k, l, i, j]
   }
```

  Note that the symmetries present on this file should be symmetries of the $d$-dimensional Lagrangian; symmetries only holding in four dimensions should not be included in this list.

- Redundancy file (compulsory for EFT models): a file called `modfilen.red` including a list of replacement rules with the redundancies, expressing the Wilson Coefficient of a physical basis in terms of the ones in the Green's basis. It can be empty if no redundancies are needed (if the physical and Green's bases coincide or if one just wants the results in the Green's basis).

- Hermiticity properties file: complex conjugation provides extra cross-checks of the correctness of the calculation in `matchmakereft`. For that reason it is important to provide the information of which WCs have special (anti)hermiticity properties. This can be provided by the user through a file `modfilen.herm` including a list called `listahermiticity`, indicating those WCs whose hermitian conjugate can be expressed in terms of the original coefficient. As an example, for the case of the hermitian operator $(\mathcal{O}_{Hq}^{(1)})_{ij} = H^\dagger \mathrm{i}\overleftrightarrow{D}_\mu H \bar{\ell}_i \gamma^\mu \ell_j$, its Wilson coefficient, denoted `alphaOHq1[i,j]` satisfies `alphaOHq1bar[i,j]=alphaOHq1[j,i]`. This relation is provided using the hermiticity file as follows:

```
listahermiticity = {
                      alphaOHq1bar[i_,j_]->alphaOHq1[j,i]
                     }
```

### 3.2.2 Gauge structure

`Matchmakereft` is especially efficient when the matching is performed in the unbroken phase of gauge theories as it keeps the gauge structure of the amplitudes completely symbolic, replacing the explicit values only at the end of the calculation. When a model is created, the name of all gauge functions, including structure constants, generators in different representations and Clebsh-Gordan coefficients cannot coincide with any function already present in `Mathematica` or `FeynRules`. Structure constants and generators do not have to be defined as `FeynRules` parameters but Clebsch-Gordan coefficients do. The numerical values of these gauge functions have to be provided in the `modfilen.gauge` file including a mathematica list called `replacegaugedata` that consists on a list of substitutions in the form of `Mathematica` sparse arrays. As a simple example, the $\mathrm{SU}(2)_L$ gauge group can be defined as follows in one of the `.fr` files:

```
M$GaugeGroups = {
  SU2L == {
    Abelian           -> False,
    CouplingConstant  -> g2,
    GaugeBoson        -> Wi,
    StructureConstant -> fsu2,
    Representations   -> {{Ta,SU2D}}
  }
},
```

where we have named the structure constant symbol and indicated one representation with generator symbol `Ta` and index definition `SU2D`. Note that the adjoint representation does not need to be explicitly defined because it is defined by the structure constants and the definition of the corresponding gauge bosons, which in this case reads:

```
M$ClassesDescription = {
  V[2] == {
    ClassName        -> Wi,
    SelfConjugate    -> True,
    Indices          -> {Index[SU2W]},
    Mass             -> 0,
    FullName        -> "light"
  }
};
```

A few comments are in order about the example above. First, we set the mass to zero because we are in the unbroken phase of the SM. Second, we define physical fields in entire gauge multiplets, rather than components (although it is actually possible to define also the field components separately as the physical fields, which can be advantageous when creating complicated models that take very long to generate in `FeynRules`). We also assign the FullName variable to "light" (`FullName->"light"`). This is compulsory in `matchmakereft`; every particle has to be defined with `FullName` equal to either `"light"` (and therefore to be kept in the EFT model) or `"heavy"` (and then integrated out of the UV model).

The corresponding indices, either gauge or flavor ones (if present), have to be defined with their respective finite ranges within the `.fr` files. As an example, we can define the ones corresponding the the adjoint (`SU2W`) and fundamental (`SU2D`) representations of $\mathrm{SU}(2)_L$, together with flavor indices for fermion generations (`Generation`), as follows:

```
IndexRange[Index[SU2W]] = Range[3];
IndexRange[Index[SU2D]] = Range[2];
IndexRange[Index[Generation]] = Range[3];
IndexStyle[SU2W,n];
IndexStyle[SU2D,l];
IndexStyle[Generation, fl];
```

Only massless particles can have flavor indices in the current version of `matchmakereft` (`1.1.0`).

In order to illustrate how new particles with non-trivial quantum numbers and Clebsch-Gordan coefficients can be defined we show here the implementation of a heavy scalar $\mathrm{SU}(2)_L$ triplet and the SM Higgs:

```
M$ClassesDescription = {
  S[105] == {
    ClassName        -> tphi,
    SelfConjugate    -> True,
    Indices          -> {Index[SU2W]},
    Mass             -> Mtphi,
    FullName        -> "heavy",
    QuantumNumbers -> {Y -> 0}
  },

  S[11] == {
    ClassName      -> Phi,
    Indices        -> {Index[SU2D]},
    SelfConjugate  -> False,
    Mass             -> muH,
    FullName        -> "light",
    QuantumNumbers -> {Y -> 1/2}
  }

};
```

where the new particle is defined as heavy and the SM Higgs is defined as light but also has a non-vanishing mass. U(1) quantum numbers also have to be defined explicitly, but their values can be symbolic. The only requirement is that U(1) invariance holds in all vertices even with symbolic charges. The symbol used for the charge has to be defined as a parameter of the model. A trilinear coupling between the heavy scalar and two Higgs bosons, which has a non-trivial gauge structure, would have a corresponding Clebsch-Gordan coefficients tensor that has to be defined explicitly, like in the following example:

```
M$Parameters = {

  C223 == {
    ParameterType     -> Internal,
    Indices -> {Index[SU2D],Index[SU2D],Index[SU2W]},
    ComplexParameter  -> True
  },

...
}
```

The corresponding Lagrangian would read:

```
Ltot := Block[{ii,jj,nn},
    2 C223[ii,jj,nn] kappatphi tphi[nn] Phibar[ii] Phi[jj] + ...]
```

As mentioned above, the explicit values of the gauge functions are given in a file called `modfilen.gauge` (assuming the last `FeynRules` model file is called `modfilen.fr`) which for our example would have to contain the following information:

```
replacegaugedata = {
   fsu2 -> SparseArray[Automatic, {3, 3, 3}, 0,
           {1, {{0, 2, 4, 6}, {{2, 3}, {3, 2},
                {1, 3}, {3, 1}, {1, 2}, {2, 1}}},
                          {1, -1, -1, 1, 1, -1}}],
       Ta -> SparseArray[Automatic, {3, 2, 2}, 0,
           {1, {{0, 2, 4, 6}, {{1, 2}, {2, 1},
                {1, 2}, {2, 1}, {1, 1}, {2, 2}}},
                {1/2, 1/2, -I/2, I/2, 1/2, -1/2}}],
       C223 -> SparseArray[Automatic, {2, 2, 3}, 0,
           {1, {{0, 3, 6}, {{1, 3}, {2, 1}, {2, 2},
                {1, 1}, {1, 2}, {2, 3}}},
                {1/2, 1/2, -I/2, 1/2, I/2, -1/2}}]}
```

where we have implemented the usual definitions, $\texttt{fsu2}[\texttt{i},\texttt{j},\texttt{k}] = \epsilon^{ijk}$, $\texttt{Ta}[\texttt{a},\texttt{i},\texttt{j}] = \sigma^a_{ij}/2$ and $\texttt{C223}[\texttt{i},\texttt{j},\texttt{a}] = \sigma^a_{ij}/2$. The simplest way to define these matrices is by applying the `Mathematica` function `SparseArray` to the corresponding arrays defined by the user and copying the output to a file. Again, this file can also be automatically created by `SOLD`, as we will see in Chapter 4.

#### 3.2.2.1 Background field method

`Matchmakereft` assumes that the BFM [85] is used when gauge theories are involved. Gauge fields are split into background and quantum configurations, and the gauge is fixed only for the latter. This implies that the effective action computed this way remains (background) gauge invariant, which, in our terms, means that the result of matching the same coefficient with different amplitudes must be the same. Following the $\mathrm{SU}(2)_L$ example, the associated quantum and ghost fields have to be defined on top of the definition of `Wi` given above:

```
 V[102] == {
    ClassName        -> WiQuantum,
```

```
    SelfConjugate    -> True,
    Indices          -> {Index[SU2W]},
    Mass             -> 0,
    FullName        -> "light"
},
  U[1] == {
    ClassName       -> ghWi,
    SelfConjugate   -> False,
    Indices      -> {Index[SU2W]},
    Ghost           -> Wi,
    QuantumNumbers  -> {GhostNumber -> 1},
    Mass            -> 0,
    FullName        -> "light"
  },
...
```

and the Lagrangian involving Wi would be given by:

```
gotoBFM={Wi[a__]->Wi[a]+WiQuantum[a]};

Ltot :=
Block[{mu,nu,ii,aa},
-1/4 (FS[Wi,mu,nu,ii] FS[Wi,mu,nu,ii])/.gotoBFM
-ghWibar[aa].DC[(DC[ghWi[aa],mu]/.gotoBFM),mu]
-DC[WiQuantum[mu,aa],mu] DC[WiQuantum[nu,aa],nu]/2
]
```

### 3.2.3 Defining an EFT model

As mentioned above, the EFT model has to be a *light* model (no heavy particles) and has to include all independent operators forming a Green's basis. The WCs in the EFT need to be named alphaXXX, where XXX stands for an arbitrary number of alpha-numeric characters. The amplitudes that matchmakereft computes are implicitly defined by the operators in the EFT. In that sense, an EFT model does not need to include all the operators of a Green's basis but at least all the operators in a certain class or sector (same fields), including redundant and evanescent ones. Matchmakereft then automatically generates a minimal set of amplitudes to match these operators. Renormalizable operators, including kinetic and mass terms, also have to be included in the EFT model in principle.

After computing the matching, matchmakereft checks that all off-shell kinematic configurations and all gauge directions are correctly matched (see next section). In the event of these checks not being satisfied, matchmakereft issues a warning and stores the relevant information. This usually happens because there is a mistake in the definition of the models, but this could happen because there are missing operators in the Green's basis. In Section 3.4 we collect some common problems and possible solutions when running matchmakereft. When doing the hard region expansion, structures of dimension equal or smaller to the highest dimension of the operators appearing in the EFT will be generated, so all operators of smaller dimensions (within the same class) have to be included. In their absence, the matching will fail but the user can check that all problems appear in sectors that are of no interest for them (for instance in lower-dimensional operators that have not been implemented). Also sometimes some amplitudes are not correctly matched due to the use of an anticommuting $\gamma^5$. Our proposed solution should be enough to ensure the correct results in the SMEFT and similar EFTs, as we discussed in Section 3.1.4, but a warning is issued anyway and the relevant information is stored so that the user can check if the solution is correct or not.

When interested in the matching results in a physical basis, the user has to provide the corresponding expression to reduce the WCs of the Green's basis into the ones of the physical basis. This has to be implemented in the `modfilen.red` file. Let us consider the following redundant operators in the SMEFT as an example:

$$\mathcal{O}_{HD} = (H^\dagger D_\mu H)^\dagger (H^\dagger D_\mu H), \tag{3.14}$$

$$\mathcal{R}_{BDH} = (H^\dagger \overleftrightarrow{D}_\mu H)\partial_\nu B^{\mu\nu} \to g_1 \mathcal{O}_{HD} + \ldots, \tag{3.15}$$

$$\mathcal{R}_{2B} = -\frac{1}{2}(\partial_\mu B^{\mu\nu})(\partial^\rho B_{\rho\nu}) \to -\frac{g_1^2}{2}\mathcal{O}_{HD} + \ldots, \tag{3.16}$$

where the $\to$ indicates an on-shell equivalence. These relations imply the following shift of the coefficient in the physical basis:

$$\texttt{alphaOHD} \to \texttt{alphaOHD} + 2g_1\texttt{alphaRBDH} - \frac{g_1^2}{2}\texttt{alphaR2B}, \tag{3.17}$$

which should be implemented in the file `modfilen.red` as follows:

```
finalruleordered={
  alphaOHD ->alphaOHD + 2*alphaRBDH*g1 - (alphaR2B*g1^2)/2,
  ...
  }
```

### 3.2.4 Protected keywords

The definition of models in `matchmakereft` is quite flexible, but there are a few keywords that are protected and should be used only for their specific purpose. In general, all variables in `matchmakereft` should be made of alphanumeric characters, without including any special characters. The list of protected variables is the following:

- `alpha`. All WCs have to be defined as `alphaXXX`, with `XXX` an arbitrary string of alphanumeric characters. Conversely, no other variable in the model can contain the substring `alpha`. However, when computing the RGEs of an EFT the WCs in the UV model can keep their original `alphaXXX` name (as in the EFT) and this will be changed into `WCXXX` automatically.

- `Ltot`. The complete Lagrangian of the model has to be declared as Ltot and it should not be used for anything else.

- `Quantum`. Since we use BFM, gauge bosons are split into a classical background and a quantum excitation. The quantum excitation has to be defined by `ClassName->VnameQuantum`, with `ClassName->Vname` the name of the classical counterpart.

- `invepsilonbar`. It denotes the dimensional regularization variable $1/\bar{\epsilon}$ so it should not be used explicitly in the definition of a model. Similarly, `epsilonbar` is used for $\bar{\epsilon}$.

- `Eps[]` denotes the `FeynRules` Levi-civita tensor. When containing four indices, `matchmakereft` interprets it as the Minkowskian (with $+---$ metric signature) totally antisymmetric tensor and should therefore not be used for the Euclidean one (if the number of indices is different from four it can be used as the Euclidean one). In case one needs to use the totally antisymmetric rank-4 tensor both with Minkowskian and Euclidean signatures, the latter should be explicitly defined as a gauge function and its numerical value defined in the corresponding `modfilen.gauge` file.
- `ee[]`, `dd[]`. These are internally used to denote the totally antisymmetric tensor and the Euclidean metric and they cannot be used in the model definition.
- `onelooporder` is a dummy variable to identify the one-loop order contribution.
- `sSS` is a dummy variable to identify the order in external momenta of a specific contribution.

## 3.3 Matchmakereft usage

In this section, we explain how to use all the commands available in `matchmakereft`. An updated version of the manual can be found, once `matchmakereft` is installed, in the directory `matchmakereft-location/matchmakereft/docs/` where `matchmakereft-location` is the directory listed under `Location` when the command `pip show matchmakereft` is used or the analogous location in Anaconda.

### 3.3.1 Installation

`Matchmakereft` is available both in the Python Package Index (PyPI) `https://pypi.org/project/matchmakereft/` and in the Anaconda Python distribution `https://anaconda.org/matchmakers/matchmakereft`. If `pip` is installed in the system, `matchmakereft` can be installed by just typing the following in a terminal:

```
> python3 -m pip install matchmakereft --user
```

or equivalently:

```
> pip install matchmakereft --user
```

Alternatively, if the distribution file has been directly downloaded from the repository, it can be installed using:

```
> python3 -m pip install matchmakereft-x.x.x.tar.gz  --user
```

where `x.x.x` corresponds to the version being installed.

The following command displays information about `matchmakereft`:

```
> pip3 show matchmakereft
Name: matchmakereft
Version: 1.1.0
Summary: Automated matching of general models onto general effective field
    theories
Home-page: https://ftae.ugr.es/matchmakereft/
Author: Adrian Carmona, Achilleas Lazopoulos, Pablo Olgoso, Jose Santiago
```

```
Author-email: adrian@ugr.es, lazopoulos@itp.phys.ethz.ch, pablolgoso@ugr.es,
    jsantiago@ugr.es
License: GNU General Public License GPLv3
Location: /Users/usuario/Library/Python/3.9/lib/python/site-packages
Requires: colorama, requests, setuptools, tqdm, version-comparison, yolk3k
Required-by:
```

Once `matchmakereft` is already installed in the system, one can check for possible updates by writing:

```
> pip install --upgrade matchmakereft --user
```

or uninstall it by typing:

```
> pip uninstall matchmakereft
```

For users employing Anaconda python distribution, `matchmakereft` can be installed using:

```
conda install -c matchmakers matchmakereft
```

Before running `matchmakereft`, however, some prerequisites are needed. These include having `Mathematica` (version 10 or higher), `FORM` and `QGRAF` installed in the system, as well as `Python` (3.5 or higher) and the `FeynRules` package. Moreover, `matchmakereft`'s executable has to be included in the user path. See the manual for further details.

### 3.3.2 `Matchmakereft` commmand line interface

`Matchmakereft` can be run in two different ways. The same commands are available in both running modes, although the syntax is slightly different on each of them. We will use the command line interface (CLI) for the examples, as it is the most straight-forward way to use `matchmakereft`. Once it is installed, we can access the CLI by typing on the terminal:

```
> matchmakereft
Checking for updates.
matchmakereft is up-to-date.

Welcome to matchmakereft v1.1.0
Please refer to SciPost Phys. 12, 198 (2022) arXiv:2112.10787 when using this
code.
For documentation please check the manual in matchmakereft-location/
matchmakereft/docs/manual.pdf

matchmakereft>
```

Inside the CLI tab-completion is available and all file paths can be absolute or relative. The command `help` gives information on all available commands. The core commands in `matchmakereft` CLI are:

- `matchmakereft> test_installation`

  This command runs a number of minimal tests to check that `matchmakereft` has been correctly installed. The process is verbose and provides information on what is being computed. It takes about 6 minutes to complete in a core-`i7@3.00 GHz` laptop.

- `matchmakereft> copy_models Location`

This command copies a number of sample models, including the complete baryon-number conserving SMEFT at dimension six, in the directory `Location` (which can be `.` for the current directory).

➤ `matchmakereft> create_model modfile1.fr ... modfilen.fr`

This command creates a `matchmakereft` model called `modfilen_MM` from the `FeynRules` model defined in one or more files with names `modfile1.fr ... modfilen.fr`, as described in detail in Section 3.2. The `matchmakereft` model is created in the same directory where `modfilen.fr` is present. Both relative and absolute paths can be given as input. All models provided with the distribution, that can be obtained via the `copy_models` command, that are extensions of the SM require calling also the file `UnbrokenSM_BFM.fr` as the first file in when using this command. In Section 3.5.2 we provide a specific example.

➤ `matchmakereft> match_model_to_eft UVModelName EFTModelName`

This command performs the complete tree-level and one-loop matching of a `matchmakereft` UV model with name `UVModelName` onto a `matchmakereft` EFT model with name `EFTModelName`. The result of the matching is written in a file called `MatchingResult.dat` in the `UVModelName` directory. Any possible problems with the matching are reported and stored in a file called `MatchingProblems.dat` under the same directory.

As of version `v1.1.0` there are two optional arguments for this function (and any `matchmakereft` function that includes the calculation of amplitudes) that can be called in arbitrary order:

- `matchmakereft> match_model_to_eft --parallel`

  This computes the relevant amplitudes in parallel, using the available cores in the computer.

- `matchmakereft> match_model_to_eft --chunksize=xx`

  This option splits any amplitude with a number of diagrams larger than `xx` into subprocesses with `xx` diagrams, whose results are combined once all of them have been computed.

The result of the matching stored in `MatchingResult.dat` is a mathematica list called `MatchingResult` with four entries and the following structure:

```
MatchingResult={
{
{{GreenTree,GreenTreeProblems},{GreenLoop,GreenLoopProblems}},
{{NormGreenTree,NormGreenTreeProblems},{NormGreenLoop,
    NormGreenLoopProblems}},
{PhysTreeLoop},
{GaugeCouplingMatching}
}
```

where GreenTree and GreenLoop stands for the tree level and one-loop matching in the Green basis, respectively and GreenTreeProblems,GreenLoopProblems are filled if problems were found in the process of impossing hermiticity as discussed in Section 3.1.4. The second level with the Norm prefix includes the matching in the Green basis (again separately for tree level and one-loop) after canonical normalization. The third level, denoted PhysTreeLoop, consists of the matching in the physical basis in which the tree level and one-loop contributions have been merged into a single expression (with the dummy variable onelooporder identifying the one-loop contribution). If no physical basis is defined by providing an empty modfilen.red file then the Green basis is used as a physical basis. Finally, the fourth level, denoted as GaugeCouplingMatching, provides the redefinition of the gauge couplings after matching as fixed by the corresponding gauge boson canonical normalization in the background gauge.

The file MatchingProblems.dat provides partial information of the problems encountered during the process of matching. It consists of a list with the following data: a number denoting the loop order (plus one) at which the problem was encountered, the external particles of the amplitude that was not correctly matched, and the result of these amplitudes. Non-vanishing values of the amplitudes indicate contributions that could not be matched by the EFT. At this point, all gauge information is lost and only kinematic information is retained. This gives only partial information (we plan to provide more detailed information in future versions of matchmakereft) but it can still be useful to debug possible problems. As an example, it is common that models that involve couplings proportional to $\gamma^5$ report some problems, due to the ambiguous terms in the anti-commuting $\gamma^5$ scheme that matchmakereft uses. In this case all non-vanishing amplitudes are proportional to ee[], as we will see in the example in Section 3.5.

```
matchmakereft> match_model_to_eft_onlytree UVModelName EFTModelName
```

Identical to match_model_to_eft but only the tree level matching is computed. With this feature, matchmakereft can be used as an automated basis translator, as one can simply use the corresponding EFT in a different basis as UV model and the matching will provide the complete translation between the two bases (see Section 3.5 for an explicit example).

```
matchmakereft> compute_rge_model_to_eft UVModelName EFTModelName
```

This command runs match_model_to_eft UVModelName EFTModelName in RGEmaker mode (notice that the UV model has to be a light model) and then computes the beta functions for the WCs of the EFT given the UV model. They are stored in a file called RGEResult.dat under directory UVModelName. We define the beta function of a Wilson Coefficient $C$ as

$$\beta(C) = \mu \frac{\mathrm{d}C}{\mathrm{d}\mu}. \tag{3.18}$$

```
matchmakereft> clean_model ModelName
```

Matchmakereft is designed for the maximal efficiency so that if a specific process has been already computed it is not computed again. If for any reason the user wants to recreate the calculation of all the amplitudes this command should be invoked to clean the previous calculations.

- ```
  matchmakereft> check_linear_dependence EFTModelName
  ```

  Given a set of operators, defined as an EFT model in directory `EFTModelName`, this command checks if they are off-shell linearly independent or not (in $d$ dimensions). This command is useful to find a Green's basis, as sometimes the off-shell relations between different operators are difficult to obtain analytically. If the set is not linearly independent `matchmakereft` will provide the relations between the different WCs (see Section 3.5 for an explicit example).

- ```
  matchmakereft> exit
  ```

  This command exits the CLI.

For the sake of flexibility the following commands are also available to perform independently some of the steps of the calculations:

- ```
  matchmakereft> match_model_to_eft_amplitudes UVModelName EFTModelName
  ```

  This command is used to compute all the relevant amplitudes in the UV model and the EFT, but no calculation of the WCs is done.

- ```
  matchmakereft> match_model_to_eft_amplitudes_onlytree UVModelName
      EFTModelName
  ```

  This command is identical to `match_model_to_eft_amplitudes` but performs only the tree level calculation.

- ```
  matchmakereft> compute_wilson_coefficients UVModelName EFTModelName
  ```

  This command should be run after the call to either `match_model_to_eft_amplitudes` or `match_model_to_eft_amplitudes_onlytree` and it computes the WCs to complete the matching.

### 3.3.3 Matchmakereft as a Python module

The python CLI described in the previous section provides an interactive experience to the user. However, `matchmakereft` can be also run by importing `matchmakereft` into a python script, a iPython shell or a Jupyter notebook as a module and then running the same commands as in the CLI adding the parameters of the corresponding function as a string. As an example, the commands to create a model stored in model `UVmodel.fr` and to match it to the EFT stored in directory `EFT_MM` (which we assume has been already created) are given by:

```
from matchmakereft.libs.mm_offline import *
create_model("UVmodel.fr")
match_model_to_eft("UVmodel_MM EFT_MM")
```

All other commands in the CLI are also available to use as functions in a script that imports `matchmakereft`.
```

## 3.4 Troubleshooting in `matchmakereft`

`Matchmakereft` provides a significant number of cross-checks that usually catch problems with the installation or with the definition of the models. When a problem is encountered, `matchmakereft` tries to provide a useful warning message that can be used to figure out the origin of the problem. If the user encounters a problem that cannot be solved from the information provided by `matchmakereft` we encourage them to check the troubleshooting section in the latest `matchmakereft` manual and the `Gitlab` `matchmakereft` issue tracker (`https://gitlab.com/m4103/matchmaker-eft/-/issues`) to see if the problem has been encountered by other users and a solution is available. If no solution can be found, the issue tracker should be used to pose questions to the `matchmakereft` developers or to file possible bugs.

Most of the times an unsuccessful matching is due to an error in the definition of the model(s). Some common pitfalls are:

- The name for the complete Lagrangian of the model has to be `Ltot`. Using a different name results in `matchmakereft` not creating the model properly.
- Operators badly defined in `FeynRules` (for instance, with indices not properly contracted). This results in wrong Feynman rules that lead to an incorrect matching.
- Model generation takes too long. This can happen with complicated models, in particular with effective operators of high mass dimension. As an example, the generation of the SMEFT model can easily take more than 30 minutes in a core-`i7@3.00 GHz` laptop. In this case it is useful to compute the Feynman rules directly with `FeynRules` to check that the model does not have any obvious problems. Also sometimes expanding in the gauge components can significantly speed up model creation (at the expense of a reduced gauge degeneracy and therefore a smaller set of cross-checks).
- `QGRAF` not running correctly. This could happen when vertices with a larger number of particles than the limit set in `QGRAF` are present. The solution is to modify correspondingly the limit in the `QGRAF` source and compile it again.
- `FORM` not running correctly. This is normally due to variables not being correctly defined (again due to an incorrect implementation of the model). Running directly with `FORM` the offending file can give hints on what is happening.
- `FORM` taking too long to run. Amplitudes with many external legs usually involve a very large number of diagrams that can take a long time to compute. The simplest solution is to not include the corresponding operators in the EFT model if the user is not interested in their matching (in the SMEFT case at dimension six the operator $\mathcal{O}_H = (H^\dagger H)^3$ is usually the one that takes the longest to be matched). Other solution would be to use the `parallel` and `chunksize` options to reduce the running time of the process.
- All amplitudes are computed but the matching is unsuccessful. This can be due to a number of reasons, the most common ones being: the WCs of the EFT model or the couplings in the UV model have some symmetry properties that have not been

implemented in the corresponding `modfilen.symm` file, the hermiticity properties of the couplings in the UV model have not been properly defined, either in the definition of the model itself or in the corresponding `modfilen.herm` file, there are some missing operators in the Green's basis of the EFT model...

## 3.5 Physics applications

A preliminary version of `matchmakereft` had already been used in a number of physical applications [12, 71, 86, 65, 87–89] even before its release, and has currently been used in some works ever since (see [90–92] for some examples). In this section we list some examples of the applications of `matchmakereft`.

### 3.5.1 Cross-checks

As we have emphasized, the large redundancy inherent in the off-shell matching in the BFM that we use gives us confidence on the correctness of the results computed with `matchmakereft`. Nevertheless we have tested `matchmakereft` against some of the few available complete one-loop matching results in the literature. We have found complete agreement except when explicitly described. The list of models we have compared includes:

- `RGEmaker` mode:
  - Complete RGEs for the ALP-SMEFT up to mass dimension-5 as computed in [12]. Exact agreement was found up to a typo in the original reference.
  - RGEs for the purely bosonic and two-fermion operators in the Warsaw basis [27] as computed in [68–70] and implemented in `DSixTools` [93, 73]. Complete agreement was found.
- `Matching` mode:
  - Scalar singlet. The complete matching up to one-loop order of an extension of the SM with a scalar singlet was recently completed in [94], after several partial attempts [41, 95]. We have found complete agreement with the results in [94].
  - Type-I see-saw model, as computed in [96]. Complete agreement was found.
  - Scalar leptoquarks, as computed in [63]. We have found some minor differences that we are discussing with the authors.
  - Charged scalar electroweak singlet, as computed in [97]. We agree with the result except for a sign in Eqs. (4.14), the terms with Pauli matrices in (4.15), (B.4) and (B.5) (the latter is the culprit of the opposite sign in terms with Pauli matrices) and a factor of 2 in Eq. (4.17) and of 4 in (B.7). We have contacted the authors about these differences.
  - Some partial cross-checks have been performed against the results in [98] with full agreement.

### 3.5.2 Complete one-loop matching of a new charged vector-like lepton singlet

In this section we provide the complete tree-level and one-loop matching of an extension of the SM with a new electroweak singlet vector-like lepton $E$ of hypercharge $-1$. The Lagrangian of this model is given by:

$$\mathcal{L} = \mathcal{L}_{\rm SM} + \bar{E}(\mathrm{i}\not{D} - M_E)E - [\tilde{\lambda}_i \bar{\ell}_i H E_R + \mathrm{h.c.}], \tag{3.19}$$

where $i$ denotes a SM flavor index. See [99] for direct experimental limits on such an extension of the SM.

This model is included in the distribution of `matchmakereft` and can be obtained via the `copy_models` command. Once the model is downloaded, and inside the corresponding directory, the following commands will generate the complete one-loop matching, including the complete matching in the Green's basis. We use the CLI as an example and replace the output given by `matchmakereft` with ... ,

```
matchmakereft> create_model UnbrokenSM_BFM.fr VLL_Singlet_Y_m1_BFM.fr
...
matchmakereft> match_model_to_eft VLL_Singlet_Y_m1_BFM_MM
    SMEFT_Green_Bpreserving_MM
...
```

Note that, due to the presence of $\gamma^5$ `matchmakereft` will warn the user that some problems are present and they are reported in the `MatchingProblems.dat` file. A close look at this file will show that all the non-vanishing amplitudes are proportional to the `ee[]` symbol and therefore they are indeed related to our $\gamma^5$ prescription. As we argue in 3.1.4, the procedure followed by `matchmakereft` guarantees the correct result in the SMEFT. Nevertheless we prefer `matchmakereft` to give the warning to alert the user of the $\gamma^5$ issue and the solution adopted.

The non vanishing WCs in the Warsaw basis, including one-loop accuracy are given in the next sections. In order to reduce clutter we only write explicitly flavor indices when necessary. We use the following notation:

$$\lfloor \tilde{\lambda}\tilde{\lambda}^* \rfloor \equiv \tilde{\lambda}_i \tilde{\lambda}_i^*, \qquad \lfloor \tilde{\lambda}\mathcal{M}\tilde{\lambda}^* \rfloor \equiv \tilde{\lambda}_i \mathcal{M}_{ij} \tilde{\lambda}_j^*, \tag{3.20}$$

with $\mathcal{M}_{ij}$ an arbitrary matrix with flavor indices. We also define:

$$L_E \equiv \log(\mu^2/M_E^2). \tag{3.21}$$

The tree level result agrees with the calculation in [100] (when taking into account the different notation in the Yukawa coupling). The result also agrees with the one computed in [45].

#### 3.5.2.1 SM couplings

The SM couplings receive the following (one-loop) corrections:

$$\mu_H^2 = \mu_H^{(0)\,2} + \frac{\lfloor\tilde{\lambda}^*\tilde{\lambda}\rfloor}{16\pi^2}\left[2M_E^2 - \frac{1}{2}\mu_H^{(0)\,2} - \frac{1}{3}\frac{\mu_H^{(0)\,4}}{M_E^2} - (\mu_H^{(0)\,2} - 2M_E^2)L_E\right], \tag{3.22}$$

$$\begin{aligned}\lambda = \lambda^{(0)} &+ \frac{1}{16\pi^2}\left[\frac{\lfloor\tilde{\lambda}^*\tilde{\lambda}\rfloor(5g_2^{(0)\,2}\mu_H^{(0)\,2} - 6\lambda^{(0)}(4\mu_H^{(0)\,2} + 3M_E^2) + 18\mu_H^{(0)\,2}\lfloor\tilde{\lambda}^*\tilde{\lambda}\rfloor)}{18M_E^2}\right.\\ &\left.+\frac{(2M_E^2 - \mu_H^{(0)\,2})\lfloor\tilde{\lambda}^* Y_e^{(0)} Y_e^{(0)\,\dagger}\tilde{\lambda}\rfloor}{M_E^2}\right] \qquad (3.23)\\ &- \frac{1}{16\pi^2}\left[\frac{\lfloor\tilde{\lambda}^*\tilde{\lambda}\rfloor[-g_2^{(0)\,2}\mu_H^{(0)\,2} + 6\lambda^{(0)}M_E^2 - 3M_E^2\lfloor\tilde{\lambda}^*\tilde{\lambda}\rfloor]}{3M_E^2}\right.\\ &\left.+\frac{2(-M_E^2 + \mu_H^{(0)\,2})\lfloor\tilde{\lambda}^* Y_e^{(0)} Y_e^{(0)\,\dagger}\tilde{\lambda}\rfloor}{M_E^2}\right] L_E, \qquad (3.24)\end{aligned}$$

$$Y_u = Y_u^{(0)} - \frac{1}{16\pi^2}\left[\left(\frac{1}{4} + \frac{\mu_H^{(0)\,2}}{3M_E^2}\right) Y_u^{(0)}\lfloor\tilde{\lambda}^*\tilde{\lambda}\rfloor + \frac{1}{2}Y_u^{(0)}\lfloor\tilde{\lambda}^*\tilde{\lambda}\rfloor L_E\right], \tag{3.25}$$

$$Y_d = Y_d^{(0)} - \frac{1}{16\pi^2}\left[\left(\frac{1}{4} + \frac{\mu_H^{(0)\,2}}{3M_E^2}\right) Y_d^{(0)}\lfloor\tilde{\lambda}^*\tilde{\lambda}\rfloor + \frac{1}{2}Y_d^{(0)}\lfloor\tilde{\lambda}^*\tilde{\lambda}\rfloor L_E\right], \tag{3.26}$$

$$\begin{aligned}(Y_e)_{ij} = (Y_e^{(0)})_{ij} &- \frac{1}{16\pi^2}\left[\left(\frac{1}{4} + \frac{\mu_H^{(0)\,2}}{3M_E^2}\right)(Y_e^{(0)})_{ij}\lfloor\tilde{\lambda}^*\tilde{\lambda}\rfloor + \left(\frac{3}{8} + \frac{3\mu_H^{(0)\,2}}{4M_E^2}\right)\tilde{\lambda}_i\tilde{\lambda}_k^*(Y_e^{(0)})_{kj}\right]\\ &- \frac{1}{16\pi^2}\left[\frac{1}{2}(Y_e^{(0)})_{ij}\lfloor\tilde{\lambda}^*\tilde{\lambda}\rfloor + \left(\frac{1}{4} + \frac{\mu_H^{(0)\,2}}{2M_E^2}\right)\tilde{\lambda}_i\tilde{\lambda}_k^*(Y_e^{(0)})_{kj}\right] L_E, \qquad (3.27)\end{aligned}$$

where the (0) superscript denotes the original parameters in the SM Lagrangian. All other SM couplings receive no corrections. In the following we express our results in terms of the physical SM couplings, the ones on the left hand side of Eqs. (3.22-3.27).

#### 3.5.2.2 Bosonic operators

Turning now to dimension 6 bosonic operators, we obtain the following non-vanishing WCs.

$$\alpha_{HW} = \frac{1}{16\pi^2}\frac{g_2^2\lfloor\tilde{\lambda}\tilde{\lambda}^*\rfloor}{24M_E^2}, \tag{3.28}$$

$$\alpha_{HB} = \frac{1}{16\pi^2}\frac{g_1^2\lfloor\tilde{\lambda}\tilde{\lambda}^*\rfloor}{8M_E^2}, \tag{3.29}$$

$$\alpha_{HWB} = -\frac{1}{16\pi^2}\frac{g_1 g_2\lfloor\tilde{\lambda}\tilde{\lambda}^*\rfloor}{6M_E^2}, \tag{3.30}$$

$$\begin{aligned}\alpha_{H\Box} =& \frac{1}{16\pi^2}\frac{1}{M_E^2}\left[-\frac{g_1^4}{30} + \left(\frac{13g_1^2}{72} - \frac{5g_2^2}{24} - \frac{\lfloor\tilde{\lambda}\tilde{\lambda}^*\rfloor}{3}\right)\lfloor\tilde{\lambda}\tilde{\lambda}^*\rfloor + \frac{3}{2}\lfloor\tilde{\lambda}^* Y_e Y_e^\dagger\tilde{\lambda}\rfloor\right] \\ &+ \frac{1}{16\pi^2}\frac{1}{M_E^2}\left[\left(\frac{g_1^2}{12} - \frac{g_2^2}{4}\right)\lfloor\tilde{\lambda}\tilde{\lambda}^*\rfloor + \lfloor\tilde{\lambda}^* Y_e Y_e^\dagger\tilde{\lambda}\rfloor\right] L_E,\end{aligned} \tag{3.31}$$

$$\begin{aligned}\alpha_{HD} =& \frac{1}{16\pi^2}\frac{1}{M_E^2}\left[-\frac{2g_1^4}{15} + \left(\frac{13g_1^2}{18} - \frac{\lfloor\tilde{\lambda}\tilde{\lambda}^*\rfloor}{2}\right)\lfloor\tilde{\lambda}\tilde{\lambda}^*\rfloor + \frac{1}{2}\lfloor\tilde{\lambda}^* Y_e Y_e^\dagger\tilde{\lambda}\rfloor\right] \\ &+ \frac{1}{16\pi^2}\frac{1}{M_E^2}\left[\frac{g_1^2}{3}\lfloor\tilde{\lambda}\tilde{\lambda}^*\rfloor + \lfloor\tilde{\lambda}^* Y_e Y_e^\dagger\tilde{\lambda}\rfloor\right] L_E,\end{aligned} \tag{3.32}$$

$$\begin{aligned}\alpha_{H} =& \frac{1}{16\pi^2}\frac{1}{M_E^2}\Bigg[\left(\frac{4\lambda^2}{3} - \frac{5\lambda g_2^2}{9} - 2\lambda\lfloor\tilde{\lambda}\tilde{\lambda}^*\rfloor + \frac{\lfloor\tilde{\lambda}\tilde{\lambda}^*\rfloor\lfloor\tilde{\lambda}\tilde{\lambda}^*\rfloor}{3} + 2\lfloor\tilde{\lambda}^* Y_e Y_e^\dagger\tilde{\lambda}\rfloor\right)\lfloor\tilde{\lambda}\tilde{\lambda}^*\rfloor \\ &\qquad + 2\lambda\lfloor\tilde{\lambda}^* Y_e Y_e^\dagger\tilde{\lambda}\rfloor - 2\lfloor\tilde{\lambda}^* Y_e Y_e^\dagger Y_e Y_e^\dagger\tilde{\lambda}\rfloor\Bigg] \\ &+ \frac{1}{16\pi^2}\frac{1}{M_E^2}\left[-\frac{2\lambda g_2^2}{3}\lfloor\tilde{\lambda}\tilde{\lambda}^*\rfloor + 4\lambda\lfloor\tilde{\lambda}^* Y_e Y_e^\dagger\tilde{\lambda}\rfloor - 2\lfloor\tilde{\lambda}^* Y_e Y_e^\dagger Y_e Y_e^\dagger\tilde{\lambda}\rfloor\right] L_E.\end{aligned} \tag{3.33}$$

All other bosonic operators do not receive any corrections up to one loop.

#### 3.5.2.3 Bi-fermion operators

Regarding operators in the Warsaw basis with two fermion fields, the non-vanishing contributions in our model are the following.

$$
\begin{aligned}
(\alpha_{eW})_{ij} =& -\frac{1}{16\pi^2}\frac{g_2}{24M_E^2}\tilde{\lambda}_i\tilde{\lambda}_k^*(Y_e)_{kj}, && (3.34)\\
(\alpha_{eB})_{ij} =& -\frac{1}{16\pi^2}\frac{g_1}{12M_E^2}\tilde{\lambda}_i\tilde{\lambda}_k^*(Y_e)_{kj}, && (3.35)\\
(\alpha^{(1)}_{Hq})_{ij} =& \frac{g_1^2}{16\pi^2}\frac{1}{M_E^2}\left[-\frac{g_1^2}{45}+\frac{13}{216}\lfloor\tilde{\lambda}\tilde{\lambda}^*\rfloor+\frac{1}{36}\lfloor\tilde{\lambda}\tilde{\lambda}^*\rfloor L_E\right]\delta_{ij}, && (3.36)\\
(\alpha^{(3)}_{Hq})_{ij} =& \frac{g_2^2}{16\pi^2}\frac{1}{M_E^2}\left[-\frac{5}{72}\lfloor\tilde{\lambda}\tilde{\lambda}^*\rfloor-\frac{1}{12}\lfloor\tilde{\lambda}\tilde{\lambda}^*\rfloor L_E\right]\delta_{ij}, && (3.37)\\
(\alpha_{Hu})_{ij} =& \frac{g_1^2}{16\pi^2}\frac{1}{M_E^2}\left[-\frac{4g_1^2}{45}+\frac{13}{54}\lfloor\tilde{\lambda}\tilde{\lambda}^*\rfloor+\frac{1}{9}\lfloor\tilde{\lambda}\tilde{\lambda}^*\rfloor L_E\right]\delta_{ij}, && (3.38)\\
(\alpha_{Hd})_{ij} =& \frac{g_1^2}{16\pi^2}\frac{1}{M_E^2}\left[\frac{2g_1^2}{45}-\frac{13}{108}\lfloor\tilde{\lambda}\tilde{\lambda}^*\rfloor-\frac{1}{18}\lfloor\tilde{\lambda}\tilde{\lambda}^*\rfloor L_E\right]\delta_{ij}, && (3.39)\\
(\alpha^{(1)}_{H\ell})_{ij} =& -\frac{\tilde{\lambda}_i\tilde{\lambda}_j^*}{4M_E^2}+\frac{1}{16\pi^2}\frac{1}{M_E^2}\left[\left(\frac{g_1^4}{15}-\frac{13g_1^2\lfloor\tilde{\lambda}\tilde{\lambda}^*\rfloor}{72}\right)\delta_{ij}+\left(\frac{31g_1^2}{288}-\frac{33g_2^2}{32}+\frac{13}{16}\lfloor\tilde{\lambda}\tilde{\lambda}^*\rfloor\right)\tilde{\lambda}_i\tilde{\lambda}_j^*\right.\\
&\left.-\frac{1}{2}\tilde{\lambda}_i\tilde{\lambda}_k^*(Y_e)_{kl}(Y_e^\dagger)_{lj}-\frac{1}{2}(Y_e)_{ik}(Y_e^\dagger)_{kl}\tilde{\lambda}_l\tilde{\lambda}_j^*\right]\\
&+\frac{1}{16\pi^2}\frac{1}{M_E^2}\left[-\frac{g_1^2\lfloor\tilde{\lambda}\tilde{\lambda}^*\rfloor}{12}\delta_{ij}+\left(\frac{25g_1^2}{48}-\frac{9g_2^2}{16}+\frac{3\lfloor\tilde{\lambda}\tilde{\lambda}^*\rfloor}{8}\right)\tilde{\lambda}_i\tilde{\lambda}_j^*\right.\\
&\left.-\frac{1}{2}\tilde{\lambda}_i\tilde{\lambda}_k^*(Y_e)_{kl}(Y_e^\dagger)_{lj}-\frac{1}{2}(Y_e)_{ik}(Y_e^\dagger)_{kl}\tilde{\lambda}_l\tilde{\lambda}_j^*\right]L_E, && (3.40)\\
(\alpha^{(3)}_{H\ell})_{ij} =& -\frac{\tilde{\lambda}_i\tilde{\lambda}_j^*}{4M_E^2}+\frac{1}{16\pi^2}\frac{1}{M_E^2}\left[-\frac{5g_2^2\lfloor\tilde{\lambda}\tilde{\lambda}^*\rfloor}{72}\delta_{ij}+\left(\frac{9g_1^2}{32}+\frac{77g_2^2}{288}+\frac{5}{16}\lfloor\tilde{\lambda}\tilde{\lambda}^*\rfloor\right)\tilde{\lambda}_i\tilde{\lambda}_j^*\right]\\
&+\frac{1}{16\pi^2}\frac{1}{M_E^2}\left[-\frac{g_2^2\lfloor\tilde{\lambda}\tilde{\lambda}^*\rfloor}{12}\delta_{ij}+\left(\frac{9g_1^2}{16}+\frac{7g_2^2}{48}+\frac{3\lfloor\tilde{\lambda}\tilde{\lambda}^*\rfloor}{8}\right)\tilde{\lambda}_i\tilde{\lambda}_j^*\right]L_E, && (3.41)\\
(\alpha_{He})_{ij} =& \frac{1}{16\pi^2}\frac{1}{M_E^2}\left[g_1^2\left(\frac{2g_1^2}{15}-\frac{13\lfloor\tilde{\lambda}\tilde{\lambda}^*\rfloor}{36}\right)\delta_{ij}+\frac{1}{24}(Y_e^\dagger)_{ik}\tilde{\lambda}_k\tilde{\lambda}_l^*(Y_e)_{lj}\right.\\
&\left.+\left(-\frac{g_1^2}{6}\lfloor\tilde{\lambda}\tilde{\lambda}^*\rfloor\delta_{ij}+\frac{1}{4}(Y_e^\dagger)_{ik}\tilde{\lambda}_k\tilde{\lambda}_l^*(Y_e)_{lj}\right)L_E\right], && (3.42)
\end{aligned}
$$

$$(\alpha_{uH})_{ij} = \frac{1}{16\pi^2}\frac{1}{M_E^2}\left[\left(\frac{2}{3}\lambda - \frac{5g_2^2}{36} - \frac{1}{2}\lfloor\tilde{\lambda}\tilde{\lambda}^*\rfloor\right)\lfloor\tilde{\lambda}\tilde{\lambda}^*\rfloor + \frac{1}{2}\lfloor\tilde{\lambda}^* Y_e Y_e^\dagger \tilde{\lambda}\rfloor \right.$$
$$\left. + \left(-\frac{g_2^2}{6}\lfloor\tilde{\lambda}\tilde{\lambda}^*\rfloor + \lfloor\tilde{\lambda}^* Y_e Y_e^\dagger \tilde{\lambda}\rfloor\right) L_E\right](Y_u)_{ij}, \tag{3.43}$$

$$(\alpha_{dH})_{ij} = \frac{1}{16\pi^2}\frac{1}{M_E^2}\left[\left(\frac{2}{3}\lambda - \frac{5g_2^2}{36} - \frac{1}{2}\lfloor\tilde{\lambda}\tilde{\lambda}^*\rfloor\right)\lfloor\tilde{\lambda}\tilde{\lambda}^*\rfloor + \frac{1}{2}\lfloor\tilde{\lambda}^* Y_e Y_e^\dagger \tilde{\lambda}\rfloor \right.$$
$$\left. + \left(-\frac{g_2^2}{6}\lfloor\tilde{\lambda}\tilde{\lambda}^*\rfloor + \lfloor\tilde{\lambda}^* Y_e Y_e^\dagger \tilde{\lambda}\rfloor\right) L_E\right](Y_d)_{ij}, \tag{3.44}$$

$$(\alpha_{eH})_{ij} = \frac{\tilde{\lambda}_i\tilde{\lambda}_k^*(Y_e)_{kj}}{2M_E^2} + \frac{1}{16\pi^2}\frac{1}{M_E^2}\left[\left(\frac{2}{3}\lambda - \frac{5g_2^2}{36} - \frac{1}{2}\lfloor\tilde{\lambda}\tilde{\lambda}^*\rfloor\right)\lfloor\tilde{\lambda}\tilde{\lambda}^*\rfloor(Y_e)_{ij} + \frac{1}{2}\lfloor\tilde{\lambda}^* Y_e Y_e^\dagger \tilde{\lambda}\rfloor(Y_e)_{ij}\right.$$
$$\left. + \left(5\lambda - \frac{14}{16}\lfloor\tilde{\lambda}\tilde{\lambda}^*\rfloor\right)\tilde{\lambda}_i\tilde{\lambda}_k^*(Y_e)_{kj} + \frac{37}{24}(Y_e)_{ik}(Y_e^\dagger)_{kl}\tilde{\lambda}_l\tilde{\lambda}_m^*(Y_e)_{mj} - \frac{1}{4}\tilde{\lambda}_i\tilde{\lambda}_k^*(Y_e)_{kl}(Y_e^\dagger)_{lm}(Y_e)_{mj}\right]$$
$$+ \frac{1}{16\pi^2}\frac{1}{M_E^2}\left[-\frac{g_2^2}{6}\lfloor\tilde{\lambda}\tilde{\lambda}^*\rfloor(Y_e)_{ij} + \lfloor\tilde{\lambda}^* Y_e Y_e^\dagger \tilde{\lambda}\rfloor(Y_e)_{ij} + \left(4\lambda - \frac{3}{4}\lfloor\tilde{\lambda}\tilde{\lambda}^*\rfloor\right)\tilde{\lambda}_i\tilde{\lambda}_k^*(Y_e)_{kj}\right.$$
$$\left. + \frac{3}{4}(Y_e)_{ik}(Y_e^\dagger)_{kl}\tilde{\lambda}_l\tilde{\lambda}_m^*(Y_e)_{mj}\right] L_E. \tag{3.45}$$

#### 3.5.2.4 Four-fermion operators

Finally, the following four-fermion operators receive non-vanishing WCs.

$$(\alpha_{qq}^{(1)})_{ijkl} = -\frac{1}{16\pi^2}\frac{g_1^4}{270M_E^2}\delta_{ij}\delta_{kl}, \tag{3.46}$$

$$(\alpha_{uu})_{ijkl} = -\frac{1}{16\pi^2}\frac{8g_1^4}{135M_E^2}\delta_{ij}\delta_{kl}, \tag{3.47}$$

$$(\alpha_{dd})_{ijkl} = -\frac{1}{16\pi^2}\frac{2g_1^4}{135M_E^2}\delta_{ij}\delta_{kl}, \tag{3.48}$$

$$(\alpha_{ud}^{(1)})_{ijkl} = \frac{1}{16\pi^2}\frac{8g_1^4}{135M_E^2}\delta_{ij}\delta_{kl}, \tag{3.49}$$

$$(\alpha_{qu}^{(1)})_{ijkl} = -\frac{1}{16\pi^2}\frac{1}{M_E^2}\left[\frac{4g_1^4}{135}\delta_{ij}\delta_{kl} + \frac{1}{18}\lfloor\tilde{\lambda}\tilde{\lambda}^*\rfloor(Y_u)_{il}(Y_u^\dagger)_{kj}\right], \tag{3.50}$$

$$(\alpha_{qu}^{(8)})_{ijkl} = -\frac{1}{16\pi^2}\frac{1}{3M_E^2}\lfloor\tilde{\lambda}\tilde{\lambda}^*\rfloor(Y_u)_{il}(Y_u^\dagger)_{kj}, \tag{3.51}$$

$$(\alpha_{qd}^{(1)})_{ijkl} = \frac{1}{16\pi^2}\frac{1}{M_E^2}\left[\frac{2g_1^4}{135}\delta_{ij}\delta_{kl} - \frac{1}{18}\lfloor\tilde{\lambda}\tilde{\lambda}^*\rfloor(Y_d)_{il}(Y_d^\dagger)_{kj}\right], \tag{3.52}$$

$$(\alpha_{qd}^{(8)})_{ijkl} = -\frac{1}{16\pi^2}\frac{1}{3M_E^2}\lfloor\tilde{\lambda}\tilde{\lambda}^*\rfloor(Y_d)_{il}(Y_d^\dagger)_{kj}, \tag{3.53}$$

$$(\alpha_{quqd}^{(1)})_{ijkl} = \frac{1}{16\pi^2}\frac{1}{3M_E^2}\lfloor\tilde{\lambda}\tilde{\lambda}^*\rfloor(Y_u)_{ij}(Y_d)_{kl}, \tag{3.54}$$

$$
\begin{aligned}
(\alpha_{\ell\ell})_{ijkl} =& \frac{1}{16\pi^2}\frac{1}{M_E^2}\left[-\frac{g_1^4}{30}\delta_{ij}\delta_{kl} + \frac{25g_1^2+11g_2^2}{288}(2\delta_{ij}\tilde{\lambda}_k\tilde{\lambda}_l^*)\right.\\
&\left.-\frac{11g_2^2}{144}(\delta_{il}\tilde{\lambda}_k\tilde{\lambda}_j^* + \delta_{jk}\tilde{\lambda}_i\tilde{\lambda}_l^*) - \frac{1}{8}\tilde{\lambda}_i\tilde{\lambda}_j^*\tilde{\lambda}_k\tilde{\lambda}_l^* + \frac{3}{16}(\tilde{\lambda}_i\tilde{\lambda}_l^*(Y_e)_{km}(Y_e^\dagger)_{mj} + \tilde{\lambda}_k\tilde{\lambda}_j^*(Y_e)_{im}(Y_e^\dagger)_{ml})\right]\\
&+\frac{1}{16\pi^2}\frac{1}{M_E^2}\left[\frac{g_1^2+g_2^2}{48}(2\delta_{ij}\tilde{\lambda}_k\tilde{\lambda}_l^*) - \frac{g_2^2}{24}(\delta_{il}\tilde{\lambda}_k\tilde{\lambda}_j^* + \delta_{jk}\tilde{\lambda}_i\tilde{\lambda}_l^*)\right.\\
&\left.+\frac{1}{8}(\tilde{\lambda}_i\tilde{\lambda}_l^*(Y_e)_{km}(Y_e^\dagger)_{mj} + \tilde{\lambda}_k\tilde{\lambda}_j^*(Y_e)_{im}(Y_e^\dagger)_{ml})\right] L_E,
\end{aligned} \tag{3.55}
$$

$$
(\alpha_{ee})_{ijkl} = -\frac{1}{16\pi^2}\frac{2g_1^4}{15M_E^2}\delta_{ij}\delta_{kl}, \tag{3.56}
$$

$$
\begin{aligned}
(\alpha_{\ell e})_{ijkl} =& \frac{1}{16\pi^2}\frac{1}{M_E^2}\left[-\frac{2g_1^4}{15}\delta_{ij}\delta_{kl} + \frac{25g_1^2}{72}\tilde{\lambda}_i\tilde{\lambda}_j^*\delta_{kl} - \frac{1}{6}\lfloor\tilde{\lambda}\tilde{\lambda}^*\rfloor(Y_e)_{il}(Y_e^\dagger)_{kj} - \frac{3}{8}\tilde{\lambda}_i\tilde{\lambda}_j^*(Y_e^\dagger)_{km}(Y_e)_{ml}\right]\\
&+\frac{1}{16\pi^2}\frac{1}{M_E^2}\left[+\frac{g_1^2}{12}\tilde{\lambda}_i\tilde{\lambda}_j^*\delta_{kl} - \frac{1}{4}\tilde{\lambda}_i\tilde{\lambda}_j^*(Y_e^\dagger)_{km}(Y_e)_{ml}\right] L_E,
\end{aligned} \tag{3.57}
$$

$$
\begin{aligned}
(\alpha_{\ell q}^{(1)})_{ijkl} =& \frac{1}{16\pi^2}\frac{1}{M_E^2}\left[\frac{g_1^4}{45}\delta_{ij}\delta_{kl} - \frac{25g_1^2}{432}\tilde{\lambda}_i\tilde{\lambda}_j^*\delta_{kl} + \frac{3}{16}\tilde{\lambda}_i\tilde{\lambda}_j^*\Big((Y_d)_{km}(Y_d^\dagger)_{ml} - (Y_u)_{km}(Y_u^\dagger)_{ml}\Big)\right]\\
&+\frac{1}{16\pi^2}\frac{1}{M_E^2}\left[-\frac{g_1^2}{72}\tilde{\lambda}_i\tilde{\lambda}_j^*\delta_{kl} + \frac{1}{8}\tilde{\lambda}_i\tilde{\lambda}_j^*\Big((Y_d)_{km}(Y_d^\dagger)_{ml} - (Y_u)_{km}(Y_u^\dagger)_{ml}\Big)\right] L_E,
\end{aligned} \tag{3.58}
$$

$$
\begin{aligned}
(\alpha_{\ell q}^{(3)})_{ijkl} =& \frac{1}{16\pi^2}\frac{1}{M_E^2}\left[-\frac{11g_2^2}{144}\tilde{\lambda}_i\tilde{\lambda}_j^*\delta_{kl} + \frac{3}{16}\tilde{\lambda}_i\tilde{\lambda}_j^*\Big((Y_d)_{km}(Y_d^\dagger)_{ml} + (Y_u)_{km}(Y_u^\dagger)_{ml}\Big)\right]\\
&+\frac{1}{16\pi^2}\frac{1}{M_E^2}\left[-\frac{g_2^2}{24}\tilde{\lambda}_i\tilde{\lambda}_j^*\delta_{kl} + \frac{1}{8}\tilde{\lambda}_i\tilde{\lambda}_j^*\Big((Y_d)_{km}(Y_d^\dagger)_{ml} + (Y_u)_{km}(Y_u^\dagger)_{ml}\Big)\right] L_E,
\end{aligned} \tag{3.59}
$$

$$
(\alpha_{eu})_{ijkl} = \frac{1}{16\pi^2}\frac{8g_1^4}{45M_E^2}\delta_{ij}\delta_{kl}, \tag{3.60}
$$

$$
(\alpha_{ed})_{ijkl} = -\frac{1}{16\pi^2}\frac{4g_1^4}{45M_E^2}\delta_{ij}\delta_{kl}, \tag{3.61}
$$

$$
(\alpha_{qe})_{ijkl} = \frac{1}{16\pi^2}\frac{2g_1^4}{45M_E^2}\delta_{ij}\delta_{kl}, \tag{3.62}
$$

$$
\begin{aligned}
(\alpha_{\ell u})_{ijkl} =& \frac{1}{16\pi^2}\frac{1}{M_E^2}\left[\frac{4g_1^4}{45}\delta_{ij}\delta_{kl} - \frac{25g_1^2}{108}\tilde{\lambda}_i\tilde{\lambda}_j^*\delta_{kl} + \frac{3}{8}\tilde{\lambda}_i\tilde{\lambda}_j^*(Y_u^\dagger)_{km}(Y_u)_{ml}\right]\\
&+\frac{1}{16\pi^2}\frac{1}{M_E^2}\left[-\frac{g_1^2}{18}\tilde{\lambda}_i\tilde{\lambda}_j^*\delta_{kl} + \frac{1}{4}\tilde{\lambda}_i\tilde{\lambda}_j^*(Y_u^\dagger)_{km}(Y_u)_{ml}\right] L_E,
\end{aligned} \tag{3.63}
$$

$$
\begin{aligned}
(\alpha_{\ell d})_{ijkl} =& \frac{1}{16\pi^2}\frac{1}{M_E^2}\left[-\frac{2g_1^4}{45}\delta_{ij}\delta_{kl} + \frac{25g_1^2}{216}\tilde{\lambda}_i\tilde{\lambda}_j^*\delta_{kl} - \frac{3}{8}\tilde{\lambda}_i\tilde{\lambda}_j^*(Y_d^\dagger)_{km}(Y_d)_{ml}\right]\\
&+\frac{1}{16\pi^2}\frac{1}{M_E^2}\left[\frac{g_1^2}{36}\tilde{\lambda}_i\tilde{\lambda}_j^*\delta_{kl} - \frac{1}{4}\tilde{\lambda}_i\tilde{\lambda}_j^*(Y_d^\dagger)_{km}(Y_d)_{ml}\right] L_E,
\end{aligned} \tag{3.64}
$$

$$
(\alpha_{\ell edq})_{ijkl} = \frac{1}{16\pi^2}\frac{1}{3M_E^2}\lfloor\tilde{\lambda}\tilde{\lambda}^*\rfloor(Y_e)_{ij}(Y_d^\dagger)_{kl}, \tag{3.65}
$$

$$
(\alpha_{\ell equ}^{(1)})_{ijkl} = -\frac{1}{16\pi^2}\frac{1}{3M_E^2}\lfloor\tilde{\lambda}\tilde{\lambda}^*\rfloor(Y_e)_{ij}(Y_u)_{kl}. \tag{3.66}
$$

### 3.5.3 Basis translation

Given a specific EFT, defined by its field content and symmetries, the choice of a basis of operators (either Green or physical) is not unique. Different bases are useful for different purposes and it is very useful to have a systematic way to translate the results from one basis to another. The `Rosetta` code [101] can be used to translate between popular physical bases for the dimension six SMEFT. Nevertheless, `matchmakereft` provides a more general approach, applicable to different EFTs and any two bases (not necessarily physical). This is done by performing a tree-level matching with the new basis as a UV model and the old one as an EFT.

As a trivial example we consider the following two operators that appear in the one-loop integration of a scalar singlet as shown in [95]:

$$\begin{aligned} O_R =&(H^\dagger H)(D_\mu H^\dagger D^\mu H) \\ &\to 2\lambda\mathcal{O}_H + \frac{1}{2}\mathcal{O}_{H\Box} + \frac{1}{2}\Big((Y_u)_{ij}(\mathcal{O}_{uH})_{ij} + (Y_d)_{ij}(\mathcal{O}_{dH})_{ij} + (Y_e)_{ij}(\mathcal{O}_{eH})_{ij} + \text{h.c.}\Big), \end{aligned} \tag{3.67}$$

$$O_T =\frac{1}{2}(H^\dagger \overleftrightarrow{D}_\mu H)^2 \to -2\mathcal{O}_{HD} - \frac{1}{2}\mathcal{O}_{H\Box}, \tag{3.68}$$

where the arrow denotes their expression in terms of the corresponding operators in the Warsaw basis.

When using `matchmakereft` to match at tree level a UV model consisting of the SM plus the two operators in the new basis, $O_R$ and $O_T$, onto the SMEFT in the basis described in Appendix B we obtain the following tree-level matching in the physical basis (we use $\beta$ for the WCs of the operators in the new basis) :

$$\alpha_H =2\lambda\beta_R, \qquad \alpha_{HD} =-2\beta_T, \qquad \alpha_{H\Box} =\frac{1}{2}(\beta_R - \beta_T), \tag{3.69}$$

$$\alpha_{uH} =\frac{1}{2}\beta_R(Y_u)_{ij}, \qquad \alpha_{dH} =\frac{1}{2}\beta_R(Y_d)_{ij}, \qquad \alpha_{eH} =\frac{1}{2}\beta_R(Y_e)_{ij}, \tag{3.70}$$

which exactly reproduce the above equations. This is of course just a minimal example to show the application of `matchmakereft` to basis translation but complete bases (both Green and physical) can be translated in an automated way using this procedure.

### 3.5.4 Off-shell operator independence

The process of construction of a Green's basis, as reviewed in Section 2.3, can be sometimes quite cumbersome in practice, in particular as the number of fields and indices increases. `Matchmakereft` can be used in this case to check if the operators defined in the EFT are linearly independent in $d$ dimensions for arbitrary off-shell kinematics or not. This can be done, as explained in Section 2.5, by checking the rank of the system of equations obtained by matching the EFT to all vanishing amplitudes. If several operators are linearly dependent, the rank will be smaller than the number of operators and `matchmakereft` will solve the system of equations to provide the relationship of the list of the dependent operators in terms of a particular set of independent ones. In order to do this one has to define an EFT with all the relevant operators (including possibly linearly dependent ones) and run the command `check_linear_dependece EFTModel`.

## 3.6 A minimal complete example

This section is devoted to illustrate many of the features of `matchmakereft` with a concrete example involving two scalar fields: a light (but not massless) field $\phi$ and a heavy field $\Phi$. Our model is described by the Lagrangian:

$$\mathcal{L} = \frac{1}{2}(\partial_\mu\phi)^2 - \frac{1}{2}m_L^2\phi^2 + \frac{1}{2}(\partial_\mu\Phi)^2 - \frac{1}{2}M_H^2\Phi^2 - \frac{\lambda_0}{4!}\phi^4 - \frac{\lambda_2}{4}\phi^2\Phi^2 - \frac{\kappa}{2}\phi^2\Phi, \tag{3.71}$$

which we want to match to an EFT without the heavy scalar, given by (up to dimension six):

$$\mathcal{L}_{\text{EFT}} = \frac{\alpha_{4k}}{2}(\partial_\mu\phi)^2 - \frac{\alpha_2}{2}\phi^2 - \frac{\alpha_4}{4!}\phi^4 - \frac{\alpha_6}{6!}\phi^6 - \frac{\tilde{\alpha}_6}{4!}\phi^3\partial^2\phi - \frac{\hat{\alpha}_6}{2}\left(\partial^2\phi\right)^2. \tag{3.72}$$

This conforms a Green's basis for the real (light) scalar field. Subsequently, the kinetic term can be canonically normalized, and the redundant operators can be eliminated. Two of the three operators of dimension six are redundant. We choose $\phi^6$ as the independent operator. Using equations of motion we can readily find that:

$$\phi^3\partial^2\phi \to -\alpha_2\phi^4 - \frac{1}{3!}\alpha_4\phi^6, \tag{3.73}$$

$$\left(\partial^2\phi\right)^2 \to \alpha_2^2\phi^2 + \frac{\alpha_2\alpha_4}{3}\phi^4 + \frac{\alpha_4^2}{36}\phi^6. \tag{3.74}$$

Eliminating these operators from the Lagrangian would induce the shifts

$$\alpha_2 \to \alpha_2 + \alpha_2^2\hat{\alpha}_6 \tag{3.75}$$

$$\alpha_4 \to \alpha_4 - \tilde{\alpha}_6\alpha_2 + 4\alpha_2\alpha_4\hat{\alpha}_6 \tag{3.76}$$

$$\alpha_6 \to \alpha_6 - 5\tilde{\alpha}_6\alpha_4 + 10\hat{\alpha}_6\alpha_4^2 \tag{3.77}$$

The coupling $\kappa$ of this model is a dimensionful coupling, and is expected to be parametrically of the order of the heavy mass scale $M_H$. Thus, $\kappa/M_H$ is of $\mathcal{O}(1)$ and is kept throughout the matching procedure consistently.

The `FeynRules` file for the UV model, saved at `two_scalars.fr`, is shown below.

```
(* --- Contents of Feynrules file two_scalars.fr --- *)
M$ModelName = "two_scalars";
(* **** Particle classes **** *)
M$ClassesDescription = {
S[1] == {ClassName -> phiH, SelfConjugate -> True, Mass -> MH,
         FullName -> "heavy"},
S[2] == {ClassName -> phi, SelfConjugate -> True, Mass -> mL,
         FullName -> "light"}
};
(* *****   Parameters   ***** *)
M$Parameters = {
MH == {ParameterType -> Internal, ComplexParameter -> False},
mL == {ParameterType -> Internal, ComplexParameter -> False},
```

```
V == {ParameterType -> Internal, ComplexParameter -> False},
lambda0 == {ParameterType -> Internal, ComplexParameter -> False},
kappa == {ParameterType -> Internal, ComplexParameter -> False},
lambda2 == {ParameterType -> Internal, ComplexParameter -> False}
};
(* *****   Lagrangian   ***** *)
Ltot := Block[{mu},
  + 1/2 * del[phi,mu] *  del[phi,mu]  + 1/2 *del[phiH,mu] * del[phiH,mu]
  - 1/2 * MH^2 * phiH^2 - 1/2 * mL^2 * phi^2
  - lambda0 / 24 * phi^4 - kappa / 2  * phi^2 * phiH
  - lambda2 / 4 * phi^2 * phiH^2
  ];
```

Note that we use the keyword `FullName` to characterize each field as `"heavy"` or `"light"`. This is mandatory, as emphasized in Section 3.2, since it indicates `matchmakereft` which fields have to be integrated out. Also note that all the parameters that are used in the Lagrangian, masses as well as couplings, must be declared. In this example all parameters are real.

The `FeynRules` file for the EFT model, saved at `one_scalar.fr`, is:

```
(* --- Contents of Feynrules file for the EFT model  one_scalar.fr --- *)
M$ModelName = "one_scalar";
(* **** Particle classes **** *)
M$ClassesDescription = {
S[2] == {ClassName -> phi, SelfConjugate -> True, Mass -> 0,
         FullName -> "light"}
};
(* *****   Parameters   ***** *)
M$Parameters = {
alpha4kin == {ParameterType -> Internal, ComplexParameter -> False},
alpha2mass == {ParameterType -> Internal, ComplexParameter -> False},
alpha4 == {ParameterType -> Internal, ComplexParameter -> False},
alpha6 == {ParameterType -> Internal, ComplexParameter -> False},
alpha6Rtilde == {ParameterType -> Internal, ComplexParameter -> False},
alpha6Rhat == {ParameterType -> Internal, ComplexParameter -> False}
};
(* *****   Lagrangian   ***** *)
Ltot := Block[{mu,mu2},
  1/2 * alpha4kin * del[phi,mu] * del[phi,mu]
  - 1/2 * alpha2mass * phi^2
  - alpha4/24 * phi^4
  - alpha6 * phi^6/720
  - alpha6Rtilde/24 * phi^3 * del[del[phi,mu],mu]
  - alpha6Rhat/2 * del[del[phi,mu],mu]  *  del[del[phi,mu2],mu2]
  ];
```

Note that we have also included WCs (denoted by `alphaXXX`) also for the kinetic and mass terms (squared), besides the rest of operators. In order for `matchmakereft` to perform the reduction to the physical basis, we need to provide the set of relations that express the redundant WCs in terms of the irreducible ones, as in Eq. (3.77). This has to be done in a `one_scalar.red` file:

```
(* --- Contents of one_scalar.red --- *)
finalruleordered = {
  alpha6 -> - alpha6Rtilde * alpha4 *5 + alpha6Rhat * alpha4^2 * 10 + alpha6 ,
```

```
alpha4 -> alpha4 - alpha6Rtilde * alpha2mass + 4 * alpha6Rhat * alpha2mass *
   alpha4 ,
alpha4kin -> alpha4kin ,
alpha2mass -> alpha2mass +  alpha6Rhat * alpha2mass^2
}
```

These rules are used at the end of the calculation, when both redundant and non-redundant WCs have been matched and are known functions of the parameters of the UV theory. The rules are therefore instructions on how to update the non-redundant WCs, to include the effect of the redundant ones.

With these files prepared, since there is no gauge structure or further symmetries in the model, we are ready to proceed with matching. In the matching directory, where `two_scalars.fr`, `one_scalar.fr` and `one_scalar.red` are present, we can run `matchmakereft` and enter the CLI. The first step is then to create the `matchmakereft` models, that can be done by:

```
matchmakereft> create_model two_scalars.fr
```

with the following output:

```
Creating model two_scalars_MM. This might take some time depending on the
complexity of the model
Model two_scalars_MM created
It took 7 seconds to create it.
```

The model is now created in the directory `two_scalars_MM`. We proceed in the same way to create the EFT model:

```
matchmakereft> create_model one_scalar.fr
Creating model one_scalar_MM. This might take some time depending on the
complexity of the model
Model one_scalar_MM created
It took 7 seconds to create it.
```

and now we can perform the matching calculation by using the `match_model_to_eft` command:

```
matchmakereft> match_model_to_eft two_scalars_MM one_scalar_MM
```

Once the process finishes, the results are stored in the UV model directory. The file `two_scalars_MM/MatchingProblems.dat` contains troubleshooting information in case the matching procedure failed. In our case it is an empty list, indicating no problems:

```
problist = {}
```

The matching results are stored in `two_scalars_MM/MatchingResults.dat`, as a Mathematica file with a list of lists of replacement rules. The off-shell matching gives the following results for the WCs of the Green's basis. At tree level the non-vanishing contributions are,

$$\alpha_2^{(0)} = m_L^2, \tag{3.78}$$

$$\alpha_4^{(0)} = \lambda_0 - \frac{3\kappa^2}{M_H^2}, \tag{3.79}$$

$$\alpha_6^{(0)} = \frac{45\lambda_2\kappa^2}{M_H^4}, \tag{3.80}$$

$$\tilde{\alpha}_6^{(0)} = \frac{4\kappa^2}{M_H^4}. \tag{3.81}$$

At one loop, keeping terms up to $\mathcal{O}\left(\frac{\kappa^{2n}}{M_H^{2n}}\frac{m_L^2}{M_H^2}\right)$, we get:

$$\alpha_2^{(1)} = -\frac{1}{16\pi^2}\left(1+L_M\right)\left(\frac{\kappa^2 m_L^4}{M_H^4}+\frac{\kappa^2 m_L^2}{M_H^2}+\frac{1}{2}\lambda_2 M_H^2+\kappa^2\right), \tag{3.82}$$

$$\alpha_{4k}^{(1)} = \frac{1}{16\pi^2}\left(\frac{5\kappa^2 m_L^2}{2M_H^4}+\frac{\kappa^2}{2M_H^2}\right)+\frac{1}{16\pi^2}\frac{\kappa^2 m_L^2}{M_H^4}L_M, \tag{3.83}$$

$$\alpha_4^{(1)} = \frac{1}{16\pi^2}\left(\frac{48\kappa^4 m_L^2}{M_H^6}+\frac{24\lambda_2\kappa^2 m_L^2}{M_H^4}-\frac{12\lambda_0\kappa^2 m_L^2}{M_H^4}+\frac{18\kappa^4}{M_H^4}+\frac{18\lambda_2\kappa^2}{M_H^2}-\frac{6\lambda_0\kappa^2}{M_H^2}\right) \tag{3.84}$$

$$+\frac{1}{16\pi^2}\left(\frac{36\kappa^4 m_L^2}{M_H^6}+\frac{18\lambda_2\kappa^2 m_L^2}{M_H^4}-\frac{12\lambda_0\kappa^2 m_L^2}{M_H^4}+\frac{12\kappa^4}{M_H^4}+\frac{12\lambda_2\kappa^2}{M_H^2}-\frac{6\lambda_0\kappa^2}{M_H^2}-\frac{3\lambda_2^2}{2}\right)L_M, \tag{3.85}$$

$$\alpha_6^{(1)} = \frac{1}{16\pi^2 M_H^2}\left(-\frac{1290\kappa^6}{M_H^6}+\frac{720\lambda_0\kappa^4}{M_H^4}-\frac{1665\lambda_2\kappa^4}{M_H^4}+\frac{360\lambda_0\lambda_2\kappa^2}{M_H^2}-\frac{90\lambda_0^2\kappa^2}{M_H^2}-\frac{495\lambda_2^2\kappa^2}{M_H^2}+\frac{15\lambda_2^3}{2}\right) \tag{3.86}$$

$$+\frac{1}{16\pi^2 M_H^2}\left(-\frac{810\kappa^6}{M_H^6}+\frac{540\lambda_0\kappa^4}{M_H^4}-\frac{945\lambda_2\kappa^4}{M_H^4}+\frac{270\lambda_0\lambda_2\kappa^2}{M_H^2}-\frac{90\lambda_0^2\kappa^2}{M_H^2}-\frac{270\lambda_2^2\kappa^2}{M_H^2}\right)L_M, \tag{3.87}$$

$$\tilde{\alpha}_6^{(1)} = \frac{1}{16\pi^2 M_H^2}\left(-\frac{107\kappa^4}{3M_H^4}+\frac{9\lambda_0\kappa^2}{M_H^2}-\frac{77\lambda_2\kappa^2}{3M_H^2}+\frac{\lambda_2^2}{3}\right)$$
$$+\frac{1}{16\pi^2 M_H^2}\left(-\frac{14\kappa^4}{M_H^4}+\frac{2\lambda_0\kappa^2}{M_H^2}-\frac{16\lambda_2\kappa^2}{M_H^2}\right)L_M, \tag{3.88}$$

$$\hat{\alpha}_6^{(1)} = -\frac{\kappa^2}{96\pi^2 M_H^4}, \tag{3.89}$$

where we define $L_M \equiv \log(\frac{\mu^2}{M_H^2})$. We can see in the equations above how the kinetic operator receives a correction and therefore $\phi$ is no longer canonically normalized. A field redefinition is needed to obtain a canonically normalized theory on which we can apply the corresponding redundancies to go to the physical basis. `Matchmakereft` does these two processes (canonical normalization and reduction to the physical basis) automatically. The resulting WCs in the physical basis, up to one-loop order and $\mathcal{O}\left(\frac{\kappa^{2n}}{M_H^{2n}}\frac{m_L^2}{M_H^2}\right)$, read:

$$\alpha_2 = m_L^2-\frac{1}{16\pi^2}\left(\frac{11\kappa^2 m_L^4}{3M_H^4}+\frac{3\kappa^2 m_L^2}{2M_H^2}+\frac{1}{2}\lambda_2 M_H^2+\kappa^2\right) \tag{3.90}$$
$$-\frac{1}{16\pi^2}\left(\frac{2\kappa^2 m_L^4}{M_H^4}+\frac{\kappa^2 m_L^2}{M_H^2}+\frac{1}{2}\lambda_2 M_H^2+\kappa^2\right)L_M,$$

$$\alpha_4 = \lambda_0-\frac{4\kappa^2 m_L^2}{M_H^4}-\frac{3\kappa^2}{M_H^2} \tag{3.91}$$
$$+\frac{1}{16\pi^2}\left(\frac{332\kappa^4 m_L^2}{3M_H^6}-\frac{80\lambda_0\kappa^2 m_L^2}{3M_H^4}+\frac{149\lambda_2\kappa^2 m_L^2}{3M_H^4}-\frac{\lambda_2^2 m_L^2}{3M_H^2}+\frac{25\kappa^4}{M_H^4}-\frac{7\lambda_0\kappa^2}{M_H^2}+\frac{20\lambda_2\kappa^2}{M_H^2}\right)$$
$$+\frac{1}{16\pi^2}\left(\frac{60\kappa^4 m_L^2}{M_H^6}-\frac{16\lambda_0\kappa^2 m_L^2}{M_H^4}+\frac{34\lambda_2\kappa^2 m_L^2}{M_H^4}+\frac{16\kappa^4}{M_H^4}-\frac{6\lambda_0\kappa^2}{M_H^2}+\frac{14\lambda_2\kappa^2}{M_H^2}-\frac{3\lambda_2^2}{2}\right)L_M,$$

$$
\begin{aligned}
\alpha_6 = {}& \frac{1}{M_H^2}\left(\frac{60\kappa^4}{M_H^4} - \frac{20\lambda_0\kappa^2}{M_H^2} + \frac{45\lambda_2\kappa^2}{M_H^2}\right) \\
&+ \frac{1}{16\pi^2 M_H^2}\left(-\frac{1560\kappa^6 m_L^2}{M_H^8} + \frac{440\lambda_0\kappa^4 m_L^2}{M_H^6} - \frac{1635\lambda_2\kappa^4 m_L^2}{2M_H^6} - \frac{2320\kappa^6}{M_H^6} + \frac{3610\lambda_0\kappa^4}{3M_H^4}\right. \\
&\qquad \left. - \frac{4955\lambda_2\kappa^4}{2M_H^4} - \frac{410\lambda_0^2\kappa^2}{3M_H^2} - \frac{490\lambda_2^2\kappa^2}{M_H^2} + \frac{1465\lambda_0\lambda_2\kappa^2}{3M_H^2} + \frac{15\lambda_2^3}{2} - \frac{5\lambda_0\lambda_2^2}{3}\right) \\
&+ \frac{1}{16\pi^2 M_H^2}\left(-\frac{960\kappa^6 m_L^2}{M_H^8} + \frac{320\lambda_0\kappa^4 m_L^2}{M_H^6} - \frac{495\lambda_2\kappa^4 m_L^2}{M_H^6} - \frac{1260\kappa^6}{M_H^6} + \frac{760\lambda_0\kappa^4}{M_H^4}\right. \\
&\qquad \left. - \frac{1425\lambda_2\kappa^4}{M_H^4} - \frac{100\lambda_0^2\kappa^2}{M_H^2} - \frac{240\lambda_2^2\kappa^2}{M_H^2} + \frac{350\lambda_0\lambda_2\kappa^2}{M_H^2}\right) L_M .
\end{aligned} \tag{3.92}
$$

Next, we will illustrate how to compute the RGE equations for both models. With this purpose, we need first to create a new pair of `FeynRules` files for each model. Let us start with the UV model, for which we will define a file `rge_two_scalars_uv.fr` that is the same as `two_scalars.fr` but declaring here the heavy field `phiH` as "light":

```
S[1] == {ClassName-> phiH, SelfConjugate->True, Mass->MH,
    FullName->"light"}

(* ***** Lagrangian ***** *)
Ltot := Block[{mu},
+ 1/2 * del[phi,mu] * del[phi,mu]
+ 1/2 *del[phiH,mu] * del[phiH,mu]
- 1/2 * MH^2 * phiH^2
- 1/2 * mL^2 * phi^2
-lambda0/24*phi^4
-kappa/2 *phi^2*phiH
- lambda2 / 4 * phi^2 * phiH^2
];
```

Next, we define the target model in a file called `rge_two_scalars_eft.fr`. It consists of an EFT Lagrangian with the field `phiH` now considered as a light field:

```
 (* ---  Contents of rge_two_scalars_eft.fr  --- *)
M$ModelName = "rge_two_scalars_eft";
(* **** Particle classes **** *)
M$ClassesDescription = {
S[1] == {ClassName ->  phiH, SelfConjugate -> True, Mass -> 0,
         FullName -> "light"},
S[2] == {ClassName -> phi,SelfConjugate -> True,Mass -> 0,
         FullName -> "light"}
};
(* *****   Parameters   ***** *)
M$Parameters = {
alpha4kinphi == {ParameterType -> Internal, ComplexParameter -> False},
alpha4kinH == {ParameterType -> Internal, ComplexParameter -> False},
alpha2MH == {ParameterType -> Internal, ComplexParameter -> False},
alpha2ML == {ParameterType -> Internal, ComplexParameter -> False},
alpha4 == {ParameterType -> Internal, ComplexParameter -> False},
alphaV == {ParameterType -> Internal, ComplexParameter -> False},
alpha1 == {ParameterType -> Internal, ComplexParameter -> False},
alpha2 == {ParameterType -> Internal, ComplexParameter -> False}
```

```
20 };
21 (* *****   Lagrangian   ***** *)
22 Ltot := Block[{mu},
23   alphaV *  phiH
24   +1/2 * alpha4kinphi* del[phi,mu] *  del[phi,mu]
25   + 1/2 * alpha4kinH * del[phiH,mu] * del[phiH,mu]
26   - 1/2 * alpha2MH * phiH^2
27   -1/2 * alpha2ML * phi^2
28   - alpha4 / 24 * phi^4
29   -  alpha1 / 2  * phi^2 * phiH
30   - alpha2 / 4 * phi^2 * phiH^2
31 ];
```

Note the presence of the tadpole term for the heavy scalar, that we will justify shortly. Also note that we now have a WC also for the kinetic term of the $\Phi$ field.

All dimension four operators present in the model are physical, so a `.red` file is not needed in this case. We can now create the two models with:

```
matchmakereft> create_model rge_two_scalars_uv.fr
```

```
matchmakereft> create_model rge_two_scalars_eft.fr
```

and then proceed to compute the RGEs using:

```
matchmakereft> compute_rge_model_to_eft  rge_two_scalars_uv_MM
    rge_two_scalars_eft_MM
```

As it happened before, we obtain an empty problem file `MatchingProblems.dat`, as well as a `MatchingResults.dat` file inside the `rge_two_scalars_uv_MM` directory. In addition, another file, `RGEResult.dat`, is written with the results for the beta functions of our UV model:

```
RGEResult = {
\[Beta][alphaV] -> -1/16*(kappa*mL^2)/Pi^2
\[Beta][alpha4kinphi] -> 0,
\[Beta][alpha4kinH] -> 0,
\[Beta][alpha2MH] -> kappa^2/(16*Pi^2)+(lambda2*mL^2)/(16*Pi^2),
\[Beta][alpha2ML] -> kappa^2/(8*Pi^2)+(lambda2*MH^2)/(16*Pi^2) +
       (lambda0*mL^2)/(16*Pi^2),
\[Beta][alpha4] -> (3*lambda0^2)/(16*Pi^2) +
       (3*lambda2^2)/(16*Pi^2),
\[Beta][alpha1] ->(lambda0*kappa)/(16*Pi^2) + (kappa*lambda2)/(4*Pi^2),
\[Beta][alpha2] -> (lambda0*lambda2)/(16*Pi^2) + lambda2^2/(4*Pi^2)}
```

Let us now see how we can deal tadpole contributions, which will also justify the reason for adding the $\alpha_V \Phi$ operator defined in line 23 of `rge_two_scalars_eft.fr`. The model we are studying contains many tadpole contributions in 1lPI diagrams due to the presence of the $\kappa\phi^2\Phi$ operator, that are accounted for during the matching procedure. These tadpoles would vanish if the light field was massless, but they give a finite contribution otherwise. However, the corresponding poles, which contribute to the beta functions of $m_L$ and $\kappa$ are disregarded during the RGE computation, since they do not belong to 1PI diagrams. Nevertheless, there is an easy way to account for them. By adding the $\alpha_V \Phi$ term in the Lagrangian of `rge_two_scalars_eft.fr`, we can match the divergence of the one-point function. Indeed, as we see from line 2 of RGEResult.dat, we have:

$$\beta(\alpha_V) = -\frac{1}{16\pi^2}\kappa m_L^2. \tag{3.93}$$

We can then perform a shift in the field $\Phi \to \Phi + V$, with $V = \frac{\alpha_V}{M_H^2}$, to eliminate the tadpole from the theory, which would modify the mass term for the light scalar, $m_L$, and the $\kappa$ coupling:

$$\tilde{m}_L^2 = m_L^2 + \kappa V + \frac{1}{2}\lambda_2 V^2 \quad , \quad \tilde{\kappa} = \kappa + \lambda_2 V. \tag{3.94}$$

The beta functions we read from RGEResult.dat should be consequently modified, to account for the tadpole pole:

$$\delta\beta(m_L^2) = \beta(\kappa V) = \frac{\kappa}{M_H^2}\beta(\alpha_V) = -\frac{\kappa^2}{16\pi^2}\frac{m_L^2}{M_H^2}, \tag{3.95}$$

$$\delta\beta(\kappa) = \beta(\lambda_2 V) = \frac{\lambda_2}{M_H^2}\beta(\alpha_V) = -\frac{\kappa\lambda_2}{16\pi^2}\frac{m_L^2}{M_H^2}. \tag{3.96}$$

The results of RGEResult.dat, including these contributions, read:

$$\beta(m_L^2) = \frac{\lambda_2 M_H^2}{16\pi^2} + \frac{\kappa^2}{8\pi^2} + \frac{\lambda_0 m_L^2}{16\pi^2} - \frac{\kappa^2}{16\pi^2}\frac{m_L^2}{M_H^2}, \tag{3.97}$$

$$\beta(M_H^2) = \frac{\kappa^2}{16\pi^2} + \frac{\lambda_2 m_L^2}{16\pi^2}, \tag{3.98}$$

$$\beta(\lambda_0) = \frac{3\lambda_0^2}{16\pi^2} + \frac{3\lambda_2^2}{16\pi^2}, \tag{3.99}$$

$$\beta(\kappa) = \frac{\lambda_0\kappa}{16\pi^2} + \frac{\lambda_2\kappa}{4\pi^2} - \frac{\kappa\lambda_2}{16\pi^2}\frac{m_L^2}{M_H^2}, \tag{3.100}$$

$$\beta(\lambda_2) = \frac{\lambda_2^2}{4\pi^2} + \frac{\lambda_0\lambda_2}{16\pi^2}. \tag{3.101}$$

We can repeat the same procedure to obtain the RGEs of the EFT model. We create the model via the following rge_one_scalar_uv.fr file

```
M$ModelName = "rge_one_scalar_uv";
(* **** Particle classes **** *)
M$ClassesDescription = {
S[2] == {ClassName -> phi,SelfConjugate -> True,Mass -> mL,
          FullName -> "light"}
};
(* *****   Parameters   ***** *)
M$Parameters = {
mL == {ParameterType -> Internal, ComplexParameter -> False},
a4 == {ParameterType -> Internal, ComplexParameter -> False},
a6 == {ParameterType -> Internal, ComplexParameter -> False}
};
(* *****   Lagrangian   ***** *)
Ltot := Block[{mu,mu2},
  1/2  * del[phi,mu] * del[phi,mu] - 1/2 * mL^2 * phi^2
  -a4/24 phi^4 - a6 * phi^6/720
  ];

```

which contains the physical operators of the EFT model. Note that we have changed the names of the couplings to something other than `alphaXXX`, although it is allowed and `matchmakereft` automatically would have changed them to `WCXXX`. We also create `rge_one_scalar_eft.fr` and `rge_one_scalar_eft.red` that are identical with `one_scalar.fr` and `one_scalar.red` defined above. Once again, we can create the two models and run `compute_rge_model_to_eft`. The result is:

$$\beta(\alpha_2) = \frac{\alpha_2\alpha_4}{16\pi^2}, \tag{3.102}$$

$$\beta(\alpha_4) = \frac{3\alpha_4^2}{16\pi^2} + \frac{\alpha_2\alpha_6}{16\pi^2}, \tag{3.103}$$

$$\beta(\alpha_6) = \frac{15\alpha_4\alpha_6}{16\pi^2}. \tag{3.104}$$

We can now check whether the matching conditions and the RGE equations are consistent with each other: if we match at $\mu = M_H$ and we evolve all couplings using the RGEs of the UV and the EFT model, to a lower scale $Q$, we should find the same expressions as when we match directly at $\mu = Q$. Let us check this explicitly in the case of the mass coefficient, $\alpha_2$. The matching condition for $\alpha_2$, at scale $\mu = M_H$, gives, see Eq. (3.90),

$$\alpha_2(M_H) = m_L^2(M_H) - \frac{1}{16\pi^2}\left(\frac{11\kappa^2 m_L^4}{3M_H^4} + \frac{3\kappa^2 m_L^2}{2M_H^2} + \frac{1}{2}\lambda_2 M_H^2 + \kappa^2\right). \tag{3.105}$$

We can use Eq. (3.102) to evolve $\alpha_2$ from $M_H$ to a lower scale $Q$. In the leading-log approximation it reads:

$$\alpha_2(Q) = \alpha_2(M_H) + \frac{1}{2}L_Q\beta(\alpha_2) = \alpha_2(M_H) + \frac{1}{2}L_Q\frac{\alpha_2\alpha_4}{16\pi^2}, \tag{3.106}$$

where $L_Q \equiv \log(\frac{Q^2}{M_H^2})$. Replacing the tree-level matched values of $\alpha_2$ and $\alpha_4$ we get:

$$\alpha_2(Q) \;=\; m_L^2(M_H) - \frac{1}{16\pi^2}\left(\frac{11\kappa^2 m_L^4}{3M_H^4} + \frac{3\kappa^2 m_L^2}{2M_H^2} + \frac{1}{2}\lambda_2 M_H^2 + \kappa^2\right) \tag{3.107}$$

$$-\frac{L_Q}{16\pi^2}\left(\frac{2\kappa^2 m_L^4}{M_H^4} + \frac{3\kappa^2 m_L^2}{2M_H^2} - \frac{\lambda_0 m_L^2}{2}\right). \tag{3.108}$$

Finally, we need to use the $m_L$ RGE of the UV model Eq. (3.97), to evolve it to the scale $Q$. We then get:

$$\alpha_2(Q) \;=\; m_L^2(Q) - \frac{1}{16\pi^2}\left(\frac{11\kappa^2 m_L^4}{3M_H^4} + \frac{3\kappa^2 m_L^2}{2M_H^2} + \frac{1}{2}\lambda_2 M_H^2 + \kappa^2\right) \tag{3.109}$$

$$-\frac{L_Q}{16\pi^2}\left(\frac{2\kappa^2 m_L^4}{M_H^4} + \frac{\kappa^2 m_L^2}{M_H^2} + \frac{\lambda_2 M_H^2}{2} + \kappa^2\right). \tag{3.110}$$

If we had matched directly at the scale $\mu = Q$ using Eq. (3.90), we would have found exactly the same result.

Similarly for $\alpha_4$, matching at $\mu = M_H$ and evolving to $\mu = Q$, with the help of the RGEs for both the UV and the EFT couplings, gives:

$$\begin{aligned}\alpha_4(Q) \;=\;& \lambda_0 - \frac{4\kappa^2 m_L^2}{M_H^4} - \frac{3\kappa^2}{M_H^2} + \frac{1}{16\pi^2}\left(\frac{332\kappa^4 m_L^2}{3M_H^6} + \frac{149\lambda_2\kappa^2 m_L^2}{3M_H^4} - \frac{80\lambda_0\kappa^2 m_L^2}{3M_H^4}\right.\\ &\left. - \frac{\lambda_2^2 m_L^2}{3M_H^2} + \frac{25\kappa^4}{M_H^4} + \frac{20\lambda_2\kappa^2}{M_H^2} - \frac{7\lambda_0\kappa^2}{M_H^2}\right) + \frac{1}{16\pi^2}L_Q\left(\frac{60\kappa^4 m_L^2}{M_H^6} + \frac{34\lambda_2\kappa^2 m_L^2}{M_H^4}\right.\\ &\left. - \frac{16\lambda_0\kappa^2 m_L^2}{M_H^4} + \frac{16\kappa^4}{M_H^4} + \frac{14\lambda_2\kappa^2}{M_H^2} - \frac{6\lambda_0\kappa^2}{M_H^2} - \frac{3\lambda_2^2}{2}\right), \qquad (3.111)\end{aligned}$$

in agreement with what we would get by matching directly at $\mu = Q$, see Eq. (3.91).

## 3.7 The future of `matchmakereft`

In this chapter, we have introduced `matchmakereft`, an automatic tool to perform the one-loop matching between general UV theories and EFTs and to compute their RGEs. `Matchmakereft` is a very active code, subjected to constant development. In fact, since its initial release, there have already been some modifications like the added functionality of computing amplitudes in parallel.

We believe that `matchmakereft` is a very powerful tool that can be used in many calculations in the context of EFTs and we plan to extend it in the future to exploit all its capabilities. This section provides an outlook of the major improvements we want to perform.

### On-shell matching

One of the ongoing developments in `matchmakereft` is to perform the matching on-shell. This has the disadvantage of increasing the number of diagrams, and the appearance of light bridges with poles in the external momenta that have to be cancelled with terms from the numerator. We plan to overcome these challenges by using numerical values for on-shell configurations of external momenta (see M. Chala's talk in SMEFT-Tools).

Once this option is implemented, the most useful application will be to compute the redundancies of any EFT, given a Green's and a physical basis. This can be trivially achieved by matching at tree level the Green's basis to the physical one on-shell, the result being directly the redundancies. This will not only severely ease the matching to any EFTs, but also open the door to the computation of several IR/UV dictionaries (see Chapter 4).

### Evanescent shifts

The reduction of a ($d$-dimensional) Green's basis into a physical one defines implicitly some evanescent structures that vanish in four dimensions, but which can produce finite, physical effects when inserted in loop diagrams, as discussed in Section 2.4. These effects can be absorbed by a shift of the physical WCs, but these one-loop contributions have to be computed in the EFT.

In the current version of `matchmakereft`, these evanescent shifts have to be manually added by the user the definition of the redundancies of the EFT. However, we plan to add a routine to compute them automatically in the future.

The idea is to have the user's input of which WCs define, through their reduction, an evanescent structure. From the redundancies of the model, we can read then the expression of the evanescent operators as the difference between the original ones and their reductions. Then, we can compute all their one-loop insertions and match them to the original EFT, in a very similar way to our RGE computation, but keeping the finite terms instead. Thus, the results are the shifts for the physical coefficients to be added to the redundancies.

### BMHV scheme

In `matchmakereft` we use a NDR scheme for $\gamma_5$. This was proven, in Section 3.1, to be sufficient for the SMEFT at dimension six and theories with operators of the form $\phi_1^\dagger \phi_2 X^{\mu\nu} \tilde{X}_{\mu\nu}$. However, fixing the ambiguities in general would require a case by case study, possibly fixing a reading point convention for the traces, to be followed also in the calculations in the EFT. A more general and flexible solution would therefore be convenient for other theories.

The Breitenlohner-Maison/t'Hooft-Veltman (BMHV) scheme [82] is the only one within dimensional regularization that has been proven to be consistent at all orders in perturbation theory. It basically consists on giving up on the anticommutation relations of $\gamma_5$ in order to obtain a consistent definition of it. This has been already partially automated in a experimental version of `matchmakereft`.

Nevertheless, in chiral gauge theories, the regularization of the fermionic action breaks gauge invariance, leading to a non-gauge invariant quantum effective action at one loop. Concretely, the Ward Identities would not be satisfied. This would translate for `matchmakereft` in a failure of the process of matching, as the same coefficient would receive different values depending on the amplitude used for its matching.

Gauge invariance can be restored, though, by the addition of some local counterterms in the theory [83, 84]. These counterterms, that are clearly non gauge invariant, have to compensate the insertions of (evanescent) non gauge invariant vertices of the regularized action in divergent loop integrals. Therefore the process can be thought as the matching of these operators into all the local, non gauge invariant independent structures in your theory, and consequently suitable to be performed using `matchmakereft`. The creation of a basis of all these structures is not trivial but it could be automatized.

`Matchmakereft` has already been used, in fact, to reproduce some of the results in [83]. Once the process is further automatized, it could be used to compute these counterterms for the complete SM (which are yet unknown), the SMEFT or, eventually, any given theory.

# 4

# Towards the SMEFT one-loop dictionary

In the previous chapter we presented `Matchmakereft`, a tool to perform automatic matching calculations. Thanks to it, comparing the experimental implications of a model of new physics is significantly simpler. However, there are still infinite models to compare, and our imagination to propose new realistic candidates to extend the Standard Model is endless. Without a compass to point a direction in the vast space of possible models, the problem does not seem to have been simplified very much. Some theoretical arguments can of course be used to get some orientation, but the increasingly stringent limits set by experiments have rendered them less convincing. In this sense, Effective Field Theories prove themselves useful once again allowing us to construct IR/UV dictionaries: a map we can use to guide our way in this overwhelming search.

In this chapter, we present the first stone in our way to a complete one-loop dictionary for the SMEFT, providing the full sector of one-loop generated operators from heavy scalars and fermions. The results are provided in a `Mathematica` package called `SOLD` (SMEFT One-Loop Dictionary), that includes some further functionalities like generating Lagrangians and `matchmakereft` models automatically. We start motivating our vision of dictionaries as a new guiding principle in Section 4.1, followed by a discussion on the target and methods of our study in Section 4.2. In Section 4.3 we review how the dictionary is constructed, and present the results in Section 4.4. Finally, Section 4.5 includes a phenomenological example of the application of the dictionary and we provide an outlook on possible future developments in Section 4.6.

## 4.1 Dictionaries: a new guiding principle

Over decades, the naturalness principle guided most theoretical model-building endeavors. A never-ending list of exotic models of new physics were waiting to be probed by the Large Hadron Collider (LHC). However, a decade after the Higgs discovery, an intensive experimental scrutiny by the LHC and other experiments has shown that new physics is not likely to be as close around the corner as we expected. In fact, there seems to be a energy gap between the scales we are currently able to probe and the scale of new physics, which, as discussed in Chapter 2, made EFTs suitable for this search.

Naturalness arguments can still play a relevant role in the discovery and interpretation of physics beyond the SM, but they cannot be in the spotlight as our only guiding principle anymore. The existence of increasingly stringent limits on the scale of new physics and the vast number of models to test suggest that we should find alternative guiding principles in our quest to unravel what lies beyond the SM. This is precisely where the power of EFTs comes into play; perturbation theory and power counting arguments provide an ordering principle that allows us to estimate the size of the different coefficients in our IR effective description, and order them accordingly. Thus, working (as we always do) at finite precision, only a finite number of WCs are actually observable and need to be considered. This opens up the possibility of classifying, using symmetry or topological arguments, all the observable models of new physics, relating them with the coefficients up to a certain order in the mass and loop expansion. This information is organized into what we call IR/UV dictionaries. As its name suggests, it consists of a mapping between UV extensions and IR effects in such a way that one can readily access the list of coefficients generated by a UV model and the list of all models that generate a particular Wilson Coefficient.

IR/UV dictionaries have the potential to become a leading guiding principle in the search of new physics. They comprise all the information about which models (and only those) are experimentally accessible, including all possible correlations between different experimental observables and, even more strikingly, including models that have never been thought of by theorists. Accessibility is of course dictated by the precision of experiments, and this changes not only with time, but also depends on the particular observable. Therefore, in order to match this precision, dictionaries have to be computed up to the relevant order.

The leading, tree level dictionary for the SMEFT at dimension six was published in [102], building on previous partial calculations [103, 100, 104, 105] (see [106] for an alternative way of constructing the dictionary). While extremely useful for sizeable effects, it is not sufficient when more precise experimental measurements are considered. Moreover, there are some effects whose leading order is one loop, so they are completely overlooked by the tree level dictionary. This motivates the extension of the dimension six SMEFT dictionary up to one-loop order, that we partially computed in [49] and present in this chapter.

Given the significant challenges inherent the task, we will restrict ourselves at first to a subset of dimension six operators that cannot be generated at tree level in any weakly coupled extension of the SM [107, 108][1], and whose leading order is therefore one loop. We will also consider only renormalizable extensions of the SM with an arbitrary number of heavy scalar and fermion fields.

[1]See [98] for a related analysis and [109, 110] for recent efforts towards the calculation of the dictionary for four-fermion interactions. See also [111–113] for results on generic UV extensions for a set of operators in the low energy EFT (LEFT).

## 4.2 The one-loop generated sector in the SMEFT

The translation that the dictionary encodes is, naturally, given by the matching of the UV models to the SMEFT at one loop. This can be achieved in different ways (see Chapter 2), our approach being to perform a diagrammatic off-shell matching because then we can make use of `matchmakereft` [64]. This requires the definition of a physical basis and a Green's basis. We adopt the Warsaw basis [27] for the former and the basis in Appendix B, also provided in `matchmakereft`, for the latter. After the matching, operators in the Green's basis have to be reduced to the ones in the physical basis. Thus, considering the UV origin of a specific operator in the Warsaw basis requires including the contribution to all redundant and evanescent operators that contribute to it.

Any operator in an EFT can be generated at different orders in perturbation theory, depending on the specific UV model. Some operators, however, can never be generated at tree level in any weakly coupled extension of the SM. For the SMEFT at dimension six, this was shown in [107], using simple topological arguments, in a basis along the lines of the Warsaw one. The complete list of operators in the Warsaw basis that cannot be generated at tree level is grouped in three classes and collected in Table 4.1. These are operators with three field strength tensors (class $X^3$), operators with two field strength tensors and two Higgs bosons (class $X^2H^2$) and finally dipole operators (class $\psi^2 XH$).

| $X^3$ | $X^2H^2$ | $\psi^2XH + \text{h.c.}$ |
|---|---|---|
| $\mathcal{O}_{3G} = f^{ABC}G_\mu^{A\nu}G_\nu^{B\rho}G_\rho^{C\mu}$ | $\mathcal{O}_{HG} = G^A_{\mu\nu}G^{A\,\mu\nu}H^\dagger H$ | $\mathcal{O}_{uG} = (\overline{q}T^A\sigma^{\mu\nu}u)\widetilde{H}G^A_{\mu\nu}$ |
| $\mathcal{O}_{3\widetilde{G}} = f^{ABC}\widetilde{G}_\mu^{A\nu}G_\nu^{B\rho}G_\rho^{C\mu}$ | $\mathcal{O}_{H\widetilde{G}} = \widetilde{G}^A_{\mu\nu}G^{A\,\mu\nu}H^\dagger H$ | $\mathcal{O}_{uW} = (\overline{q}\sigma^{\mu\nu}u)\sigma^I\widetilde{H}W^I_{\mu\nu}$ |
| $\mathcal{O}_{3W} = \epsilon^{IJK}W_\mu^{I\nu}W_\nu^{J\rho}W_\rho^{K\mu}$ | $\mathcal{O}_{HW} = W^I_{\mu\nu}W^{I\,\mu\nu}H^\dagger H$ | $\mathcal{O}_{uB} = (\overline{q}\sigma^{\mu\nu}u)\widetilde{H}B_{\mu\nu}$ |
| $\mathcal{O}_{3\widetilde{W}} = \epsilon^{IJK}\widetilde{W}_\mu^{I\nu}W_\nu^{J\rho}W_\rho^{K\mu}$ | $\mathcal{O}_{H\widetilde{W}} = \widetilde{W}^I_{\mu\nu}W^{I\,\mu\nu}H^\dagger H$ | $\mathcal{O}_{dG} = (\overline{q}T^A\sigma^{\mu\nu}d)HG^A_{\mu\nu}$ |
| | $\mathcal{O}_{HB} = B_{\mu\nu}B^{\mu\nu}H^\dagger H$ | $\mathcal{O}_{dW} = (\overline{q}\sigma^{\mu\nu}d)\sigma^I HW^I_{\mu\nu}$ |
| | $\mathcal{O}_{H\widetilde{B}} = \widetilde{B}_{\mu\nu}B^{\mu\nu}H^\dagger H$ | $\mathcal{O}_{dB} = (\overline{q}\sigma^{\mu\nu}d)HB_{\mu\nu}$ |
| | $\mathcal{O}_{HWB} = W^I_{\mu\nu}B^{\mu\nu}H^\dagger\sigma^I H$ | $\mathcal{O}_{eW} = (\overline{\ell}\sigma^{\mu\nu}e)\sigma^I HW^I_{\mu\nu}$ |
| | $\mathcal{O}_{H\widetilde{W}B} = \widetilde{W}^I_{\mu\nu}B^{\mu\nu}H^\dagger\sigma^I H$ | $\mathcal{O}_{eB} = (\overline{\ell}\sigma^{\mu\nu}e)HB_{\mu\nu}$ |

**Table 4.1:** One-loop generated operators in the Warsaw basis. Shaded operators are generated at two or higher order loops in SM extensions with fermions and scalars.

Let us outline the structure of one-loop contributions to each operator class in turn. In particular, we are interested in the UV origin of such contributions, namely, which heavy scalar or fermion fields can give rise to these operators at one-loop order. The fact that both light and heavy fields belong to complete, independent representations of the SM gauge group means that any gauge boson insertion in an amplitude does not change the type of field. Thus, gauge boson insertions do not affect the following discussion and can be ignored (naturally, all required gauge boson insertions will be properly taken into account in the actual calculation). Operators in classes $X^3$ and $X^2H^2$ do not receive contributions from redundant or evanescent operators so we only need to focus on the generation of the physical operators. Operators in the former class, $X^3$, can be computed from three gauge boson off-shell amplitudes. Neglecting the gauge boson insertions these amplitudes are simply vacuum bubbles of a single heavy scalar or fermion that is charged under the corresponding gauge group. Thus, any fermion or scalar that is not a singlet will, in principle, contribute to the corresponding operator. $X^2H^2$ class operators

| $\psi^2 D^3$ | | $\psi^2 X D$ | | | |
|---|---|---|---|---|---|
| $\mathcal{R}_{qD}$ | $\frac{\mathrm{i}}{2}\bar{q}\left\{D_\mu D^\mu, \not{D}\right\} q$ | $\mathcal{R}_{Gq}$ | $(\bar{q}T^A\gamma^\mu q)D^\nu G^A_{\mu\nu}$ | $\mathcal{R}_{Bd}$ | $(\bar{d}\gamma^\mu d)\partial^\nu B_{\mu\nu}$ |
| $\mathcal{R}_{uD}$ | $\frac{\mathrm{i}}{2}\bar{u}\left\{D_\mu D^\mu, \not{D}\right\} u$ | $\mathcal{R}'_{Gq}$ | $\frac{1}{2}(\bar{q}T^A\gamma^\mu \mathrm{i}\overleftrightarrow{D}^\nu q)G^A_{\mu\nu}$ | $\mathcal{R}'_{Bd}$ | $\frac{1}{2}(\bar{d}\gamma^\mu i\overleftrightarrow{D}^\nu d)B_{\mu\nu}$ |
| $\mathcal{R}_{dD}$ | $\frac{\mathrm{i}}{2}\bar{d}\left\{D_\mu D^\mu, \not{D}\right\} d$ | $\mathcal{R}'_{\widetilde{G}q}$ | $\frac{1}{2}(\bar{q}T^A\gamma^\mu \mathrm{i}\overleftrightarrow{D}^\nu q)\widetilde{G}^A_{\mu\nu}$ | $\mathcal{R}'_{\widetilde{B}d}$ | $\frac{1}{2}(\bar{d}\gamma^\mu \mathrm{i}\overleftrightarrow{D}^\nu d)\widetilde{B}_{\mu\nu}$ |
| $\mathcal{R}_{\ell D}$ | $\frac{\mathrm{i}}{2}\bar{\ell}\left\{D_\mu D^\mu, \not{D}\right\} \ell$ | $\mathcal{R}_{Wq}$ | $(\bar{q}\sigma^I\gamma^\mu q)D^\nu W^I_{\mu\nu}$ | $\mathcal{R}_{W\ell}$ | $(\bar{\ell}\sigma^I\gamma^\mu \ell)D^\nu W^I_{\mu\nu}$ |
| $\mathcal{R}_{eD}$ | $\frac{\mathrm{i}}{2}\bar{e}\left\{D_\mu D^\mu, \not{D}\right\} e$ | $\mathcal{R}'_{Wq}$ | $\frac{1}{2}(\bar{q}\sigma^I\gamma^\mu \mathrm{i}\overleftrightarrow{D}^\nu q)W^I_{\mu\nu}$ | $\mathcal{R}'_{W\ell}$ | $\frac{1}{2}(\bar{\ell}\sigma^I\gamma^\mu \mathrm{i}\overleftrightarrow{D}^\nu \ell)W^I_{\mu\nu}$ |
| **$\psi^2 H D^2$ + h.c.** | | $\mathcal{R}'_{\widetilde{W}q}$ | $\frac{1}{2}(\bar{q}\sigma^I\gamma^\mu \mathrm{i}\overleftrightarrow{D}^\nu q)\widetilde{W}^I_{\mu\nu}$ | $\mathcal{R}'_{\widetilde{W}\ell}$ | $\frac{1}{2}(\bar{\ell}\sigma^I\gamma^\mu \mathrm{i}\overleftrightarrow{D}^\nu \ell)\widetilde{W}^I_{\mu\nu}$ |
| $\mathcal{R}_{uHD1}$ | $(\bar{q}u)D_\mu D^\mu \widetilde{H}$ | $\mathcal{R}_{Bq}$ | $(\bar{q}\gamma^\mu q)\partial^\nu B_{\mu\nu}$ | $\mathcal{R}_{B\ell}$ | $(\bar{\ell}\gamma^\mu \ell)\partial^\nu B_{\mu\nu}$ |
| $\mathcal{R}_{uHD2}$ | $(\bar{q}\,\mathrm{i}\sigma_{\mu\nu}D^\mu u)D^\nu \widetilde{H}$ | $\mathcal{R}'_{Bq}$ | $\frac{1}{2}(\bar{q}\gamma^\mu \mathrm{i}\overleftrightarrow{D}^\nu q)B_{\mu\nu}$ | $\mathcal{R}'_{B\ell}$ | $\frac{1}{2}(\bar{\ell}\gamma^\mu \mathrm{i}\overleftrightarrow{D}^\nu \ell)B_{\mu\nu}$ |
| $\mathcal{R}_{uHD3}$ | $(\bar{q}D_\mu D^\mu u)\widetilde{H}$ | $\mathcal{R}'_{\widetilde{B}q}$ | $\frac{1}{2}(\bar{q}\gamma^\mu i\overleftrightarrow{D}^\nu q)\widetilde{B}_{\mu\nu}$ | $\mathcal{R}'_{\widetilde{B}\ell}$ | $\frac{1}{2}(\bar{\ell}\gamma^\mu \mathrm{i}\overleftrightarrow{D}^\nu \ell)\widetilde{B}_{\mu\nu}$ |
| $\mathcal{R}_{uHD4}$ | $(\bar{q}D_\mu u)D^\mu \widetilde{H}$ | $\mathcal{R}_{Gu}$ | $(\bar{u}T^A\gamma^\mu u)D^\nu G^A_{\mu\nu}$ | $\mathcal{R}_{Be}$ | $(\bar{e}\gamma^\mu e)\partial^\nu B_{\mu\nu}$ |
| $\mathcal{R}_{dHD1}$ | $(\bar{q}d)D_\mu D^\mu H$ | $\mathcal{R}'_{Gu}$ | $\frac{1}{2}(\bar{u}T^A\gamma^\mu \mathrm{i}\overleftrightarrow{D}^\nu u)G^A_{\mu\nu}$ | $\mathcal{R}'_{Be}$ | $\frac{1}{2}(\bar{e}\gamma^\mu \mathrm{i}\overleftrightarrow{D}^\nu e)B_{\mu\nu}$ |
| $\mathcal{R}_{dHD2}$ | $(\bar{q}\,\mathrm{i}\sigma_{\mu\nu}D^\mu d)D^\nu H$ | $\mathcal{R}'_{\widetilde{G}u}$ | $\frac{1}{2}(\bar{u}T^A\gamma^\mu \mathrm{i}\overleftrightarrow{D}^\nu u)\widetilde{G}^A_{\mu\nu}$ | $\mathcal{R}'_{\widetilde{B}e}$ | $\frac{1}{2}(\bar{e}\gamma^\mu \mathrm{i}\overleftrightarrow{D}^\nu e)\widetilde{B}_{\mu\nu}$ |
| $\mathcal{R}_{dHD3}$ | $(\bar{q}D_\mu D^\mu d)H$ | $\mathcal{R}_{Bu}$ | $(\bar{u}\gamma^\mu u)\partial^\nu B_{\mu\nu}$ | | |
| $\mathcal{R}_{dHD4}$ | $(\bar{q}D_\mu d)D^\mu H$ | $\mathcal{R}'_{Bu}$ | $\frac{1}{2}(\bar{u}\gamma^\mu \mathrm{i}\overleftrightarrow{D}^\nu u)B_{\mu\nu}$ | | |
| $\mathcal{R}_{eHD1}$ | $(\bar{\ell}e)D_\mu D^\mu H$ | $\mathcal{R}'_{\widetilde{B}u}$ | $\frac{1}{2}(\bar{u}\gamma^\mu \mathrm{i}\overleftrightarrow{D}^\nu u)\widetilde{B}_{\mu\nu}$ | | |
| $\mathcal{R}_{eHD2}$ | $(\bar{\ell}\,\mathrm{i}\sigma_{\mu\nu}D^\mu e)D^\nu H$ | $\mathcal{R}_{Gd}$ | $(\bar{d}T^A\gamma^\mu d)D^\nu G^A_{\mu\nu}$ | | |
| $\mathcal{R}_{eHD3}$ | $(\bar{\ell}D_\mu D^\mu e)H$ | $\mathcal{R}'_{Gd}$ | $\frac{1}{2}(\bar{d}T^A\gamma^\mu \mathrm{i}\overleftrightarrow{D}^\nu d)G^A_{\mu\nu}$ | | |
| $\mathcal{R}_{eHD4}$ | $(\bar{\ell}D_\mu e)D^\mu H$ | $\mathcal{R}'_{\widetilde{G}d}$ | $\frac{1}{2}(\bar{d}T^A\gamma^\mu \mathrm{i}\overleftrightarrow{D}^\nu d)\widetilde{G}^A_{\mu\nu}$ | | |

**Table 4.2:** One-loop generated redundant operators. Operators in gray do not contribute to one loop generated operators in the Warsaw basis. Shaded operators are generated at two or higher order loops in SM extensions with fermions and scalars.

can be computed from $H^\dagger H\, X\, X$ amplitudes which, ignoring again gauge boson insertions, can be computed simply from $H^\dagger H$ two-point functions. Dipole operators, on the other hand, receive contributions also from redundant and evanescent operators, collected in Tables B.2 and B.4. Note that following the nomenclature in [64], evanescent operators are redundant ones that define evanescent structures through their reduction, but the shifts generated by these evanescent remnants are also taking into account. All the relevant operators for this class can be computed from amplitudes of the form $\bar{\psi}\psi(V)$ and $\bar{\psi}_L\psi_R H^{(\dagger)}(V)$, where $V$ stands for the corresponding gauge boson, $\psi_L = \{l_L, q_L\}$ stand for the left-handed fermions of the SM, $\psi_R = \{u_R, d_R, e_R\}$ for the right-handed ones and $\psi = \{\psi_L, \psi_R\}$ includes both. Neglecting again the gauge boson insertions we just need to consider $\bar{\psi}\psi$ and $\bar{\psi}_L\psi_R H^{(\dagger)}$ amplitudes.

Once we know which amplitudes contribute to each class, we can use topological considerations to list the actual Feynman diagrams for each amplitude. Any one loop Feynman diagram satisfies the following relation between the number of external particles, $E$, and the number of vertices:

$$E = \sum_{n=3}^{E+2} (n-2)V_n, \tag{4.1}$$

where $n$ denotes the order (number of fields) of the vertices and $V_n$ the number of vertices of order $n$ in the diagram. The sum ends at $n = E+2$ because higher order vertices would result in more than $E$ external legs at one loop. In particular we are interested in the cases $E = 2, 3,$

| $\Psi^2 XH + \text{h.c.}$ | | $\Psi^2 XD$ | | | |
|---|---|---|---|---|---|
| $\mathcal{E}_{uG}$ | $\bar{q}T^A\sigma^{\mu\nu}u\widetilde{H}\widetilde{G}^A_{\mu\nu}$ | $\mathcal{E}_{Gq}$ | $\bar{q}T^A(\sigma^{\mu\nu}\gamma^\rho+\gamma^\rho\sigma^{\mu\nu})qD_\rho\widetilde{G}^A_{\mu\nu}$ | $\mathcal{E}_{Gd}$ | $\bar{d}T^A(\sigma^{\mu\nu}\gamma^\rho+\gamma^\rho\sigma^{\mu\nu})dD_\rho\widetilde{G}^A_{\mu\nu}$ |
| $\mathcal{E}_{uW}$ | $\bar{q}\sigma^I\sigma^{\mu\nu}u\widetilde{H}\widetilde{W}^I_{\mu\nu}$ | $\mathcal{E}'_{Gq}$ | $\mathrm{i}\bar{q}(T^A\sigma^{\mu\nu}\slashed{D}-\overleftarrow{\slashed{D}}\sigma^{\mu\nu}T^A)qG^A_{\mu\nu}$ | $\mathcal{E}'_{Gd}$ | $\mathrm{i}\bar{d}(T^A\sigma^{\mu\nu}\slashed{D}-\overleftarrow{\slashed{D}}\sigma^{\mu\nu}T^A)dG^A_{\mu\nu}$ |
| $\mathcal{E}_{uB}$ | $\bar{q}\sigma^{\mu\nu}u\widetilde{H}\widetilde{B}_{\mu\nu}$ | $\mathcal{E}'_{\widetilde{G}q}$ | $\mathrm{i}\bar{q}(T^A\sigma^{\mu\nu}\slashed{D}-\overleftarrow{\slashed{D}}\sigma^{\mu\nu}T^A)q\widetilde{G}^A_{\mu\nu}$ | $\mathcal{E}'_{\widetilde{G}d}$ | $\mathrm{i}\bar{d}(T^A\sigma^{\mu\nu}\slashed{D}-\overleftarrow{\slashed{D}}\sigma^{\mu\nu}T^A)d\widetilde{G}^A_{\mu\nu}$ |
| $\mathcal{E}_{dG}$ | $\bar{q}T^A\sigma^{\mu\nu}dH\widetilde{G}^A_{\mu\nu}$ | $\mathcal{E}_{Wq}$ | $\bar{q}\sigma^I(\sigma^{\mu\nu}\gamma^\rho+\gamma^\rho\sigma^{\mu\nu})qD_\rho\widetilde{W}^I_{\mu\nu}$ | $\mathcal{E}_{Bd}$ | $\bar{d}(\sigma^{\mu\nu}\gamma^\rho+\gamma^\rho\sigma^{\mu\nu})d\partial_\rho\widetilde{B}_{\mu\nu}$ |
| $\mathcal{E}_{dW}$ | $\bar{q}\sigma^I\sigma^{\mu\nu}dH\widetilde{W}^I_{\mu\nu}$ | $\mathcal{E}'_{Wq}$ | $\mathrm{i}\bar{q}(\sigma^I\sigma^{\mu\nu}\slashed{D}-\overleftarrow{\slashed{D}}\sigma^{\mu\nu}\sigma^I)qW^I_{\mu\nu}$ | $\mathcal{E}'_{Bd}$ | $\mathrm{i}\bar{d}(\sigma^{\mu\nu}\slashed{D}-\overleftarrow{\slashed{D}}\sigma^{\mu\nu})dB^A_{\mu\nu}$ |
| $\mathcal{E}_{dB}$ | $\bar{q}\sigma^{\mu\nu}dH\widetilde{B}_{\mu\nu}$ | $\mathcal{E}'_{\widetilde{W}q}$ | $\mathrm{i}\bar{q}(\sigma^I\sigma^{\mu\nu}\slashed{D}-\overleftarrow{\slashed{D}}\sigma^{\mu\nu}\sigma^I)q\widetilde{W}^I_{\mu\nu}$ | $\mathcal{E}'_{\widetilde{B}d}$ | $\mathrm{i}\bar{d}(\sigma^{\mu\nu}\slashed{D}-\overleftarrow{\slashed{D}}\sigma^{\mu\nu})d\widetilde{B}_{\mu\nu}$ |
| $\mathcal{E}_{eW}$ | $\bar{\ell}\sigma^I\sigma^{\mu\nu}eH\widetilde{W}^I_{\mu\nu}$ | $\mathcal{E}_{Bq}$ | $\bar{q}(\sigma^{\mu\nu}\gamma^\rho+\gamma^\rho\sigma^{\mu\nu})q\partial_\rho\widetilde{B}_{\mu\nu}$ | $\mathcal{E}_{W\ell}$ | $\bar{\ell}\sigma^I(\sigma^{\mu\nu}\gamma^\rho+\gamma^\rho\sigma^{\mu\nu})\ell D_\rho\widetilde{W}^I_{\mu\nu}$ |
| $\mathcal{E}_{eB}$ | $\bar{\ell}\sigma^{\mu\nu}eH\widetilde{B}_{\mu\nu}$ | $\mathcal{E}'_{Bq}$ | $\mathrm{i}\bar{q}(\sigma^{\mu\nu}\slashed{D}-\overleftarrow{\slashed{D}}\sigma^{\mu\nu})qB_{\mu\nu}$ | $\mathcal{E}'_{W\ell}$ | $\mathrm{i}\bar{\ell}(\sigma^I\sigma^{\mu\nu}\slashed{D}-\overleftarrow{\slashed{D}}\sigma^{\mu\nu}\sigma^I)\ell W^I_{\mu\nu}$ |
| $\psi^2 HD^2 + \text{h.c.}$ | | $\mathcal{E}'_{\widetilde{B}q}$ | $\mathrm{i}\bar{q}(\sigma^{\mu\nu}\slashed{D}-\overleftarrow{\slashed{D}}\sigma^{\mu\nu})q\widetilde{B}_{\mu\nu}$ | $\mathcal{E}'_{\widetilde{W}\ell}$ | $\mathrm{i}\bar{\ell}(\sigma^I\sigma^{\mu\nu}\slashed{D}-\overleftarrow{\slashed{D}}\sigma^{\mu\nu}\sigma^I)\ell\widetilde{W}^I_{\mu\nu}$ |
| $\mathcal{E}_{uH}$ | $\bar{q}\sigma^{\mu\nu}D^\rho uD^\sigma\widetilde{H}\epsilon_{\mu\nu\rho\sigma}$ | $\mathcal{E}_{Gu}$ | $\bar{u}T^A(\sigma^{\mu\nu}\gamma^\rho+\gamma^\rho\sigma^{\mu\nu})uD_\rho\widetilde{G}^A_{\mu\nu}$ | $\mathcal{E}_{B\ell}$ | $\bar{\ell}(\sigma^{\mu\nu}\gamma^\rho+\gamma^\rho\sigma^{\mu\nu})\ell\partial_\rho\widetilde{B}_{\mu\nu}$ |
| $\mathcal{E}_{dH}$ | $\bar{q}\sigma^{\mu\nu}D^\rho dD^\sigma H\epsilon_{\mu\nu\rho\sigma}$ | $\mathcal{E}'_{Gu}$ | $\mathrm{i}\bar{u}(T^A\sigma^{\mu\nu}\slashed{D}-\overleftarrow{\slashed{D}}\sigma^{\mu\nu}T^A)uG^A_{\mu\nu}$ | $\mathcal{E}'_{B\ell}$ | $\mathrm{i}\bar{\ell}(\sigma^{\mu\nu}\slashed{D}-\overleftarrow{\slashed{D}}\sigma^{\mu\nu})\ell B_{\mu\nu}$ |
| $\mathcal{E}_{eH}$ | $\bar{\ell}\sigma^{\mu\nu}D^\rho eD^\sigma H\epsilon_{\mu\nu\rho\sigma}$ | $\mathcal{E}'_{\widetilde{G}u}$ | $\mathrm{i}\bar{u}(T^A\sigma^{\mu\nu}\slashed{D}-\overleftarrow{\slashed{D}}\sigma^{\mu\nu}T^A)u\widetilde{G}^A_{\mu\nu}$ | $\mathcal{E}'_{\widetilde{B}\ell}$ | $\mathrm{i}\bar{\ell}(\sigma^{\mu\nu}\slashed{D}-\overleftarrow{\slashed{D}}\sigma^{\mu\nu})\ell\widetilde{B}_{\mu\nu}$ |
| | | $\mathcal{E}_{Bu}$ | $\bar{u}(\sigma^{\mu\nu}\gamma^\rho+\gamma^\rho\sigma^{\mu\nu})u\partial_\rho\widetilde{B}_{\mu\nu}$ | $\mathcal{E}_{Be}$ | $\bar{e}(\sigma^{\mu\nu}\gamma^\rho+\gamma^\rho\sigma^{\mu\nu})e\partial_\rho\widetilde{B}_{\mu\nu}$ |
| | | $\mathcal{E}'_{Bu}$ | $\mathrm{i}\bar{u}(\sigma^{\mu\nu}\slashed{D}-\overleftarrow{\slashed{D}}\sigma^{\mu\nu})uB_{\mu\nu}$ | $\mathcal{E}'_{Be}$ | $\mathrm{i}\bar{e}(\sigma^{\mu\nu}\slashed{D}-\overleftarrow{\slashed{D}}\sigma^{\mu\nu})eB_{\mu\nu}$ |
| | | $\mathcal{E}'_{\widetilde{B}u}$ | $\mathrm{i}\bar{u}(\sigma^{\mu\nu}\slashed{D}-\overleftarrow{\slashed{D}}\sigma^{\mu\nu})u\widetilde{B}_{\mu\nu}$ | $\mathcal{E}'_{\widetilde{B}e}$ | $\mathrm{i}\bar{e}(\sigma^{\mu\nu}\slashed{D}-\overleftarrow{\slashed{D}}\sigma^{\mu\nu})e\widetilde{B}_{\mu\nu}$ |

**Table 4.3:** One-loop generated evanescent operators. Operators in gray do not contribute to one loop generated operators in the Warsaw basis. Shaded operators are generated at two or higher order loops in SM extensions with fermions and scalars.

for which we have:

$$E = 2 = V_3 + 2V_4, \tag{4.2}$$

$$E = 3 = V_3 + 2V_4 + 3V_5. \tag{4.3}$$

Using these expressions and the form of possible renormalizable vertices (which further limits $n \leq 4$) between heavy and light fermions and scalars one can draw all generic 1lPI amplitudes. Moreover, since we extract the hard region part of the amplitude, loops involving light particles are directly not considered (because they yield scaleless integrals). Once we have the list of diagrams, we can immediately determine the quantum numbers of all possible UV completions that contribute to the operators we are interested in[2]. In practice, we can also determine the quantum numbers of those completions *a posteriori*, by using the result of the matching to a generic UV model as we describe in detail in the next section.

From all the operators in Table 4.1, the CP-violating operators in the $X^3$ class, namely $\mathcal{O}_{3\widetilde{W}}$ and $\mathcal{O}_{3\widetilde{G}}$, can only be generated at two-loop order in weakly coupled extensions of the SM with heavy scalars and fermions. This feature was already pointed out, within some simplifying assumptions, in [115].

[2]See [114, 115] for a similar approach to the classification of UV completions for the SMEFT under some simplifying assumptions.

The contributions for the $X^3$ class are simple enough that the complete classification and even the full result can be given in closed form. We can define the following operator:

$$\mathcal{O}_{3V} = \alpha_{3V} f^{ABC} V_\mu^{A\nu} V_\nu^{B\rho} V_\rho^{C\mu}, \tag{4.4}$$

for a general (non-abelian) gauge symmetry, with $f^{ABC}$ the structure constants of the group. This allows us to give the results for both $\alpha_{3W}$ and $\alpha_{3G}$ in the SMEFT. The only restriction on the heavy fields is that they are charged under the gauge symmetry, irrespectively on their hypercharge. The matching condition is the following [41]:

$$\alpha_{3V} = -\frac{1}{(4\pi)^2} \sum_R \frac{c_R\, g^3}{90 M_R^2} \mu(R), \quad c_R = \begin{cases} 1, & \text{Dirac fermions} \\ \frac{1}{2}, & \text{Majorana fermions} \\ -\frac{1}{2}, & \text{complex scalars} \\ -\frac{1}{4}, & \text{real scalars} \end{cases}, \tag{4.5}$$

with $\mathrm{Tr}(T_R^A T_R^B) = \mu(R)\delta^{AB}$ where $R$ runs over all the heavy fields in the model, $T_R$ are the generators of the group in $R$'s representation, $g$ is the gauge group's coupling constant.

## 4.3 Constructing the dictionary

In this section we review how the dictionary is computed in both directions, i.e., the matching results of particular models and the classification of models contributing to one coefficient.

### 4.3.1 Matching procedure

Let us start by explaining precisely how the matching is performed. Notice, in the first place, that the operators we are interested in are generated at least at one-loop order. Therefore, we do not need to take into account "universal" contributions in the form of wave-function renormalization or one-loop corrections to renormalizable couplings, that would give additional contributions at one-loop order only via tree level generated operators. Thus, all of these corrections (tree level generated operators and one-loop corrections to couplings or kinetic terms) will be disregarded in the following. The only caveat is the presence of tree level evanescent structures that shift the dipole operators in the Warsaw basis at one loop, that we do take into account following the results from [33] (see subsection 4.3.1.1).

The matching is performed using `matchmakereft` (see Chapter 3), therefore adopting a diagrammatic off-shell approach. Since we do not know *a priori* the representations of the heavy particles under the SM gauge group, we proceed in two steps. First we define a generic model consisting of the most general extension of the SM with heavy (Dirac or Majorana) fermions and (real or complex) scalars with all the renormalizable couplings allowed by Lorentz symmetry but leaving their gauge quantum numbers, and therefore the corresponding Clebsch-Gordan (CG) coefficients, arbitrary. The only assumptions made on this generic model are the following:

- It respects the SM gauge group symmetry, under which the new heavy particles transform in some arbitrary representation.

- The interaction basis coincides with the mass-eigenstates basis, i.e., mass terms are diagonal at tree level.
- Heavy fermions are vector-like, i.e., both chiralities transform under the same representation of the gauge group, so the UV theory has no chiral anomaly.

Denoting all fermions (both light and heavy) by a single field $\Psi_a$ and all scalars (light and heavy) by another one $\Phi_b$, where the indices, $a, b$, run over all relevant multiplets of the gauge group, we can write the generic form of the Lagrangian as follows:

$$\begin{aligned}\mathcal{L}_{\mathrm{UV}} =& \delta_{\Psi_a}\bar{\Psi}_a\Big[\mathrm{i}\not{D} - M_{\Psi_a}\Big]\Psi_a + \delta_{\Phi_a}\Big[|D_\mu\Phi_a|^2 - M^2_{\Phi_a}|\Phi_a|^2\Big]\\ &+ \sum_{\chi=L,R}\Big[Y^\chi_{abc}\overline{\Psi}_a P_\chi \Psi_b \Phi_c + \widetilde{Y}^\chi_{abc}\overline{\Psi}_a P_\chi\Psi_b\Phi^\dagger_c\\ &\qquad + X^\chi_{abc}\overline{\Psi^c}_a P_\chi\Psi_b\Phi_c + \widetilde{X}^\chi_{abc}\overline{\Psi^c}_a P_\chi\Psi_b\Phi^\dagger_c + \text{h.c.}\Big]\\ &+\Big[\kappa_{abc}\Phi_a\Phi_b\Phi_c + \kappa'_{abc}\Phi_a\Phi_b\Phi^\dagger_c + \lambda_{abcd}\Phi_a\Phi_b\Phi_c\Phi_d\\ &\quad + \lambda'_{abcd}\Phi_a\Phi_b\Phi_c\Phi^\dagger_d + \lambda''_{abcd}\Phi_a\Phi_b\Phi^\dagger_c\Phi^\dagger_d + \text{h.c.}\Big],\end{aligned} \tag{4.6}$$

where $\Psi^c \equiv \mathcal{C}\overline{\Psi}^T$ with $\mathcal{C}$ the charge conjugation matrix, $\delta_{\Psi_a}$ is 1 (1/2) times the identity matrix for complex (Majorana, satisfying $\Psi^c_a = \Psi_a$) fermions and $\delta_{\Phi_a}$ is 1 (1/2) times the identity matrix for complex (real, satisfying $\Phi^\dagger_a = \Phi_a$) scalars and all the light fields are massless except for the SM Higgs doublet. The remaining couplings represent, for each fixed value of the indices, coupling constants times CG tensors. Our convention for the covariant derivative is the following:

$$D_\mu\Psi = (\partial_\mu - \mathrm{i}g_1 B_\mu Y_\Psi - \mathrm{i}g_2 W^a_\mu T^a_W - \mathrm{i}g_3 G^a_\mu T^a_G)\Psi, \tag{4.7}$$

where $T_W(T_G)$ are the generators of SU(2) (SU(3)) in the representation of $\Psi$, and $Y_\Psi$ is its hypercharge. Also note that, despite the explicit sign for the interactions in Eq. (4.6), we still follow conventions for the SM interactions stated in Appendix A:

$$\widetilde{Y}^R_{q^i u^j \phi} = -\,\mathrm{i}\sigma^2 (Y_u)_{ij}, \tag{4.8}$$
$$Y^R_{q^i d^j \phi} = -\,(Y_d)_{ij}, \tag{4.9}$$
$$Y^R_{l^i e^j \phi} = -\,(Y_e)_{ij}, \tag{4.10}$$
$$\lambda''_{\phi^4} = -\,\lambda/2, \tag{4.11}$$

with $\sigma^2$ the second Pauli matrix. Given this generic model, we use `matchmakereft` to perform the calculation of the hard region of the amplitudes. As explained in Section 3.1, the first time an EFT model is matched using `matchmakereft`, we obtain a solution for the Wilson Coefficients in terms of arbitrary coefficients of kinematic and gauge structures in the UV. This information, for the case of the SMEFT, is then used to extract directly the relevant kinematic structures from our result. The gauge information is however still left generic at this point. This result is stored internally, as it will be common for any extension of the SM, so that we do not need to repeat this calculation. In a second step, once the specific quantum numbers for the heavy fields are fixed, we use `GroupMath` [116] to perform the remaining group-theoretic calculation.

Results in the Warsaw basis are computed obtaining first all the relevant coefficients in the Green's basis and then using the redundancies provided in [64] to project into the physical basis. We follow the NDR prescription for $\gamma^5$, as implemented in `matchmakereft`, which is compatible with the scheme introduced in [33] to compute the evanescent contributions.

#### 4.3.1.1 Evanescent contribution to the dipole operators

As mentioned above, tree level generated operators can produce tree level evanescent structures that would shift the coefficients of the physical basis. This was studied in detail in [33] with the result that, among the three classes of operators considered in this work, only the dipole operators receive a contribution from evanescent ones. Given the small number of extensions in which this effect is relevant, collected in Table **??**, we present below the results explicitly. The shifts in the dipole operators, as computed in [33], using the conventions in [64], read:

$$(\alpha_{eB})_{ij} \to (\alpha_{eB})_{ij} + \frac{g_1}{(4\pi)^2}\left[\frac{3}{8}(\gamma_{le})_{ijst}(Y_e)_{ts} - \frac{5}{8}(1-\xi_{rp})(Y_u)^*_{ts}(\gamma^c_{uelq})_{sjit} \right. \\ \left. + \frac{5}{8}(1-\xi_{rp})(\gamma_{luqe})_{itsj}(Y_u)^*_{st}\right], \tag{4.12}$$

$$(\alpha_{eW})_{ij} \to (\alpha_{eW})_{ij} + \frac{g_2}{(4\pi)^2}\left[-\frac{1}{8}(Y_e)_{ts}(\gamma_{le})_{ijst} + \frac{3}{8}(1-\xi_{rp})(Y_u)^*_{ts}(\gamma^c_{uelq})_{sjit} \right. \\ \left. - \frac{3}{8}(1-\xi_{rp})(Y_u)^*_{st}(\gamma_{luqe})_{itsj}\right], \tag{4.13}$$

$$(\alpha_{uB})_{ij} \to (\alpha_{uB})_{ij} - \frac{g_1}{(4\pi)^2}\frac{5}{8}(Y_u)_{ts}(\gamma_{qu})_{ijst}, \tag{4.14}$$

$$(\alpha_{uW})_{ij} \to (\alpha_{uW})_{ij} - \frac{g_2}{(4\pi)^2}\frac{3}{8}(Y_u)_{ts}(\gamma_{qu})_{ijst}, \tag{4.15}$$

$$(\alpha_{uG})_{ij} \to (\alpha_{uG})_{ij} - \frac{g_3}{(4\pi)^2}\frac{1}{4}(Y_u)_{ts}(\gamma^{(8)}_{qu})_{ijst}, \tag{4.16}$$

$$(\alpha_{dB})_{ij} \to (\alpha_{dB})_{ij} + \frac{g_1}{(4\pi)^2}\frac{1}{8}(Y_d)_{ts}(\gamma_{qd})_{ijst}, \tag{4.17}$$

$$(\alpha_{dW})_{ij} \to (\alpha_{dW})_{ij} - \frac{g_2}{(4\pi)^2}\frac{3}{8}(Y_d)_{ts}(\gamma_{qd})_{ijst}, \tag{4.18}$$

$$(\alpha_{dG})_{ij} \to (\alpha_{dG})_{ij} - \frac{g_3}{(4\pi)^2}\frac{1}{4}(Y_d)_{ts}(\gamma^{(8)}_{qd})_{ijst}. \tag{4.19}$$

In the equations above $Y_{u,d,e}$ stand for the up-type, down-type and charged electron Yukawa couplings, respectively, and $\xi_{rp}$ represents a reading point parameter and has `xRP` as output format in `SOLD` (see [33] for more details). The remaining coefficients correspond to tree-level contributions to evanescent structures. Using the notation in the tree level dictionary [102] they correspond to the following expressions:

$$(\gamma_{le})_{ijkl} = \frac{(y^e_\varphi)^*_{ji}(y^e_\varphi)_{kl}}{M^2_\varphi}, \tag{4.20}$$

$$(\gamma^c_{uelq})_{ijkl} = -\frac{(y^{eu}_{\omega_1})_{ji}(y^{ql}_{\omega_1})^*_{lk}}{M^2_{\omega_1}}, \tag{4.21}$$

$$(\gamma_{luqe})_{ijkl} = \frac{(y^{lu}_{\Pi_7})_{ij}(y^{eq}_{\Pi_7})^*_{lk}}{M^2_{\Pi_7}}, \tag{4.22}$$

| Heavy Field | Shifted operator |
|---|---|
| $\varphi \sim (1, 2, \frac{1}{2})$ | $\mathcal{O}_{eB}, \mathcal{O}_{eW}, \mathcal{O}_{uB}, \mathcal{O}_{uW}, \mathcal{O}_{dB}, \mathcal{O}_{dW}$ |
| $\omega_1 \sim (3, 1, -\frac{1}{3})$ | $\mathcal{O}_{eB}, \mathcal{O}_{eW}$ |
| $\Phi \sim (8, 2, \frac{1}{2})$ | $\mathcal{O}_{uG}, \mathcal{O}_{dG}$ |
| $\Pi_7 \sim (3, 2, \frac{7}{6})$ | $\mathcal{O}_{eB}, \mathcal{O}_{eW}$ |

**Table 4.4:** List of all the SM extensions that generate a tree level evanescent structure that shifts the dipole operators in the Warsaw basis. The notation for the heavy fields follows the conventions in [102].

$$(\gamma_{qu})_{ijkl} = \frac{(y^u_\varphi)_{ij}(y^u_\varphi)^*_{lk}}{M^2_\varphi}, \tag{4.23}$$

$$(\gamma_{qd})_{ijkl} = \frac{(y^d_\varphi)^*_{ji}(y^d_\varphi)_{kl}}{M^2_\varphi}, \tag{4.24}$$

$$(\gamma^{(8)}_{qu})_{ijkl} = \frac{(y^u_\Phi)_{ij}(y^u_\Phi)^*_{lk}}{M^2_\Phi}, \tag{4.25}$$

$$(\gamma^{(8)}_{qd})_{ijkl} = \frac{(y^d_\Phi)^*_{ji}(y^d_\Phi)_{kl}}{M^2_\Phi}. \tag{4.26}$$

### 4.3.2 Model classification

The complementary, bottom-up use of the dictionary, as mentioned above, consists of the classification of all possible (renormalizable) SM extensions including heavy scalar and fermion fields whose one-loop contribution to a certain WC, either in the SMEFT Warsaw or Green's basis, is allowed by gauge symmetry. Notice that, contrary to what happens in the tree level case, the list of all possible models is infinite. The reason is that couplings that are quadratic in heavy fields can contribute for the first time at one-loop order, thus allowing for loop topologies in which the gauge representations for the fields running in the loop are not fixed, but only their product is. Consequently, one can only impose the restrictions that the fields must satisfy to contribute through a certain diagram, but these can be fulfilled by an infinite number of representations.

Nevertheless, the classification of all possible new physics models can still be given in a closed form using two different levels: on the first level we provide a complete, finite list of the restrictions to be fulfilled by the new fields; on a second level we give a list of the allowed specific representations that satisfy any of these conditions, up to certain dimension of such representations (the list being infinite otherwise). As we will see below, the `Mathematica` package `SOLD`, that encodes the one-loop dictionary, includes routines to perform both tasks.

The list of restrictions (at first level) can be easily computed in a comprehensive way making use of the intermediate results of the matching as discussed in the previous section. Once a specific WC is matched and expressed in terms of a combination of CG tensors, one can simply check the restrictions on the quantum numbers of the heavy fields so that each diagram is allowed by gauge symmetry. Note, however, that we are just imposing that the result is non-zero *a priori*; the particular value of the gauge structure depends on specific choices for the representations, so it could happen that it vanishes for some of them, or even that some cancellation happens between different diagrams. The list of restrictions for each diagram defines implicitly a new possible extension and it is added to the complete list. These restrictions are then reduced so that they contain the minimum number of different fields needed to satisfy them. Finally, we eliminate from the complete list those models that are related by conjugation of one of the fields, since they are physically equivalent. In the case of the classification for coefficients in the Warsaw basis, we compute this list for every coefficient that can contribute to it through redundancies.

The complete list of models, even at the first level, is too long to be reported here and is given in electronic form via the `SOLD` package. The only exception is the operators in the $X^3$ class, for which both the classification and the result are given in Section 4.1. An interesting result of our calculation is that the two CP-violating operators with three field strength tensors, namely, $\mathcal{O}_{\widetilde{3W}}$ and $\mathcal{O}_{\widetilde{3G}}$, are not generated at one-loop order in any renormalizable extension of the SM with heavy scalars or fermions.

## 4.4 `SOLD` usage

This section is devoted to provide a detailed description of the `Mathematica` package `SOLD`, that encodes the calculation of the sector of the SMEFT one-loop dictionary described above.

### 4.4.1 Installation

`SOLD` is publicly available in the following Gitlab repository: `https://gitlab.com/jsantiago_ugr/sold`. Before using `SOLD`, one should make sure that `GroupMath` is already installed (otherwise, a reminder will be issued when installing `SOLD`). The same applies to `matchmakereft` if the user is interested in the functionalities that make use of it (see below). There are two ways of installing the package:

1. **Automatic installation**. `SOLD` can be installed in a fully automated way by typing the following command on a `Mathematica` notebook:

```
In[1]:= Import["https://gitlab.com/jsantiago_ugr/sold/-/raw/main
        /install.m"]
```

   This will download the package and place it in the `Applications` folder of `Mathematica`'s base directory. The same command will (re)install the latest version available in the repository.

2. **Manual installation**. The alternative way is to manually download the package from the `SOLD` repository and place it in the `Applications` folder of `Mathematica`'s base directory, or a different directory as long as it is included in the variable `$Path`.

Once it is correctly installed, `SOLD` can be loaded in any `Mathematica` notebook in the usual way:

```
In[2]:= << SOLD`
```

with an output shown in Fig. 4.1. When loading `SOLD`, it automatically checks the latest version available and raises a warning if the installed version is outdated.

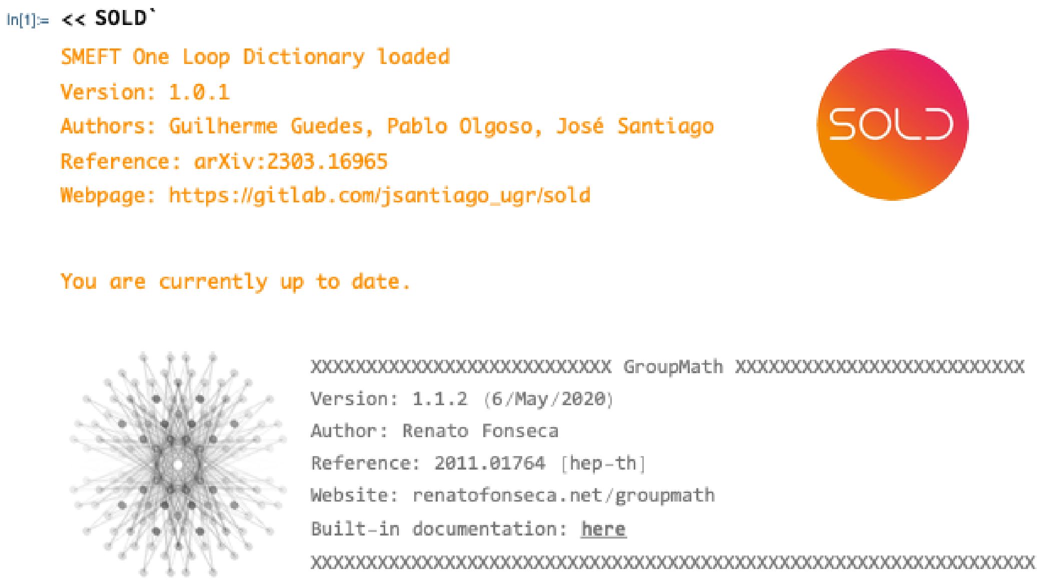


**Figure 4.1:** Output generated by loading `SOLD`, given that the latest version is installed.

### 4.4.2 List of functions

We describe below the list of all the functions available in the `SOLD` package. The usual help command in `Mathematica` can be used to obtain more information on them, while some detailed examples of their usage and output can be found in next section. An updated version of the manual can be found in `SOLD`'s installation directory.

- `OneLoopOperatorsGrid`. Displays a grid with the SMEFT operators in the Warsaw basis whose leading contribution is at one loop (see Table 4.1). When the mouse is on top of each entry the expression of the operator is displayed, and when clicked, the different contributions from redundant coefficients of the Green's basis are shown.

- `ListModelsWarsaw[coefficient]`. Returns a list with all possible SM extensions (sometimes implicitly defined by restrictions in the product of some representations, as described in the previous section) whose contribution to `coefficient` in the SMEFT Warsaw basis is allowed by gauge symmetry. The notation for the name of the coefficients follow `matchmakereft` and a list of all coefficients is stored in the variable `AllCoefficientsWarsaw`. Each entry of the result represents a different SM extension. For each entry of the list, the first item indicates the field content of the model (number and spin of heavy fields, with $\psi i$ and $\phi i$ indicating fermions and scalars, respectively, with $i$ a numeric tag), the second item contains the restrictions that the $\mathrm{SU}(3)\otimes\mathrm{SU}(2)$ representations of the new fields should fulfill, and the last item indicates the restrictions on the hypercharge.

- `ListModelsGreen[coefficient]`. Identical to the previous function but for operators in the Green's basis.

- `ListValidQNs[listrestrictions,<MaxDimSU3>,<MaxDimSU2>]`. Computes the valid representations under $\mathrm{SU}(3)\otimes\mathrm{SU}(2)$, up to dimensions `MaxDimSU3` and `MaxDimSU2`, respectively, allowed by `listrestrictions`, for the fields contained in it. `listrestrictions` can be either the direct output of `ListModelsWarsaw` or `ListModelsGreen`, a sublist of its entries or just an entry's second item. `MaxDimSU3` and `MaxDimSU2` are optional arguments and their default values are 15 and 5, respectively.

- `Match2Warsaw[coefficient, extension]`. Computes the contribution to a particular WC `coefficient` in the Warsaw basis generated by a model defined by `extension`, where `extension` is a list of replacement rules with a tag to identify the heavy particle (that must begin with an S or F, depending on whether the heavy particle is a scalar or a fermion respectively and be followed by an identifying letter) and a list of its quantum numbers under SU(3) $\otimes$ SU(2) $\otimes$ U(1). As an explicit example, if we wanted to compute the matching condition of $(\mathcal{O}_{eW})_{i,j}$ from the SM extended with an SU(2) triplet vector-like lepton of hypercharge -1, a triplet scalar leptoquark of hypercharge -1/3 and a triplet vector-like quark of hypercharge -4/3 [89], we would need to write:

```
In[3]:= Match2Warsaw[alphaOeW[i,j],
            {Sa->{3,3,-1/3},Fa->{1,3,-1},Fb->{3,3,-4/3}}]
```

  Note that the definitions of `coefficient` follow `matchmakereft` convention. Explicit numerical values for the flavor indices are also allowed.

  In order to allow for different, non-equivalent SU(3) representations of the same dimension, as well as conjugated ones, Dynkin indices can be used as a valid input for SU(3). Note that this is not necessary for SU(2). An explicit example of an input in this format is provided in the next section. Symbolic hypercharges for the heavy fields are also supported, as long as they are called `Yi`, where `i` is an integer character. However, only vertices that formally conserve hypercharge will be taken as non-zero. This means, for instance, that fields with symbolic hypercharge will never couple linearly with SM.

- `Match2Green[coefficient,extension]`. Computes the contribution to `coefficient` in the Green's basis of Appendix B. The conventions for `coefficient` and `extension` are the same as for the function `Match2Warsaw`.

- `NiceOutput[result,<ListSubstitutions>]`. Returns a more readable expression of `result`. `ListSubstitutions` is optional and set to `False` by default. If set to `True`, it prints a list of the substitutions performed.

- `SOLDInputForm[fieldreps]`. Translates the gauge representation of a field (including its hypercharge) from the output form given by `ListValidQNs` to a valid input form usable by `Match2Warsaw`, `Match2Green`, `CreateLag`, `GenerateMMEModel` or `CompleteOneLoopMatching`. An explicit example of this function is given in the next section.

- `CreateLag[extension]`. Returns the full Lagrangian internally used to compute results produced by `extension`, including the numerical values of each of the CG tensors, which are presented as `TSi` or `TCi` for the SU(2) and SU(3) contraction respectively, where `i` corresponds to an identifying numeric tag.

- `GenerateMMEModel[extension, modelname, <outputdirectory>]`. Generates, in the `outputdirectory`, the `matchmakereft` model needed for the full one loop computation (the files included are also useful to use with other tools such as FeynRules). The file modelname.fr contains the full Lagrangian of extension, as computed by CreateLag, the heavy particles and parameter definitions, all in FeynRules format. The file SM_SOLD.fr contains the SM definition in FeynRules format and in case that the heavy particles in extension have exotic representations under the SM gauge group, it adds these representations to the definition of the gauge groups. The file modelname.gauge contains the numerical definitions of the CG tensors considered in the definition of the Lagrangian. outputdirectory is optional and set to Mathematica's current working directory by default.

- CompleteOneLoopMatching[extension, modelname, <EFTname>,<outputdirectory>]. Runs matchmakereft to obtain the complete one-loop matching conditions between a UV extension and an effective theory EFTname. If there is no modelname_MM in outputdirectory, the model is first created by calling GenerateMMEModel. EFTname is an optional argument and takes the default value of the matchmakereft's model for the SMEFT, SMEFT_Green_BPreserving_MM. outputdirectory is also optional and set to Mathematica's current working directory by default. Before doing the calculation, matchmakereft's installed version is checked to be the latest available one to avoid possible errors.

Note that matchmakereft must be installed to run these last two functions, GenerateMMEModel and CompleteOneLoopMatching. When these two functions are used to run matchmakereft from a Mathematica notebook, the output is only printed at the end of whole calculation. For a more informative process we recommend the user to create the model within SOLD using the GenerateMMEModel function and then run the matching from matchmakereft in the terminal directly. Likewise, we strongly recommend that the latest version of matchmakereft is always used in conjuction with SOLD, as this could be the culprit of some errors otherwise.

### 4.4.3 Example of usage

In this subsection we provide an example to illustrate in more detail the usage of the different functions in the package in sequential order. In preparation for the phenomenological study in the next section, we will consider that the user is interested in using the dictionary to explore the UV completions which could generate the SMEFT operator $\mathcal{O}_{dG}$.

After loading SOLD, the natural first step is listing the conditions on the models that can generate this operator. This can be achieved by the command:

```
In[4]:= ListModelsWarsaw[alphaOdG[i,j]]
```

whose output is partially shown in Fig. 4.2.

Note that, for the $\mathrm{SU}(3)\otimes\mathrm{SU}(2)$ restrictions a rule is used to indicate that the representation for the corresponding particle is fixed whereas the symbol $\supset$ appears when only the product is constrained. For the case of U(1) an unconstrained hypercharge is explicitly written only when it does not appear in other conditions. We also include redundant restrictions such as $\phi 2\otimes\overline{\phi 2}\supset 1\otimes 1$ because, while $\phi 2$ in this case can have any quantum numbers, there

In[2]:=
```
listofmodels = ListModelsWarsaw[alphaOdG[i, j]];
MatrixForm[Join[Take[listofmodels⟦1⟧, {1, 3}], {{"....", "....", "...."}}, Take[listofmodels⟦1⟧, {20, 22}],
  {{"....", "....", "...."}}, Take[listofmodels⟦1⟧, {145, 146}], {{"....", "....", "...."}}]]
```

Out[3]//MatrixForm=

| Field Content | SU(3) ⊗ SU(2) | U(1) |
|---|---|---|
| $\{\phi 1\}$ | $\{\phi 1 \to \mathbf{\bar{3}} \otimes \mathbf{1}\}$ | $\{Y_{\phi 1} \to \frac{1}{3}\}$ |
| $\{\phi 1\}$ | $\{\phi 1 \to \mathbf{\bar{3}} \otimes \mathbf{1}\}$ | $\{Y_{\phi 1} \to \frac{4}{3}\}$ |
| .... | .... | .... |
| $\{\phi 1, \phi 2\}$ | $\{\phi 1 \to \mathbf{8} \otimes \mathbf{2},\ \phi 2 \otimes \overline{\phi 2} \supset \mathbf{8} \otimes \mathbf{3}\}$ | $\{Y_{\phi 1} \to -\frac{1}{2},\ Y_{\phi 2}\}$ |
| $\{\phi 1, \psi 1\}$ | $\{\psi 1 \otimes \overline{\phi 1} \supset \mathbf{\bar{3}} \otimes \mathbf{1}\}$ | $\{Y_{\psi 1} \to \frac{1}{3} + Y_{\phi 1}\}$ |
| $\{\phi 1, \psi 1\}$ | $\{\psi 1 \otimes \overline{\phi 1} \supset \mathbf{\bar{3}} \otimes \mathbf{2}\}$ | $\{Y_{\psi 1} \to -\frac{1}{6} + Y_{\phi 1}\}$ |
| .... | .... | .... |
| $\{\phi 1, \psi 1, \psi 2\}$ | $\{\psi 1 \otimes \overline{\phi 1} \supset \mathbf{\bar{3}} \otimes \mathbf{2},\ \psi 1 \otimes \psi 2 \supset \mathbf{1} \otimes \mathbf{2},\ \psi 2 \otimes \phi 1 \supset \mathbf{3} \otimes \mathbf{1}\}$ | $\{Y_{\psi 1} \to -\frac{1}{6} + Y_{\phi 1},\ Y_{\psi 2} \to -\frac{1}{3} - Y_{\phi 1}\}$ |
| $\{\phi 1, \psi 1, \psi 2\}$ | $\{\psi 1 \otimes \overline{\phi 1} \supset \mathbf{\bar{3}} \otimes \mathbf{2},\ \psi 2 \otimes \overline{\psi 1} \supset \mathbf{1} \otimes \mathbf{2},\ \psi 2 \otimes \overline{\phi 1} \supset \mathbf{3} \otimes \mathbf{1}\}$ | $\{Y_{\psi 1} \to -\frac{1}{6} + Y_{\phi 1},\ Y_{\psi 2} \to \frac{1}{3} + Y_{\phi 1}\}$ |
| .... | .... | .... |

**Figure 4.2:** Partial output of the command `ListModelsWarsaw[alphaOdG[i,j]]`.

has to be information that it exists in the extension so that it is included when finding the valid quantum numbers that respect the restrictions.

After obtaining the restrictions, the subsequent step is to find the actual combinations of quantum numbers which respect them. As such, we would have to use the command:

In[5]:=
```
ListValidQNs[conditions]
```

where `conditions` stands for the output of the `ListModelsWarsaw[...]` command or a sublist of it. The resulting list of models, using as condition the second one from the bottom appearing in Fig. 4.2, is partially shown in Fig. 4.3. The output consist of a list in which each entry is a different extension respecting the restriction given by the previous command.

In[13]:=
```
modelQNs = ListValidQNs[listofmodels⟦1, 145⟧];
Print["Model restriction :", listofmodels⟦1, 145⟧, "\nList of Models:\n",
 MatrixForm[Join[Take[modelQNs, {1, 3}], {{"....", "....", "...."}}, Take[modelQNs, {-3, -1}]]]]
```

Model restriction : $\{\{\phi 1, \psi 1, \psi 2\}, \{\psi 1 \otimes \overline{\phi 1} \supset \mathbf{\bar{3}} \otimes \mathbf{2},\ \psi 1 \otimes \psi 2 \supset \mathbf{1} \otimes \mathbf{2},\ \psi 2 \otimes \phi 1 \supset \mathbf{3} \otimes \mathbf{1}\}, \{Y_{\psi 1} \to -\frac{1}{6} + Y_{\phi 1},\ Y_{\psi 2} \to -\frac{1}{3} - Y_{\phi 1}\}\}$

List of Models:

| | | |
|---|---|---|
| $\phi 1 \to \mathbf{1} \otimes \mathbf{1} \otimes Y_{\phi 1}$ | $\psi 1 \to \mathbf{\bar{3}} \otimes \mathbf{2} \otimes \left(-\frac{1}{6} + Y_{\phi 1}\right)$ | $\psi 2 \to \mathbf{3} \otimes \mathbf{1} \otimes \left(-\frac{1}{3} - Y_{\phi 1}\right)$ |
| $\phi 1 \to \mathbf{1} \otimes \mathbf{2} \otimes Y_{\phi 1}$ | $\psi 1 \to \mathbf{\bar{3}} \otimes \mathbf{1} \otimes \left(-\frac{1}{6} + Y_{\phi 1}\right)$ | $\psi 2 \to \mathbf{3} \otimes \mathbf{2} \otimes \left(-\frac{1}{3} - Y_{\phi 1}\right)$ |
| $\phi 1 \to \mathbf{1} \otimes \mathbf{2} \otimes Y_{\phi 1}$ | $\psi 1 \to \mathbf{\bar{3}} \otimes \mathbf{3} \otimes \left(-\frac{1}{6} + Y_{\phi 1}\right)$ | $\psi 2 \to \mathbf{3} \otimes \mathbf{2} \otimes \left(-\frac{1}{3} - Y_{\phi 1}\right)$ |
| .... | .... | .... |
| $\phi 1 \to \mathbf{15'} \otimes \mathbf{4} \otimes Y_{\phi 1}$ | $\psi 1 \to \mathbf{10} \otimes \mathbf{3} \otimes \left(-\frac{1}{6} + Y_{\phi 1}\right)$ | $\psi 2 \to \mathbf{\overline{10}} \otimes \mathbf{4} \otimes \left(-\frac{1}{3} - Y_{\phi 1}\right)$ |
| $\phi 1 \to \mathbf{15'} \otimes \mathbf{4} \otimes Y_{\phi 1}$ | $\psi 1 \to \mathbf{10} \otimes \mathbf{5} \otimes \left(-\frac{1}{6} + Y_{\phi 1}\right)$ | $\psi 2 \to \mathbf{\overline{10}} \otimes \mathbf{4} \otimes \left(-\frac{1}{3} - Y_{\phi 1}\right)$ |
| $\phi 1 \to \mathbf{15'} \otimes \mathbf{5} \otimes Y_{\phi 1}$ | $\psi 1 \to \mathbf{10} \otimes \mathbf{4} \otimes \left(-\frac{1}{6} + Y_{\phi 1}\right)$ | $\psi 2 \to \mathbf{\overline{10}} \otimes \mathbf{5} \otimes \left(-\frac{1}{3} - Y_{\phi 1}\right)$ |

**Figure 4.3:** Output of the `ListValidQNs` command for one restriction, i.e., one entry from the output of `ListModelsWarsaw[alphaOdG[i,j]]`.

From this list of possible extensions, let us suppose that we want to focus on studying, for instance, the first one appearing in Fig. 4.3. It consists of one heavy scalar and two heavy fermions with the following quantum numbers: $\phi_a \sim (1, 1, \mathrm{Y1})$; $\psi_a \sim (\bar{3}, 2, \mathrm{Y1} - 1/6)$ and $\psi_b \sim (3, 1, -\mathrm{Y1} - 1/3)$. We can obtain the one-loop matching result for the WC of the $(\mathcal{O}_{dG})_{ij}$ operator in this model by simply typing the following command (using the Dynkin index notation for the SU(3) representations):

```
In[6]:= Match2Warsaw[alphaOdG[i,j],
          {Sa->{{0,0},1,Y1},Fa->{{0,1},2,-(1/6)+Y1},Fb->{{1,0},1,-(1/3)-Y1}}]
```

Note that the correct format for the model such that it can be used as an input in `Match2Warsaw` can be obtained using the `ListValidQNs[...]` command as follows:

```
In[7]:= ourModel = SOLDInputForm /@ modelQNs[[1]]

Out[7]= {Sa->{{0,0},1,Y1},Fa->{{0,1},2,-(1/6)+Y1},Fb->{{1,0},1,-(1/3)-Y1}}
```

where `modelQNs` is defined in Fig. 4.3. The result from `Match2Warsaw` is given in Fig. 4.4, in the limit of equal masses and vanishing down-type Yukawa couplings.

```
In[2]:= Limit[
          Match2Warsaw[alphaOdG[i, j], {Sa → {{0, 0}, 1, Y1}, Fa → {{0, 1}, 2, -(1 / 6) + Y1},
             Fb → {{1, 0}, 1, -(1 / 3) - Y1}}] /. L1[qLbar, dR, phi][__] → 0, {MFa → MSa, MFb → MSa}] //
         FullSimplify

Out[2]= -(1/(384 MSa^2 π^2)) g3 (L1[Fa, Fb, phi, L] - 3 L1[Fa, Fb, phi, R]) × L1bar[dRbar, Fb, Sa][j] × L1bar[Sabar, Fa, qL][i]
```

**Figure 4.4:** Result for the WC of the $(\mathcal{O}_{dG})_{ij}$ operator in the Warsaw basis for a particular extension (see the text for more details) in the limit of degenerate masses and neglecting terms proportional to the down-type Yukawa couplings.

The couplings of the SM extension in the output of `Match2Warsaw` and `Match2Green` are denoted as `Li`, with `i` an identifying integer. A `bar` is appended when the coupling corresponds to the hermitian conjugate of the corresponding operator. These couplings are identified by two possible sets of arguments: the first one corresponds to the fields which compose the corresponding renormalizable operator (and an $R$ or $L$ in the case of operators with two heavy fermions, denoting the two independent chiralities); the second set corresponds to flavor indices in case the operator contains light fermions. The number `i` distinguishes couplings of operators with the same field content but with different gauge contractions. The masses of the heavy fields are defined as `MX` where `X` is the tag, given by the user, of the heavy state. This raw result might seem a bit intricate and not easy to read, but it is given as the default output to facilitate the user to easily make any desired simplifications, such as the one shown in Fig. 4.4, where the down-type Yukawa was sent to zero.

Nevertheless, a more readable expression can be obtained using the `NiceOutput` function, whose output is shown in Fig. 4.5. In `NiceOutput` format, couplings are represented by $\lambda$ (or other greek letters in case there is more than one relevant operator with the same field content), except for the Yukawa couplings which are hard-coded to be written as $y$. The subscript of these couplings denotes the fields composing the corresponding operator, whereas the superscript can be either $R$ or $L$, depending on whether the operator has a right- or left-handed projector (for operators with two heavy fermions) or the flavor indices for operators with light fermions. Notice that, when set to true, the optional argument in `NiceOutput` has the effect of printing a list of the correspondence between the couplings in both the default and the `NiceOutput` formats.

Besides the informative output format, one can naturally check the precise definition of any coupling by calling the function `CreateLag`, whose output is the complete Lagrangian of the UV

```
In[3]:= NiceOutput[
         Limit[
           Match2Warsaw[alphaOdG[i, j], {Sa → {{0, 0}, 1, Y1}, Fa → {{0, 1}, 2, -(1/6) + Y1},
              Fb → {{1, 0}, 1, -(1/3) - Y1}}] /. L1[qLbar, dR, phi][__] → 0, {MFa → MSa, MFb → MSa}] // FullSimplify,
         True]
```

$\{$g3 $\to g_3$, MSa $\to M_{Sa}$, L1[Fa, Fb, phi, L] $\to \lambda^{[L]}{}_{Fa,Fb,\phi}$, L1[Fa, Fb, phi, R] $\to \lambda^{[R]}{}_{Fa,Fb,\phi}$, L1bar[dRbar, Fb, Sa][j] $\to \overline{\lambda}_{\overline{dR},Fb,Sa}{}^{[j]}$, L1bar[Sabar, Fa, qL][i] $\to \overline{\lambda}_{\overline{Sa},Fa,qL}{}^{[i]}\}$

Out[3]= $-\dfrac{g_3\left(\lambda^{[L]}{}_{Fa,Fb,\phi}-3\,\lambda^{[R]}{}_{Fa,Fb,\phi}\right)\overline{\lambda}_{\overline{dR},Fb,Sa}{}^{[j]}\,\overline{\lambda}_{\overline{Sa},Fa,qL}{}^{[i]}}{384\,\pi^2\,M_{Sa}^2}$

**Figure 4.5:** Warsaw basis result for the WC of the $(\mathcal{O}_{dG})_{ij}$ operator for the same extension (see text), in the limit of degenerate masses and vanishing down-type Yukawa couplings, using the `NiceOutput` function to obtain a more readable expression. The last argument, set to `True` in this example, prints a list of the replacements performed to the output in Figure 4.4 to obtain this one.

extension. This not only includes the correspondence between couplings and interaction terms but also the numerical values used for the CG coefficients for each coupling. The Lagrangian is given in `FeynRules` [77] notation, where the arguments of the fields correspond to their indices, and the CG tensors are named as `TCi` and `TSi` for the SU(3) and SU(2) contractions, respectively, with `i` an identifying integer. Kinetic terms are omitted and follow the conventions in Eq. (4.6). The explicit values for the group generators can be obtained using the routine `RepMatrices` in `GroupMath`. An example of the output of `CreateLag` is shown in Fig. 4.6.

```
In[2]:= CreateLag[{Sa → {{0, 0}, 1, Y1}, Fa → {{0, 1}, 2, -(1/6) + Y1}, Fb → {{1, 0}, 1, -(1/3) - Y1}}]
```

Out[2]= $\{$Sa$^2$ Sabar$^2$ $\lambda_{\overline{Sa},\overline{Sa},Sa,Sa}$ + Sa DRbar[sp1, ff0, cc0].Fb[sp1, cc1] $\lambda_{\overline{dR},Fb,Sa}{}^{[ff0]}$ TC51[cc0, cc1] +
Sa Sabar Phi[ss2] × Phibar[ss0] $\lambda_{\overline{\phi},\overline{Sa},\phi,Sa}$ TS11[ss0, ss2] +
CC[Fabar[sp1, ss0, cc0]].left[Fb[sp1, cc1]] × Phi[ss2] $\lambda^{[L]}{}_{Fa,Fb,\phi}$ TC31[cc0, cc1] × TS31[ss0, ss2] +
CC[Fabar[sp1, ss0, cc0]].right[Fb[sp1, cc1]] × Phi[ss2] $\lambda^{[R]}{}_{Fa,Fb,\phi}$ TC31[cc0, cc1] × TS31[ss0, ss2] +
Sabar CC[Fabar[sp1, ss1, cc1]].QL[sp1, ss2, ff0, cc2] $\lambda_{\overline{Sa},Fa,qL}{}^{[ff0]}$ TC41[cc1, cc2] × TS41[ss1, ss2],
{TS11 → {{1, 0}, {0, 1}}, TC31 → {{1, 0, 0}, {0, 1, 0}, {0, 0, 1}}, TS31 → {{0, -1}, {1, 0}},
TC41 → {{1, 0, 0}, {0, 1, 0}, {0, 0, 1}}, TS41 → {{0, -1}, {1, 0}}, TC51 → {{1, 0, 0}, {0, 1, 0}, {0, 0, 1}}}$\}$

**Figure 4.6:** Output of the CreateLag function.

Finally, one can be interested in studying the implications of this model in other operators or observables. The function `GenerateMMEModel` allows then to generate automatically a `matchmakereft` model by simply specifying the representations of the new heavy fields:

```
In[8]:= GenerateMMEModel[{Sa->{{0,0},1,Y1},Fa->{{0,1},2,-(1/6)+Y1},
        Fb->{{1,0},1,-(1/3)-Y1}},"model"]
```

and we can perform the complete one-loop matching to the SMEFT (or any other EFT) using `matchmakereft` by simply running following the command:

```
In[9]:= CompleteOneLoopMatching[{Sa->{{0,0},1,Y1},Fa->{{0,1},2,-(1/6)+Y1},
        Fb->{{1,0},1,-(1/3)-Y1}},"model"]
```

## 4.5 A phenomenological example

The ultimate goal of the one-loop IR/UV dictionary is to improve the efficiency in the search for new physics and, as such, to use it in phenomenologically relevant applications. The purpose of this section is to illustrate how the dictionary can be used in practice with a simple but phenomenologically motivated example, before performing a more detailed and extensive study in the next chapter.

Even in its current partial form, the dictionary can still be used to classify in a comprehensive way the origin, and the corresponding phenomenological implications in other experimental measurements, of experimental anomalies eventually reported. We will consider, for the sake of the exposition, a recently reported tension (around $\sim 2\sigma$ in significance) in different non-leptonic decays of B mesons [117]. A discussion on this tension and its interpretations in terms of SMEFT operators is beyond the scope of this section, so we refer to the original article for all the relevant details and simply use one of the proposed solutions in terms of the following effective Lagrangian:

$$\mathcal{L} = \frac{G_F}{2}\frac{g_3}{4\pi^2} m_b \sum_{q=d,s} C_{8gq}(V_{ub}V_{uq}^* + V_{cb}V_{cq}^*)\bar{q}_L\sigma^{\mu\nu}T^A b_R G^A_{\mu\nu} + \ldots, \tag{4.27}$$

where the dots comprise the hermitian conjugate and other operators that are not relevant for our discussion here. Besides the conventions stated in Appendix A, $G_F$ denotes the Fermi constant, $m_b$ the bottom mass and $V_{ij}$ the corresponding entries of the CKM matrix. One way of alleviating the mentioned tension among the different B-meson decays is generating the $C_{8gd}$ and $C_{8gs}$ coefficients in the following ranges (with some correlation on the upper range for the latter):

$$0.13 \lesssim C_{8gd}(m_b) \lesssim 0.33, \quad -0.45 \lesssim C_{8gs}(m_b) \lesssim 0.03, \tag{4.28}$$

where the value in parenthesis denotes the scale ($\mu = m_b$) at which the WCs are renormalized.

Given this bottom-up interpretation of the effect, we can wonder which new physics models can be held accountable of this deviation. Note how the proposed explanation is in terms of dipole operators which, as discussed in this chapter, are first generated at one loop. Thus, we can use our dictionary to completely classify all possible extensions of the SM (with new scalars or fermions) that can generate these non-vanishing values. However, as discussed in Section 2.7, we first have to express the $C_{8gq}$ coefficients in terms of the corresponding WC in the LEFT, then use the LEFT (one-loop) RGEs to write them in terms of the LEFT WCs defined at the matching scale with SMEFT, perform the one-loop matching and finally use the SMEFT RGEs to express everything in terms of the WCs defined at a high scale $\mu = \Lambda$, whose values we can read off from our dictionary. All these steps can be simplified by automated tools like `DSixTools` [93, 73]. During this whole process we can take into account that some SMEFT coefficients can only be generated at one loop and therefore their effect via running or one-loop matching is formally a two-loop effect that can be disregarded.

In the following discussion, we will denote generically the anomalous dimension of a WC $\alpha_i$

$$\dot{\alpha}_i \equiv 16\pi^2\mu\frac{\mathrm{d}\alpha_i}{\mathrm{d}\mu}, \tag{4.29}$$

and working to the leading log approximation (fixed order one-loop effects), we have

$$\alpha_i(\mu) = \alpha_i(\mu_0) + \frac{\dot{\alpha}_i(\alpha_j^{\text{tree}})}{32\pi^2}\log\left(\frac{\mu^2}{\mu_0^2}\right), \tag{4.30}$$

where $\dot{\alpha}_i$ can be evaluated at any scale and, as we have explicitly written, only the tree level contribution for the relevant WCs needs to be included, since it would be formally two-loops order otherwise. Note that our convention for the covariant derivative is the opposite to the one used in the references above. Thus, we have changed the signs of the gauge couplings whenever necessary.

The relevant part of the LEFT Lagrangian reads:

$$\mathcal{L}_{\text{LEFT}} = (L_{dG})_{ij}\bar{d}_{L\,i}\sigma^{\mu\nu}T^A d_{R\,j}G^A_{\mu\nu} + \dots, \tag{4.31}$$

so, by comparison:

$$C_{8gq} = \frac{F_q}{g_3}(L_{dG})_{qb}, \tag{4.32}$$

where

$$F_q \equiv \left[\frac{G_F}{8\pi^2}m_b(V_{ub}V_{uq}^* + V_{cb}V_{cq}^*)\right]^{-1} \approx \begin{cases} 1.8\times 10^5\ \mathrm{e}^{0.9\mathrm{i}\pi}\ \text{TeV}, & [q=d], \\ 3.8\times 10^4\ \text{TeV}, & [q=s]. \end{cases} \tag{4.33}$$

Likewise, the relevant part of the LEFT RGEs, in the up basis, reads:

$$\begin{aligned}(\dot{L}_{dG})_{ij} &= -g_3\textstyle\sum_{q_u=u,c} m_{q_u}\left[(L^{S1,RR}_{uddu})_{q_u j i q_u} - \frac{1}{6}(L^{S8,RR}_{uddu})_{q_u j i q_u}\right] + \dots \\ &= \phantom{-}g_3\textstyle\sum_{q_u=u,c} m_{q_u}\left[(C^{(1)}_{quqd})_{i q_u q_u j} - \frac{1}{6}(C^{(8)}_{quqd})_{i q_u q_u j}\right] + \dots,\end{aligned} \tag{4.34}$$

where the dots stand for contributions that are either one-loop generated or receive no contribution from the SMEFT, and we have used in the second line the following tree level matching between the SMEFT and the LEFT:

$$(L^{S1,RR}_{uddu})_{ijkl} = -(C^{(1)}_{quqd})_{klij}, \quad (L^{S8,RR}_{uddu})_{ijkl} = -(C^{(8)}_{quqd})_{klij}. \tag{4.35}$$

We can therefore write:

$$\begin{aligned}C_{8gq}\frac{g_s}{F_q}\Big|_{\mu=m_b} &= (L_{dG})_{qb}\Big|_{\mu=m_b} \\ &= (L_{dG})_{qb}\Big|_{\mu=m_t} + \frac{g_s}{32\pi^2}\sum_{q_u=u,c} m_{q_u}\left[(C^{(1)}_{quqd})_{q q_u q_u b} - \frac{1}{6}(C^{(8)}_{quqd})_{q q_u q_u b}\right]\log\left(\frac{m_b^2}{m_t^2}\right)\Big|_{\mu=\Lambda},\end{aligned} \tag{4.36}$$

where the SMEFT coefficients on the last term can already be evaluated at the high scale (other effects being formally of two-loops order) and for later convenience we have chosen the top quark mass for the matching scale between the SMEFT and LEFT.

Using the one-loop matching between SMEFT and LEFT we obtain:

$$
\begin{aligned}
(L_{dG})_{qb} = &\frac{v}{\sqrt{2}} V^\dagger_{qk} (C_{dG})_{kb} + \frac{g_3}{64\pi^2} F_1(x_W) \frac{V^\dagger_{qt} V_{tb} m_b}{v_T^2} \\
&+ \frac{g_3}{36\pi^2}\left(1 - \frac{m_W^2}{m_Z^2}\right) m_q (C_{Hd})_{qb} + \frac{g_3}{64\pi^2} F_2(x_W) m_t V^\dagger_{qt} (C_{Hud})_{tb} \\
&- \frac{g_3}{72\pi^2}\Big(1 + \frac{2m_W^2}{m_Z^2}\Big) m_b V^\dagger_{qk} (C^{(1)}_{Hq})_{kl} V_{lb} \\
&- \frac{g_3}{576\pi^2} m_b \Big\{ 8\left(7 + 2\frac{m_W^2}{m_Z^2}\right) V^\dagger_{qk} (C^{(3)}_{Hq})_{kl} V_{lb} - 9 F_1(x_W) [V^\dagger_{qt} (C^{(3)}_{Hq})_{tk} V_{kb} + V^\dagger_{qk} (C^{(3)}_{Hq})_{kt} V_{tb}] \Big\} + \ldots,
\end{aligned}
\tag{4.37}
$$

where the dots stand for two-loop effects and, at the order given, $v \approx 246$ GeV. This equality should be understood at a scale $\mu = m_t$ but, again, all terms but the first one can already be evaluated at the cut-off scale, as any running effect will be of two-loop order. We have defined:

$$
x_W \equiv \frac{m_W^2}{m_t^2}, \tag{4.38}
$$

$$
F_1(x) = \frac{1 - 6x + 3x^2 + 2x^3 - 6x^2 \log(x)}{(1-x)^4}, \tag{4.39}
$$

$$
F_2(x) = \frac{1 - 3x^2 + 4x^3 - 6x^2 \log(x)}{(1-x)^3}. \tag{4.40}
$$

The last term in the first line of Eq. (4.37) corresponds to the SM contribution which, using the relation between the measured Fermi constant in muon decay and the Higgs vacuum expectation value (vev), $v_T$, [70]

$$
\frac{1}{v_T^2} = \sqrt{2} G_F + \frac{1}{2}[(C_{ll})_{2112} + (C_{ll})_{1221}] - [(C^{(3)}_{Hl})_{11} - (C^{(3)}_{Hl})_{22}] \equiv \sqrt{2} G_F + \Delta G_F, \tag{4.41}
$$

gives the following new physics contribution:

$$
\frac{g_3}{64\pi^2} F_1(x_W) \frac{V^\dagger_{qt} V_{tb} m_b}{v_T^2} = \mathrm{SM} - \frac{g_3}{64\pi^2} (V_{ub} V^*_{uq} + V_{cb} V^*_{cq}) F_1(x_W) m_b \Delta G_F. \tag{4.42}
$$

Finally, we have to include the RGE of $C_{dG}$ in the SMEFT, which reads,

$$
(\dot{C}_{dG})_{qb} = g_3 \left( C^{(1)}_{quqd} - \frac{1}{6} C^{(8)}_{quqd} \right)_{qklb} (Y_u^\dagger)_{kl} + \ldots, \tag{4.43}
$$

where the dots denote, once again, terms that correspond to two-loop effects. We therefore have:

$$
(C_{dG})_{qb}\big|_{\mu = m_t} = \left[ (C_{dG})_{qb} + \frac{g_3}{32\pi^2} \left( C^{(1)}_{quqd} - \frac{1}{6} C^{(8)}_{quqd} \right)_{qklb} (Y_u^\dagger)_{kl} \log\left(\frac{m_t^2}{\Lambda^2}\right) \right]_{\mu = \Lambda} + \ldots, \tag{4.44}
$$

where, as explicitly stated, this expression is already evaluated at the high scale. Putting everything together we arrive to the following expression for the new physics contribution:

$$
\begin{aligned}
C_{8gq}\frac{g_s}{F_q}\Big|_{\mu=m_b} = & \frac{g_s}{32\pi^2}\sum_{q_u=u,c} m_{q_u}\Big[(C^{(1)}_{quqd})_{qq_uq_ub} - \frac{1}{6}(C^{(8)}_{quqd})_{qq_uq_ub}\Big]\log\left(\frac{m_b^2}{m_t^2}\right) \\
& + \frac{v}{\sqrt{2}}V^\dagger_{qk}(C_{dG})_{kb} + \frac{g_s}{64\pi^2}F_1(x_W)V^\dagger_{qt}V_{tb}m_b\Delta G_F \\
& + \frac{g_s}{36\pi^2}\left(1-\frac{m_W^2}{m_Z^2}\right)m_q(C_{Hd})_{qb} + \frac{g_s}{64\pi^2}F_2(x_W)m_tV^\dagger_{qt}(C_{Hud})_{tb} \\
& - \frac{g_s}{72\pi^2}\Big(1+\frac{2m_W^2}{m_Z^2}\Big)m_bV^\dagger_{qk}(C^{(1)}_{Hq})_{kl}V_{lb} \\
& - \frac{g_s}{576\pi^2}m_b\Big\{8\left(7+2\frac{m_W^2}{m_Z^2}\right)V^\dagger_{qk}(C^{(3)}_{Hq})_{kl}V_{lb} - 9F_1(x_W)[V^\dagger_{qt}(C^{(3)}_{Hq})_{tk}V_{kb} + V^\dagger_{qk}(C^{(3)}_{Hq})_{kt}V_{tb}]\Big\} \\
& + V^\dagger_{qk}\left[\frac{g_s}{32\pi^2}\left(C^{(1)}_{quqd} - \frac{1}{6}C^{(8)}_{quqd}\right)_{qkkb}(m_u)_k\log\left(\frac{m_t^2}{\Lambda^2}\right)\right] + \ldots,
\end{aligned} \tag{4.45}
$$

where in the last line we neglected higher loop and mass dimension effects to write the mass of the up-type quarks in terms of their Yukawa couplings and the Higgs vev. In the equation above the first line corresponds to the running in the LEFT between $\mu = m_b$ and $\mu = m_t$, the second to fifth to the matching between the SMEFT and the LEFT at $\mu = m_t$ and the last to the SMEFT running between $\mu = m_t$ and the cut-off scale $\mu = \Lambda$. All the SMEFT WCs are to be evaluated at the cut-off scale and only their tree level contributions should be included to be consistent (except for $C_{dG}$).

Thanks to equation (4.45), we can "read" low energy effects in $C_{8gq}$ (like the reported tension in B decays) in terms of physics generated at a high scale $\Lambda$. Thus, we can directly use the dictionaries to classify all possible SM extensions (with scalars and fermions for the one loop one) that can explain this tension.

The analysis can be simplified by first checking which WCs can give a sizeable contribution to our coefficient at low energy. In order to do that we will select a benchmark point with:

$$
C_{8gd}^{\text{benchm.}} = 0.25, \quad C_{8gs}^{\text{benchm.}} = -0.1, \tag{4.46}
$$

allowed from the study of [117]. Rescaling all coefficients with an explicit power of the cut-off:

$$
C = \frac{c}{\Lambda^2}, \tag{4.47}
$$

with $c$ now a dimensionless coefficient, and dropping all contributions that require the relevant $c$ to be larger than 10 (to be on the conservative side) to reproduce the benchmark points, we find, for $\Lambda = 2$ TeV,

$$\begin{aligned}
C_{8gd} \approx\ & [-6.9 + 2.9\mathrm{i}] \times 10^3\ (c_{dG})_{1,3} + [1.6 - 0.66\mathrm{i}] \times 10^3\ (c_{dG})_{2,3} - 65.5\ (c_{dG})_{3,3} \\
& + [3.22 - 1.34\mathrm{i}] \times 10^{-2}\ (c^{(1)}_{Hq})_{1,2} + [0.80 - 0.33\mathrm{i}]\ (c^{(1)}_{Hq})_{1,3} - [0.18 - 0.08\mathrm{i}]\ (c^{(1)}_{Hq})_{2,3} \\
& + [0.11 - 0.04\mathrm{i}]\ (c^{(3)}_{Hq})_{1,2} + [2.38 - 0.99\mathrm{i}]\ (c^{(3)}_{Hq})_{1,3} - [2.5 - 1.0\mathrm{i}] \times 10^{-2}\ (c^{(3)}_{Hq})_{2,2} \\
& - [0.55 - 0.23\mathrm{i}]\ (c^{(3)}_{Hq})_{2,3} - 0.39\ (c_{Hud})_{3,3} + [1.23 - 0.51\mathrm{i}]\ (c^{(1)}_{quqd})_{1,2,2,3} \\
& + 1.18\ (c^{(1)}_{quqd})_{1,3,3,3} - [0.21 - 0.09\mathrm{i}]\ (c^{(8)}_{quqd})_{1,2,2,3} - 0.20\ (c^{(8)}_{quqd})_{1,3,3,3}, \qquad (4.48)\\
C_{8gs} \approx\ & [373 + 7\mathrm{i}]\ (c_{dG})_{1,3} + [1600 + 30\mathrm{i}]\ (c_{dG})_{2,3} - 65.5\ (c_{dG})_{3,3} \\
& - 0.043\ (c^{(1)}_{Hq})_{1,3} - 0.18\ (c^{(1)}_{Hq})_{2,3} - 0.13\ (c^{(3)}_{Hq})_{1,3} - 0.025\ (c^{(3)}_{Hq})_{2,2} \\
& - [0.55 + 0.01\mathrm{i}]\ (c^{(3)}_{Hq})_{2,3} + 0.02\ (c^{(3)}_{Hq})_{3,3} - 0.39\ (c_{Hud})_{3,3} - [0.58 + 0.01\mathrm{i}]\ (c^{(1)}_{quqd})_{2,2,2,3} \\
& + 1.2\ (c^{(1)}_{quqd})_{2,3,3,3} + [0.096 + 0.002\mathrm{i}]\ (c^{(8)}_{quqd})_{2,2,2,3} - 0.20 (c^{(8)}_{quqd})_{2,3,3,3}. \qquad (4.49)
\end{aligned}$$

Contributions from tree level generated operators can be directly read off from the tree level dictionary [102], so we will classify in the following the contribution from the one-loop generated WC $C_{dG}$, taking full advantage of the sector of the one-loop dictionary that we have computed. We are interested, then, in models that do not contribute at tree level to the SMEFT operators in the equation above and just consider the simpler case of:

$$\begin{aligned}
C_{8gd} &\approx [-6.9 + 2.9\mathrm{i}] \times 10^3\ (c_{dG})_{1,3} + [1.6 - 0.66\mathrm{i}] \times 10^3\ (c_{dG})_{2,3} - 65.5\ (c_{dG})_{3,3} \\
&= [-27.6 + 11.6\mathrm{i}] \times 10^3\ (C_{dG})_{1,3} + [6.4 - 2.64\mathrm{i}] \times 10^3\ (C_{dG})_{2,3} - 262.\ (C_{dG})_{3,3}, \qquad (4.50)\\
C_{8gs} &\approx [373 + 7\mathrm{i}]\ (c_{dG})_{1,3} + [1600 + 30\mathrm{i}]\ (c_{dG})_{2,3} - 65.5\ (c_{dG})_{3,3} \\
&= [1492 + 28\mathrm{i}]\ (C_{dG})_{1,3} + [6400 + 120\mathrm{i}]\ (C_{dG})_{2,3} - 262.\ (C_{dG})_{3,3}, \qquad (4.51)
\end{aligned}$$

where the second line (of each equation) has been rewritten in terms of dimensionful Wilson Coefficients (arbitrary $\Lambda$. All dimensionful quantities hereafter will be measured in TeV. There is a continuum of solutions for these observables to match the benchmark values. An example of such solution is:

$$(C_{dG})_{1,3} \approx -(1.1 + 0.3\mathrm{i}) \times 10^{-5}, \quad (C_{dG})_{2,3} \approx -1 \times 10^{-5}, \quad (C_{dG})_{3,3} \approx 10^{-4}, \qquad (4.52)$$

all in units of $\mathrm{TeV}^{-2}$ and the complex value for the $1,3$ component is just to accommodate the assumption of real WC made in [117].

One can check that in general it is easy to generate these values in phenomenologically viable models. We are in position now, using `SOLD`, to see the list of all possible extensions that can generate these coefficients. This was computed in Section 4.4 and partially shown in Figure 4.2. From this (long) list we eliminate the cases in which at least one heavy field has all its quantum numbers fixed, as they correspond to linear couplings to the SM and therefore contribute at tree level to other operators.

All the remaining models have three heavy fields. We choose one of the simplest ones that has "chirally enhanced" contributions, not suppressed by the down-type quark Yukawa couplings (for simplicity we will use the conjugated field of the first fermion with respect to the one given by SOLD):

$$\Phi \sim (1,1)_{\mathrm{Y}_\Phi}, \quad \Psi_1 \sim (3,2)_{\frac{1}{6}-\mathrm{Y}_\Phi}, \quad \Psi_2 \sim (3,1)_{-\frac{1}{3}-\mathrm{Y}_\Phi}, \tag{4.53}$$

where the hypercharge of the heavy scalar $\mathrm{Y}_\Phi$ is arbitrary up to the limitation (under our assumption) of no tree level contributions, that restricts $\mathrm{Y}_\Phi \neq 0, -1$. The complete expression can be obtained by the command

```
In[10]:= Match2Warsaw[alphaOdG[i,j],{Sa ->{1,1,Y1},Fa->{3,2,1/6-Y1},
         Fb->{3,1,-1/3-Y1}}]
```

For simplicity we report here the expression in the large scalar mass limit and neglecting terms suppressed by the down-type quark masses:

$$\begin{aligned}(C_{dG})_{ij} = &-\frac{g_3}{64\pi^2}\frac{(\lambda_{qa})_i(\lambda_{bd})_j}{M_\Phi^2(M_a^2-M_b^2)}\Bigg[2M_aM_b\log\left(\frac{M_a^2}{M_b^2}\right)\lambda_{ab}^R \\ &+\left(2M_b^2\log\left(\frac{M_a^2}{M_b^2}\right)+(M_a^2-M_b^2)\left(3+2\log\left(\frac{M_a^2}{M_\Phi^2}\right)\right)\right)\lambda_{ab}^L\Bigg]+\mathcal{O}\left(\frac{M_{a,b}^2}{M_\Phi^4}\right),\end{aligned} \tag{4.54}$$

where the parameters are defined by the following Lagrangian:

$$\begin{aligned}\mathcal{L} \supset &-M_\Phi^2\Phi^\dagger\Phi - M_a\bar{\Psi}_a\Psi_a - M_b\bar{\Psi}_b\Psi_b \\ &-\bar{\Psi}_a[\lambda_{ab}^LP_L+\lambda_{ab}^RP_R]\Psi_b - (\lambda_{qa})_i\bar{q}_iP_R\Psi_a\Phi - (\lambda_{bd})_i\bar{\Psi}_bP_Rd_i\Phi^\dagger.\end{aligned} \tag{4.55}$$

Using the full expression given by SOLD, we can obtain, for instance, the following parameter point, respecting the values in Eq. (4.52):

$$\begin{aligned}&M_a = 1.5\ \text{TeV}, \quad M_b = 2.0\ \text{TeV}, \quad M_a = 4.0\ \text{TeV}, \\ &\lambda_{ab}^L = 0, \quad (\lambda_{qa})_i = \frac{(0.084+0.023\mathrm{i}, 0.077, -0.776)}{\lambda_{ab}^R(\lambda_{bc})_3}.\end{aligned} \tag{4.56}$$

We can then proceed to perform the full one-loop matching of this model via the function `CompleteOneLoopMatching`. The result has been exported to WCxf format [118] and `smelli` [119–121] has been used to check the viability of the model. Indeed the following values of the remaining parameters:

$$\lambda_{ab}^R = -0.7, \quad (\lambda_{bc})_3 = 0.9, \tag{4.57}$$

relax the corresponding tension for the considered operators without conflicting with other experimental observables (the global pull with respect to the SM is of 3.4 $\sigma$ when considering all other relevant observables encoded in `smelli`).

Note that, given the choice of quantum numbers, there is no linear coupling of the new fields to SM particles. This means that the lightest one, $\Psi_a$ for our choice, is stable. However, we can still make a choice of $\mathrm{Y}_\Phi$ that ensures that $\Psi_a$ can still decay via higher dimensional operators, with a non-standard decay pattern, evading current experimental limits. See [122] for a detailed discussion.

## 4.6 Outlook

We have presented in this chapter the results of the one-loop dictionary for the SMEFT at dimension six for a sector of operators whose leading contribution is at this order. Even in its current partial form, it can be already applied to phenomenological examples, as presented in Section 4.5 and as we will see in the next chapter. However, there are a few clear limitations that we should be able to overcome thanks to all the machinery constructed.

The first future step would be clearly to extend the dictionary to all dimension six operators in the SMEFT. Even if the remaining operators can receive tree-level contributions, this is still necessary to perform a complete one-loop analysis of the connection between models and observables. The changes needed to accommodate the rest of operators are minimal and we plan to include them in the future.

Likewise, we also want to include extensions of the SM with new heavy vector bosons, which are theoretically very motivated. Before that, we want to study in detail how to construct consistently a generic UV theory with massive vector bosons without details of their representations [123].

Another slight improvement could be implementing flavor indices for the heavy fields in the models defined by the user. Note that same physical result can be already obtained with the current version of `SOLD` by defining different heavy particles with the same quantum numbers (which is what we call flavor). However, the results would be much more compact and readable introducing a flavor index for the heavy fields. This will be taken care of following their inclusion in `matchmakereft`. Besides, we plan to add a `Mathematica` interface between `SOLD` (and `matchmakereft`) and the `MatchingDB` format [124] that will allow for a flexible use of these highly non-trivial dictionaries.

Finally, given the way in which the dictionary is constructed, the power to extend the results to other EFTs is at hand. Since we work with generic field multiplets, without specifying their components or gauge representations right until the end of the calculation, we can consider other EFTs by only matching them to a generic theory. This can be easily achieved with `matchmakereft`, only limited by the reduction of a general EFT to a physical basis. Once this is implemented, we would “instantly” have dictionaries for theories like $\nu$SMEFT, ALP EFTs, SMEFT at dimension eight, etc.

# 5

# A `SOLD` bridge to new physics

Motivated by the increasing precision in experiments and the intention to capture higher order effects, we constructed the one-loop dictionary for heavy scalars and fermions for the sector of SMEFT generated for the first time at one loop. We reviewed how the dictionary is constructed and encoded in the package `SOLD`, and provided an example of a phenomenological application.

In this chapter, we want to demonstrate how IR/UV dictionaries can play a relevant role as a guiding principle in our search for new physics, and how it is important to be systematic and "leave no stone unturned". With that purpose, we show how the dictionary was used to propose a whole new class of models to explain the anomaly in the magnetic dipole moment of the muon ($a_\mu$). After an introduction to the problem in Sections 5.1 and 5.2, we present generic (with gauge representations unspecified) and specific results for $a_\mu$ in this class of models in Sections 5.3, 5.4 and 5.5. Finally we exemplify how the models contained in the dictionary, in particular the ones discussed in this chapter, can have the freedom to accommodate well-known explanations of different anomalies, by proposing an specific model in Section 5.6.

## 5.1 The anomalous magnetic moment of the muon

The Fermilab Muon g-2 Experiment [125] recently performed a measurement of the anomalous magnetic moment of the muon which, together with the previous measurement by Brookhaven National Laboratory [126], combines to a 4.2$\sigma$ tension with the Standard Model (SM) result [127–162],

$$a_\mu^{\mathrm{EXP}} - a_\mu^{\mathrm{SM}} = (251 \pm 59) \times 10^{-11}. \tag{5.1}$$

This exciting tension strongly suggests the presence of new physics coupling to muons, and has fueled significant efforts in the community in order to explain its origin. This SM value, however, does not take into account the latest lattice results from the hadronic vacuum polarization (HVP) SM contribution, presented by the BMW collaboration [163, 164], which would reduce the tension in g-2 to $\sim 1.5\sigma$. Nevertheless, there is a disagreement in the size of prediction for the HVP contribution between these lattice results and the data-driven method, which introduces another tension in $e^+e^- \to$ hadrons cross-section [165–168] that amounts to $\sim 3\sigma$.

In the following, we will neglect this discrepancy and acknowledge the g-2 measurement as an anomaly. Our rationale behind this is that, even if the tension eventually vanishes, this chapter still sets the example as an illustration of how the dictionaries can be used to interpret future anomalies and how a systematic scrutiny of models can open up several new physics possibilities.

Under the assumption that the physics responsible for the g-2 tension is heavy, we will use once again the formalism of Effective Field Theories in our study. From the SMEFT perspective, the heavy physics contribution to $a_\mu$ (at tree-level) is given by:

$$\Delta a_\mu = a_\mu^{\rm NP} - a_\mu^{\rm SM} = \frac{4m_\mu v}{\sqrt{2}e}\Big(\mathrm{Re}([\alpha_{eB}]_{2,2})c_W - \mathrm{Re}([\alpha_{eW}]_{2,2})s_W\Big) \equiv \frac{4m_\mu v}{\sqrt{2}e}[\alpha_{e\gamma}]_{2,2}\,, \tag{5.2}$$

where $m_\mu$ is the mass of the muon, $v$ the vacuum expectation value (VEV) of the Higgs, $e$ the electric charge, $c_W$ ($s_W$) the co-sine (sine) of the Weinberg angle and $\alpha_{eB}$ and $\alpha_{eW}$ the coefficients of the leptonic dipole operators (see Appendix B):

$$[\mathcal{O}_{eB}]_{i,j} = (\bar{\ell}_i\sigma^{\mu\nu}e_j)HB_{\mu\nu}, \tag{5.3}$$
$$[\mathcal{O}_{eW}]_{i,j} = (\bar{\ell}_i\sigma^{\mu\nu}e_j)\sigma^I HW^I_{\mu\nu}\,, \tag{5.4}$$

with $i$ and $j$ denoting flavor indices. At lower energies, the contribution to $a_\mu$ at tree level in the LEFT is given by the photon dipole operator, whose Wilson coefficient is $L_{e\gamma} = \frac{v}{\sqrt{2}}\alpha_{e\gamma}$ [75]. Therefore, we will quote our results as contributions to $\alpha_{e\gamma}$ hereafter.

As discussed in Chapter 4, the SMEFT dipole operators are generated only at loop level by weakly-coupled UV theories. Since the measurement is performed at low energies, a consistent calculation at one loop needs to include the effects of running of coefficients besides the one-loop finite contributions at low energy (see Section 2.7). A calculation along the lines of the one in Section 4.5 was done in [48], and showed that besides the mentioned dipole operators, the only remaining relevant contribution to $a_\mu$ arises as a one-loop effect from the $\mathcal{O}^{(3)}_{\ell equ}$ operator, setting a cut-off of $\Lambda = 10$ TeV (lower cut-offs result in even more negligible remaining terms, since the running effects are less important). Since it is already a one-loop contribution, we only need to consider the tree-level generation of this operator, which only occurs for extensions including one of the two scalar leptoquarks $S_1$ or $S_2$ [102]. These have been well studied [102, 48] so, following the purpose of exploring one-loop generated operators, we will focus only on the contributions to the leptonic dipoles.

Several works have been dedicated in the last years to propose SM extensions (containing a number of different fields) that generate these operators. A comprehensive review of the status of such models can be found in [169] (and references therein). Among all of these explanations, chirally enhanced solutions, i.e., solutions in which the contribution to $a_\mu$ is not suppressed by the muon Yukawa coupling, are particularly interesting because they can explain the observed value with masses for the new heavy particles typically large enough to avoid current experimental constraints. These chirally enhanced contributions have been studied for a wide range of extensions (see, for instance, [170, 171, 112, 98, 172, 173]).

All of these extensions are included in the one-loop dictionary, since they give finite contributions to the dipole operators $\mathcal{O}_{eB}, \mathcal{O}_{eW}$. We can examine the complete list by using the following command in SOLD:

```
In[11]:=    ListModelsWarsaw[alphaOeW[2,2]]
```

The complete set of models is technically the union of the sets contributing to the $\mathcal{O}_{eB}$ *and* $\mathcal{O}_{eW}$ operators, but we use here only $\mathcal{O}_{eW}$ as an example. Among this long list, we can find some models:

```
Out[11]= {...
         {{ϕ1,ψ1,ψ2}, {ψ1→1⊗2, ϕ1⊗ϕ1̄⊃1⊗3, ψ2⊗ϕ1̄⊃1⊗2},
         {Y_ψ1→-1/2,Y_ψ2→Y_ϕ1-1/2}},
         {{ϕ1, ψ1, ψ2}, {ψ1→1⊗2, ψ2⊗ϕ1̄⊃1⊗2, ψ2⊗ψ2̄ ⊃1⊗3},
         {Y_ψ1→1/2, Y_ψ2→Y_ϕ1+1/2}},
         {{ϕ1, ψ1, ψ2}, {ψ2==ϕ1, ψ1→1⊗1, ϕ1⊗ϕ1̄ ⊃1⊗3}, {Y_ψ1→1, Y_ψ2→1+Y_ϕ1}},
         {{ϕ1, ψ1, ψ2}, {ψ2==ϕ1, ψ1→1⊗3, ϕ1⊗ϕ1̄ ⊃1⊗3}, {Y_ψ1→1, Y_ψ2→1+Y_ϕ1}},
         ...}
```

that had not been studied, to the best of our knowledge, prior to this work. This completions have in common that they yield chirally enhanced contributions to $a_\mu$ produced by the topology of Fig. 5.2, which we will refer to as *bridge* hereafter, and contain one vector-like lepton (VLL) that couples linearly to the SM. Note that the VLL connecting the loop and 2 external states (the bridge) and one of the particles in the loop must be heavy (otherwise the hard region of the loop would vanish), but the remaining one can be heavy or light. As such, either 2- or 3-field extensions can generate this type of topology, besides the ones listed above.

While the bridge diagram has been studied in the context of some particular cases of 2-field extensions with two VLLs [174, 175], in this chapter we perform the complete classification of the subset of all possible 2 and 3 fields extensions of the SM (included in the dictionary) that can produce this topology. Chirally enhanced solutions from 3-field extensions, like the ones in [171, 112, 98, 172, 173, 170], contributed to $a_\mu$ through a box diagram[1] (see Figure C.2). The heavy fields allowed by gauge symmetry to generate that topology are different from the ones which can generate the bridge one, and, as such, the latter constitute a new class of models that can alleviate the observed tension. Notice, however, that some of these extensions will also contribute to $a_\mu$ through a box diagram.

Adopting the SMEFT perspective also allowed us to consider several 2-field extensions which had been overlooked in the literature, where only the lepton Yukawa-suppressed contributions to $a_\mu$ were took into account, thus excluding these models as explanations of the anomaly either by direct searches or due to a wrong sign in the contribution. The bridge-like contribution in these 2-field models restores them as plausible explanations for the g-2 anomaly.

[1] From the LEFT perspective, this box corresponds to the triangle diagram, which is the one usually considered in the literature, when the Higgs takes a VEV.

## 5.2 Computation of $a_\mu$

In this section we review the technicalities pertinent to the calculation of $a_\mu$ from an EFT perspective. Even if in the rest of the chapter we consider SM extensions with two or three heavy fermions or scalars that can generate the bridge topology, but the procedure presented in this section is completely general and applies for any type of model. Moreover, we will neglect contributions suppressed either by lepton Yukawa couplings or by the Higgs mass (terms of the form $m_H/M$) throughout all computations, since they are negligible in comparison with the chirally enhanced contribution that we are interested in.

The matching condition of the dipole operators can naturaly be obtained through a diagrammatic off-shell approach, as we have been doing on the previous chapters, computing the relevant 1lPI amplitudes and then reducing the result to the Warsaw basis:

$$\alpha_{eB} = \alpha_{eB}^G - \frac{g_1}{8}\beta_{eHD2}^G + \frac{g_1}{8}\beta_{eHD4}^G - \frac{g_1}{2}\beta_{eHD3}^G\,, \tag{5.5}$$

$$\alpha_{eW} = \alpha_{eW}^G - \frac{g_2}{8}\beta_{eHD2}^G + \frac{g_2}{8}\beta_{eHD4}^G\,, \tag{5.6}$$

where we have added explicitly the superscript $G$ to denote the Wilson coefficients in the Green's basis. In this expression we neglected Yukawa-suppressed contributions and coefficients not generated at one loop by renormalizable extensions (see Chapter 4). Following from Eq. (5.2), we can then express the contribution to $a_\mu$ in terms of these coefficients in the Green's basis as:

$$\Delta a_\mu = \frac{4m_\mu v}{\sqrt{2}}\left(\frac{1}{g_1}\,\left[\alpha_{eB}^G\right]_{2,2} - \frac{1}{g_2}\,\left[\alpha_{eW}^G\right]_{2,2} - \frac{1}{2}\,\left[\beta_{eHD3}^G\right]_{2,2}\right). \tag{5.7}$$

This procedure was applied to cross-check with `matchmakereft` [64] all the results presented in the next sections (and, when possible, compared against those in the literature).

However, in the following we will adopt a different approach to compute $a_\mu$, simpler in our case of interest. We will compute the on-shell amplitude $\langle \bar{\ell}_L\, e_R\, H\, B/W\rangle$[2], taking all momenta incoming, in the full theory and in the SMEFT. For simplicity, we set the momentum of the Higgs, $p_H$, to zero. The dipole operators are uniquely defined by the kinematic structure $\not{q}\not{\epsilon}$, where $q$ is the gauge boson momentum and $\epsilon$ its polarization vector. This structure can be traded on-shell by $\epsilon\cdot p_e$, since:

$$\overline{v_\ell}\,\not{q}\not{\epsilon}\,u_e = -\overline{v_\ell}\,(\not{p}_\ell + \not{p}_e)\not{\epsilon}\,u_e = -2\epsilon\cdot p_e\,\overline{v_\ell}\,u_e\;, \tag{5.8}$$

where $p_{e(\ell)}$ is the momentum of the right-handed (left-handed) electron, and $v_\ell, u_e$ are the corresponding external spinors. In the second equality we applied the on-shell conditions $\overline{v_\ell}\,\not{p}_\ell = 0$ and $\not{p}_e\,u_e = 0$ (which hold for massless fermions). Therefore, $\epsilon\cdot p_e$ ends up being the only relevant kinematic structure for the matching calculation.

On-shell matching is particularly efficient in this specific case, since we do not have to consider any connected diagrams other than the box (if present) and the bridge ones. The reason is that, first, we are neglecting diagrams with insertions of the lepton Yukawas. Second, one could also think of diagrams with the gauge bosons attached to the external legs instead

[2] Note that in practice one can directly calculate the diagram with the photon insertion and consider the appropriate electric charge; however, to keep the language coherent within the SMEFT picture, we will refer to diagrams with both $W$ and $B$ bosons.

of in the internal propagators. However, when the gauge boson is attached to the fermions, the diagram will either result in a contribution proportional to $\not{p}_\ell \not{\epsilon}$ or $\not{\epsilon}\not{p}_e$, or, when the photon couples to the Higgs, proportional to $q \cdot \epsilon = 0$ or $p_H \cdot \epsilon = 0$.

Moreover, the same happens when the gauge boson is attached to the fermionic bridge. In this case, all contributions are proportional either to $\not{p}_\ell \not{\epsilon}$ or $\not{\epsilon}\not{p}_e$, being therefore zero in light of the arguments presented above. Consequently, we can compute only the diagrams with insertions of gauge bosons in the particles in the loop. The same arguments can be used to realize that only the mass insertion in the bridge propagator contributes, fixing the chirality of the coupling between the two (or three) heavy fields.

## 5.3 General results

In this section we present the contributions to $a_\mu$ produced by the bridge topology for general representations of the new heavy fields. Among the bridge topologies, we can distinguish three cases depending on the particle that runs in the bridge. Note that it can never be a SM particle because it would give a Yukawa-suppressed contribution. The possible heavy particles in the bridge couple linearly to SM particles and their representations are therefore fixed:

- **Scalar bridge.** A heavy scalar in the bridge must couple to the left- and right-handed muon, fixing its quantum numbers to be the same as the SM Higgs. The contributions to $a_\mu$ through these diagrams are always zero (they are proportional to $\epsilon \cdot q$).
- **Fermion bridge coupled to right-handed muon.** In this case the heavy fermion has a Yukawa-like interaction to the Higgs and right-handed muon, so it is fixed to be a heavy copy of the SM left-handed lepton, $\Delta \sim (1, 2, -1/2)$. The numbers in parenthesis denote the representations under $SU(3)_c$, $SU(2)_L$ and $U(1)_Y$, respectively.
- **Fermion bridge coupled to left-handed muon.** The Yukawa-like interaction leaves us in this case with two possibilities for the quantum numbers of the heavy fermion: those of a SM right-handed lepton, $E \sim (1, 1, -1)$, or an SU(2) triplet, $\Sigma \sim (1, 3, -1)$.

The next subsections include the contribution to $a_\mu$ for each of these VLL bridges. Note that some of the extensions we consider can also contribute to $a_\mu$ through the box diagrams shown in Figs. C.1 and C.2. Therefore, for completeness, we present in Appendix C the general results arising from box diagrams. With these and the ones from the bridge topology one can in principle calculate the full contribution to $a_\mu$ for arbitrary UV extensions of the SM. Furthermore, for some particular representations, some 3-field extensions can also generate diagrams with only two or one heavy propagators, which have different kinematic factors and must also be included in the calculation of the full result[3]. When presenting results for particular extensions in Sections 5.4 and 5.5, we obviously include all possible contributions to $a_\mu$.

Moreover, extensions including $\varphi$, $\omega_1$ or $\Pi_7$ scalars (see Table **??**) also feature a shift of the dipole coefficients in the Warsaw basis to account for the evanescent structures generated at tree level, which affects the result for $a_\mu$. See Section 4.3 for the results of this contribution.

[3]For instance, 3-field extensions with a heavy Higgs also include diagrams generated by substituting it by the SM Higgs. Note, in addition, that the heavy Higgs generates by itself a contribution to $a_\mu$.

For concreteness, our results will always be presented assuming one specific orientation of the internal propagators shown in the diagrams (in particular, we always avoid the presence of fermion-number violating interactions). To translate from these results to those with a flipped propagator – which may be needed for some choices of the gauge representations of the heavy fields –, it is sufficient to add a minus sign in the contribution corresponding to a gauge boson insertion in the flipped propagator.

### 5.3.1 VLL doublet bridge

Considering a fermionic bridge, we sitll have three possible combinations inside the loop: one extra heavy fermion, $\Psi$ with the SM Higgs (Fig. 5.1a), one heavy scalar, $\Phi$, and one heavy fermion (Fig. 5.2), and one heavy scalar and an SM fermion (Fig. 5.1b). The latter contribution to $a_\mu$ vanishes because, since a mass insertion in the bridge propagator is needed (as discussed in the previous section), the chirality of the external fermions requires another mass insertion from the fermion propagator in the loop, which is massless. We will therefore neglect this possibility in the following.

The most general Lagrangian, extending the SM with the VLL doublet, $\Delta$, that can generate a bridge-like contribution to $a_\mu$ is the following:

$$\begin{aligned}\mathcal{L} \supset\, & gY_\Psi \overline{\Psi}\gamma_\mu \Psi B^\mu + g_W T^{W,\Psi}_{IKI'} \overline{\Psi_I}\gamma_\mu \Psi_{I'} W^\mu_K \\ & - igY_\Phi B^\mu(\partial_\mu \Phi^\dagger \Phi - \Phi^\dagger \partial_\mu \Phi) - ig_W T^{W,\Phi}_{JKJ'} W^\mu_K (\partial_\mu \Phi^\dagger_J \Phi_{J'} - \Phi^\dagger_J \partial_\mu \Phi_{J'}) \\ & + y_M \overline{\Delta}\, e_R\, H + T_{IKJ}\left(y^R_b\, \overline{\Psi}_I\, P_R\, \Delta_K \Phi_J + y^L_b\, \overline{\Psi}_I\, P_L\, \Delta_K \Phi_J\right) + y_F\, T'_{KIJ}\, \overline{\ell_{L,K}} \Psi_I \Phi^\dagger_J + \text{h.c.}\,,\end{aligned} \tag{5.9}$$

where $\Phi$ can stand generically for a heavy scalar or the SM Higgs ($H$ always stands for the SM Higgs) and $\Psi$ is a heavy fermion. Flavor indices in the couplings with the SM leptons are omitted because we are only interested in the coupling to the muons. The indices $I^{(\prime)}$, $J^{(\prime)}$, $K^{(\prime)}$ denote the SU(2) components of the fields, $Y_{\Psi(\Phi)}$ represents the hypercharge of $\Psi(\Phi)$, and $T^W$, $T$ and $T'$ are the Clebsch-Gordan coefficients of the fields in the corresponding interaction term.

Defining $T^{\gamma,\psi}_{ij} \equiv Y_\psi \delta_{ij} + T^{W,\psi}_{i3j}$, where $\psi$ here represents any particle, we can write the generic bridge result for $\alpha_{e\gamma}$ as:

$$[\alpha_{e\gamma}]_{2,2} = \frac{iNe}{4} y_M y_F y^R_b \sum_{IJ} T_{I2J}\left[\gamma_\Psi T^{\gamma,\Psi}_{I'I} T'_{2JI'} + \gamma_\Phi T^{\gamma,\Phi}_{JJ'} T'_{2IJ'}\right]\,, \tag{5.10}$$

where $N$ denotes the dimension of the $SU(3)$ representation of $\Psi$ (and $\Phi$, by extension, when denoting a heavy scalar). $\gamma_{\Psi,\Phi}$, which will be defined below, are different kinematic factors corresponding to the insertion of the gauge bosons on the fermion and scalar, respectively. Their explicit expression depends on the number of heavy propagators. Note that $T^{\gamma,\psi}$ would be diagonal and proportional to the electric charge if the charge eigenstate basis is chosen for the $\psi$ multiplet, i.e., $T^{W,\psi}$ is diagonal.

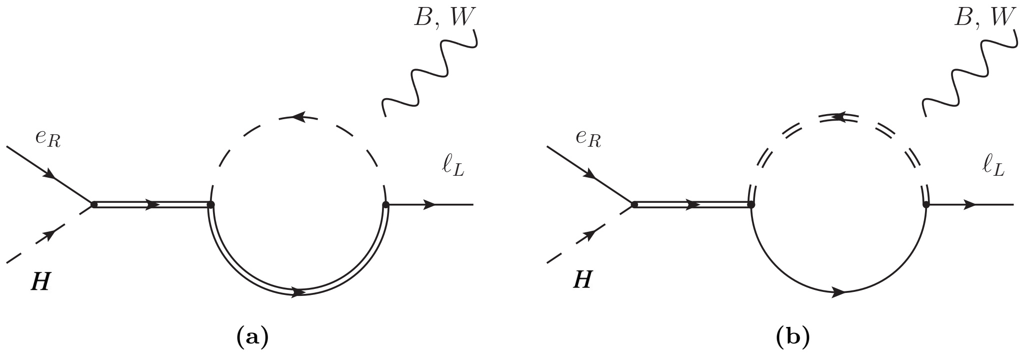


**Figure 5.1:** Bridge topology for the fermionic bridge with: (a) an extra heavy fermion and the SM Higgs; (b) an extra heavy scalar and a SM fermion. Double lines represent heavy particles whereas single lines are SM particles. The gauge boson ($B$ or $W$) is represented outside the diagram since it can be attached to any of the internal propagators.

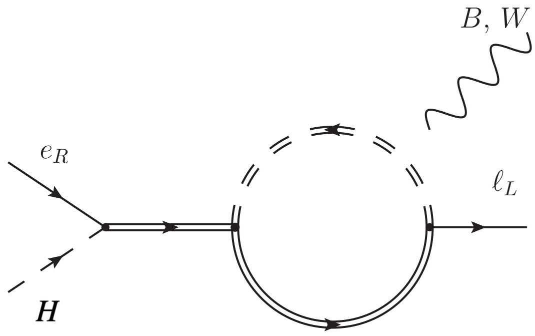


**Figure 5.2:** Bridge topology for the fermionic bridge with an extra heavy fermion and a heavy scalar. Double lines represent heavy particles, whereas single lines are SM particles. The gauge boson ($B$ or $W$) is represented outside the diagram since it can be attached to any of the internal propagators.

Let us define, for convenience, these two functions of the masses:

$$f(M_A, M_B, M_C) \equiv -\frac{iM_B}{(4\pi)^2 M_A}\,\frac{M_B^4 - 4M_B^2M_C^2 + 3M_C^4 + 2M_C^4\,\mathrm{Log}\,[M_B^2/M_C^2]}{(M_B^2 - M_C^2)^3}\,, \tag{5.11}$$

$$h(M_A, M_B, M_C) \equiv -\frac{iM_B}{(4\pi)^2 M_A}\,\frac{M_B^4 - M_C^4 - 2M_B^2M_C^2\,\mathrm{Log}\,[M_B^2/M_C^2]}{(M_B^2 - M_C^2)^3}\,. \tag{5.12}$$

as all the kinematic factors $\gamma_{\Psi,\Phi}$ defined throughout this section can always be expressed in terms of them. For the case in which the loop contains a heavy fermion, $\Psi$, and the SM Higgs (Fig. 5.1a), the kinematic factors in Eq. (5.10) are given by:

$$\gamma_\Psi = \gamma_\Phi = \lim_{M_\Phi \to 0} f(M_\Delta, M_\Psi, M_\Phi) = \frac{-i}{(4\pi)^2 M_\Delta M_\Psi}\,. \tag{5.13}$$

Likewise, for the bridge diagram with three heavy propagators (Fig. 5.2), the kinematic factors read:

$$\gamma_\Psi = f(M_\Delta, M_\Psi, M_\Phi)\,, \tag{5.14}$$

$$\gamma_\Phi = h(M_\Delta, M_\Psi, M_\Phi)\,. \tag{5.15}$$

### 5.3.2 VLL singlet (triplet) bridge

The relevant diagrams for the case of a VLL singlet or triplet bridge are the same ones presented in the previous subsection, changing only the flow of the fermionic current because the bridge is attached now to the left-handed muon.

The relevant Lagrangian for an extension of the SM with a triplet, $\Sigma$, that generates the bridge diagram is given by:

$$\mathcal{L} \supset y_M \bar{\ell}_L \sigma^I H P_R \Sigma_I + y_F \overline{\Psi}_I \Phi_I e_R + T_{KIJ} \left( y_b^R \,\overline{\Sigma}_K P_R \Psi_I \Phi_J^\dagger + y_b^L \,\overline{\Sigma}_K P_L \Psi_I \Phi_J^\dagger \right) + \text{h.c.}\,, \tag{5.16}$$

where we use the same gauge conventions and general notation introduced in Eqs. (5.9) and (5.10). Thus, we can write the general bridge result for $\alpha_{e\gamma}$ as:

$$[\alpha_{e\gamma}]_{2,2} = -\frac{iNe}{4} y_M y_F y_b^R \sum_{IJ} T_{3IJ} \left[ \gamma_\Psi T_{IJ}^{\gamma,\Psi} + \gamma_\Phi T_{IJ}^{\gamma,\Phi} \right] . \tag{5.17}$$

In the case of a singlet bridge, $E$, the relevant Lagrangian is the following:

$$\mathcal{L} \supset y_M \bar{\ell}_L H P_R E + y_F \overline{\Psi}_I \Phi_I e_R + y_b^R \overline{E} P_R \Psi_I \Phi_I^\dagger + y_b^L \overline{E} P_L \Psi_I \Phi_I^\dagger + \text{h.c.}\,, \tag{5.18}$$

using once again the conventions in Eqs. (5.9), (5.10). The contributions to $\alpha_{e\gamma}$ are given by:

$$[\alpha_{e\gamma}]_{2,2} = \frac{iNe}{4} y_M y_F y_b^R \left( \text{Tr}\,[T^{\gamma,\Psi}] \gamma_\Psi + \text{Tr}\,[T^{\gamma,\Phi}] \gamma_\Phi \right) . \tag{5.19}$$

The kinematic factors, common to Eqs. (5.17) and (5.19), for diagrams with a loop including one heavy fermion and the SM Higgs, read

$$\gamma_\Psi = \gamma_\Phi = \lim_{M_\Phi \to 0} f(M_{E(\Sigma)}, M_\Psi, M_\Phi)\,, \tag{5.20}$$

whereas for the case of two heavy particles running in the loop, they are given by:

$$\gamma_\psi = f(M_{E(\Sigma)}, M_\Psi, M_\Phi)\,, \tag{5.21}$$

$$\gamma_\Phi = h(M_{E(\Sigma)}, M_\Psi, M_\Phi)\,. \tag{5.22}$$

## 5.4 Two-field extensions

Since there are not many two field extensions that generate one of the bridge topologies previously discussed, we present in this section the specific $\alpha_{e\gamma}$ results for all of them.

The list of all possible completions that can generate a bridge topology with only one heavy propagator in the loop in collected in Table 5.1. Note that, since the representation of the bridge is fixed, the quantum numbers of the other heavy particle are also fixed, and therefore the possibilities are finite.

**Table 5.1:** 2-field UV completions which generate the bridge topology, with only two heavy propagators. The $a_\mu$ results include, however, all possible topologies for each extension.

| Bridge | Other Fermion | $a_\mu$ result |
|---|---|---|
| $E \sim (1,1,-1)$ | $\Delta \sim (1,2,-1/2)$ | Eq. (5.23) |
| | $\Delta_3 \sim (1,2,-3/2)$ | Eq. (5.24) |
| $\Delta \sim (1,2,-1/2)$ | $E \sim (1,1,-1)$ | Eq. (5.23) |
| | $\Sigma \sim (1,3,-1)$ | Eq. (5.25) |
| | $N \sim (1,1,0)$ | Eq. (5.26) |
| | $\Sigma_0 \sim (1,3,0)$ | Eq. (5.27) |
| $\Sigma \sim (1,3,-1)$ | $\Delta \sim (1,2,-1/2)$ | Eq. (5.25) |
| | $\Delta_3 \sim (1,2,-3/2)$ | Eq. (5.28) |

The chirally enhanced contribution to $\alpha_{e\gamma}$ from all these extensions can be readily obtained using the SOLD package:

```
In[12]:= alpha0egamma[ex_] :=
          16 Pi^2*(Match2Warsaw[alpha0eB[2, 2], ex_]/g1 -
            Match2Warsaw[alpha0eW[2, 2], ex_]/gw) /.
         L1[lLbar, eR, phi][a_, b_] -> 0 // NiceOutput // Simplify
```

We list below the individual results, again, all of them to be understood as divided by the loop factor ($16\pi^2$):

- $E \sim (1,1,-1)$ and $\Delta \sim (1,2,-1/2)$

  Note that in this particular extension, there are two different bridge diagrams that contribute, because both heavy fermions can act as the bridge.

$$[\alpha_{e\gamma}]_{2,2} = -\frac{e\, y_M y_F y_b^R}{4 M_E M_\Delta}\,. \tag{5.23}$$

  The couplings above can therefore be interpreted within the Lagrangian in Eq. (5.9) or Eq. (5.18).

- $E \sim (1,1,-1)$ and $\Delta_3 \sim (1,2,-3/2)$

$$[\alpha_{e\gamma}]_{2,2} = -\frac{5e\, y_M y_F y_b^R}{4 M_E M_{\Delta_3}}\,. \tag{5.24}$$

- $\Delta \sim (1,2,-1/2)$ and $\Sigma \sim (1,3,-1)$

  There are also two bridge diagrams relevant for this extension: one with the doublet on the bridge and the triplet in the loop, and vice-versa.

$$[\alpha_{e\gamma}]_{2,2} = -\frac{9e\, y_M y_F y_b^R}{4 M_\Delta M_\Sigma}\,. \tag{5.25}$$

Both (5.9) and (5.16) can be used to interpret this result.

- $\Delta \sim (1,2,-1/2)$ and $N \sim (1,1,0)$

$$[\alpha_{e\gamma}]_{2,2} = 0\,. \tag{5.26}$$

This zero has been extensively discussed in the literature in Refs. [174, 175].

- $\Delta \sim (1,2,-1/2)$ and $\Sigma_0 \sim (1,3,0)$

$$[\alpha_{e\gamma}]_{2,2} = -\frac{e\, y_M y_F y_b^R}{2M_\Delta M_{\Sigma_0}}\,. \tag{5.27}$$

- $\Sigma \sim (1,3,-1)$ and $\Delta_3 \sim (1,2,-3/2)$

$$[\alpha_{e\gamma}]_{2,2} = -\frac{5e\, y_M y_F y_b^R}{4M_\Sigma M_{\Delta_3}}\,. \tag{5.28}$$

These results were cross-checked against those in [176, 175, 177], and found agreement except for the numerical factors in Eq. (4.8) from Ref. [176] for VLLs with doubly charged components.

In addition, some 2-field extensions can also generate a bridge topology with 3 heavy propagators (Fig. 5.2), given that the fermion in the bridge is the same as the fermion in the loop. These extensions are obviously limited and are listed in Table 5.2. The corresponding contributions to $\alpha_{e\gamma}$ are:

- $E \sim (1,1,-1)$ and $\mathcal{S}_0 \sim (1,1,0)$

$$[\alpha_{e\gamma}]_{2,2} = -e y_b^R y_M y_F \frac{M_E^4 - 4M_E^2 M_{\mathcal{S}_0}^2 + 3M_{\mathcal{S}_0}^4 + 2M_{\mathcal{S}_0}^4 \,\mathrm{Log}\,[M_E^2/M_{\mathcal{S}_0}^2]}{4(M_E^2 - M_{\mathcal{S}_0}^2)^3}\,; \tag{5.29}$$

- $E \sim (1,1,-1)$ and $\mathcal{S}_2 \sim (1,1,-2)$

$$[\alpha_{e\gamma}]_{2,2} = e y_b^R y_M y_F \frac{3M_E^4 - 4M_E^2 M_{\mathcal{S}_2}^2 + M_{\mathcal{S}_2}^4 + (2M_{\mathcal{S}_2}^4 - 4M_E^2 M_{\mathcal{S}_2}^2)\,\mathrm{Log}\,[M_E^2/M_{\mathcal{S}_2}^2]}{2(M_E^2 - M_{\mathcal{S}_2}^2)^3}\,; \tag{5.30}$$

- $\Delta \sim (1,2,-1/2)$ and $\mathcal{S}_0 \sim (1,1,0)$

$$[\alpha_{e\gamma}]_{2,2} = -e y_b^R y_M y_F \frac{M_\Delta^4 - 4M_\Delta^2 M_{\mathcal{S}_0}^2 + 3M_{\mathcal{S}_0}^4 + 2M_{\mathcal{S}_0}^4 \,\mathrm{Log}\,[M_\Delta^2/M_{\mathcal{S}_0}^2]}{4(M_\Delta^2 - M_{\mathcal{S}_0}^2)^3}\,; \tag{5.31}$$

- $\Delta \sim (1,2,-1/2)$ and $\mathcal{S}_1 \sim (1,1,-1)$

$$[\alpha_{e\gamma}]_{2,2} = 0\,; \tag{5.32}$$

- $\Delta \sim (1,2,-1/2)$ and $\Xi_0 \sim (1,3,0)$

$$[\alpha_{e\gamma}]_{2,2} = e y_b^R y_M y_F \frac{M_\Delta^4 + 4M_\Delta^2 M_{\Xi_0}^2 - 5M_{\Xi_0}^4 - (4M_{\Xi_0}^2 M_\Delta^2 + 2M_{\Xi_0}^4)\,\mathrm{Log}\,[M_\Delta^2/M_{\Xi_0}^2]}{4(M_\Delta^2 - M_{\Xi_0}^2)^3}\,; \tag{5.33}$$

- $\Delta \sim (1,2,-1/2)$ and $\Xi_1 \sim (1,3,-1)$

$$[\alpha_{e\gamma}]_{2,2} = -e y_b^R y_M y_F \frac{7M_\Delta^4 - 8M_\Delta^2 M_{\Xi_1}^2 + M_{\Xi_1}^4 + (-10M_{\Xi_1}^2 M_\Delta^2 + 4M_{\Xi_1}^4)\,\mathrm{Log}\,[M_\Delta^2/M_{\Xi_1}^2]}{2(M_\Delta^2 - M_{\Xi_1}^2)^3}\,; \tag{5.34}$$

- $\Sigma \sim (1,3,-1)$ and $\Xi_0 \sim (1,3,0)$

$$[\alpha_{e\gamma}]_{2,2} = -e y_b^R y_M y_F \frac{M_\Sigma^2 - M_{\Xi_0}^2 + M_{\Xi_0}^2\,\mathrm{Log}\,[M_{\Xi_0}^2/M_\Sigma^2]}{(M_\Sigma^2 - M_{\Xi_0}^2)^2}\,; \tag{5.35}$$

- $\Sigma \sim (1,3,-1)$ and $\Xi_2 \sim (1,3,-2)$

$$[\alpha_{e\gamma}]_{2,2} = 0\,. \tag{5.36}$$

A few comments are in order concerning these results. First, we are not considering here flavor for the heavy particles for simplicity. Therefore, in this type of completions, where the bridge coupling $y_b$ involves two fermions that are equal, it will vanish when the gauge structure is antisymmetric. This is the case for completions (5.32) and (5.36). Note that this is not true in general when dealing with multiple families for heavy fields. On the other hand, for models (5.29), (5.31), (5.33) and (5.35), the couplings $y_b^R$ and $y_b^L$ are related by hermitian conjugation; therefore, we redefine $y_b^R \equiv y_b^R + y_b^{L\,*}$ as the effective coupling with the right-handed chirality and write our results using such convention.

These models have been considered previously in the literature [178, 170, 177], apart from the ones that involve fermion number violating (FNV) vertices which, to the best of our knowledge, are first explored here. However, only the Yukawa-proportional contribution (neglected here) was considered, which resulted in most of the models in Tab. 5.2 being excluded as explanations of $\Delta a_\mu$, since this was driven the mass of the new particles to be lighter than what was allowed by experiments. Performing, as we do, the calculations in the unbroken phase of the SM, it becomes easier to see the chirally enhanced contribution coming from the bridge diagram, which allows for the new particles to be heavier while explaining $a_\mu$ and avoiding the constraints. Consequently, this opens up this class of models as possible explanations of the anomaly.

A particularly interesting example is the case of the model with $\Delta \sim (1,2,-1/2) + \Xi_0 \sim (1,3,0)$, where the contribution is quoted to be always negative in the literature (and as such worsening the tension with the observed value). However, we can see from Eq. (5.33) that the dependence on the couplings makes it always possible to take a positive contribution and account for the observed $\Delta a_\mu$.

**Table 5.2:** 2 field fermion-scalar UV extensions which generate the bridge topology with 3 heavy propagators. Completions in gray color involve fermion number violating interactions.

| Fermion | Scalar | Result |
|---|---|---|
| $E \sim (1,1,-1)$ | $\mathcal{S}_0 \sim (1,1,0)$ | Eq. (5.29) |
| | $\mathcal{S}_2 \sim (1,1,-2)$ | Eq. (5.30) |
| $\Delta \sim (1,2,-1/2)$ | $\mathcal{S}_0 \sim (1,1,0)$ | Eq. (5.31) |
| | $\mathcal{S}_1 \sim (1,1,-1)$ | Eq. (5.32) |
| | $\Xi_0 \sim (1,3,0)$ | Eq. (5.33) |
| | $\Xi_1 \sim (1,3,-1)$ | Eq. (5.34) |
| $\Sigma \sim (1,3,-1)$ | $\Xi_0 \sim (1,3,0)$ | Eq. (5.35) |
| | $\Xi_2 \sim (1,3,-2)$ | Eq. (5.36) |

## 5.5 Three-field extensions

In the case of three-field extension, there is an infinite number of extensions that generate the bridge diagram of Fig. 5.2, since the representation of particles in the loop is not fixed, but only their product is. Therefore, we collect in this section the restrictions of the quantum numbers of the fields in the loop in order to contribute through this diagram. This can be done using the results included in the one-loop dictionary, collecting the models contributing to either $\mathcal{O}_{eB}$ or $\mathcal{O}_{eW}$ and selecting the extensions that produce a bridge diagram, as partially shown in Section 5.1.

The conditions that the extra heavy scalar, $\Phi$, and heavy fermion, $\Psi$, must respect are the following:

- VLL singlet bridge:

$$\begin{cases} \mathrm{Y}_\Psi - \mathrm{Y}_\Phi = -1 \\ \mathrm{SU}(2)_\Phi \otimes \mathrm{SU}(2)_\Psi \supset 1 \end{cases} \tag{5.37}$$

- VLL doublet bridge:

$$\begin{cases} \mathrm{Y}_\Psi - \mathrm{Y}_\Phi = -1/2 \\ \mathrm{SU}(2)_\Phi \otimes \mathrm{SU}(2)_\Psi \supset 2 \end{cases} \tag{5.38}$$

- VLL triplet bridge:

$$\begin{cases} \mathrm{Y}_\Psi - \mathrm{Y}_\Phi = -1 \\ \mathrm{SU}(2)_\Phi \otimes \mathrm{SU}(2)_\Psi \supset 3 \\ \mathrm{SU}(2)_\Phi \otimes \mathrm{SU}(2)_\Psi \supset 1 \end{cases} \tag{5.39}$$

In the case of SU(3) representations, the condition is to always form a singlet with the two fields in the loop, $\Phi$ and $\Psi$. Introducing large color representations results in an enhancement factor to the diagram, as explored in [172] for completions with box diagrams.

**Table 5.3:** Three-field UV extensions which generate the bridge topology, up to the triplet representation of SU(2). Only SU(2) representations are shown because the color representations must be the conjugates of each other and the conditions on the hypercharge are specified above. Switching the assigned $SU(2)$ representations between $\Phi$ and $\Psi$ also corresponds to a possible extension.

| Bridge | $(\mathrm{SU}(2)_\Psi\,,\mathrm{SU}(2)_\Phi)$ | Result |
|---|---|---|
| $E \sim (1,1,-1)$ | (1,1) | Eq. (5.40) |
| | (2,2) | Eq. (5.41) |
| | (3,3) | Eq. (5.42) |
| $\Delta \sim (1,2,-1/2)$ | (2,1) | Eqs. (5.43), (5.44) |
| | (2,3) | Eqs. (5.45), (5.46) |
| $\Sigma \sim (1,3,-1)$ | (2,2) | Eq. (5.47) |
| | (3,3) | Eq. (5.48) |

Using the `ListValidQNs` routine in `SOLD`, we can compute the specific quantum numbers that fulfill these conditions. Limiting ourselves to, at most, triplet representations of SU(2), the UV completions which can generate the bridge topology are listed in Table 5.3.

Notice that none of these completions can be found among the ones explored in Refs. [170, 171, 112, 98, 172, 173] and as such represent a new class of SM extensions that can in principle contribute to $a_\mu$. We will present, for completeness, the results from the models in Table 5.3, using again the notation in Eqs. (5.9), (5.16) and (5.18). This corresponds only to the chirally enhanced contributions (terms proportional to the lepton Yukawa are neglected) and, once again, a factor $1/16\pi^2$ is omitted. We do not fix the hypercharge of the new fields, expressing the results in terms of a symbolic one for $\Psi$, $Y_\Psi$, and we use the notation $(\Psi,\Phi) \sim (\mathrm{SU}(2)_\Psi, \mathrm{SU}(2)_\Phi)$ to label the SU(2) representations of the fields.

- $E \sim (1,1,-1) \quad + \quad (\Psi,\Phi) \sim (1,1)$

$$[\alpha_{e\gamma}]_{2,2} = \frac{eNM_\Psi y_M y_F y_b^R}{4M_E(M_\Psi^2 - M_\Phi^2)^3}\Big\{(M_\Psi^2 - M_\Phi^2)(M_\Phi^2(1-2Y_\Psi) + M_\Psi^2(1+2Y_\Psi)) \\ - 2(-M_\Phi^4 Y_\Psi + M_\Psi^2 M_\Phi^2(1+Y_\Psi))\,\mathrm{Log}\,[M_\Psi^2/M_\Phi^2]\Big\}\,; \tag{5.40}$$

- $E \sim (1,1,-1) \quad + \quad (\Psi,\Phi) \sim (2,2)$

$$[\alpha_{e\gamma}]_{2,2} = \frac{eNM_\Psi y_M y_F y_b^R}{2M_E(M_\Psi^2 - M_\Phi^2)^3}\Big\{(M_\Psi^2 - M_\Phi^2)(M_\Phi^2(1-2Y_\Psi) + M_\Psi^2(1+2Y_\Psi)) \\ -2(-M_\Phi^4 Y_\Psi + M_\Psi^2 M_\Phi^2(1+Y_\Psi))\,\mathrm{Log}\,[M_\Psi^2/M_\Phi^2]\Big\}\,; \tag{5.41}$$

- $E \sim (1,1,-1) \quad + \quad (\Psi,\Phi) \sim (3,3)$

$$[\alpha_{e\gamma}]_{2,2} = \frac{3eNM_\Psi y_M y_F y_b^R}{4M_E(M_\Psi^2-M_\Phi^2)^3}\Big\{(M_\Psi^2-M_\Phi^2)(M_\Phi^2(1-2Y_\Psi)+M_\Psi^2(1+2Y_\Psi)) \\ -2(-M_\Phi^4 Y_\Psi + M_\Psi^2 M_\Phi^2(1+Y_\Psi))\,\mathrm{Log}\,[M_\Psi^2/M_\Phi^2]\Big\}\,; \tag{5.42}$$

- $\Delta \sim (1,2,-1/2) \quad + \quad (\Psi,\Phi) \sim (2,1)$

$$[\alpha_{e\gamma}]_{2,2} = \frac{eNM_\Psi y_M y_F y_b^R}{4M_\Delta(M_\Psi^2-M_\Phi^2)^3}\Big\{2(M_\Psi^2-M_\Phi^2)(M_\Phi^2(1-Y_\Psi)+M_\Psi^2 Y_\Psi) \\ -(M_\Phi^4(1-2Y_\Psi) + M_\Psi^2 M_\Phi^2(1+2Y_\Psi))\,\mathrm{Log}\,[M_\Psi^2/M_\Phi^2]\Big\}\,; \tag{5.43}$$

- $\Delta \sim (1,2,-1/2) \quad + \quad (\Psi,\Phi) \sim (1,2)$

$$[\alpha_{e\gamma}]_{2,2} = \frac{eNM_\Psi y_M y_F y_b^R}{4M_\Delta(M_\Psi^2-M_\Phi^2)^3}\Big\{(M_\Psi^2-M_\Phi^2)(M_\Phi^2(1-2Y_\Psi)+M_\Psi^2(1+2Y_\Psi)) \\ -2(-M_\Phi^4 Y_\Psi + M_\Psi^2 M_\Phi^2(1+Y_\Psi))\,\mathrm{Log}\,[M_\Psi^2/M_\Phi^2]\Big\}\,; \tag{5.44}$$

- $\Delta \sim (1,2,-1/2) \quad + \quad (\Psi,\Phi) \sim (2,3)$

$$[\alpha_{e\gamma}]_{2,2} = \frac{eNM_\Psi y_M y_F y_b^R}{4M_\Delta(M_\Psi^2-M_\Phi^2)^3}\Big\{2(M_\Psi^2-M_\Phi^2)(M_\Phi^2(1-3Y_\Psi)+M_\Psi^2(2+3Y_\Psi)) \\ +(M_\Phi^4(1+6Y_\Psi) - M_\Psi^2 M_\Phi^2(7+6Y_\Psi))\,\mathrm{Log}\,[M_\Psi^2/M_\Phi^2]\Big\}\,; \tag{5.45}$$

- $\Delta \sim (1,2,-1/2) \quad + \quad (\Psi,\Phi) \sim (3,2)$

$$[\alpha_{e\gamma}]_{2,2} = -\frac{eNM_\Psi y_M y_F y_b^R}{4M_\Delta(M_\Psi^2-M_\Phi^2)^3}\Big\{(M_\Psi^2-M_\Phi^2)(M_\Phi^2(7-6Y_\Psi)+M_\Psi^2(-1+6Y_\Psi)) \\ -2(M_\Phi^4(2-3Y_\Psi) + M_\Psi^2 M_\Phi^2(1+3Y_\Psi))\,\mathrm{Log}\,[M_\Psi^2/M_\Phi^2]\Big\}\,; \tag{5.46}$$

- $\Sigma \sim (1,3,-1) \quad + \quad (\Psi,\Phi) \sim (2,2)$

$$[\alpha_{e\gamma}]_{2,2} = -\frac{eNM_\Psi y_M y_F y_b^R}{2M_\Sigma(M_\Psi^2-M_\Phi^2)^2}\Big\{M_\Psi^2 - M_\Phi^2 - M_\Phi^2\,\mathrm{Log}\,[M_\Psi^2/M_\Phi^2]\Big\}\,; \tag{5.47}$$

- $\Sigma \sim (1,3,-1) \quad + \quad (\Psi,\Phi) \sim (3,3)$

$$[\alpha_{e\gamma}]_{2,2} = -\frac{eNM_\Psi y_M y_F y_b^R}{M_\Sigma(M_\Psi^2-M_\Phi^2)^2}\Big\{M_\Psi^2 - M_\Phi^2 - M_\Phi^2\,\mathrm{Log}\,[M_\Psi^2/M_\Phi^2]\Big\}\,. \tag{5.48}$$

## 5.6 A step beyond the bridge

So far, we have focused on models explaining the tension in $a_\mu$ because it is an effect that arises at one loop and constitutes a realistic and relevant phenomenological example of the use of the dictionary. In this last section of the chapter, we want to show how the models within it have enough flexibility to accommodate other (present or future) anomalous observations by proposing a specific model as an example.

### 5.6.1 General phenomenological considerations

First, let us briefly discuss some general considerations that apply to the class of bridge models. Among the new particles introduced, the one that is typically more constrained by experiment a priori is the VLL in the bridge, since it is the only one, in principle, coupling linearly to SM particles.

The mixing of VLLs with the SM muon is bounded by electroweak precision observables (EWPO) [179, 180]:

$$\frac{v}{M_E} y_M \lesssim 0.03\,(0.04)\,, \tag{5.49}$$

$$\frac{v}{M_\Delta} y_M \lesssim 0.065\,(0.075)\,, \tag{5.50}$$

$$\frac{v}{M_\Sigma} y_M \lesssim 0.1\,(0.11)\,, \tag{5.51}$$

for the singlet, doublet and triplet of SU(2), respectively, at 1 (2) $\sigma$ confidence levels.

We can find lower limits on the masses of these VLLs set by direct searches at colliders. [181] set a limit of $M_E \gtrsim 175\,\mathrm{GeV}$ for a singlet VLL decaying through muon or electron channels. In [99], however, it is estimated that the HL phase of the LHC could exclude masses lighter than 800 GeV. The doublet has recently been probed by CMS [182], excluding masses below $\sim 800\,\mathrm{GeV}$. These results are conservative for our specific case, since only tau decays were considered, whereas we need a coupling to muons to address the $a_\mu$ tension. In the case of the triplet, the discovery reach of the LHC at $3\,\mathrm{ab}^{-1}$ at $5\,\sigma$ was estimated in [183] to be of approximately 1.4 TeV.

Other direct bounds typically apply to the particles running in the loop (EW or QCD pair production, for instance). However, these are clearly model-dependent and performing a specific study of the phenomenology and general constraints for different types of bridge models is beyond the scope of this section.

Finally, a common feature of chirally enhanced solutions to $a_\mu$ is typically a large contribution to the muon Yukawa through the same mechanism responsible of generating the $a_\mu$ contribution. In fact, the same diagrams contribute in principle to both, without insertions of the gauge boson in the Yukawa ones. In the case of the VLL triplet bridge diagram this does not suppose a problem, since without an insertion of a $W$-boson the loop vanishes. In the other two cases, in turn, a sizable contribution to the muon Yukawa is indeed expected, needing then to explain the cancellation between this contribution and a possible tree-level coefficient. This motivates the idea of UV scenarios in which the Yukawa couplings and the dipole operators have the same origin [184–186].

### 5.6.2 The triple triplet model

Before introducing the model, let us briefly review the anomalous observations that it is designed to address. The LHCb collaboration measurements of $B$-meson decays seemed to suggest an exciting violation of lepton flavor universality. The ratio:

$$R_K^{(*)} = \frac{\mathrm{BR}(B \to K^{(*)}\overline{\mu}\mu)}{\mathrm{BR}(B \to K^{(*)}\overline{e}e)} \tag{5.52}$$

is close to 1 in the SM, but there was a deficit in the observations of muon decays with a combined deviation from the SM prediction of more than $4\,\sigma$ [187–191]. This set of observables was known as the neutral $B$ anomalies, and triggered an active field of research [192–197]. However, the latest measurements reveal that the ratios seem to be compatible with SM [198, 199]. In spite of it, we will still consider here the old measurements in order to illustrate how one could proceed in the event of a future anomalous observable.

Another observed tension is a possible violation of unitarity in the first row of the CKM matrix, known as the Cabibbo Angle Anomaly (CAA). Measurements of $V_{us}$ which assume CKM unitarity coming from super-allowed $\beta$ decays are in tension with those coming from direct measurements from leptonic kaon decays [200, 201], with a significance of 3 to $5\,\sigma$, depending on the parametrization of the $\beta$ decays. See [202–204] for some examples of models explaining this tension. We will parametrize this deviation as the difference from unity of the $R(V_{us})$ observable, defined as the ratio of the values of $V_{us}$ extracted directly from kaon decays and assuming unitarity [205, 206]. This deviation is shown in [205, 206] to be directly related to a correction in the muon vertex with the $W$ boson, denoted by $\epsilon_{\mu\mu}$:

$$\mathcal{L} \supset \frac{g_2}{\sqrt{2}} W_\mu^- \overline{\ell}_i \gamma^\mu P_L \nu_j (\delta_{ij} + \epsilon_{ij}), \tag{5.53}$$

where $i, j$ run over lepton flavors.

The idea of this section is to construct one specific realization of the last class of models in Table 5.3 that is able to alleviate the tension in these observables, besides $a_\mu$. We will show how this can be achieved by extending the SM with the vector-like lepton triplet, $\Sigma$, a triplet scalar leptoquark with hypercharge $-1/3$, $S_3$, and a triplet vector-like quark, $\Psi_Q$, with hypercharge $-4/3$.

First, the triplet leptoquark has been extensively studied and is well-known to provide a tree-level solution for the neutral $B$ anomalies [47, 197, 207, 208]. The VLL triplet, in turn, is able to explain the CAA, in spite of creating some tension with EWPO [180, 206][4]. The constraint of explaining $a_\mu$ including these two particles and using a bridge topology fixes the representation of $\Psi_Q$.

The Lagrangian of this model reads:

$$\begin{aligned} \mathcal{L} \supset\ & y_T^i \overline{\ell}_{Li} H \sigma^I \Sigma_R^I + y_Q^i \overline{\Psi}_{QL}^I S_3^I\, e_{Ri} + i y_b^L \epsilon^{IJK} \overline{\Sigma}_R^I \Psi_{Q,L}^J S_3^{K\dagger} + i y_b^R \epsilon^{IJK} \overline{\Sigma}_L^I \Psi_{Q,R}^J S_3^{K\dagger} \\ & + \lambda_S^{ij} \overline{q}_{Li}^c i\sigma^2 \sigma^I \ell_{Lj} S_3^{I\dagger} + \lambda_U^i \overline{u_{Ri}}\, \Sigma^{c,I} S_3^I + \text{h.c.}, \end{aligned} \tag{5.54}$$

where, again, $q^c \equiv \mathcal{C}\overline{q}^T$ with $\mathcal{C}$ the charge conjugation matrix. We will assume the SM doublets $q_L$ and $\ell_L$ to be in the down-quark and charged lepton diagonal basis, respectively.

[4]This tension between the CAA and EWPO significantly increases with one takes into account the latest CDF II measurement of the $W$-boson mass [209](see [210] for a recent analysis). We will, however, neglect this tension.

| Observable | SM Prediction | Model Prediction | Experiment | Pull model ($\sigma$) | Pull SM ($\sigma$) |
|---|---|---|---|---|---|
| $a_\mu$ | 0.0011659181(4) | 0.0011659201(4) | 0.0011659206(4) | 0.82 | 4.22 |
| $\langle R_{\mu e}\rangle(B^\pm \to K^\pm \ell^+\ell^-)^{[1.0,6.0]}$ | 1 | 0.79 | 0.85(5) | 1.41 | 3.21 |
| $\langle R_{\mu e}\rangle(B^0 \to K^{*0} \ell^+\ell^-)^{[0.045,1.1]}$ | 0.93 | 0.87 | 0.65(12) | 1.98 | 2.39 |
| $\langle R_{\mu e}\rangle(B^0 \to K^{*0} \ell^+\ell^-)^{[1.1,6.0]}$ | 0.99 | 0.79 | 0.68(12) | 1.04 | 2.55 |
| $\epsilon_{\mu\mu}$ | 0 | 0.40e-3 | 0.58(15)e-3 | 1.20 | 3.87 |
| $\Delta M_s$ | 1.25(8)e-11 | 1.25(8)e-11 | 1.1688(14)e-11 | 1.08 | 1.07 |
| $\Delta M_d$ | 3.9(5)e-13 | 3.9(5)e-13 | 3.33(15)e-13 | 1.25 | 1.25 |
| $M_W$ | 80.36 | 80.35 | 80.379(12) | 2.28 | 1.72 |
| $A_e$ | 0.147 | 0.146 | 0.151(2) | 2.77 | 2.22 |

**Table 5.4:** Individual values for the SM prediction, model prediction, experimental measure and pulls of the most relevant observables as given by `smelli`. Definitions of these observables (and updated values) can be read from the `flavio` [54] documentation, which `smelli` uses to calculate contributions from the Wilson coefficients to low energy observables.

Limiting ourselves to the simplest version of this model, we will only consider the minimal set of couplings which allow us to explain the anomalies in $B$-meson decays, $V_{\rm CKM}$ unitarity and $\Delta a_\mu$. We will therefore suppose just one flavor of heavy particles and assume that new physics only couples to second generation leptons (see [211–213] for some works on the implications of g-2 in the flavor structure of new physics). This also helps to avoid some constraints like the Lepton Flavor Violating (LFV) decay $\mu \to e\gamma$. In the quark sector, we will only allow for second and third generation couplings in $\lambda_S^{ij}$, namely $\lambda_S^{s\mu}$ and $\lambda_S^{b\mu}$.

The aforementioned anomalies can be explained in this model due to the generation of $\mathcal{O}_{\ell q}^{(1),(3)}$ at tree-level by $S_3$ exchange, $\mathcal{O}_{H\ell}^{(3)}$ also at tree-level by $\Sigma$ exchange and a bridge-like one-loop contribution to $\Delta a_\mu$. The expressions for the relevant Wilson coefficients are:

$$[\alpha_{\ell q}^{(1)}]_{i,j,k,l} = \frac{3\lambda_S^{*ki}\lambda_S^{lj}}{4M_{S_3}^2} + \mathcal{O}\Big(\frac{1}{16\pi^2}\Big)\,, \tag{5.55}$$

$$[\alpha_{\ell q}^{(3)}]_{i,j,k,l} = \frac{\lambda_S^{*ki}\lambda_S^{lj}}{4M_{S_3}^2} + \mathcal{O}\Big(\frac{1}{16\pi^2}\Big)\,, \tag{5.56}$$

$$[\alpha_{H\ell}^{(3)}]_{i,j} = \frac{y_T^i y_T^{*j}}{4M_\Sigma^2} + \mathcal{O}\Big(\frac{1}{16\pi^2}\Big)\,, \tag{5.57}$$

$$[\alpha_{eB}]_{i,j} \simeq 0\,, \tag{5.58}$$

$$[\alpha_{eW}]_{i,j} \simeq \frac{3g_W y_b^R\, y_T^i y_Q^j}{16\pi^2}\frac{M_{\Psi_Q}}{M_\Sigma}\left(\frac{M_{\Psi_Q}^2 - M_{S_3}^2 + M_{S_3}^2\ \mathrm{Log}\left[\frac{M_{S_3}^2}{M_{\Psi_Q}^2}\right]}{(M_{\Psi_Q}^2 - M_{S_3}^2)^2}\right)\,, \tag{5.59}$$

where the $\simeq$ means that we are once again neglecting Yukawa-suppressed contributions.

Explaining $R_K^{(*)}$ and CAA essentially fixes the ratios $x_S \equiv \lambda_S^{*s\mu}\lambda_S^{b\mu}/M_{S_3}^2$ and $x_T \equiv y_T^\mu/M_\Sigma$, up to small one-loop corrections that break the scale invariance in couplings over masses. In spite of this, the loop suppression is enough for observables to be approximately flat on the values of the masses (within a certain range). The $x_T$ ratio contributes to the expression of $\Delta a_\mu$ as well, but the couplings $y_b^R$ and $x_F \equiv y_Q^\mu/M_{\Psi_Q}$ provide enough freedom to fix both observables to the desired value. Note also that, since they couple two and three heavy fields,

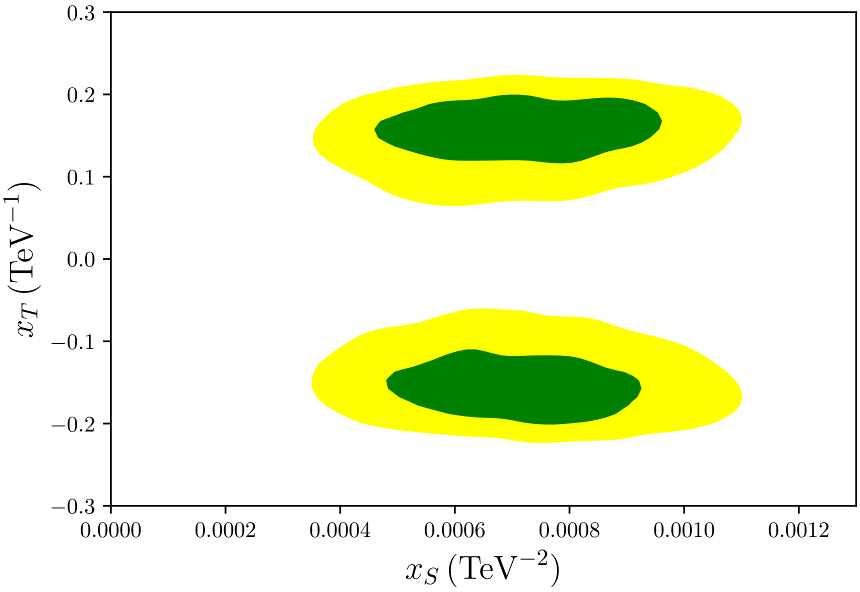


**Figure 5.3:** The 1 (2)-$\sigma$ regions in green (yellow) around the model's best fit point. For each $x_S$ and $x_T$ point in the plot, the other couplings were marginalized in order to minimize the $\chi^2$. The observables included in the fit were the ones available in `smelli` in the classes EWPO, leptonic observables, lepton flavor universality for neutral currents and quark flavor observables, and $\epsilon_{\mu\mu}$.

both $y_b$ and $x_F$ generate Wilson Coefficients starting at one-loop order, so in principle a wider parameter space could be expected in comparison to other couplings.

With the goal of studying the one-loop low-energy phenomenology of the model, we used `matchmakereft` [64] to compute the complete one-loop matching of the model and constructed, using `smelli` [214, 215, 74, 54], a $\chi^2$ function from the relevant observables at low energy in terms of the Wilson Coefficients defined at the cut-off scale. Finally, we performed a fit, minimizing the $\chi^2$ function using the `iminuit` [216] python package. The likelihood includes the observables given in `smelli` in the classes of leptonic observables (with magnetic dipole moments for leptons), lepton flavor universality for neutral currents (for anomalies in $B$ decays such as $R_K^{(*)}$), EWPO (containing observables sensitive to deviations in the electroweak vertices) and quark flavor related observables (which include meson decays and mixing)[5]. Besides these observables taken directly from `smelli`, we also added $\epsilon_{\mu\mu}$.

In addition to the flavor assumptions listed above, we further imposed the couplings to be lower than 1, and fixed the values of the masses to $M_\Sigma = 3.4$ TeV, $M_{S_3} = 2$ TeV and $M_{\Psi_Q} = 4.6$ TeV. As discussed above, the observables were indeed essentially flat for masses between 1-5 TeV, so this hierarchy was chosen just as an example that avoided current experimental detection limits but that could be reached by upcoming searches. Other hierarchies and values for the masses between 1-5 TeV are also feasible and yield similar results.

The best fit point in this setup is:

$$\begin{aligned} x_F &= 0.2\ \mathrm{TeV}^{-1}, & x_S &= 0.00078\ \mathrm{TeV}^{-2}, \\ x_T &= 0.17\ \mathrm{TeV}^{-1}, & \lambda_S^{b\mu} &= 0.07, \\ y_b^L &= 0.10, & y_b^R &= 0.13, \end{aligned} \tag{5.60}$$

[5]See Appendix D of [214] to find more details on all the observables included in these classes.

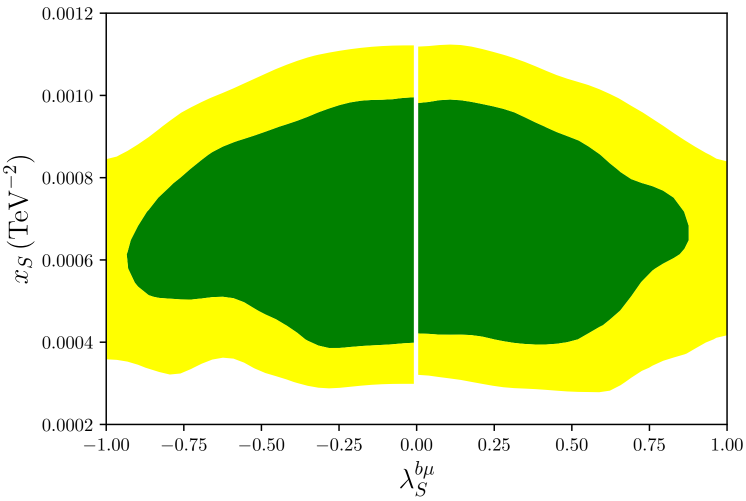


**Figure 5.4:** The 1 (2)-$\sigma$ regions in green (yellow) around the model's best fit point. For each point in the plot, the other couplings were marginalized in order to minimize the $\chi^2$. The observables included in the fit were the ones available in `smelli` in the classes EWPO, leptonic observables, lepton flavor universality for neutral currents and quark flavor observables, and $\epsilon_{\mu\mu}$. Values of $\lambda_S^{b\mu}$ very close to zero were not plotted because that would imply $\lambda_S^{s\mu}$ larger than 1 for a fixed $x_S$ and $M_{S_3}$.

which corresponds to a global pull from the SM of 6.2 $\sigma$. This pull was computed from the observables included in the likelihood, i.e., the ones available in `smelli` in the classes EWPO, leptonic observables, lepton flavor universality for neutral currents and quark flavor observables; we do not include $\epsilon_{\mu\mu}$ since we did not consider its correlations with the observables in the stated classes. Some of the individual pulls for the most relevant observables, both from experiment and SM, are collected in Table 5.4.

Figures 5.3 and 5.4 show the 1- and 2-$\sigma$ regions from the best-fit point for the parameters of the model that generate Wilson Coefficients at tree level, using the global likelihood constructed with `smelli`. For each point in the grid, the value of $\chi^2$ was minimized by varying the remaining parameters. The profiles in the rest of the variables, that contribute for the firs time at one loop, are very similar to what one would expect from only taking the tree level solutions (i.e. they feature somewhat flat directions), showing that the model has enough freedom to explain $\Delta a_\mu$ without spoiling the anomalies independently explained at tree level. These flat directions are illustrated in the plots of Fig. 5.5, where the couplings on the $x$-axis only enter at one-loop. Note that $y_b^L$ is the only coupling allowed to vanish because it does not contribute to the relevant anomalies.

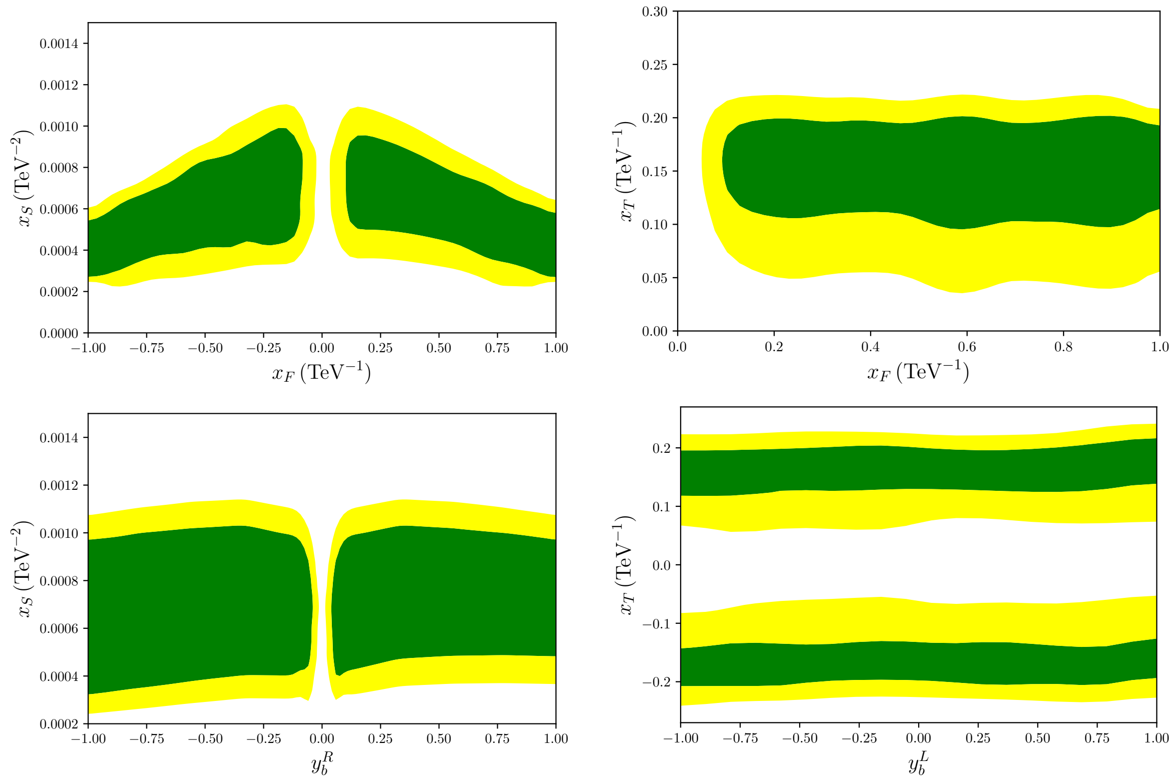


**Figure 5.5:** The 1 (2)-$\sigma$ regions in green (yellow) around the model's best fit point. For every plot, the vertical axis represents a coupling that enters observables a tree-level, whereas the horizontal axis represents one that only contributes at one-loop. For each point in the plot, the other couplings were marginalized in order to minimize the $\chi^2$. The observables included in the fit were the ones available in `smelli` in the classes EWPO, leptonic observables, lepton flavor universality for neutral currents and quark flavor observables, and $\epsilon_{\mu\mu}$.

# 6 Conclusions

The Standard Model meant a huge success in the history of particle physics, but we have many reasons to believe there must be new physics beyond it. Decades of theoretical efforts and experimental searches have left us with a myriad of models and no clue of where this new physics is hiding. Some would advocate for stopping the waste of time and giving up our search, but others see this situation as a time of opportunities. Indeed, we can follow the trail of what the data are hinting: new physics seems to be waiting for us behind an energy gap greater than we expected, and this opens up the possibility of using Effective Field Theories. The works comprised in this thesis have the purpose of pushing forward the use of EFTs, both developing tools for the community and exploring new physics scenarios ourselves to be able to obtain the most out of it.

We discussed in Chapter 2 how EFTs had the advantage of splitting the problem in two independent steps. Through the bottom-up approach, we can parametrize and constrain all possible deviations from SM in a highly agnostic way. We dispose of an ordering principle that allows us to list all the coefficients that can be observed at a certain experimental precision, and use them to perform calculations just once. However, this tells us nothing about new physics by itself; we need a connection – the top down approach – between these coefficients and the models among which we want to discriminate, given by the process of matching. After many collective efforts, the running in SMEFT and LEFT and the matching between them have been computed at one loop and are available in computer tools. Likewise, the matching of arbitrary models onto the SMEFT has been solved at tree level and dimension six. However, performing a complete one-loop analysis of the implications of new physics models still means to match them at one loop, which is very cumbersome in practice and needs to be repeated for every model.

In Chapter 3 we introduced `matchmakereft` [64], a tool designed to compute automatically the matching between two arbitrary theories up to one loop. In particular, we provide the model for the the B-preserving sector of the SMEFT at dimension six, which can be used to complete the mentioned chain in the translation between new physics and experimental implications. `Matchmakereft` is robust, efficient and flexible, and have been extensively cross-checked to ensure the reliability of our results. In fact, it has already been used in several physical applications which, due to its flexibility, are many more than just the matching to the SMEFT. The possibility of defining arbitrary EFTs makes it usable for extending the matching of SMEFT to higher dimensions or for the matching to other motivated EFTs, like the ones including an axion-like particle or a right-handed neutrino [217]. Another relevant use is the calculation of the RGEs of arbitrary theories (renormalizable or not). Other applications include the automated basis translation between two EFT bases (either Green's or physical) or the extraction of the relations between a set of linearly dependent operators in $d$ dimensions. All these features will allow the particle physics community to analyze in a automated way the one-loop phenomenology or arbitrary new physics models.

Moreover, `matchmakereft` is constantly growing in efficiency and functionalities. The parallelization of the calculations, already available, can significantly decrease the time of execution. The current input from the user only consists of giving the details about the UV and EFT models, but we plan to reduce it even further. With the generation of EFT bases greatly automatized in the last few years, the main bottleneck is the reduction from a Green's basis to a physical one. This not only involves the computation of redundancies, but also the evanescent shifts to the physical basis. Given the flexibility that `matchmakereft` offers, we are already planning to use it to solve both problems.

The power of EFTs, however, goes beyond simplifying the comparison between models and experimental data. Given the vast number of possible models of new physics, even being able of perform the matching automatically, we need a way of guiding or organizing the search. Since the number of coefficients at any observable order in the mass and loop expansion is finite, we can classify all the models which have observable consequences. This allows us to obtain, in a systematic way, the complete phenomenological implications of any model: new physics, whatever it is, will be included in that list as long as it is observable. This is the idea behind IR/UV dictionaries, that encode the correspondence between Wilson Coefficients and extensions of the Standard Model (at a given order). The leading tree-level dictionary for the SMEFT at dimension six was computed only recently, but in order to make a competitive, realistic analysis given the current experimental precision we need to extend it to include one-loop effects.

Chapter 4 presents the first step towards the calculation of the IR/UV dictionary for the SMEFT at mass dimension 6 and one-loop order. In particular, we classify all SM extensions including new heavy fermions and scalars that contribute to the sector of the SMEFT that cannot be generated at tree level, so that the contributions considered are the leading ones for them. A key feature, absent at tree level, is that infinite different extensions can generate a coefficient, since representations of heavy fields are not fixed but only their product is. However, we can still provide the list in a closed form by indicating the restrictions that these representations have to fulfill in order to contribute to a certain coefficient. The results are provided in electronic form via the `Mathematica` package `SOLD` [49] (SMEFT One Loop Dictionary), together with routines to obtain the value of these WCs for arbitrary extensions and specify the representations that can satisfy any given restriction.

Moreover, we have included routines that, for a particular SM extension, automatically create the `matchmakereft` model and compute the complete one-loop matching of the model using `matchmakereft`. The only inputs from the user are the spin and quantum numbers of the heavy fermions and scalars in the extension, which significantly increases the efficiency in the use of `matchmakereft`.

Finally, we have illustrated how the dictionary, even in its current, partial form, can still be used for relevant phenomenological studies, first with a brief example about a recently reported tension in some $B$ decays, and second with its application to the g-2 anomaly in Chapter 5. In this chapter we perform a detailed, systematic study of the chirally enhanced contributions to $a_\mu$ arising from bridge topologies [89]. General results for two and three field extensions generating this topology, with gauge representations unspecified, are provided, together with specific results for all two field extensions and some of the three field ones (since there is an infinite number of them). These general results are also provided for the usual box topology considered in the literature in Appendix C.

Within these two field extensions, we arrive at a class of them, with a fermion and a scalar, which had been previously discarded in the literature but that, when considering this bridge diagram contribution, can in principle be viable solutions to alleviate the $a_\mu$ tension. Moreover, the set of three field extensions considered represent a completely new class of models which, to the best of our knowledge, were not considered in the literature.

We have shown, in addition, how the systematic study of effects arising at one-loop (in our case, the anomalous magnetic moment of the muon) can open up the possibility of a common explanation with other observations, even at tree level. We demonstrate this with a toy model designed to address the anomalies in the neutral $B$ decays, the $V_{CKM}$ unitarity and the anomalous magnetic moment of the muon. Using `matchmakereft` and `smelli`, we perform a one-loop analysis of its phenomenology and show the allowed regions in parameter space. Even if all these tensions with the SM eventually fade away, we believe that this analysis sets an example of how the provided dictionary can be used if (when) new anomalous observations are found, and how dictionaries simplify the scrutiny of observable models of new physics.

We do not know how or where new physics will finally be revealed to us. The field is living a time of changes and uncertainty, in which the challenge could be precisely how to address this situation. In the next years we will have to decide the experiments that will determine the future of the field in half a century, so we need to extract the most information out of what we have. In this sense, it is essential to proceed systematically and agnostically, and Effective Field Theories are a very useful ally in this quest. We need to develop all the tools necessary to make this search in the most smart and efficient way, and be prepared to explore all possibilities in the light of future data. In this time of uncertainty only one thing is clear: the search continues.

# A

# Conventions

In this Appendix we collect a set of different conventions that we adopt throughout this thesis. In first place, we will use the following Lagrangian for the Standard Model:

$$
\begin{aligned}
\mathcal{L}_{\rm SM} &= -\frac{1}{4}G^A_{\mu\nu}G^{A\,\mu\nu} - \frac{1}{4}W^I_{\mu\nu}W^{I\,\mu\nu} - \frac{1}{4}B_{\mu\nu}B^{\mu\nu} + (D_\mu H)^\dagger D^\mu H - m^2 H^\dagger H - \lambda(H^\dagger H)^2 \\
&+ \mathrm{i}[\bar{\ell}\not{D}\ell + \bar{e}\not{D}e + \bar{q}\not{D}q + \bar{u}\not{D}u + \bar{d}\not{D}d] - [\bar{\ell}Y_e eH + \bar{q}Y_u u\tilde{H} + \bar{q}Y_d dH + \text{h.c.}]\ . \quad \text{(A.1)}
\end{aligned}
$$

We will omit in general gauge and flavor indices. When necessary, we will tipically use $i, j, k, l, \ldots$ as flavour indices and $A, B, C, \ldots$ and $I, J, K, \ldots$ for the adjoint representation of SU(3) and SU(2), respectively. On the other hand, $a, b, c, \ldots$ and $r, s, t, \ldots$ will be used for the fundamental representations their respective fundamental representations. $\tilde{H}$ is defined as $\tilde{H} = \mathrm{i}\sigma^2 H^*$ and we use the following convention for the covariant derivative:

$$
D_\mu q = (\partial_\mu - \mathrm{i}g_3 T^A G^A_\mu - \mathrm{i}g_2 \frac{\sigma^I}{2} W^I_\mu - \mathrm{i}g_1 Y B_\mu)q, \tag{A.2}
$$

where $T^A = \lambda^A/2$ and $\lambda^A$, $\sigma^I$ are the Gell-Mann and Pauli matrices, respectively. Correspondingly, the field strength tensors are:

$$
\begin{aligned}
G^A_{\mu\nu} &= \partial_\mu G^A_\nu - \partial_\nu G^A_\mu + g_3 f^{ABC} G^B_\mu G^C_\nu, && \text{(A.3)}\\
W^I_{\mu\nu} &= \partial_\mu W^I_\nu - \partial_\nu W^I_\mu + g_2 \epsilon^{IJK} W^J_\mu W^K_\nu, && \text{(A.4)}\\
B_{\mu\nu} &= \partial_\mu B_\nu - \partial_\nu B_\mu, && \text{(A.5)}
\end{aligned}
$$

and their covariant derivatives:

$$
\begin{aligned}
(D_\rho G_{\mu\nu})^A &= \partial_\rho G^A_{\mu\nu} + g_3 f^{ABC} G^B_\rho G^C_{\mu\nu}, && \text{(A.6)}\\
(D_\rho W_{\mu\nu})^I &= \partial_\rho W^I_{\mu\nu} + g_2 \epsilon^{IJK} W^J_\rho W^K_{\mu\nu}, && \text{(A.7)}\\
(D_\rho B_{\mu\nu}) &= \partial_\rho B_{\mu\nu}, && \text{(A.8)}
\end{aligned}
$$

with $f^{ABC}$ and $\epsilon^{IJK}$ the $SU(3)$ and $SU(2)$ structure constants, respectively.

The chiral projectors are defined as usual:

$$P_{R,L} = \frac{1}{2}(1 \pm \gamma_5), \tag{A.9}$$

and we use:

$$\sigma^{\mu\nu} = \frac{\mathrm{i}}{2}[\gamma^\mu, \gamma^\nu] \tag{A.10}$$

for the commutator of gamma matrices. We use the convention $\epsilon_{0123} = -1$ with $\epsilon^{\alpha\beta\mu\nu}$ the Levi-Civita tensor, in such a way that for $D = 4$ e.g.

$$\sigma^{\mu\nu}\epsilon_{\mu\nu\rho\sigma} = -2\mathrm{i}\sigma_{\rho\sigma}\gamma_5, \tag{A.11}$$

and

$$\gamma_5 = \mathrm{i}\gamma^0\gamma^1\gamma^2\gamma^3 = -\frac{i}{4!}\epsilon_{\mu\nu\alpha\beta}\gamma^\mu\gamma^\nu\gamma^\alpha\gamma^\beta. \tag{A.12}$$

Dual tensors are defined by:

$$\tilde{X}_{\mu\nu} = \frac{1}{2}\epsilon_{\mu\nu\alpha\beta}X^{\mu\nu}, \quad \text{with} \quad X = G, W, B. \tag{A.13}$$

# B

# SMEFT Green's Basis

| $\boldsymbol{X^3}$ | | $\boldsymbol{X^2H^2}$ | | $\boldsymbol{H^2D^4}$ | |
|---|---|---|---|---|---|
| $\mathcal{O}_{3G}$ | $f^{ABC}G_\mu^{A\nu}G_\nu^{B\rho}G_\rho^{C\mu}$ | $\mathcal{O}_{HG}$ | $G^A_{\mu\nu}G^{A\mu\nu}(H^\dagger H)$ | $\mathcal{R}_{DH}$ | $(D_\mu D^\mu H)^\dagger(D_\nu D^\nu H)$ |
| $\mathcal{O}_{3\widetilde{G}}$ | $f^{ABC}\widetilde{G}_\mu^{A\nu}G_\nu^{B\rho}G_\rho^{C\mu}$ | $\mathcal{O}_{H\widetilde{G}}$ | $\widetilde{G}^A_{\mu\nu}G^{A\mu\nu}(H^\dagger H)$ | $\boldsymbol{H^4D^2}$ | |
| $\mathcal{O}_{3W}$ | $\epsilon^{IJK}W_\mu^{I\nu}W_\nu^{J\rho}W_\rho^{K\mu}$ | $\mathcal{O}_{HW}$ | $W^I_{\mu\nu}W^{I\mu\nu}(H^\dagger H)$ | $\mathcal{O}_{H\Box}$ | $(H^\dagger H)\Box(H^\dagger H)$ |
| $\mathcal{O}_{3\widetilde{W}}$ | $\epsilon^{IJK}\widetilde{W}_\mu^{I\nu}W_\nu^{J\rho}W_\rho^{K\mu}$ | $\mathcal{O}_{H\widetilde{W}}$ | $\widetilde{W}^I_{\mu\nu}W^{I\mu\nu}(H^\dagger H)$ | $\mathcal{O}_{HD}$ | $(H^\dagger D^\mu H)^\dagger(H^\dagger D_\mu H)$ |
| $\boldsymbol{X^2D^2}$ | | $\mathcal{O}_{HB}$ | $B_{\mu\nu}B^{\mu\nu}(H^\dagger H)$ | $\mathcal{R}'_{HD}$ | $(H^\dagger H)(D_\mu H)^\dagger(D^\mu H)$ |
| $\mathcal{R}_{2G}$ | $-\frac{1}{2}(D_\mu G^{A\mu\nu})(D^\rho G^A_{\rho\nu})$ | $\mathcal{O}_{H\widetilde{B}}$ | $\widetilde{B}_{\mu\nu}B^{\mu\nu}(H^\dagger H)$ | $\mathcal{R}''_{HD}$ | $(H^\dagger H)D_\mu(H^\dagger \mathrm{i}\overleftrightarrow{D}^\mu H)$ |
| $\mathcal{R}_{2W}$ | $-\frac{1}{2}(D_\mu W^{I\mu\nu})(D^\rho W^I_{\rho\nu})$ | $\mathcal{O}_{HWB}$ | $W^I_{\mu\nu}B^{\mu\nu}(H^\dagger\sigma^I H)$ | $\boldsymbol{H^6}$ | |
| $\mathcal{R}_{2B}$ | $-\frac{1}{2}(\partial_\mu B^{\mu\nu})(\partial^\rho B_{\rho\nu})$ | $\mathcal{O}_{H\widetilde{W}B}$ | $\widetilde{W}^I_{\mu\nu}B^{\mu\nu}(H^\dagger\sigma^I H)$ | $\mathcal{O}_H$ | $(H^\dagger H)^3$ |
| | | $\boldsymbol{H^2XD^2}$ | | | |
| | | $\mathcal{R}_{WDH}$ | $D_\nu W^{I\mu\nu}(H^\dagger \mathrm{i}\overleftrightarrow{D}^I_\mu H)$ | | |
| | | $\mathcal{R}_{BDH}$ | $\partial_\nu B^{\mu\nu}(H^\dagger \mathrm{i}\overleftrightarrow{D}_\mu H)$ | | |

**Table B.1:** Physical and redundant bosonic operators.

| $\psi^2 D^3$ | | $\psi^2 XD$ | | $\psi^2 DH^2$ | |
|---|---|---|---|---|---|
| $\mathcal{R}_{qD}$ | $\frac{\mathrm{i}}{2}\bar{q}\left\{D_\mu D^\mu, \slashed{D}\right\} q$ | $\mathcal{R}_{Gq}$ | $(\bar{q}T^A\gamma^\mu q)D^\nu G^A_{\mu\nu}$ | $\mathcal{O}^{(1)}_{Hq}$ | $(\bar{q}\gamma^\mu q)(H^\dagger \mathrm{i}\overleftrightarrow{D}_\mu H)$ |
| $\mathcal{R}_{uD}$ | $\frac{\mathrm{i}}{2}\bar{u}\left\{D_\mu D^\mu, \slashed{D}\right\} u$ | $\mathcal{R}'_{Gq}$ | $\frac{1}{2}(\bar{q}T^A\gamma^\mu \mathrm{i}\overleftrightarrow{D}^\nu q)G^A_{\mu\nu}$ | $\mathcal{R}'^{(1)}_{Hq}$ | $(\bar{q}\,\mathrm{i}\overleftrightarrow{\slashed{D}}\,q)(H^\dagger H)$ |
| $\mathcal{R}_{dD}$ | $\frac{\mathrm{i}}{2}\bar{d}\left\{D_\mu D^\mu, \slashed{D}\right\} d$ | $\mathcal{R}'_{\widetilde{G}q}$ | $\frac{1}{2}(\bar{q}T^A\gamma^\mu \mathrm{i}\overleftrightarrow{D}^\nu q)\widetilde{G}^A_{\mu\nu}$ | $\mathcal{R}''^{(1)}_{Hq}$ | $(\bar{q}\gamma^\mu q)\partial_\mu(H^\dagger H)$ |
| $\mathcal{R}_{\ell D}$ | $\frac{\mathrm{i}}{2}\bar{\ell}\left\{D_\mu D^\mu, \slashed{D}\right\} \ell$ | $\mathcal{R}_{Wq}$ | $(\bar{q}\sigma^I\gamma^\mu q)D^\nu W^I_{\mu\nu}$ | $\mathcal{O}^{(3)}_{Hq}$ | $(\bar{q}\sigma^I\gamma^\mu q)(H^\dagger \mathrm{i}\overleftrightarrow{D}^I_\mu H)$ |
| $\mathcal{R}_{eD}$ | $\frac{\mathrm{i}}{2}\bar{e}\left\{D_\mu D^\mu, \slashed{D}\right\} e$ | $\mathcal{R}'_{Wq}$ | $\frac{1}{2}(\bar{q}\sigma^I\gamma^\mu \mathrm{i}\overleftrightarrow{D}^\nu q)W^I_{\mu\nu}$ | $\mathcal{R}'^{(3)}_{Hq}$ | $(\bar{q}\,\mathrm{i}\overleftrightarrow{\slashed{D}}^I q)(H^\dagger\sigma^I H)$ |
| **$\psi^2 HD^2$ + h.c.** | | $\mathcal{R}'_{\widetilde{W}q}$ | $\frac{1}{2}(\bar{q}\sigma^I\gamma^\mu \mathrm{i}\overleftrightarrow{D}^\nu q)\widetilde{W}^I_{\mu\nu}$ | $\mathcal{R}''^{(3)}_{Hq}$ | $(\bar{q}\sigma^I\gamma^\mu q)D_\mu(H^\dagger\sigma^I H)$ |
| $\mathcal{R}_{uHD1}$ | $(\bar{q}u)D_\mu D^\mu \widetilde{H}$ | $\mathcal{R}_{Bq}$ | $(\bar{q}\gamma^\mu q)\partial^\nu B_{\mu\nu}$ | $\mathcal{O}_{Hu}$ | $(\bar{u}\gamma^\mu u)(H^\dagger \mathrm{i}\overleftrightarrow{D}_\mu H)$ |
| $\mathcal{R}_{uHD2}$ | $(\bar{q}\,\mathrm{i}\sigma_{\mu\nu}D^\mu u)D^\nu \widetilde{H}$ | $\mathcal{R}'_{Bq}$ | $\frac{1}{2}(\bar{q}\gamma^\mu \mathrm{i}\overleftrightarrow{D}^\nu q)B_{\mu\nu}$ | $\mathcal{R}'_{Hu}$ | $(\bar{u}\,\mathrm{i}\overleftrightarrow{\slashed{D}}\,u)(H^\dagger H)$ |
| $\mathcal{R}_{uHD3}$ | $(\bar{q}D_\mu D^\mu u)\widetilde{H}$ | $\mathcal{R}'_{\widetilde{B}q}$ | $\frac{1}{2}(\bar{q}\gamma^\mu i\overleftrightarrow{D}^\nu q)\widetilde{B}_{\mu\nu}$ | $\mathcal{R}''_{Hu}$ | $(\bar{u}\gamma^\mu u)\partial_\mu(H^\dagger H)$ |
| $\mathcal{R}_{uHD4}$ | $(\bar{q}D_\mu u)D^\mu \widetilde{H}$ | $\mathcal{R}_{Gu}$ | $(\bar{u}T^A\gamma^\mu u)D^\nu G^A_{\mu\nu}$ | $\mathcal{O}_{Hd}$ | $(\bar{d}\gamma^\mu d)(H^\dagger \mathrm{i}\overleftrightarrow{D}_\mu H)$ |
| $\mathcal{R}_{dHD1}$ | $(\bar{q}d)D_\mu D^\mu H$ | $\mathcal{R}'_{Gu}$ | $\frac{1}{2}(\bar{u}T^A\gamma^\mu \mathrm{i}\overleftrightarrow{D}^\nu u)G^A_{\mu\nu}$ | $\mathcal{R}'_{Hd}$ | $(\bar{d}\,\mathrm{i}\overleftrightarrow{\slashed{D}}\,d)(H^\dagger H)$ |
| $\mathcal{R}_{dHD2}$ | $(\bar{q}\,\mathrm{i}\sigma_{\mu\nu}D^\mu d)D^\nu H$ | $\mathcal{R}'_{\widetilde{G}u}$ | $\frac{1}{2}(\bar{u}T^A\gamma^\mu \mathrm{i}\overleftrightarrow{D}^\nu u)\widetilde{G}^A_{\mu\nu}$ | $\mathcal{R}''_{Hd}$ | $(\bar{d}\gamma^\mu d)\partial_\mu(H^\dagger H)$ |
| $\mathcal{R}_{dHD3}$ | $(\bar{q}D_\mu D^\mu d)H$ | $\mathcal{R}_{Bu}$ | $(\bar{u}\gamma^\mu u)\partial^\nu B_{\mu\nu}$ | $\mathcal{O}_{Hud}$ | $(\bar{u}\gamma^\mu d)(\widetilde{H}^\dagger \mathrm{i}D_\mu H)$ |
| $\mathcal{R}_{dHD4}$ | $(\bar{q}D_\mu d)D^\mu H$ | $\mathcal{R}'_{Bu}$ | $\frac{1}{2}(\bar{u}\gamma^\mu \mathrm{i}\overleftrightarrow{D}^\nu u)B_{\mu\nu}$ | $\mathcal{O}^{(1)}_{H\ell}$ | $(\bar{\ell}\gamma^\mu \ell)(H^\dagger \mathrm{i}\overleftrightarrow{D}_\mu H)$ |
| $\mathcal{R}_{eHD1}$ | $(\bar{\ell}e)D_\mu D^\mu H$ | $\mathcal{R}'_{\widetilde{B}u}$ | $\frac{1}{2}(\bar{u}\gamma^\mu \mathrm{i}\overleftrightarrow{D}^\nu u)\widetilde{B}_{\mu\nu}$ | $\mathcal{R}'^{(1)}_{H\ell}$ | $(\bar{\ell}i\overleftrightarrow{\slashed{D}}\,\ell)(H^\dagger H)$ |
| $\mathcal{R}_{eHD2}$ | $(\bar{\ell}\,\mathrm{i}\sigma_{\mu\nu}D^\mu e)D^\nu H$ | $\mathcal{R}_{Gd}$ | $(\bar{d}T^A\gamma^\mu d)D^\nu G^A_{\mu\nu}$ | $\mathcal{R}''^{(1)}_{H\ell}$ | $(\bar{\ell}\gamma^\mu \ell)\partial_\mu(H^\dagger H)$ |
| $\mathcal{R}_{eHD3}$ | $(\bar{\ell}D_\mu D^\mu e)H$ | $\mathcal{R}'_{Gd}$ | $\frac{1}{2}(\bar{d}T^A\gamma^\mu \mathrm{i}\overleftrightarrow{D}^\nu d)G^A_{\mu\nu}$ | $\mathcal{O}^{(3)}_{H\ell}$ | $(\bar{\ell}\sigma^I\gamma^\mu \ell)(H^\dagger \mathrm{i}\overleftrightarrow{D}^I_\mu H)$ |
| $\mathcal{R}_{eHD4}$ | $(\bar{\ell}D_\mu e)D^\mu H$ | $\mathcal{R}'_{\widetilde{G}d}$ | $\frac{1}{2}(\bar{d}T^A\gamma^\mu \mathrm{i}\overleftrightarrow{D}^\nu d)\widetilde{G}^A_{\mu\nu}$ | $\mathcal{R}'^{(3)}_{H\ell}$ | $(\bar{\ell}\mathrm{i}\overleftrightarrow{\slashed{D}}^I \ell)(H^\dagger\sigma^I H)$ |
| **$\psi^2 XH$ + h.c.** | | $\mathcal{R}_{Bd}$ | $(\bar{d}\gamma^\mu d)\partial^\nu B_{\mu\nu}$ | $\mathcal{R}''^{(3)}_{H\ell}$ | $(\bar{\ell}\sigma^I\gamma^\mu \ell)D_\mu(H^\dagger\sigma^I H)$ |
| $\mathcal{O}_{uG}$ | $(\bar{q}T^A\sigma^{\mu\nu}u)\widetilde{H}G^A_{\mu\nu}$ | $\mathcal{R}'_{Bd}$ | $\frac{1}{2}(\bar{d}\gamma^\mu i\overleftrightarrow{D}^\nu d)B_{\mu\nu}$ | $\mathcal{O}_{He}$ | $(\bar{e}\gamma^\mu e)(H^\dagger \mathrm{i}\overleftrightarrow{D}_\mu H)$ |
| $\mathcal{O}_{uW}$ | $(\bar{q}\sigma^{\mu\nu}u)\sigma^I\widetilde{H}W^I_{\mu\nu}$ | $\mathcal{R}'_{\widetilde{B}d}$ | $\frac{1}{2}(\bar{d}\gamma^\mu i\overleftrightarrow{D}^\nu d)\widetilde{B}_{\mu\nu}$ | $\mathcal{R}'_{He}$ | $(\bar{e}\,\mathrm{i}\overleftrightarrow{\slashed{D}}\,e)(H^\dagger H)$ |
| $\mathcal{O}_{uB}$ | $(\bar{q}\sigma^{\mu\nu}u)\widetilde{H}B_{\mu\nu}$ | $\mathcal{R}_{W\ell}$ | $(\bar{\ell}\sigma^I\gamma^\mu \ell)D^\nu W^I_{\mu\nu}$ | $\mathcal{R}''_{He}$ | $(\bar{e}\gamma^\mu e)\partial_\mu(H^\dagger H)$ |
| $\mathcal{O}_{dG}$ | $(\bar{q}T^A\sigma^{\mu\nu}d)HG^A_{\mu\nu}$ | $\mathcal{R}'_{W\ell}$ | $\frac{1}{2}(\bar{\ell}\sigma^I\gamma^\mu \mathrm{i}\overleftrightarrow{D}^\nu \ell)W^I_{\mu\nu}$ | **$\psi^2 H^3$ + h.c.** | |
| $\mathcal{O}_{dW}$ | $(\bar{q}\sigma^{\mu\nu}d)\sigma^I HW^I_{\mu\nu}$ | $\mathcal{R}'_{\widetilde{W}\ell}$ | $\frac{1}{2}(\bar{\ell}\sigma^I\gamma^\mu \mathrm{i}\overleftrightarrow{D}^\nu \ell)\widetilde{W}^I_{\mu\nu}$ | $\mathcal{O}_{uH}$ | $(H^\dagger H)\bar{q}\widetilde{H}u$ |
| $\mathcal{O}_{dB}$ | $(\bar{q}\sigma^{\mu\nu}d)HB_{\mu\nu}$ | $\mathcal{R}_{B\ell}$ | $(\bar{\ell}\gamma^\mu \ell)\partial^\nu B_{\mu\nu}$ | $\mathcal{O}_{dH}$ | $(H^\dagger H)\bar{q}Hd$ |
| $\mathcal{O}_{eW}$ | $(\bar{\ell}\sigma^{\mu\nu}e)\sigma^I HW^I_{\mu\nu}$ | $\mathcal{R}'_{B\ell}$ | $\frac{1}{2}(\bar{\ell}\gamma^\mu \mathrm{i}\overleftrightarrow{D}^\nu \ell)B_{\mu\nu}$ | $\mathcal{O}_{eH}$ | $(H^\dagger H)\bar{\ell}He$ |
| $\mathcal{O}_{eB}$ | $(\bar{\ell}\sigma^{\mu\nu}e)HB_{\mu\nu}$ | $\mathcal{R}'_{\widetilde{B}\ell}$ | $\frac{1}{2}(\bar{\ell}\gamma^\mu \mathrm{i}\overleftrightarrow{D}^\nu \ell)\widetilde{B}_{\mu\nu}$ | | |
| | | $\mathcal{R}_{Be}$ | $(\bar{e}\gamma^\mu e)\partial^\nu B_{\mu\nu}$ | | |
| | | $\mathcal{R}'_{Be}$ | $\frac{1}{2}(\bar{e}\gamma^\mu \mathrm{i}\overleftrightarrow{D}^\nu e)B_{\mu\nu}$ | | |
| | | $\mathcal{R}'_{\widetilde{B}e}$ | $\frac{1}{2}(\bar{e}\gamma^\mu \mathrm{i}\overleftrightarrow{D}^\nu e)\widetilde{B}_{\mu\nu}$ | | |

**Table B.2:** Physical and redundant operators with two fermions.

| Four-quark | | Four-lepton | | Semileptonic | |
|---|---|---|---|---|---|
| $\mathcal{O}_{qq}^{(1)}$ | $(\bar{q}\gamma^\mu q)(\bar{q}\gamma_\mu q)$ | $\mathcal{O}_{\ell\ell}$ | $(\bar{\ell}\gamma^\mu \ell)(\bar{\ell}\gamma_\mu \ell)$ | $\mathcal{O}_{\ell q}^{(1)}$ | $(\bar{\ell}\gamma^\mu \ell)(\bar{q}\gamma_\mu q)$ |
| $\mathcal{O}_{qq}^{(3)}$ | $(\bar{q}\gamma^\mu \sigma^I q)(\bar{q}\gamma_\mu \sigma^I q)$ | $\mathcal{O}_{ee}$ | $(\bar{e}\gamma^\mu e)(\bar{e}\gamma_\mu e)$ | $\mathcal{O}_{\ell q}^{(3)}$ | $(\bar{\ell}\gamma^\mu \sigma^I \ell)(\bar{q}\gamma_\mu \sigma^I q)$ |
| $\mathcal{O}_{uu}$ | $(\bar{u}\gamma^\mu u)(\bar{u}\gamma_\mu u)$ | $\mathcal{O}_{\ell e}$ | $(\bar{\ell}\gamma^\mu \ell)(\bar{e}\gamma_\mu e)$ | $\mathcal{O}_{eu}$ | $(\bar{e}\gamma^\mu e)(\bar{u}\gamma_\mu u)$ |
| $\mathcal{O}_{dd}$ | $(\bar{d}\gamma^\mu d)(\bar{d}\gamma_\mu d)$ | | | $\mathcal{O}_{ed}$ | $(\bar{e}\gamma^\mu e)(\bar{d}\gamma_\mu d)$ |
| $\mathcal{O}_{ud}^{(1)}$ | $(\bar{u}\gamma^\mu u)(\bar{d}\gamma_\mu d)$ | | | $\mathcal{O}_{qe}$ | $(\bar{q}\gamma^\mu q)(\bar{e}\gamma_\mu e)$ |
| $\mathcal{O}_{ud}^{(8)}$ | $(\bar{u}\gamma^\mu T^A u)(\bar{d}\gamma_\mu T^A d)$ | | | $\mathcal{O}_{\ell u}$ | $(\bar{\ell}\gamma^\mu \ell)(\bar{u}\gamma_\mu u)$ |
| $\mathcal{O}_{qu}^{(1)}$ | $(\bar{q}\gamma^\mu q)(\bar{u}\gamma_\mu u)$ | | | $\mathcal{O}_{\ell d}$ | $(\bar{\ell}\gamma^\mu \ell)(\bar{d}\gamma_\mu d)$ |
| $\mathcal{O}_{qu}^{(8)}$ | $(\bar{q}\gamma^\mu T^A q)(\bar{u}\gamma_\mu T^A u)$ | | | $\mathcal{O}_{\ell edq}$ | $(\bar{\ell}e)(\bar{d}q)$ |
| $\mathcal{O}_{qd}^{(1)}$ | $(\bar{q}\gamma^\mu q)(\bar{d}\gamma_\mu d)$ | | | $\mathcal{O}_{\ell equ}^{(1)}$ | $(\bar{\ell}_r e)\epsilon_{rs}(\bar{q}_s u)$ |
| $\mathcal{O}_{qd}^{(8)}$ | $(\bar{q}\gamma^\mu T^A q)(\bar{d}\gamma_\mu T^A d)$ | | | $\mathcal{O}_{\ell equ}^{(3)}$ | $(\bar{\ell}_r \sigma^{\mu\nu} e)\epsilon_{rs}(\bar{q}_s \sigma_{\mu\nu} u)$ |
| $\mathcal{O}_{quqd}^{(1)}$ | $(\bar{q}_r u)\epsilon_{rs}(\bar{q}_s d)$ | | | | |
| $\mathcal{O}_{quqd}^{(8)}$ | $(\bar{q}_r T^A u)\epsilon_{rs}(\bar{q}_s T^A d)$ | | | | |

**Table B.3:** Baryon and lepton number conserving operators with four fermions.

| $\boldsymbol{\Psi^2 XH}$ + h.c. | | $\boldsymbol{\Psi^2 XD}$ | | | |
|---|---|---|---|---|---|
| $\mathcal{E}_{uG}$ | $\bar{q}T^A\sigma^{\mu\nu}u\widetilde{H}\widetilde{G}^A_{\mu\nu}$ | $\mathcal{E}_{Gq}$ | $\bar{q}T^A(\sigma^{\mu\nu}\gamma^\rho+\gamma^\rho\sigma^{\mu\nu})qD_\rho\widetilde{G}^A_{\mu\nu}$ | $\mathcal{E}_{Gd}$ | $\bar{d}T^A(\sigma^{\mu\nu}\gamma^\rho+\gamma^\rho\sigma^{\mu\nu})dD_\rho\widetilde{G}^A_{\mu\nu}$ |
| $\mathcal{E}_{uW}$ | $\bar{q}\sigma^I\sigma^{\mu\nu}u\widetilde{H}\widetilde{W}^I_{\mu\nu}$ | $\mathcal{E}'_{Gq}$ | $\mathrm{i}\bar{q}(T^A\sigma^{\mu\nu}\not{D}-\overleftarrow{\not{D}}\sigma^{\mu\nu}T^A)qG^A_{\mu\nu}$ | $\mathcal{E}'_{Gd}$ | $\mathrm{i}\bar{d}(T^A\sigma^{\mu\nu}\not{D}-\overleftarrow{\not{D}}\sigma^{\mu\nu}T^A)dG^A_{\mu\nu}$ |
| $\mathcal{E}_{uB}$ | $\bar{q}\sigma^{\mu\nu}u\widetilde{H}\widetilde{B}_{\mu\nu}$ | $\mathcal{E}'_{\widetilde{G}q}$ | $\mathrm{i}\bar{q}(T^A\sigma^{\mu\nu}\not{D}-\overleftarrow{\not{D}}\sigma^{\mu\nu}T^A)q\widetilde{G}^A_{\mu\nu}$ | $\mathcal{E}'_{\widetilde{G}d}$ | $\mathrm{i}\bar{d}(T^A\sigma^{\mu\nu}\not{D}-\overleftarrow{\not{D}}\sigma^{\mu\nu}T^A)d\widetilde{G}^A_{\mu\nu}$ |
| $\mathcal{E}_{dG}$ | $\bar{q}T^A\sigma^{\mu\nu}dH\widetilde{G}^A_{\mu\nu}$ | $\mathcal{E}_{Wq}$ | $\bar{q}\sigma^I(\sigma^{\mu\nu}\gamma^\rho+\gamma^\rho\sigma^{\mu\nu})qD_\rho\widetilde{W}^I_{\mu\nu}$ | $\mathcal{E}_{Bd}$ | $\bar{d}(\sigma^{\mu\nu}\gamma^\rho+\gamma^\rho\sigma^{\mu\nu})d\partial_\rho\widetilde{B}_{\mu\nu}$ |
| $\mathcal{E}_{dW}$ | $\bar{q}\sigma^I\sigma^{\mu\nu}dH\widetilde{W}^I_{\mu\nu}$ | $\mathcal{E}'_{Wq}$ | $\mathrm{i}\bar{q}(\sigma^I\sigma^{\mu\nu}\not{D}-\overleftarrow{\not{D}}\sigma^{\mu\nu}\sigma^I)qW^I_{\mu\nu}$ | $\mathcal{E}'_{Bd}$ | $\mathrm{i}\bar{d}(\sigma^{\mu\nu}\not{D}-\overleftarrow{\not{D}}\sigma^{\mu\nu})dB^A_{\mu\nu}$ |
| $\mathcal{E}_{dB}$ | $\bar{q}\sigma^{\mu\nu}dH\widetilde{B}_{\mu\nu}$ | $\mathcal{E}'_{\widetilde{W}q}$ | $\mathrm{i}\bar{q}(\sigma^I\sigma^{\mu\nu}\not{D}-\overleftarrow{\not{D}}\sigma^{\mu\nu}\sigma^I)q\widetilde{W}^I_{\mu\nu}$ | $\mathcal{E}'_{\widetilde{B}d}$ | $\mathrm{i}\bar{d}(\sigma^{\mu\nu}\not{D}-\overleftarrow{\not{D}}\sigma^{\mu\nu})d\widetilde{B}_{\mu\nu}$ |
| $\mathcal{E}_{eW}$ | $\bar{\ell}\sigma^I\sigma^{\mu\nu}eH\widetilde{W}^I_{\mu\nu}$ | $\mathcal{E}_{Bq}$ | $\bar{q}(\sigma^{\mu\nu}\gamma^\rho+\gamma^\rho\sigma^{\mu\nu})q\partial_\rho\widetilde{B}_{\mu\nu}$ | $\mathcal{E}_{W\ell}$ | $\bar{\ell}\sigma^I(\sigma^{\mu\nu}\gamma^\rho+\gamma^\rho\sigma^{\mu\nu})\ell D_\rho\widetilde{W}^I_{\mu\nu}$ |
| $\mathcal{E}_{eB}$ | $\bar{\ell}\sigma^{\mu\nu}eH\widetilde{B}_{\mu\nu}$ | $\mathcal{E}'_{Bq}$ | $\mathrm{i}\bar{q}(\sigma^{\mu\nu}\not{D}-\overleftarrow{\not{D}}\sigma^{\mu\nu})qB_{\mu\nu}$ | $\mathcal{E}'_{W\ell}$ | $\mathrm{i}\bar{\ell}(\sigma^I\sigma^{\mu\nu}\not{D}-\overleftarrow{\not{D}}\sigma^{\mu\nu}\sigma^I)\ell W^I_{\mu\nu}$ |
| $\boldsymbol{\psi^2 HD^2}$ + h.c. | | $\mathcal{E}'_{\widetilde{B}q}$ | $\mathrm{i}\bar{q}(\sigma^{\mu\nu}\not{D}-\overleftarrow{\not{D}}\sigma^{\mu\nu})q\widetilde{B}_{\mu\nu}$ | $\mathcal{E}'_{\widetilde{W}\ell}$ | $\mathrm{i}\bar{\ell}(\sigma^I\sigma^{\mu\nu}\not{D}-\overleftarrow{\not{D}}\sigma^{\mu\nu}\sigma^I)\ell\widetilde{W}^I_{\mu\nu}$ |
| $\mathcal{E}_{uH}$ | $\bar{q}\sigma^{\mu\nu}D^\rho uD^\sigma\widetilde{H}\epsilon_{\mu\nu\rho\sigma}$ | $\mathcal{E}_{Gu}$ | $\bar{u}T^A(\sigma^{\mu\nu}\gamma^\rho+\gamma^\rho\sigma^{\mu\nu})uD_\rho\widetilde{G}^A_{\mu\nu}$ | $\mathcal{E}_{B\ell}$ | $\bar{\ell}(\sigma^{\mu\nu}\gamma^\rho+\gamma^\rho\sigma^{\mu\nu})\ell\partial_\rho\widetilde{B}_{\mu\nu}$ |
| $\mathcal{E}_{dH}$ | $\bar{q}\sigma^{\mu\nu}D^\rho dD^\sigma H\epsilon_{\mu\nu\rho\sigma}$ | $\mathcal{E}'_{Gu}$ | $\mathrm{i}\bar{u}(T^A\sigma^{\mu\nu}\not{D}-\overleftarrow{\not{D}}\sigma^{\mu\nu}T^A)uG^A_{\mu\nu}$ | $\mathcal{E}'_{B\ell}$ | $\mathrm{i}\bar{\ell}(\sigma^{\mu\nu}\not{D}-\overleftarrow{\not{D}}\sigma^{\mu\nu})\ell B_{\mu\nu}$ |
| $\mathcal{E}_{eH}$ | $\bar{\ell}\sigma^{\mu\nu}D^\rho eD^\sigma H\epsilon_{\mu\nu\rho\sigma}$ | $\mathcal{E}'_{\widetilde{G}u}$ | $\mathrm{i}\bar{u}(T^A\sigma^{\mu\nu}\not{D}-\overleftarrow{\not{D}}\sigma^{\mu\nu}T^A)u\widetilde{G}^A_{\mu\nu}$ | $\mathcal{E}'_{\widetilde{B}\ell}$ | $\mathrm{i}\bar{\ell}(\sigma^{\mu\nu}\not{D}-\overleftarrow{\not{D}}\sigma^{\mu\nu})\ell\widetilde{B}_{\mu\nu}$ |
| | | $\mathcal{E}_{Bu}$ | $\bar{u}(\sigma^{\mu\nu}\gamma^\rho+\gamma^\rho\sigma^{\mu\nu})u\partial_\rho\widetilde{B}_{\mu\nu}$ | $\mathcal{E}_{Be}$ | $\bar{e}(\sigma^{\mu\nu}\gamma^\rho+\gamma^\rho\sigma^{\mu\nu})e\partial_\rho\widetilde{B}_{\mu\nu}$ |
| | | $\mathcal{E}'_{Bu}$ | $\mathrm{i}\bar{u}(\sigma^{\mu\nu}\not{D}-\overleftarrow{\not{D}}\sigma^{\mu\nu})uB_{\mu\nu}$ | $\mathcal{E}'_{Be}$ | $\mathrm{i}\bar{e}(\sigma^{\mu\nu}\not{D}-\overleftarrow{\not{D}}\sigma^{\mu\nu})eB_{\mu\nu}$ |
| | | $\mathcal{E}'_{\widetilde{B}u}$ | $\mathrm{i}\bar{u}(\sigma^{\mu\nu}\not{D}-\overleftarrow{\not{D}}\sigma^{\mu\nu})u\widetilde{B}_{\mu\nu}$ | $\mathcal{E}'_{\widetilde{B}e}$ | $\mathrm{i}\bar{e}(\sigma^{\mu\nu}\not{D}-\overleftarrow{\not{D}}\sigma^{\mu\nu})e\widetilde{B}_{\mu\nu}$ |

**Table B.4:** Evanescent operators with two fermions.

| $\bar{L}R\bar{R}L$ | |
|---|---|
| $\mathcal{E}_{qu}$ | $(\bar{q}u)(\bar{u}q)$ |
| $\mathcal{E}_{qu}^{(8)}$ | $(\bar{q}T^A u)(\bar{u}T^A q)$ |
| $\mathcal{E}_{qd}$ | $(\bar{q}d)(\bar{d}q)$ |
| $\mathcal{E}_{qd}^{(8)}$ | $(\bar{q}T^A d)(\bar{d}T^A q)$ |
| $\mathcal{E}_{qu}^{[2]}$ | $(\bar{q}\gamma^{\mu\nu}u)(\bar{u}\gamma_{\mu\nu}q)$ |
| $\mathcal{E}_{qu}^{[2](8)}$ | $(\bar{q}\gamma^{\mu\nu}T^A u)(\bar{u}\gamma_{\mu\nu}T^A q)$ |
| $\mathcal{E}_{qd}^{[2]}$ | $(\bar{q}\gamma^{\mu\nu}d)(\bar{d}\gamma_{\mu\nu}q)$ |
| $\mathcal{E}_{qd}^{[2](8)}$ | $(\bar{q}\gamma^{\mu\nu}T^A d)(\bar{d}\gamma_{\mu\nu}T^A q)$ |

| $\bar{L}R\bar{L}R$ | |
|---|---|
| $\mathcal{E}_{quqd}^{[2]}$ | $(\bar{q}_r\gamma^{\mu\nu}u)\epsilon_{rs}(\bar{q}_s\gamma_{\mu\nu}d)$ |
| $\mathcal{E}_{quqd}^{[2](8)}$ | $(\bar{q}_r\gamma^{\mu\nu}T^A u)\epsilon_{rs}(\bar{q}_s\gamma_{\mu\nu}T^A d)$ |

| $\bar{R}R\bar{R}R$ | |
|---|---|
| $\mathcal{E}_{uu}^{(8)}$ | $(\bar{u}\gamma^{\mu}T^A u)(\bar{u}\gamma_{\mu}T^A u)$ |
| $\mathcal{E}_{uu}^{[3]}$ | $(\bar{u}\gamma^{\mu\nu\rho}u)(\bar{u}\gamma_{\mu\nu\rho}u)$ |
| $\mathcal{E}_{uu}^{[3](8)}$ | $(\bar{u}\gamma^{\mu\nu\rho}T^A u)(\bar{u}\gamma_{\mu\nu\rho}T^A u)$ |
| $\mathcal{E}_{dd}^{(8)}$ | $(\bar{d}\gamma^{\mu}T^A d)(\bar{d}\gamma_{\mu}T^A d)$ |
| $\mathcal{E}_{dd}^{[3]}$ | $(\bar{d}\gamma^{\mu\nu\rho}d)(\bar{d}\gamma_{\mu\nu\rho}d)$ |
| $\mathcal{E}_{dd}^{[3](8)}$ | $(\bar{d}\gamma^{\mu\nu\rho}T^A d)(\bar{d}\gamma_{\mu\nu\rho}T^A d)$ |
| $\mathcal{E}_{ud}$ | $(\bar{u}\gamma^{\mu}d)(\bar{d}\gamma_{\mu}u)$ |
| $\mathcal{E}_{ud}^{(8)}$ | $(\bar{u}\gamma^{\mu}T^A d)(\bar{d}\gamma_{\mu}T^A u)$ |
| $\mathcal{E}_{ud}^{[3]}$ | $(\bar{u}\gamma^{\mu\nu\rho}d)(\bar{d}\gamma_{\mu\nu\rho}u)$ |
| $\mathcal{E}_{ud}^{[3](8)}$ | $(\bar{u}\gamma^{\mu\nu\rho}T^A d)(\bar{d}\gamma_{\mu\nu\rho}T^A u)$ |
| $\mathcal{E}_{ud}^{\prime\,[3]}$ | $(\bar{u}\gamma^{\mu\nu\rho}u)(\bar{d}\gamma_{\mu\nu\rho}d)$ |
| $\mathcal{E}_{ud}^{\prime\,[3](8)}$ | $(\bar{u}\gamma^{\mu\nu\rho}T^A u)(\bar{d}\gamma_{\mu\nu\rho}T^A d)$ |

| $\bar{L}L\bar{R}R$ | |
|---|---|
| $\mathcal{E}_{qu}^{[3]}$ | $(\bar{q}\gamma^{\mu\nu\rho}q)(\bar{u}\gamma_{\mu\nu\rho}u)$ |
| $\mathcal{E}_{qu}^{[3](8)}$ | $(\bar{q}\gamma^{\mu\nu\rho}T^A q)(\bar{u}\gamma_{\mu\nu\rho}T^A u)$ |
| $\mathcal{E}_{qd}^{[3]}$ | $(\bar{q}\gamma^{\mu\nu\rho}q)(\bar{d}\gamma_{\mu\nu\rho}d)$ |
| $\mathcal{E}_{qd}^{[3](8)}$ | $(\bar{q}\gamma^{\mu\nu\rho}T^A q)(\bar{d}\gamma_{\mu\nu\rho}T^A d)$ |

| $\bar{L}L\bar{L}L$ | |
|---|---|
| $\mathcal{E}_{qq}^{(8)}$ | $(\bar{q}\gamma^{\mu}T^A q)(\bar{q}\gamma_{\mu}T^A q)$ |
| $\mathcal{E}_{qq}^{(3,8)}$ | $(\bar{q}\gamma^{\mu}\sigma^I T^A q)(\bar{q}\gamma_{\mu}\sigma^I T^A q)$ |
| $\mathcal{E}_{qq}^{[3](1)}$ | $(\bar{q}\gamma^{\mu\nu\rho}q)(\bar{q}\gamma_{\mu\nu\rho}q)$ |
| $\mathcal{E}_{qq}^{[3](3)}$ | $(\bar{q}\gamma^{\mu\nu\rho}\sigma^I q)(\bar{q}\gamma_{\mu\nu\rho}\sigma^I q)$ |
| $\mathcal{E}_{qq}^{[3](8)}$ | $(\bar{q}\gamma^{\mu\nu\rho}T^A q)(\bar{q}\gamma_{\mu\nu\rho}T^A q)$ |
| $\mathcal{E}_{qq}^{[3](3,8)}$ | $(\bar{q}\gamma^{\mu\nu\rho}\sigma^I T^A q)(\bar{q}\gamma_{\mu\nu\rho}\sigma^I T^A q)$ |

**Table B.5:** Evanescent operators with four fermions involving only quarks.

| $\bar{L}R\bar{R}L$ | |
|---|---|
| $\mathcal{E}_{\ell u}$ | $(\bar{\ell}u)(\bar{u}\ell)$ |
| $\mathcal{E}_{\ell d}$ | $(\bar{\ell}d)(\bar{d}\ell)$ |
| $\mathcal{E}_{qe}$ | $(\bar{q}e)(\bar{e}q)$ |
| $\mathcal{E}_{\ell edq}^{[2]}$ | $(\bar{\ell}\gamma^{\mu\nu}e)(\bar{d}\gamma_{\mu\nu}q)$ |
| $\mathcal{E}_{\ell u}^{[2]}$ | $(\bar{\ell}\gamma^{\mu\nu}u)(\bar{u}\gamma_{\mu\nu}\ell)$ |
| $\mathcal{E}_{\ell d}^{[2]}$ | $(\bar{\ell}\gamma^{\mu\nu}d)(\bar{d}\gamma_{\mu\nu}\ell)$ |
| $\mathcal{E}_{qe}^{[2]}$ | $(\bar{q}\gamma^{\mu\nu}e)(\bar{e}\gamma_{\mu\nu}q)$ |

| $\bar{L}R\bar{L}R$ | |
|---|---|
| $\mathcal{E}_{\ell equ}^{[2]}$ | $(\bar{\ell}_r\gamma^{\mu\nu}e)\epsilon_{rs}(\bar{q}_s\gamma_{\mu\nu}u)$ |
| $\mathcal{E}_{\ell uqe}$ | $(\bar{\ell}_r u)\epsilon_{rs}(\bar{q}_s e)$ |
| $\mathcal{E}_{\ell uqe}^{[2]}$ | $(\bar{\ell}_r\gamma^{\mu\nu}u)\epsilon_{rs}(\bar{q}_s\gamma_{\mu\nu}e)$ |

| $\bar{R}R\bar{R}R$ | |
|---|---|
| $\mathcal{E}_{eu}$ | $(\bar{e}\gamma^{\mu}u)(\bar{u}\gamma_{\mu}e)$ |
| $\mathcal{E}_{ed}$ | $(\bar{e}\gamma^{\mu}d)(\bar{d}\gamma_{\mu}e)$ |
| $\mathcal{E}_{eu}^{[3]}$ | $(\bar{e}\gamma^{\mu\nu\rho}u)(\bar{u}\gamma_{\mu\nu\rho}e)$ |
| $\mathcal{E}_{ed}^{[3]}$ | $(\bar{e}\gamma^{\mu\nu\rho}d)(\bar{d}\gamma_{\mu\nu\rho}e)$ |
| $\mathcal{E}_{eu}^{\prime\,[3]}$ | $(\bar{e}\gamma^{\mu\nu\rho}e)(\bar{u}\gamma_{\mu\nu\rho}u)$ |
| $\mathcal{E}_{ed}^{\prime\,[3]}$ | $(\bar{e}\gamma^{\mu\nu\rho}e)(\bar{d}\gamma_{\mu\nu\rho}d)$ |

| $\bar{L}L\bar{R}R$ | |
|---|---|
| $\mathcal{E}_{\ell qde}$ | $(\bar{\ell}\gamma^{\mu}q)(\bar{d}\gamma_{\mu}e)$ |
| $\mathcal{E}_{\ell u}^{[3]}$ | $(\bar{\ell}\gamma^{\mu\nu\rho}\ell)(\bar{u}\gamma_{\mu\nu\rho}u)$ |
| $\mathcal{E}_{\ell d}^{[3]}$ | $(\bar{\ell}\gamma^{\mu\nu\rho}\ell)(\bar{d}\gamma_{\mu\nu\rho}d)$ |
| $\mathcal{E}_{qe}^{[3]}$ | $(\bar{q}\gamma^{\mu\nu\rho}q)(\bar{e}\gamma_{\mu\nu\rho}e)$ |
| $\mathcal{E}_{\ell qde}^{[3]}$ | $(\bar{\ell}\gamma^{\mu\nu\rho}q)(\bar{d}\gamma_{\mu\nu\rho}e)$ |

| $\bar{L}L\bar{L}L$ | |
|---|---|
| $\mathcal{E}_{\ell q}$ | $(\bar{\ell}\gamma^{\mu}q)(\bar{q}\gamma_{\mu}\ell)$ |
| $\mathcal{E}_{\ell q}^{(3)}$ | $(\bar{\ell}\gamma^{\mu}\sigma^I q)(\bar{q}\gamma_{\mu}\sigma^I\ell)$ |
| $\mathcal{E}_{\ell q}^{[3]}$ | $(\bar{\ell}\gamma^{\mu\nu\rho}q)(\bar{q}\gamma_{\mu\nu\rho}\ell)$ |
| $\mathcal{E}_{\ell q}^{[3](3)}$ | $(\bar{\ell}\gamma^{\mu\nu\rho}\sigma^I q)(\bar{q}\gamma_{\mu\nu\rho}\sigma^I\ell)$ |
| $\mathcal{E}_{\ell q}^{\prime\,[3]}$ | $(\bar{\ell}\gamma^{\mu\nu\rho}\ell)(\bar{q}\gamma_{\mu\nu\rho}q)$ |
| $\mathcal{E}_{\ell q}^{\prime\,[3](3)}$ | $(\bar{\ell}\gamma^{\mu\nu\rho}\sigma^I\ell)(\bar{q}\gamma_{\mu\nu\rho}\sigma^I q)$ |

**Table B.6:** Semileptonic four-fermion evanescent operators. We use the shorthand notation $\gamma^{\mu_1\cdots\mu_n}\equiv\gamma^{\mu_1}\ldots\gamma^{\mu_n}$ with no (anti)symmetrization.

| $\bar{R}R\bar{R}R$ | |
|---|---|
| $\mathcal{E}_{ee}^{[3]}$ | $(\bar{e}\gamma^{\mu\nu\rho}e)(\bar{e}\gamma_{\mu\nu\rho}e)$ |

| $\bar{L}R\bar{R}L$ | |
|---|---|
| $\mathcal{E}_{\ell e}$ | $(\bar{\ell}e)(\bar{e}\ell)$ |
| $\mathcal{E}_{\ell e}^{[2]}$ | $(\bar{\ell}\gamma^{\mu\nu}e)(\bar{e}\gamma_{\mu\nu}\ell)$ |

| $\bar{L}L\bar{L}L$ | |
|---|---|
| $\mathcal{E}_{\ell\ell}^{(3)}$ | $(\bar{\ell}\gamma^{\mu}\sigma^I\ell)(\bar{\ell}\gamma_{\mu}\sigma^I\ell)$ |
| $\mathcal{E}_{\ell\ell}^{[3]}$ | $(\bar{\ell}\gamma^{\mu\nu\rho}\ell)(\bar{\ell}\gamma_{\mu\nu\rho}\ell)$ |
| $\mathcal{E}_{\ell\ell}^{[3](3)}$ | $(\bar{\ell}\gamma^{\mu\nu\rho}\sigma^I\ell)(\bar{\ell}\gamma_{\mu\nu\rho}\sigma^I\ell)$ |

| $\bar{L}L\bar{R}R$ | |
|---|---|
| $\mathcal{E}_{\ell e}^{[3]}$ | $(\bar{\ell}\gamma^{\mu\nu\rho}\ell)(\bar{e}\gamma_{\mu\nu\rho}e)$ |

**Table B.7:** Leptonic four-fermion evanescent operators. We use the shorthand notation $\gamma^{\mu_1\cdots\mu_n}\equiv\gamma^{\mu_1}\ldots\gamma^{\mu_n}$ with no (anti)symmetrization.

| $\bar{L}^c L\bar{L}L^c$ | | $\bar{R}^c R\bar{R}R^c$ | | $\bar{L}^c R\bar{R}L^c$ | |
|---|---|---|---|---|---|
| $\mathcal{E}^{c}_{qq}$ | $(\overline{q^c}_{ar} q_{bs})(\bar{q}_{bs} q^c_{ar})$ | $\mathcal{E}^{c}_{uu}$ | $(\overline{u^c}_a u_b)(\bar{u}_b u^c_a)$ | $\mathcal{E}^{c}_{qu}$ | $(\overline{q^c}_a \gamma^{\mu} u_b)(\bar{u}_b \gamma_{\mu} q^c_a)$ |
| $\mathcal{E}^{c\prime}_{qq}$ | $(\overline{q^c}_{ar} q_{bs})(\bar{q}_{as} q^c_{br})$ | $\mathcal{E}^{c}_{dd}$ | $(\overline{d^c}_a d_b)(\bar{d}_b d^c_a)$ | $\mathcal{E}^{c}_{qd}$ | $(\overline{q^c}_a \gamma^{\mu} d_b)(\bar{d}_b \gamma_{\mu} q^c_a)$ |
| $\mathcal{E}^{c\,[2]}_{qq}$ | $(\overline{q^c}_{ar} \gamma^{\mu\nu} q_{bs})(\bar{q}_{bs} \gamma_{\mu\nu} q^c_{ar})$ | $\mathcal{E}^{c}_{ud}$ | $(\overline{u^c}_a d_b)(\bar{d}_b u^c_a)$ | $\mathcal{E}^{c\prime}_{qu}$ | $(\overline{q^c}_a \gamma^{\mu} u_b)(\bar{u}_a \gamma_{\mu} q^c_b)$ |
| $\mathcal{E}^{c\prime[2]}_{qq}$ | $(\overline{q^c}_{ar} \gamma^{\mu\nu} q_{bs})(\bar{q}_{as} \gamma_{\mu\nu} q^c_{br})$ | $\mathcal{E}^{c\prime}_{ud}$ | $(\overline{u^c}_a d_b)(\bar{d}_a u^c_b)$ | $\mathcal{E}^{c\prime}_{qd}$ | $(\overline{q^c}_a \gamma^{\mu} d_b)(\bar{d}_a \gamma_{\mu} q^c_b)$ |
| $\bar{R}^c R\bar{L}L^c$ | | $\mathcal{E}^{c\,[2]}_{uu}$ | $(\overline{u^c}_a \gamma^{\mu\nu} u_b)(\bar{u}_b \gamma_{\mu\nu} u^c_a)$ | $\mathcal{E}^{c\,[3]}_{qu}$ | $(\overline{q^c}_a \gamma^{\mu\nu\rho} u_b)(\bar{u}_b \gamma_{\mu\nu\rho} q^c_a)$ |
| $\mathcal{E}^{c}_{udqq}$ | $(\overline{u^c}_a d_b)(\bar{q}_{br} \epsilon_{rs} q^c_{as})$ | $\mathcal{E}^{c\,[2]}_{dd}$ | $(\overline{d^c}_a \gamma^{\mu\nu} d_b)(\bar{d}_b \gamma_{\mu\nu} d^c_a)$ | $\mathcal{E}^{c\,[3]}_{qd}$ | $(\overline{q^c}_a \gamma^{\mu\nu\rho} d_b)(\bar{d}_b \gamma_{\mu\nu\rho} q^c_a)$ |
| $\mathcal{E}^{c\,[2]}_{udqq}$ | $(\overline{u^c}_a \gamma^{\mu\nu} d_b)(\bar{q}_{br} \epsilon_{rs} \gamma_{\mu\nu} q^c_{as})$ | $\mathcal{E}^{c\,[2]}_{ud}$ | $(\overline{u^c}_a \gamma^{\mu\nu} d_b)(\bar{d}_b \gamma_{\mu\nu} u^c_a)$ | $\mathcal{E}^{c\prime\,[3]}_{qu}$ | $(\overline{q^c}_a \gamma^{\mu\nu\rho} u_b)(\bar{u}_a \gamma_{\mu\nu\rho} q^c_b)$ |
| | | $\mathcal{E}^{c\prime[2]}_{ud}$ | $(\overline{u^c}_a \gamma^{\mu\nu} d_b)(\bar{d}_a \gamma_{\mu\nu} u^c_b)$ | $\mathcal{E}^{c\prime\,[3]}_{qd}$ | $(\overline{q^c}_a \gamma^{\mu\nu\rho} d_b)(\bar{d}_a \gamma_{\mu\nu\rho} q^c_b)$ |

**Table B.8:** Evanescent operators with four fermions involving only quarks and featuring charge conjugation. We use the shorthand notation $\gamma^{\mu_1\cdots\mu_n} \equiv \gamma^{\mu_1}\ldots\gamma^{\mu_n}$ with no (anti)symmetrization.

| $\bar{L}^c L\bar{L}L^c$ | | $\bar{R}^c R\bar{R}R^c$ | | $\bar{L}^c R\bar{R}L^c$ | |
|---|---|---|---|---|---|
| $\mathcal{E}^{c}_{\ell\ell}$ | $(\overline{\ell^c}_r \ell_s)(\bar{\ell}_s \ell^c_r)$ | $\mathcal{E}^{c}_{ee}$ | $(\overline{e^c} e)(\bar{e} e^c)$ | $\mathcal{E}^{c}_{\ell e}$ | $(\overline{\ell^c} \gamma^{\mu} e)(\bar{e} \gamma_{\mu} \ell^c)$ |
| $\mathcal{E}^{c}_{q\ell}$ | $(\overline{q^c}_r \ell_s)(\bar{\ell}_s q^c_r)$ | $\mathcal{E}^{c}_{eu}$ | $(\overline{e^c} u)(\bar{u} e^c)$ | $\mathcal{E}^{c}_{qe}$ | $(\overline{q^c} \gamma^{\mu} e)(\bar{e} \gamma_{\mu} q^c)$ |
| $\mathcal{E}^{c\prime}_{q\ell}$ | $(\overline{q^c}_r \ell_s)(\bar{\ell}_r q^c_s)$ | $\mathcal{E}^{c}_{ed}$ | $(\overline{e^c} d)(\bar{d} e^c)$ | $\mathcal{E}^{c}_{\ell u}$ | $(\overline{\ell^c} \gamma^{\mu} u)(\bar{u} \gamma_{\mu} \ell^c)$ |
| $\mathcal{E}^{c\,[2]}_{\ell\ell}$ | $(\overline{\ell^c}_r \gamma^{\mu\nu} \ell_s)(\bar{\ell}_s \gamma_{\mu\nu} \ell^c_r)$ | $\mathcal{E}^{c\,[2]}_{ee}$ | $(\overline{e^c} \gamma^{\mu\nu} e)(\bar{e} \gamma_{\mu\nu} e^c)$ | $\mathcal{E}^{c}_{\ell d}$ | $(\overline{\ell^c} \gamma^{\mu} d)(\bar{d} \gamma_{\mu} \ell^c)$ |
| $\mathcal{E}^{c\,[2]}_{q\ell}$ | $(\overline{q^c}_r \gamma^{\mu\nu} \ell_s)(\bar{\ell}_s \gamma_{\mu\nu} q^c_r)$ | $\mathcal{E}^{c\,[2]}_{eu}$ | $(\overline{e^c} \gamma^{\mu\nu} u)(\bar{u} \gamma_{\mu\nu} e^c)$ | $\mathcal{E}^{c}_{qed\ell}$ | $(\overline{q^c} \gamma^{\mu} e)(\bar{d} \gamma_{\mu} \ell^c)$ |
| $\mathcal{E}^{c\prime[2]}_{q\ell}$ | $(\overline{q^c}_r \gamma^{\mu\nu} \ell_s)(\bar{\ell}_r \gamma_{\mu\nu} q^c_s)$ | $\mathcal{E}^{c\,[2]}_{ed}$ | $(\overline{e^c} \gamma^{\mu\nu} d)(\bar{d} \gamma_{\mu\nu} e^c)$ | $\mathcal{E}^{c\,[3]}_{\ell e}$ | $(\overline{\ell^c} \gamma^{\mu\nu\rho} e)(\bar{e} \gamma_{\mu\nu\rho} \ell^c)$ |
| $\bar{R}^c R\bar{L}L^c$ | | | | $\mathcal{E}^{c\,[3]}_{qe}$ | $(\overline{q^c} \gamma^{\mu\nu\rho} e)(\bar{e} \gamma_{\mu\nu\rho} q^c)$ |
| $\mathcal{E}^{c}_{ue\ell q}$ | $(\overline{u^c} e)(\bar{\ell}_r \epsilon_{rs} q^c_s)$ | | | $\mathcal{E}^{c\,[3]}_{\ell u}$ | $(\overline{\ell^c} \gamma^{\mu\nu\rho} u)(\bar{u} \gamma_{\mu\nu\rho} \ell^c)$ |
| $\mathcal{E}^{c\,[2]}_{ue\ell q}$ | $(\overline{u^c} \gamma^{\mu\nu} e)(\bar{\ell}_r \gamma_{\mu\nu} \epsilon_{rs} q^c_s)$ | | | $\mathcal{E}^{c\,[3]}_{\ell d}$ | $(\overline{\ell^c} \gamma^{\mu\nu\rho} d)(\bar{d} \gamma_{\mu\nu\rho} \ell^c)$ |
| | | | | $\mathcal{E}^{c\,[3]}_{qed\ell}$ | $(\overline{q^c} \gamma^{\mu\nu\rho} e)(\bar{d} \gamma_{\mu\nu\rho} \ell^c)$ |

**Table B.9:** Semileptonic and leptonic evanescent operators with four fermions featuring charge conjugation. We use the shorthand notation $\gamma^{\mu_1\cdots\mu_n} \equiv \gamma^{\mu_1}\ldots\gamma^{\mu_n}$ with no (anti)symmetrization.

C

# General results from box diagrams

For completeness, we present in this appendix the generic results, as done for the bridge topology in Chapter 5, for the contribution to $a_\mu$ produced by the box diagrams. These chirally enhanced contributions (equivalent to triangles in the LEFT) are the ones commonly considered in the literature. In the models consider in Chapter 5, however, these are only relevant for some specific representations of the new heavy fields.

For the box diagram with two heavy fermion propagators (Fig. C.1a), the generic Lagrangian reads:

$$\begin{aligned}\mathcal{L} \supset\, & y_R T_{IJ} \overline{\Psi_1}_I H_J e_R + y_L T_{IJK} \overline{\ell_L}_{,I} H_J^\dagger \Psi_{2K} + y_H^R T^H_{IJK} \overline{\Psi_2}_I H_J P_R \Psi_{1K} \\ & + T^H_{IJK} y_H^L \overline{\Psi_2}_I H_J P_L \Psi_{1K} + \text{h.c.}\,,\end{aligned} \tag{C.1}$$

where we use the same conventions for the covariant derivative of $\Psi$ and $\Phi$ as in Eq. (5.9).

The contribution to $\alpha_{e\gamma}$ is given by:

$$\begin{aligned}[\alpha_{e\gamma}]_{2,2} = \left(\frac{i}{4}\right) e\, y_R\, y_L \sum_{\chi=R,L} y_H^\chi \Big[ & T_{IJ} T_{2JK} T^\gamma_{I'I} T^H_{K2I'} \gamma^\chi_{\Psi_1} \\ & + T_{IJ} T_{2JK} T^H_{K'2I} T^\gamma_{KK'} \gamma^\chi_{\Psi_2} + T_{IJ} T_{2J'K} T^H_{K2I} T^\gamma_{J'J} \gamma^\chi_H \Big]\,,\end{aligned} \tag{C.2}$$

where $\chi$ sums over the right- and left-handed chiralities and the different kinematic factors read:

$$\begin{aligned}\gamma^L_{\Psi_1} &= 0\,, \\ \gamma^R_{\Psi_1} &= -\frac{i}{16\pi^2} \frac{M_{\Psi_2}\left(M^2_{\Psi_1} \operatorname{Log}\left(\frac{M^2_{\Psi_1}}{M^2_{\Psi_2}}\right) - M^2_{\Psi_1} + M^2_{\Psi_2}\right)}{M_{\Psi_1}\left(M^2_{\Psi_1} - M^2_{\Psi_2}\right)^2}\,,\end{aligned} \tag{C.3}$$

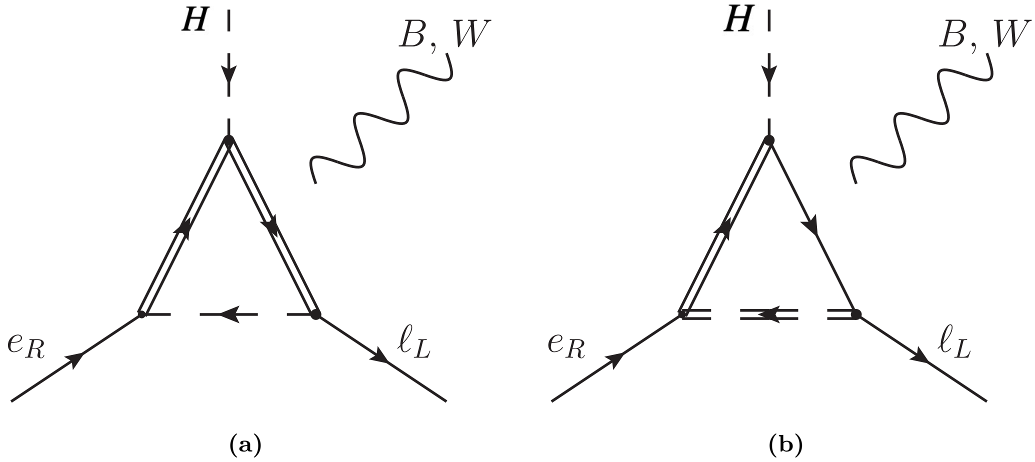


**Figure C.1:** Box diagram contribution to $\alpha_{e\gamma}$ with: (a) two heavy fermion propagators; (b) one heavy fermion and one heavy scalar propagator. Double lines represent heavy particles whereas single lines are SM particles. The gauge boson ($B$ or $W$) is represented outside the diagram since it can be attached to any of the internal propagators.

$$
\begin{aligned}
\gamma^L_{\Psi_2} &= 0\,, \\
\gamma^R_{\Psi_2} &= -\frac{i}{16\pi^2}\frac{M_{\Psi_1}\left(-M^2_{\Psi_2}\,\mathrm{Log}\left(\frac{M^2_{\Psi_1}}{M^2_{\Psi_2}}\right)+M^2_{\Psi_1}-M^2_{\Psi_2}\right)}{M_{\Psi_2}\left(M^2_{\Psi_1}-M^2_{\Psi_2}\right)^2}\,, \\
\gamma^L_H &= 0\,, \\
\gamma^R_H &= \frac{-i}{16\pi^2 M_{\Psi_1}M_{\Psi_2}}\,.
\end{aligned}
\tag{C.4}
$$

For the box diagram with a light fermion in the loop, in which the heavy fermion couples with the right-handed muon (Fig. C.1b), the Lagrangian reads:

$$
\mathcal{L} \supset y_R T^e_{IJ}\overline{\Psi_1}_I \Phi_J e_R + y_L T^1_{IJ}\overline{\psi} H_J P_L \Psi_{1I} + y_\Phi T^\Phi_{IJ}\overline{\ell_{LI}}\Phi^\dagger_J P_R \psi + \text{h.c.}\,, \tag{C.5}
$$

where $\psi$ represents any light SM fermion which fits with the heavy field representations. The resulting contribution to $\alpha_{e\gamma}$ is:

$$
\begin{aligned}
[\alpha_{e\gamma}]_{2,2} = \left(\frac{i}{4}\right) e\, N\, y_R\, y_L\, y_\Phi \Big[ & T^e_{IJ} T^\gamma_{I'I} T^1_{I'2} T^\Phi_{2J}\gamma_\Psi \\
& + T^e_{IJ} T^1_{I2} Y_\psi T^\Phi_{2J}\gamma_\psi + T^e_{IJ} T^1_{I2} T^\gamma_{JJ'} T^\Phi_{2J'}\gamma_\Phi \Big]\,,
\end{aligned}
\tag{C.6}
$$

with the following kinematic factors:

$$
\begin{aligned}
\gamma_\Psi &= -\frac{M_\Phi^2\left((M_\Psi^2+M_\Phi^2)\,\mathrm{Log}\left(\frac{M_\Psi^2}{M_\Phi^2}\right)-2M_\Psi^2+2M_\Phi^2\right)}{\left(M_\Phi^2-M_\Psi^2\right)^3}\,,\\
\gamma_\psi &= \frac{-M_\Phi^2\,\mathrm{Log}\left(\frac{M_\Psi^2}{M_\Phi^2}\right)+M_\Psi^2-M_\Phi^2}{\left(M_\Psi^2-M_\Phi^2\right)^2}\,,\\
\gamma_\Phi &= \frac{M_\Psi^4-2M_\Psi^2M_\Phi^2\,\mathrm{Log}\left(\frac{M_\Psi^2}{M_\Phi^2}\right)-M_\Phi^4}{\left(M_\Psi^2-M_\Phi^2\right)^3}\,.
\end{aligned}
\tag{C.7}
$$

In the case that the heavy fermion couples with the left-handed muon, the relevant Lagrangian can be written as:

$$
\mathcal{L}\supset y_R T^{\ell}_{IJK}\overline{\ell_L}_I\Phi^\dagger_J\Psi_{1K}+y_L T^2_{IJK}\overline{\Psi}_I H_J P_L\psi_K+y_\Phi T^\Phi_{IJ}\overline{\psi}_I\Phi_J e_R+\text{h.c.}\,,
\tag{C.8}
$$

with the following contribution to $\alpha_{e\gamma}$:

$$
\begin{aligned}
[\alpha_{e\gamma}]_{2,2} = \left(\frac{i}{4}\right) eNy_Ry_Ly_\Phi\Big[&T^\ell_{2JI}T^\gamma_{II'}T^2_{I'2K}T^\Phi_{KJ}\gamma_\Psi\\
&+T^\ell_{2JI}T^2_{I2K}T^\gamma_{KK'}T^\Phi_{K'J}\gamma_\psi+T^\ell_{2JI}T^2_{I2K}T^\Phi_{KJ'}T^\gamma_{J'J}\gamma_\Phi\Big]\,,
\end{aligned}
\tag{C.9}
$$

where:

$$
\begin{aligned}
\gamma_\Psi &= \frac{M_\Phi^2\left(\left(M_{\Psi_1}^2+M_\Phi^2\right)\mathrm{Log}\left(\frac{M_{\Psi_1}^2}{M_\Phi^2}\right)-2M_{\Psi_1}^2+2M_\Phi^2\right)}{\left(M_{\Psi_1}^2-M_\Phi^2\right)^3}\,,\\
\gamma_\psi &= -\frac{\left(M_{\Psi_1}^2\,\mathrm{Log}\left(\frac{M_{\Psi_1}^2}{M_\Phi^2}\right)-M_{\Psi_1}^2+M_\Phi^2\right)}{\left(M_{\Psi_1}^2-M_\Phi^2\right)^2}\,,\\
\gamma_\Phi &= \frac{M_\Psi^4-2M_\Psi^2M_\Phi^2\,\mathrm{Log}\left(\frac{M_\Psi^2}{M_\Phi^2}\right)-M_\Phi^4}{\left(M_\Psi^2-M_\Phi^2\right)^3}\,.
\end{aligned}
\tag{C.10}
$$

When there are only heavy propagators in the box diagram (Fig. C.2), the relevant Lagrangian reads:

$$
\begin{aligned}
\mathcal{L}\supset\, & y_R T^1_{IJ}\overline{\Psi_1}_I\Phi_J e_R+y_L T^2_{IJ}\overline{\ell_L}\Psi_{2I}\Phi^\dagger_J+y_H^R T_{IJK}\overline{\Psi_2}_I H_J P_R\Psi_{1K}\\
&+y_H^L T_{IJK}\overline{\Psi_2}_I H_J P_L\Psi_{1K}+\text{h.c.},
\end{aligned}
\tag{C.11}
$$

and the resulting $\alpha_{e\gamma}$ is given by:

$$
\begin{aligned}
[\alpha_{e\gamma}]_{2,2} = \left(\frac{i}{4}\right) y_Ry_L\sum_{\chi=R,L}y_H^\chi\Big[&T^2_{IJ}T^H_{I2K}T^\gamma_{KK'}T^1_{K'J}\gamma^\chi_{\Psi_1}\\
&+T^2_{IJ}T^\gamma_{II'}T_{I'2K}T^1_{KJ}\gamma^\chi_{\Psi_2}+T^2_{IJ}T_{I2K}T_{KJ'2}T^\gamma_{JJ'}\gamma^\chi_\Phi\Big]\,,
\end{aligned}
\tag{C.12}
$$

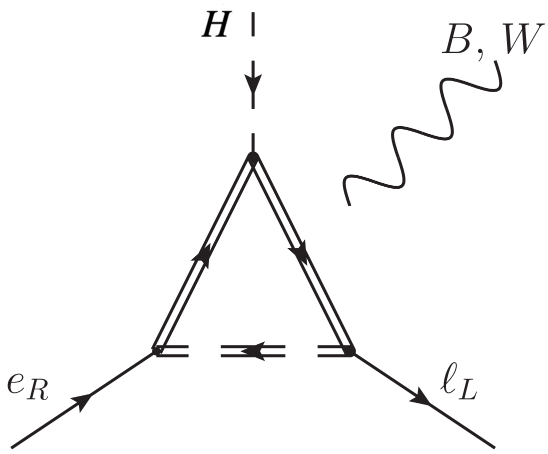


**Figure C.2:** Box diagram contribution to $\alpha_{e\gamma}$ with all heavy internal propagators. Double lines represent heavy particles, whereas single lines are SM particles. The gauge boson ($B$ or $W$) is represented outside the diagram since it can be attached to any of the internal propagators.

where:

$$\begin{aligned}\gamma^L_{\Psi_1} =& \frac{i}{16\pi^2} M_\Phi^2 \Big[ (M_{\Psi_2} - M_{\Psi_1})(M_{\Psi_1} + M_{\Psi_2}) \Big( M_\Phi^2 (M_{\Psi_2} - M_{\Psi_1})(M_{\Psi_1} + M_{\Psi_2}) \Big( M_{\Psi_1}^2 \Big( M_\Phi^2 - 2M_{\Psi_2}^2 \Big) \\ & + M_\Phi^4 \Big) \operatorname{Log}\left( \frac{M_{\Psi_1}^2}{M_\Phi^2} \right) - (M_\Phi - M_{\Psi_1})(M_{\Psi_1} + M_\Phi)(M_{\Psi_2} - M_\Phi)(M_{\Psi_2} + M_\Phi) \Big( M_{\Psi_1}^2 \Big( M_{\Psi_2}^2 - 2M_\Phi^2 \Big) \\ & + M_{\Psi_2}^2 M_\Phi^2 \Big) \Big) + M_{\Psi_2}^4 \Big( M_{\Psi_1}^2 - M_\Phi^2 \Big)^3 \operatorname{Log}\left( \frac{M_{\Psi_1}^2}{M_{\Psi_2}^2} \right) \Big] \times \\ & \frac{1}{(M_{\Psi_1} - M_{\Psi_2})^2 (M_{\Psi_1} + M_{\Psi_2})^2 \Big( M_\Phi^2 - M_{\Psi_1}^2 \Big)^3 (M_{\Psi_2} - M_\Phi)^2 (M_{\Psi_2} + M_\Phi)^2}, \end{aligned} \tag{C.13}$$

$$\begin{aligned}\gamma^R_{\Psi_1} =& \frac{i}{16\pi^2} M_{\Psi_1} \big( M_{\Psi_2} (M_{\Psi_2} - M_{\Psi_1})(M_{\Psi_1} + M_{\Psi_2}) \big( (M_{\Psi_1} - M_\Phi)(M_{\Psi_1} + M_\Phi) \\ & (M_{\Psi_2} - M_\Phi)(M_{\Psi_2} + M_\Phi) \Big( M_{\Psi_1}^2 M_{\Psi_2}^2 - 3M_{\Psi_2}^2 M_\Phi^2 + 2M_\Phi^4 \Big) + M_\Phi^4 (M_{\Psi_2} - M_{\Psi_1})(M_{\Psi_1} + M_{\Psi_2}) \\ & \Big( M_{\Psi_1}^2 + 2M_{\Psi_2}^2 - 3M_\Phi^2 \Big) \operatorname{Log}\left( \frac{M_{\Psi_1}^2}{M_\Phi^2} \right) \Big) \Big) + M_{\Psi_2}^3 \Big( M_{\Psi_1}^2 - M_\Phi^2 \Big)^3 \Big( M_{\Psi_2}^2 - 2M_\Phi^2 \Big) \operatorname{Log}\left( \frac{M_{\Psi_1}^2}{M_{\Psi_2}^2} \right) \Big) \times \\ & \frac{1}{(M_{\Psi_1} - M_{\Psi_2})^2 (M_{\Psi_1} + M_{\Psi_2})^2 (M_{\Psi_1} - M_\Phi)^3 (M_{\Psi_1} + M_\Phi)^3 (M_{\Psi_2} - M_\Phi)^2 (M_{\Psi_2} + M_\Phi)^2}, \end{aligned} \tag{C.14}$$

$$
\gamma^L_{\Psi_2} = -\frac{i}{16\pi^2}\left[M^6_{\Psi_1}\left(-\left(M^2_{\Psi_2}-M^2_{\Phi}\right)^3\right)\text{Log}\left(\frac{M^2_{\Psi_1}}{M^2_{\Phi}}\right)+M^4_{\Psi_1}(M_{\Psi_1}-M_{\Phi})(M_{\Psi_1}+M_{\Phi})\right.
$$

$$
(M_{\Psi_2}-M_{\Phi})^3(M_{\Psi_2}+M_{\Phi})^3\,\text{Log}\left(\frac{M^2_{\Psi_1}}{M^2_{\Psi_2}}\right)+(M_{\Psi_1}-M_{\Phi})(M_{\Psi_1}+M_{\Phi})\left(M^2_{\Phi}(M_{\Psi_1}-M_{\Psi_2})(M_{\Psi_1}+M_{\Psi_2})\right.
$$

$$
(M_{\Psi_2}-M_{\Phi})(M_{\Psi_2}+M_{\Phi})\left(M^2_{\Psi_1}\left(M^2_{\Psi_2}+M^2_{\Phi}\right)-2M^2_{\Psi_2}M^2_{\Phi}\right)+\left(M^4_{\Psi_1}M^6_{\Psi_2}-M^6_{\Phi}\left(M^2_{\Psi_1}-M^2_{\Psi_2}\right)^2\right.
$$

$$
\left.\left.\left.+M^2_{\Psi_1}M^4_{\Psi_2}M^2_{\Phi}\left(M^2_{\Psi_2}-3M^2_{\Psi_1}\right)+M^2_{\Psi_2}M^4_{\Phi}\left(M^4_{\Psi_1}+M^2_{\Psi_1}M^2_{\Psi_2}-M^4_{\Psi_2}\right)\right)\text{Log}\left(\frac{M^2_{\Psi_2}}{M^2_{\Phi}}\right)\right)\right]\times
$$

$$
\frac{1}{(M_{\Psi_1}-M_{\Psi_2})^2(M_{\Psi_1}+M_{\Psi_2})^2(M_{\Psi_1}-M_{\Phi})^2(M_{\Psi_1}+M_{\Phi})^2(M_{\Psi_2}-M_{\Phi})^3(M_{\Psi_2}+M_{\Phi})^3}\,, \tag{C.15}
$$

$$
\gamma^R_{\Psi_2} = \frac{i}{16\pi^2}M_{\Psi_1}M_{\Psi_2}\left(2M^2_{\Psi_1}(M_{\Psi_1}-M_{\Phi})(M_{\Psi_1}+M_{\Phi})\left(M^2_{\Phi}-M^2_{\Psi_2}\right)^3\text{Log}\left(\frac{M^2_{\Psi_1}}{M^2_{\Psi_2}}\right)\right.
$$

$$
+M^4_{\Psi_1}\left(M^2_{\Psi_2}-M^2_{\Phi}\right)^3\text{Log}\left(\frac{M^2_{\Psi_1}}{M^2_{\Phi}}\right)+(M_{\Phi}-M_{\Psi_1})(M_{\Psi_1}+M_{\Phi})\left((M_{\Psi_2}-M_{\Psi_1})(M_{\Psi_1}+M_{\Psi_2})\right.
$$

$$
(M_{\Psi_2}-M_{\Phi})(M_{\Psi_2}+M_{\Phi})\left(M^2_{\Psi_1}\left(M^2_{\Psi_2}-3M^2_{\Phi}\right)+2M^4_{\Phi}\right)+\left(M^2_{\Psi_1}M^6_{\Psi_2}+M^4_{\Psi_2}M^2_{\Phi}\left(M^2_{\Psi_2}-3M^2_{\Psi_1}\right)\right.
$$

$$
\left.\left.\left.+M^4_{\Phi}\left(-2M^4_{\Psi_1}+6M^2_{\Psi_1}M^2_{\Psi_2}-3M^4_{\Psi_2}\right)\right)\text{Log}\left(\frac{M^2_{\Psi_2}}{M^2_{\Phi}}\right)\right)\right)\times
$$

$$
\frac{1}{(M_{\Psi_1}-M_{\Psi_2})^2(M_{\Psi_1}+M_{\Psi_2})^2(M_{\Psi_1}-M_{\Phi})^2(M_{\Psi_1}+M_{\Phi})^2(M_{\Psi_2}-M_{\Phi})^3(M_{\Psi_2}+M_{\Phi})^3}\,, \tag{C.16}
$$

$$
\gamma^L_{\Phi} = \frac{iM^2_{\Phi}}{16\pi^2}\left[\frac{1}{\left(M^2_{\Psi_2}-M^2_{\Phi}\right)^3}\left(2\left(M^4_{\Psi_1}M^4_{\Psi_2}+M^6_{\Phi}\left(M^2_{\Psi_1}+M^2_{\Psi_2}\right)-3M^2_{\Psi_1}M^2_{\Psi_2}M^4_{\Phi}\right)\text{Log}\left(\frac{M^2_{\Psi_2}}{M^2_{\Phi}}\right)\right.\right.
$$

$$
-(M_{\Phi}-M_{\Psi_1})(M_{\Psi_1}+M_{\Phi})(M_{\Psi_2}-M_{\Phi})(M_{\Psi_2}+M_{\Phi})\left(M^2_{\Phi}\left(M^2_{\Psi_1}+M^2_{\Psi_2}\right)-3M^2_{\Psi_1}M^2_{\Psi_2}+M^4_{\Phi}\right)
$$

$$
\left.\left.-\frac{2M^4_{\Psi_1}\,\text{Log}\left(\frac{M^2_{\Psi_1}}{M^2_{\Psi_2}}\right)}{M^2_{\Psi_1}-M^2_{\Psi_2}}\right)\right]\times\frac{1}{(M_{\Psi_1}-M_{\Phi})^3\,(M_{\Psi_1}+M_{\Phi})^3}\,, \tag{C.17}
$$

$$
\gamma^R_{\Phi} = \frac{i}{16\pi^2}M_{\Psi_1}M_{\Psi_2}\left(2M^2_{\Psi_1}M^2_{\Phi}\left(M^2_{\Psi_2}-M^2_{\Phi}\right)^3\text{Log}\left(\frac{M^2_{\Psi_1}}{M^2_{\Psi_2}}\right)+(M_{\Psi_1}-M_{\Psi_2})(M_{\Psi_1}+M_{\Psi_2})\right.
$$

$$
\left((M_{\Psi_1}-M_{\Phi})(M_{\Psi_1}+M_{\Phi})(M_{\Psi_2}-M_{\Phi})(M_{\Psi_2}+M_{\Phi})\left(M^2_{\Phi}\left(M^2_{\Psi_1}+M^2_{\Psi_2}\right)+M^2_{\Psi_1}M^2_{\Psi_2}-3M^4_{\Phi}\right)\right.
$$

$$
\left.\left.-2M^2_{\Phi}\left(M^4_{\Psi_1}M^2_{\Psi_2}+M^2_{\Psi_1}\left(M^4_{\Psi_2}-3M^2_{\Psi_2}M^2_{\Phi}\right)+M^6_{\Phi}\right)\text{Log}\left(\frac{M^2_{\Psi_2}}{M^2_{\Phi}}\right)\right)\right)\times
$$

$$
\frac{1}{(-M^2_{\Psi_1}+M^2_{\Psi_2})(M^2_{\Psi_1}-M^2_{\Phi})^3(M^2_{\Psi_2}-M^2_{\Phi})^3}\,. \tag{C.18}
$$

This last result of the box diagram with only heavy internal propagators was cross-checked with Eq. (4.4) of Ref. [172] in the limit of degenerate masses and we found perfect agreement.

# Bibliography


[1] Super-Kamiokande collaboration, K. Abe et al., *Search for Nucleon Decay via $n \to \bar{\nu}\pi^0$ and $p \to \bar{\nu}\pi^+$ in Super-Kamiokande*, *Phys. Rev. Lett.* **113** (2014) 121802, arXiv: 1305.4391.

[2] Super-Kamiokande collaboration, K. Abe et al., *Search for proton decay via $p \to e^+\pi^0$ and $p \to \mu^+\pi^0$ in 0.31 megaton · years exposure of the Super-Kamiokande water Cherenkov detector*, *Phys. Rev. D* **95** (2017) 012004, arXiv: 1610.03597.

[3] Super-Kamiokande collaboration, S. Sussman et al., *Dinucleon and Nucleon Decay to Two-Body Final States with no Hadrons in Super-Kamiokande*, arXiv: 1811.12430.

[4] T. Appelquist and J. Carazzone, *Infrared Singularities and Massive Fields*, *Phys. Rev. D* **11** (1975) 2856.

[5] T. Cohen, *As Scales Become Separated: Lectures on Effective Field Theory*, *PoS* **TASI2018** (2019) 011, arXiv: 1903.03622.

[6] A. Pich, *Effective field theory: Course*, in *Les Houches Summer School in Theoretical Physics, Session 68: Probing the Standard Model of Particle Interactions*, pp. 949–1049, 6, 1998. arXiv: hep-ph/9806303.

[7] W. Skiba, *Effective Field Theory and Precision Electroweak Measurements*, in *Theoretical Advanced Study Institute in Elementary Particle Physics: Physics of the Large and the Small*, pp. 5–70, 2011. arXiv: 1006.2142. DOI.

[8] A. V. Manohar, *Introduction to Effective Field Theories*, arXiv: 1804.05863.

[9] G. Isidori, F. Wilsch and D. Wyler, *The Standard Model effective field theory at work*, arXiv: 2303.16922.

[10] M. Bauer, M. Neubert and A. Thamm, *Collider Probes of Axion-Like Particles*, *JHEP* **12** (2017) 044, arXiv: 1708.00443.

[11] K. Choi, S. H. Im, C. B. Park and S. Yun, *Minimal Flavor Violation with Axion-like Particles*, *JHEP* **11** (2017) 070, arXiv: 1708.00021.

[12] M. Chala, G. Guedes, M. Ramos and J. Santiago, *Running in the ALPs*, *Eur. Phys. J. C* **81** (2021) 181, arXiv: 2012.09017.

[13] F. del Aguila, S. Bar-Shalom, A. Soni and J. Wudka, *Heavy Majorana Neutrinos in the Effective Lagrangian Description: Application to Hadron Colliders*, *Phys. Lett. B* **670** (2009) 399–402, arXiv: 0806.0876.

[14] A. Aparici, K. Kim, A. Santamaria and J. Wudka, *Right-handed neutrino magnetic moments*, *Phys. Rev. D* **80** (2009) 013010, arXiv: 0904.3244.

[15] S. Bhattacharya and J. Wudka, *Dimension-seven operators in the standard model with right handed neutrinos*, *Phys. Rev. D* **94** (2016) 055022, arXiv: 1505.05264.

[16] Y. Liao and X.-D. Ma, *Operators up to Dimension Seven in Standard Model Effective Field Theory Extended with Sterile Neutrinos*, *Phys. Rev. D* **96** (2017) 015012, arXiv: 1612.04527.

[17] H.-L. Li, Z. Ren, M.-L. Xiao, J.-H. Yu and Y.-H. Zheng, *Operator bases in effective field theories with sterile neutrinos: $d \leq 9$*, *JHEP* **11** (2021) 003, arXiv: 2105.09329.

[18] A. Falkowski and R. Rattazzi, *Which EFT*, *JHEP* **10** (2019) 255, arXiv: 1902.05936.

[19] I. Brivio and M. Trott, *The Standard Model as an Effective Field Theory*, *Phys. Rept.* **793** (2019) 1–98, arXiv: 1706.08945.

[20] T. Cohen, N. Craig, X. Lu and D. Sutherland, *Is SMEFT Enough?*, *JHEP* **03** (2021) 237, arXiv: 2008.08597.

[21] S. Weinberg, *Baryon and Lepton Nonconserving Processes*, *Phys. Rev. Lett.* **43** (1979) 1566–1570.

[22] F. Bonnet, M. Hirsch, T. Ota and W. Winter, *Systematic study of the d=5 Weinberg operator at one-loop order*, *JHEP* **07** (2012) 153, arXiv: 1204.5862.

[23] D. Aristizabal Sierra, A. Degee, L. Dorame and M. Hirsch, *Systematic classification of two-loop realizations of the Weinberg operator*, *JHEP* **03** (2015) 040, arXiv: 1411.7038.

[24] R. Cepedello, R. M. Fonseca and M. Hirsch, *Systematic classification of three-loop realizations of the Weinberg operator*, *JHEP* **10** (2018) 197, arXiv: 1807.00629.

[25] C. Arzt, *Reduced effective Lagrangians*, *Phys. Lett. B* **342** (1995) 189–195, arXiv: hep-ph/9304230.

[26] J. C. Criado and M. Pérez-Victoria, *Field redefinitions in effective theories at higher orders*, *JHEP* **03** (2019) 038, arXiv: 1811.09413.

[27] B. Grzadkowski, M. Iskrzynski, M. Misiak and J. Rosiek, *Dimension-Six Terms in the Standard Model Lagrangian*, *JHEP* **10** (2010) 085, arXiv: 1008.4884.

[28] G. D'Ambrosio, G. F. Giudice, G. Isidori and A. Strumia, *Minimal flavor violation: An Effective field theory approach*, *Nucl. Phys. B* **645** (2002) 155–187, arXiv: hep-ph/0207036.

[29] D. A. Faroughy, G. Isidori, F. Wilsch and K. Yamamoto, *Flavour symmetries in the SMEFT*, *JHEP* **08** (2020) 166, arXiv: 2005.05366.

[30] A. Greljo, A. Palavrić and A. E. Thomsen, *Adding Flavor to the SMEFT*, *JHEP* **10** (2022) 010, arXiv: 2203.09561.

[31] L. Bellafronte, S. Dawson and P. P. Giardino, *The importance of flavor in SMEFT Electroweak Precision Fits*, *JHEP* **05** (2023) 208, arXiv: 2304.00029.

[32] A. Greljo and A. Palavrić, *Leading directions in the SMEFT*, arXiv: 2305.08898.

[33] J. Fuentes-Martín, M. König, J. Pagès, A. E. Thomsen and F. Wilsch, *Evanescent operators in one-loop matching computations*, *JHEP* **02** (2023) 031, arXiv: 2211.09144.

[34] J. Fuentes-Martin, J. Portoles and P. Ruiz-Femenia, *Integrating out heavy particles with functional methods: a simplified framework*, *JHEP* **09** (2016) 156, arXiv: 1607.02142.

[35] T. Cohen, X. Lu and Z. Zhang, *Functional Prescription for EFT Matching*, *JHEP* **02** (2021) 228, arXiv: 2011.02484.

[36] J. Fuentes-Martin, M. König, J. Pagès, A. E. Thomsen and F. Wilsch, *SuperTracer: A Calculator of Functional Supertraces for One-Loop EFT Matching*, *JHEP* **04** (2021) 281, arXiv: 2012.08506.

[37] T. Cohen, X. Lu and Z. Zhang, *STrEAMlining EFT Matching*, *SciPost Phys.* **10** (2021) 098, arXiv: 2012.07851.

[38] M. K. Gaillard, *The Effective One Loop Lagrangian With Derivative Couplings*, *Nucl. Phys. B* **268** (1986) 669–692.

[39] O. Cheyette, *Effective Action for the Standard Model With Large Higgs Mass*, *Nucl. Phys. B* **297** (1988) 183–204.

[40] O. Cheyette, *Derivative Expansion of the Effective Action*, *Phys. Rev. Lett.* **55** (1985) 2394.

[41] B. Henning, X. Lu and H. Murayama, *How to use the Standard Model effective field theory*, *JHEP* **01** (2016) 023, arXiv: `1412.1837`.

[42] A. Drozd, J. Ellis, J. Quevillon and T. You, *The Universal One-Loop Effective Action*, *JHEP* **03** (2016) 180, arXiv: `1512.03003`.

[43] J. C. Criado, *MatchingTools: a Python library for symbolic effective field theory calculations*, *Comput. Phys. Commun.* **227** (2018) 42–50, arXiv: `1710.06445`.

[44] S. Das Bakshi, J. Chakrabortty and S. K. Patra, *CoDEx: Wilson coefficient calculator connecting SMEFT to UV theory*, *Eur. Phys. J. C* **79** (2019) 21, arXiv: `1808.04403`.

[45] J. Fuentes-Martín, M. König, J. Pagès, A. E. Thomsen and F. Wilsch, *A Proof of Concept for Matchete: An Automated Tool for Matching Effective Theories*, arXiv: `2212.04510`.

[46] M. Beneke and V. A. Smirnov, *Asymptotic expansion of Feynman integrals near threshold*, *Nucl. Phys. B* **522** (1998) 321–344, arXiv: `hep-ph/9711391`.

[47] V. Gherardi, D. Marzocca and E. Venturini, *Low-energy phenomenology of scalar leptoquarks at one-loop accuracy*, *JHEP* **01** (2021) 138, arXiv: `2008.09548`.

[48] J. Aebischer, W. Dekens, E. E. Jenkins, A. V. Manohar, D. Sengupta and P. Stoffer, *Effective field theory interpretation of lepton magnetic and electric dipole moments*, *JHEP* **07** (2021) 107, arXiv: `2102.08954`.

[49] G. Guedes, P. Olgoso and J. Santiago, *Towards the one loop IR/UV dictionary in the SMEFT: one loop generated operators from new scalars and fermions*, arXiv: `2303.16965`.

[50] T. Giani, G. Magni and J. Rojo, *SMEFiT: a flexible toolbox for global interpretations of particle physics data with effective field theories*, *Eur. Phys. J. C* **83** (2023) 393, arXiv: `2302.06660`.

[51] J. Ellis, M. Madigan, K. Mimasu, V. Sanz and T. You, *Top, Higgs, Diboson and Electroweak Fit to the Standard Model Effective Field Theory*, *JHEP* **04** (2021) 279, arXiv: `2012.02779`.

[52] N. Castro, J. Erdmann, C. Grunwald, K. Kröninger and N.-A. Rosien, *EFTfitter—A tool for interpreting measurements in the context of effective field theories*, *Eur. Phys. J. C* **76** (2016) 432, arXiv: `1605.05585`.

[53] J. De Blas et al., *`HEPfit`: a code for the combination of indirect and direct constraints on high energy physics models*, *Eur. Phys. J. C* **80** (2020) 456, arXiv: `1910.14012`.

[54] D. M. Straub, *flavio: a Python package for flavour and precision phenomenology in the Standard Model and beyond*, arXiv: `1810.08132`.

[55] J. Aebischer, J. Kumar, P. Stangl and D. M. Straub, *A Global Likelihood for Precision Constraints and Flavour Anomalies*, *Eur. Phys. J. C* **79** (2019) 509, arXiv: `1810.07698`.

[56] L. Lehman, *Extending the Standard Model Effective Field Theory with the Complete Set of Dimension-7 Operators*, *Phys. Rev. D* **90** (2014) 125023, arXiv: `1410.4193`.

[57] C. W. Murphy, *Dimension-8 operators in the Standard Model Eective Field Theory*, *JHEP* **10** (2020) 174, arXiv: `2005.00059`.

[58] Y. Liao and X.-D. Ma, *An explicit construction of the dimension-9 operator basis in the standard model effective field theory*, *JHEP* **11** (2020) 152, arXiv: `2007.08125`.

[59] R. V. Harlander, T. Kempkens and M. C. Schaaf, *The Standard Model Effective Field Theory up to Mass Dimension 12*, arXiv: `2305.06832`.

[60] H.-L. Li, Z. Ren, M.-L. Xiao, J.-H. Yu and Y.-H. Zheng, *Low energy effective field theory operator basis at $d \leq 9$*, *JHEP* **06** (2021) 138, arXiv: 2012.09188.

[61] J. C. Criado, *BasisGen: automatic generation of operator bases*, *Eur. Phys. J. C* **79** (2019) 256, arXiv: 1901.03501.

[62] H.-L. Li, Z. Ren, M.-L. Xiao, J.-H. Yu and Y.-H. Zheng, *Operators for generic effective field theory at any dimension: on-shell amplitude basis construction*, *JHEP* **04** (2022) 140, arXiv: 2201.04639.

[63] V. Gherardi, D. Marzocca and E. Venturini, *Matching scalar leptoquarks to the SMEFT at one loop*, *JHEP* **07** (2020) 225, arXiv: 2003.12525.

[64] A. Carmona, A. Lazopoulos, P. Olgoso and J. Santiago, *Matchmakereft: automated tree-level and one-loop matching*, *SciPost Phys.* **12** (2022) 198, arXiv: 2112.10787.

[65] M. Chala, A. Díaz-Carmona and G. Guedes, *A Green's basis for the bosonic SMEFT to dimension 8*, *JHEP* **05** (2022) 138, arXiv: 2112.12724.

[66] Z. Ren and J.-H. Yu, *A Complete Set of the Dimension-8 Green's Basis Operators in the Standard Model Effective Field Theory*, arXiv: 2211.01420.

[67] E. E. Jenkins, A. V. Manohar and P. Stoffer, *Low-Energy Effective Field Theory below the Electroweak Scale: Anomalous Dimensions*, *JHEP* **01** (2018) 084, arXiv: 1711.05270.

[68] E. E. Jenkins, A. V. Manohar and M. Trott, *Renormalization Group Evolution of the Standard Model Dimension Six Operators I: Formalism and lambda Dependence*, *JHEP* **10** (2013) 087, arXiv: 1308.2627.

[69] E. E. Jenkins, A. V. Manohar and M. Trott, *Renormalization Group Evolution of the Standard Model Dimension Six Operators II: Yukawa Dependence*, *JHEP* **01** (2014) 035, arXiv: 1310.4838.

[70] R. Alonso, E. E. Jenkins, A. V. Manohar and M. Trott, *Renormalization Group Evolution of the Standard Model Dimension Six Operators III: Gauge Coupling Dependence and Phenomenology*, *JHEP* **04** (2014) 159, arXiv: 1312.2014.

[71] M. Chala, G. Guedes, M. Ramos and J. Santiago, *Towards the renormalisation of the Standard Model effective field theory to dimension eight: Bosonic interactions I*, *SciPost Phys.* **11** (2021) 065, arXiv: 2106.05291.

[72] S. Das Bakshi, M. Chala, A. Díaz-Carmona and G. Guedes, *Towards the renormalisation of the Standard Model effective field theory to dimension eight: bosonic interactions II*, *Eur. Phys. J. Plus* **137** (2022) 973, arXiv: 2205.03301.

[73] J. Fuentes-Martin, P. Ruiz-Femenia, A. Vicente and J. Virto, *DsixTools 2.0: The Effective Field Theory Toolkit*, *Eur. Phys. J. C* **81** (2021) 167, arXiv: 2010.16341.

[74] J. Aebischer, J. Kumar and D. M. Straub, *Wilson: a Python package for the running and matching of Wilson coefficients above and below the electroweak scale*, *Eur. Phys. J. C* **78** (2018) 1026, arXiv: 1804.05033.

[75] E. E. Jenkins, A. V. Manohar and P. Stoffer, *Low-Energy Effective Field Theory below the Electroweak Scale: Operators and Matching*, *JHEP* **03** (2018) 016, arXiv: 1709.04486.

[76] W. Dekens and P. Stoffer, *Low-energy effective field theory below the electroweak scale: matching at one loop*, *JHEP* **10** (2019) 197, arXiv: 1908.05295.

[77] A. Alloul, N. D. Christensen, C. Degrande, C. Duhr and B. Fuks, *FeynRules 2.0 - A complete toolbox for tree-level phenomenology*, *Comput. Phys. Commun.* **185** (2014) 2250–2300, arXiv: 1310.1921.

[78] P. Nogueira, *Automatic Feynman graph generation*, *J. Comput. Phys.* **105** (1993) 279–289.

[79] B. Ruijl, T. Ueda and J. Vermaseren, *FORM version 4.2*, arXiv: 1707.06453.

[80] A. Denner, H. Eck, O. Hahn and J. Kublbeck, *Feynman rules for fermion number violating interactions*, *Nucl. Phys. B* **387** (1992) 467–481.

[81] A. Denner, H. Eck, O. Hahn and J. Kublbeck, *Compact Feynman rules for Majorana fermions*, *Phys. Lett. B* **291** (1992) 278–280.

[82] P. Breitenlohner and D. Maison, *Dimensional Renormalization and the Action Principle*, *Commun. Math. Phys.* **52** (1977) 11–38.

[83] C. Cornella, F. Feruglio and L. Vecchi, *Gauge invariance and finite counterterms in chiral gauge theories*, *JHEP* **02** (2023) 244, arXiv: 2205.10381.

[84] H. Bélusca-Maïto, A. Ilakovac, M. Mađor-Božinović, P. Kühler and D. Stöckinger, *Gamma5 in dimensional regularization - a no-compromise approach using the BMHV scheme*, *PoS* **LL2022** (2022) 011, arXiv: 2208.02752.

[85] L. F. Abbott, *The Background Field Method Beyond One Loop*, *Nucl. Phys. B* **185** (1981) 189–203.

[86] M. Chala and J. Santiago, *Positivity bounds in the Standard Model effective field theory beyond tree level*, arXiv: 2110.01624.

[87] A. Crivellin, M. Kirk, T. Kitahara and F. Mescia, *Correlating $t \to cZ$ to the $W$ Mass and $B$ Physics with Vector-Like Quarks*, arXiv: 2204.05962.

[88] S. Bakshi Das, M. Chala, A. Díaz-Carmona and G. Guedes, *Towards the renormalisation of the Standard Model effective field theory to dimension eight: Bosonic interactions II*, arXiv: 2205.03301.

[89] G. Guedes and P. Olgoso, *A bridge to new physics: proposing new – and reviving old – explanations of $a_\mu$*, arXiv: 2205.04480.

[90] A. Crivellin, M. Kirk and A. Thapa, *$Y = 0$ Scalar Triplet Beyond the $W$ Mass: $(g-2)_\mu$, $h \to \mu^+\mu^-$ and CKM Unitarity*, arXiv: 2305.03081.

[91] M. Chala, *Constraints on anomalous dimensions from the positivity of the S-matrix*, arXiv: 2301.09995.

[92] A. Crivellin, M. Kirk, T. Kitahara and F. Mescia, *Global fit of modified quark couplings to EW gauge bosons and vector-like quarks in light of the Cabibbo angle anomaly*, *JHEP* **03** (2023) 234, arXiv: 2212.06862.

[93] A. Celis, J. Fuentes-Martin, A. Vicente and J. Virto, *DsixTools: The Standard Model Effective Field Theory Toolkit*, *Eur. Phys. J. C* **77** (2017) 405, arXiv: 1704.04504.

[94] U. Haisch, M. Ruhdorfer, E. Salvioni, E. Venturini and A. Weiler, *Singlet night in Feynman-ville: one-loop matching of a real scalar*, *JHEP* **04** (2020) 164, arXiv: 2003.05936.

[95] M. Jiang, N. Craig, Y.-Y. Li and D. Sutherland, *Complete one-loop matching for a singlet scalar in the Standard Model EFT*, *JHEP* **02** (2019) 031, arXiv: 1811.08878.

[96] D. Zhang and S. Zhou, *Complete One-loop Matching of the Type-I Seesaw Model onto the Standard Model Effective Field Theory*, arXiv: 2107.12133.

[97] M. S. Bilenky and A. Santamaria, *One loop effective Lagrangian for a standard model with a heavy charged scalar singlet*, *Nucl. Phys. B* **420** (1994) 47–93, arXiv: hep-ph/9310302.

[98] A. Crivellin and M. Hoferichter, *Consequences of chirally enhanced explanations of $(g-2)_\mu$ for $h \to \mu\mu$ and $Z \to \mu\mu$*, *JHEP* **07** (2021) 135, arXiv: 2104.03202.

[99] G. Guedes and J. Santiago, *New leptons with exotic decays: collider limits and dark matter complementarity*, *JHEP* **01** (2022) 111, arXiv: 2107.03429.

[100] F. del Aguila, J. de Blas and M. Perez-Victoria, *Effects of new leptons in Electroweak Precision Data*, *Phys. Rev. D* **78** (2008) 013010, arXiv: 0803.4008.

[101] A. Falkowski, B. Fuks, K. Mawatari, K. Mimasu, F. Riva and V. Sanz, *Rosetta: an operator basis translator for Standard Model effective field theory*, *Eur. Phys. J. C* **75** (2015) 583, arXiv: 1508.05895.

[102] J. de Blas, J. C. Criado, M. Perez-Victoria and J. Santiago, *Effective description of general extensions of the Standard Model: the complete tree-level dictionary*, *JHEP* **03** (2018) 109, arXiv: 1711.10391.

[103] F. del Aguila, M. Perez-Victoria and J. Santiago, *Observable contributions of new exotic quarks to quark mixing*, *JHEP* **09** (2000) 011, arXiv: hep-ph/0007316.

[104] F. del Aguila, J. de Blas and M. Perez-Victoria, *Electroweak Limits on General New Vector Bosons*, *JHEP* **09** (2010) 033, arXiv: 1005.3998.

[105] J. de Blas, M. Chala, M. Perez-Victoria and J. Santiago, *Observable Effects of General New Scalar Particles*, *JHEP* **04** (2015) 078, arXiv: 1412.8480.

[106] H.-L. Li, Y.-H. Ni, M.-L. Xiao and J.-H. Yu, *The Bottom-Up EFT: Complete UV Resonances of the SMEFT Operators*, arXiv: 2204.03660.

[107] C. Arzt, M. B. Einhorn and J. Wudka, *Patterns of deviation from the standard model*, *Nucl. Phys. B* **433** (1995) 41–66, arXiv: hep-ph/9405214.

[108] N. Craig, M. Jiang, Y.-Y. Li and D. Sutherland, *Loops and Trees in Generic EFTs*, *JHEP* **08** (2020) 086, arXiv: 2001.00017.

[109] R. Cepedello, F. Esser, M. Hirsch and V. Sanz, *Mapping the SMEFT to discoverable models*, *JHEP* **09** (2022) 229, arXiv: 2207.13714.

[110] R. Cepedello, F. Esser, M. Hirsch and V. Sanz, *SMEFT goes dark: Dark Matter models for four-fermion operators*, arXiv: 2302.03485.

[111] P. Arnan, L. Hofer, F. Mescia and A. Crivellin, *Loop effects of heavy new scalars and fermions in $b \to s\mu^+\mu^-$*, *JHEP* **04** (2017) 043, arXiv: 1608.07832.

[112] P. Arnan, A. Crivellin, M. Fedele and F. Mescia, *Generic Loop Effects of New Scalars and Fermions in $b \to s\ell^+\ell^-$, $(g-2)_\mu$ and a Vector-like $4^{\text{th}}$ Generation*, *JHEP* **06** (2019) 118, arXiv: 1904.05890.

[113] F. Bishara, J. Brod, M. Gorbahn and U. Moldanazarova, *Generic one-loop matching conditions for rare meson decays*, *JHEP* **07** (2021) 230, arXiv: 2104.10930.

[114] S. Das Bakshi, J. Chakrabortty, S. Prakash, S. U. Rahaman and M. Spannowsky, *EFT diagrammatica: UV roots of the CP-conserving SMEFT*, *JHEP* **06** (2021) 033, arXiv: 2103.11593.

[115] W. Naskar, S. Prakash and S. U. Rahaman, *EFT Diagrammatica. Part II. Tracing the UV origin of bosonic D6 CPV and D8 SMEFT operators*, *JHEP* **08** (2022) 190, arXiv: 2205.00910.

[116] R. M. Fonseca, *GroupMath: A Mathematica package for group theory calculations*, *Comput. Phys. Commun.* **267** (2021) 108085, arXiv: 2011.01764.

[117] A. Biswas, S. Descotes-Genon, J. Matias and G. Tetlalmatzi-Xolocotzi, *A new puzzle in non-leptonic B decays*, arXiv: 2301.10542.

[118] J. Aebischer et al., *WCxf: an exchange format for Wilson coefficients beyond the Standard Model*, *Comput. Phys. Commun.* **232** (2018) 71–83, arXiv: 1712.05298.

[119] J. Aebischer, J. Kumar, P. Stangl and D. M. Straub, *A global likelihood for precision constraints and flavour anomalies*, *The European Physical Journal C* **79** (jun, 2019) .

[120] D. M. Straub, *flavio: a Python package for flavour and precision phenomenology in the Standard Model and beyond*, arXiv: 1810.08132.

[121] J. Aebischer, J. Kumar and D. M. Straub, *Wilson: a Python package for the running and matching of Wilson coefficients above and below the electroweak scale*, *Eur. Phys. J. C* **78** (2018) 1026, arXiv: 1804.05033.

[122] J. C. Criado and M. Perez-Victoria, *Vector-like quarks with non-renormalizable interactions*, *JHEP* **01** (2020) 057, arXiv: 1908.08964.

[123] J. Fuentes-Martín, P. Olgoso, A. E. Thomsen and J. Santiago, *In preparation*, arXiv: 23xx.xxxxx.

[124] J. Criado, "Matchingdb." https://gitlab.com/jccriado/matchingdb/, 2023.

[125] Muon g-2 collaboration, B. Abi et al., *Measurement of the Positive Muon Anomalous Magnetic Moment to 0.46 ppm*, *Phys. Rev. Lett.* **126** (2021) 141801, arXiv: 2104.03281.

[126] Muon g-2 collaboration, G. W. Bennett et al., *Final Report of the Muon E821 Anomalous Magnetic Moment Measurement at BNL*, *Phys. Rev. D* **73** (2006) 072003, arXiv: hep-ex/0602035.

[127] T. Aoyama et al., *The anomalous magnetic moment of the muon in the Standard Model*, *Phys. Rept.* **887** (2020) 1–166, arXiv: 2006.04822.

[128] M. Davier, A. Hoecker, B. Malaescu and Z. Zhang, *Reevaluation of the hadronic vacuum polarisation contributions to the Standard Model predictions of the muon $g-2$ and $\alpha(m_Z^2)$ using newest hadronic cross-section data*, *Eur. Phys. J.* **C77** (2017) 827, arXiv: 1706.09436.

[129] A. Keshavarzi, D. Nomura and T. Teubner, *Muon $g-2$ and $\alpha(M_Z^2)$: a new data-based analysis*, *Phys. Rev.* **D97** (2018) 114025, arXiv: 1802.02995.

[130] G. Colangelo, M. Hoferichter and P. Stoffer, *Two-pion contribution to hadronic vacuum polarization*, *JHEP* **02** (2019) 006, arXiv: 1810.00007.

[131] M. Hoferichter, B.-L. Hoid and B. Kubis, *Three-pion contribution to hadronic vacuum polarization*, *JHEP* **08** (2019) 137, arXiv: 1907.01556.

[132] M. Davier, A. Hoecker, B. Malaescu and Z. Zhang, *A new evaluation of the hadronic vacuum polarisation contributions to the muon anomalous magnetic moment and to $\boldsymbol{\alpha}(\mathbf{m_Z^2})$*, *Eur. Phys. J.* **C80** (2020) 241, arXiv: 1908.00921.

[133] A. Keshavarzi, D. Nomura and T. Teubner, *The $g-2$ of charged leptons, $\alpha(M_Z^2)$ and the hyperfine splitting of muonium*, *Phys. Rev.* **D101** (2020) 014029, arXiv: 1911.00367.

[134] A. Kurz, T. Liu, P. Marquard and M. Steinhauser, *Hadronic contribution to the muon anomalous magnetic moment to next-to-next-to-leading order*, *Phys. Lett.* **B734** (2014) 144–147, arXiv: 1403.6400.

[135] Fermilab Lattice, LATTICE-HPQCD, MILC collaboration, B. Chakraborty et al., *Strong-Isospin-Breaking Correction to the Muon Anomalous Magnetic Moment from Lattice QCD at the Physical Point*, *Phys. Rev. Lett.* **120** (2018) 152001, arXiv: 1710.11212.

[136] Budapest-Marseille-Wuppertal collaboration, S. Borsanyi et al., *Hadronic vacuum polarization contribution to the anomalous magnetic moments of leptons from first principles*, *Phys. Rev. Lett.* **121** (2018) 022002, arXiv: 1711.04980.

[137] RBC, UKQCD collaboration, T. Blum, P. A. Boyle, V. Gülpers, T. Izubuchi, L. Jin, C. Jung et al., *Calculation of the hadronic vacuum polarization contribution to the muon anomalous magnetic moment*, *Phys. Rev. Lett.* **121** (2018) 022003, arXiv: 1801.07224.

[138] ETM collaboration, D. Giusti, V. Lubicz, G. Martinelli, F. Sanfilippo and S. Simula, *Electromagnetic and strong isospin-breaking corrections to the muon $g-2$ from Lattice QCD+QED*, *Phys. Rev.* **D99** (2019) 114502, arXiv: 1901.10462.

[139] E. Shintani and Y. Kuramashi, *Study of systematic uncertainties in hadronic vacuum polarization contribution to muon $g-2$ with 2+1 flavor lattice QCD*, *Phys. Rev.* **D100** (2019) 034517, arXiv: 1902.00885.

[140] Fermilab Lattice, LATTICE-HPQCD, MILC collaboration, C. T. H. Davies et al., *Hadronic-vacuum-polarization contribution to the muon's anomalous magnetic moment from four-flavor lattice QCD*, *Phys. Rev.* **D101** (2020) 034512, arXiv: 1902.04223.

[141] A. Gérardin, M. Cè, G. von Hippel, B. Hörz, H. B. Meyer, D. Mohler et al., *The leading hadronic contribution to $(g-2)_\mu$ from lattice QCD with $N_\mathrm{f}=2+1$ flavours of O(a) improved Wilson quarks*, *Phys. Rev.* **D100** (2019) 014510, arXiv: 1904.03120.

[142] C. Aubin, T. Blum, C. Tu, M. Golterman, C. Jung and S. Peris, *Light quark vacuum polarization at the physical point and contribution to the muon $g-2$*, *Phys. Rev.* **D101** (2020) 014503, arXiv: 1905.09307.

[143] D. Giusti and S. Simula, *Lepton anomalous magnetic moments in Lattice QCD+QED*, *PoS* **LATTICE2019** (2019) 104, arXiv: 1910.03874.

[144] K. Melnikov and A. Vainshtein, *Hadronic light-by-light scattering contribution to the muon anomalous magnetic moment revisited*, *Phys. Rev.* **D70** (2004) 113006, arXiv: hep-ph/0312226.

[145] P. Masjuan and P. Sánchez-Puertas, *Pseudoscalar-pole contribution to the $(g_\mu-2)$: a rational approach*, *Phys. Rev.* **D95** (2017) 054026, arXiv: 1701.05829.

[146] G. Colangelo, M. Hoferichter, M. Procura and P. Stoffer, *Dispersion relation for hadronic light-by-light scattering: two-pion contributions*, *JHEP* **04** (2017) 161, arXiv: 1702.07347.

[147] M. Hoferichter, B.-L. Hoid, B. Kubis, S. Leupold and S. P. Schneider, *Dispersion relation for hadronic light-by-light scattering: pion pole*, *JHEP* **10** (2018) 141, arXiv: 1808.04823.

[148] A. Gérardin, H. B. Meyer and A. Nyffeler, *Lattice calculation of the pion transition form factor with $N_f=2+1$ Wilson quarks*, *Phys. Rev.* **D100** (2019) 034520, arXiv: 1903.09471.

[149] J. Bijnens, N. Hermansson-Truedsson and A. Rodríguez-Sánchez, *Short-distance constraints for the HLbL contribution to the muon anomalous magnetic moment*, *Phys. Lett.* **B798** (2019) 134994, arXiv: 1908.03331.

[150] G. Colangelo, F. Hagelstein, M. Hoferichter, L. Laub and P. Stoffer, *Longitudinal short-distance constraints for the hadronic light-by-light contribution to $(g-2)_\mu$ with large-$N_c$ Regge models*, *JHEP* **03** (2020) 101, arXiv: 1910.13432.

[151] V. Pauk and M. Vanderhaeghen, *Single meson contributions to the muon's anomalous magnetic moment*, *Eur. Phys. J.* **C74** (2014) 3008, arXiv: 1401.0832.

[152] I. Danilkin and M. Vanderhaeghen, *Light-by-light scattering sum rules in light of new data*, *Phys. Rev.* **D95** (2017) 014019, arXiv: 1611.04646.

[153] F. Jegerlehner, *The Anomalous Magnetic Moment of the Muon*, *Springer Tracts Mod. Phys.* **274** (2017) 1–693.

[154] M. Knecht, S. Narison, A. Rabemananjara and D. Rabetiarivony, *Scalar meson contributions to $a_\mu$ from hadronic light-by-light scattering*, *Phys. Lett.* **B787** (2018) 111–123, arXiv: 1808.03848.

[155] G. Eichmann, C. S. Fischer and R. Williams, *Kaon-box contribution to the anomalous magnetic moment of the muon*, *Phys. Rev.* **D101** (2020) 054015, arXiv: 1910.06795.

[156] P. Roig and P. Sánchez-Puertas, *Axial-vector exchange contribution to the hadronic light-by-light piece of the muon anomalous magnetic moment*, *Phys. Rev.* **D101** (2020) 074019, arXiv: 1910.02881.

[157] G. Colangelo, M. Hoferichter, A. Nyffeler, M. Passera and P. Stoffer, *Remarks on higher-order hadronic corrections to the muon $g-2$*, *Phys. Lett.* **B735** (2014) 90–91, arXiv: 1403.7512.

[158] T. Blum, N. Christ, M. Hayakawa, T. Izubuchi, L. Jin, C. Jung et al., *The hadronic light-by-light scattering contribution to the muon anomalous magnetic moment from lattice QCD*, *Phys. Rev. Lett.* **124** (2020) 132002, arXiv: 1911.08123.

[159] T. Aoyama, M. Hayakawa, T. Kinoshita and M. Nio, *Complete Tenth-Order QED Contribution to the Muon $g-2$*, *Phys. Rev. Lett.* **109** (2012) 111808, arXiv: 1205.5370.

[160] T. Aoyama, T. Kinoshita and M. Nio, *Theory of the Anomalous Magnetic Moment of the Electron*, *Atoms* **7** (2019) 28.

[161] A. Czarnecki, W. J. Marciano and A. Vainshtein, *Refinements in electroweak contributions to the muon anomalous magnetic moment*, *Phys. Rev.* **D67** (2003) 073006, arXiv: hep-ph/0212229.

[162] C. Gnendiger, D. Stöckinger and H. Stöckinger-Kim, *The electroweak contributions to $(g-2)_\mu$ after the Higgs boson mass measurement*, *Phys. Rev.* **D88** (2013) 053005, arXiv: 1306.5546.

[163] S. Borsanyi et al., *Leading hadronic contribution to the muon magnetic moment from lattice QCD*, *Nature* **593** (2021) 51–55, arXiv: 2002.12347.

[164] M. Cè et al., *Window observable for the hadronic vacuum polarization contribution to the muon g-2 from lattice QCD*, *Phys. Rev. D* **106** (2022) 114502, arXiv: 2206.06582.

[165] A. Keshavarzi, W. J. Marciano, M. Passera and A. Sirlin, *Muon $g-2$ and $\Delta\alpha$ connection*, *Phys. Rev. D* **102** (2020) 033002, arXiv: 2006.12666.

[166] A. Crivellin, M. Hoferichter, C. A. Manzari and M. Montull, *Hadronic Vacuum Polarization: $(g-2)_\mu$ versus Global Electroweak Fits*, *Phys. Rev. Lett.* **125** (2020) 091801, arXiv: 2003.04886.

[167] B. Malaescu and M. Schott, *Impact of correlations between $a_\mu$ and $\alpha_{QED}$ on the EW fit*, *Eur. Phys. J. C* **81** (2021) 46, arXiv: 2008.08107.

[168] G. Colangelo, M. Hoferichter and P. Stoffer, *Constraints on the two-pion contribution to hadronic vacuum polarization*, *Phys. Lett. B* **814** (2021) 136073, arXiv: 2010.07943.

[169] P. Athron, C. Balázs, D. H. J. Jacob, W. Kotlarski, D. Stöckinger and H. Stöckinger-Kim, *New physics explanations of $a_\mu$ in light of the FNAL muon $g-2$ measurement*, *JHEP* **09** (2021) 080, arXiv: 2104.03691.

[170] L. Calibbi, R. Ziegler and J. Zupan, *Minimal models for dark matter and the muon $g-2$ anomaly*, *JHEP* **07** (2018) 046, arXiv: 1804.00009.

[171] L. Calibbi, T. Li, Y. Li and B. Zhu, *Simple model for large CP violation in charm decays, B-physics anomalies, muon g-2 and dark matter*, *JHEP* **10** (2020) 070, arXiv: 1912.02676.

[172] L. Allwicher, L. Di Luzio, M. Fedele, F. Mescia and M. Nardecchia, *What is the scale of new physics behind the muon g-2?*, *Phys. Rev. D* **104** (2021) 055035, arXiv: 2105.13981.

[173] G. Arcadi, L. Calibbi, M. Fedele and F. Mescia, *Muon $g-2$ and B-anomalies from Dark Matter*, *Phys. Rev. Lett.* **127** (2021) 061802, arXiv: 2104.03228.

[174] N. Arkani-Hamed and K. Harigaya, *Naturalness and the muon magnetic moment*, *JHEP* **09** (2021) 025, arXiv: 2106.01373.

[175] L. D. Rose, B. von Harling and A. Pomarol, *Wilson Coefficients and Natural Zeros from the On-Shell Viewpoint*, arXiv: 2201.10572.

[176] K. Kannike, M. Raidal, D. M. Straub and A. Strumia, *Anthropic solution to the magnetic muon anomaly: the charged see-saw*, *JHEP* **02** (2012) 106, arXiv: 1111.2551.

[177] A. Freitas, J. Lykken, S. Kell and S. Westhoff, *Testing the Muon g-2 Anomaly at the LHC*, *JHEP* **05** (2014) 145, arXiv: 1402.7065.

[178] K. Kowalska and E. M. Sessolo, *Expectations for the muon g-2 in simplified models with dark matter*, *JHEP* **09** (2017) 112, arXiv: 1707.00753.

[179] J. de Blas, *Electroweak limits on physics beyond the Standard Model*, *EPJ Web Conf.* **60** (2013) 19008, arXiv: 1307.6173.

[180] A. Crivellin, F. Kirk, C. A. Manzari and M. Montull, *Global Electroweak Fit and Vector-Like Leptons in Light of the Cabibbo Angle Anomaly*, *JHEP* **12** (2020) 166, arXiv: 2008.01113.

[181] ATLAS collaboration, G. Aad et al., *Search for heavy lepton resonances decaying to a Z boson and a lepton in pp collisions at $\sqrt{s} = 8$ TeV with the ATLAS detector*, *JHEP* **09** (2015) 108, arXiv: 1506.01291.

[182] CMS collaboration, A. M. Sirunyan et al., *Search for vector-like leptons in multilepton final states in proton-proton collisions at $\sqrt{s}$ = 13 TeV*, *Phys. Rev. D* **100** (2019) 052003, arXiv: 1905.10853.

[183] S. Ashanujjaman, D. Choudhury and K. Ghosh, *Search for exotic leptons in final states with two or three leptons and fat-jets at 13 TeV LHC*, arXiv: 2201.09645.

[184] M. J. Baker, P. Cox and R. R. Volkas, *Radiative muon mass models and $(g-2)_\mu$*, *JHEP* **05** (2021) 174, arXiv: 2103.13401.

[185] A. Greljo, Y. Soreq, P. Stangl, A. E. Thomsen and J. Zupan, *Muonic force behind flavor anomalies*, *JHEP* **04** (2022) 151, arXiv: 2107.07518.

[186] W. Yin, *Radiative lepton mass and muon $g-2$ with suppressed lepton flavor and CP violations*, *JHEP* **08** (2021) 043, arXiv: 2103.14234.

[187] LHCb collaboration, R. Aaij et al., *Test of lepton universality with $B^0 \to K^{*0}\ell^+\ell^-$ decays*, *JHEP* **08** (2017) 055, arXiv: 1705.05802.

[188] LHCb collaboration, R. Aaij et al., *Search for lepton-universality violation in $B^+ \to K^+\ell^+\ell^-$ decays*, *Phys. Rev. Lett.* **122** (2019) 191801, arXiv: 1903.09252.

[189] M. Algueró, B. Capdevila, A. Crivellin, S. Descotes-Genon, P. Masjuan, J. Matias et al., *Emerging patterns of New Physics with and without Lepton Flavour Universal contributions*, *Eur. Phys. J. C* **79** (2019) 714, arXiv: 1903.09578.

[190] J. Aebischer, W. Altmannshofer, D. Guadagnoli, M. Reboud, P. Stangl and D. M. Straub, *B-decay discrepancies after Moriond 2019*, *Eur. Phys. J. C* **80** (2020) 252, arXiv: 1903.10434.

[191] M. Ciuchini, A. M. Coutinho, M. Fedele, E. Franco, A. Paul, L. Silvestrini et al., *New Physics in $b \to s\ell^+\ell^-$ confronts new data on Lepton Universality*, *Eur. Phys. J. C* **79** (2019) 719, arXiv: 1903.09632.

[192] D. Buttazzo, A. Greljo, G. Isidori and D. Marzocca, *B-physics anomalies: a guide to combined explanations*, *JHEP* **11** (2017) 044, arXiv: 1706.07808.

[193] C. Cornella, D. A. Faroughy, J. Fuentes-Martin, G. Isidori and M. Neubert, *Reading the footprints of the B-meson flavor anomalies*, *JHEP* **08** (2021) 050, arXiv: 2103.16558.

[194] D. Marzocca, *Addressing the B-physics anomalies in a fundamental Composite Higgs Model*, *JHEP* **07** (2018) 121, arXiv: 1803.10972.

[195] J. Fuentes-Martin, G. Isidori, J. M. Lizana, N. Selimovic and B. A. Stefanek, *Flavor hierarchies, flavor anomalies, and Higgs mass from a warped extra dimension*, *Phys. Lett. B* **834** (2022) 137382, arXiv: 2203.01952.

[196] L. Alasfar, A. Azatov, J. de Blas, A. Paul and M. Valli, *$B$ anomalies under the lens of electroweak precision*, *JHEP* **12** (2020) 016, arXiv: 2007.04400.

[197] A. Angelescu, D. Bečirević, D. A. Faroughy, F. Jaffredo and O. Sumensari, *Single leptoquark solutions to the B-physics anomalies*, *Phys. Rev. D* **104** (2021) 055017, arXiv: 2103.12504.

[198] LHCb collaboration, *Test of lepton universality in $b \to s\ell^+\ell^-$ decays*, arXiv: 2212.09152.

[199] LHCb collaboration, *Measurement of lepton universality parameters in $B^+ \to K^+\ell^+\ell^-$ and $B^0 \to K^{*0}\ell^+\ell^-$ decays*, arXiv: 2212.09153.

[200] Y. Grossman, E. Passemar and S. Schacht, *On the Statistical Treatment of the Cabibbo Angle Anomaly*, *JHEP* **07** (2020) 068, arXiv: 1911.07821.

[201] B. Belfatto, R. Beradze and Z. Berezhiani, *The CKM unitarity problem: a trace of new physics at the TeV scale?*, *The European Physical Journal C* **80** (feb, 2020) .

[202] B. Capdevila, A. Crivellin, C. A. Manzari and M. Montull, *Explaining $b \to s\ell^+\ell^-$ and the Cabibbo angle anomaly with a vector triplet*, *Phys. Rev. D* **103** (2021) 015032, arXiv: 2005.13542.

[203] A. Crivellin, C. A. Manzari, M. Alguero and J. Matias, *Combined Explanation of the $Z\to bb^-$ Forward-Backward Asymmetry, the Cabibbo Angle Anomaly, and $\tau\to\mu\nu\nu$ and $b\to s\ell+\ell$- Data*, *Phys. Rev. Lett.* **127** (2021) 011801, arXiv: 2010.14504.

[204] D. Marzocca and S. Trifinopoulos, *Minimal Explanation of Flavor Anomalies: B-Meson Decays, Muon Magnetic Moment, and the Cabibbo Angle*, *Phys. Rev. Lett.* **127** (2021) 061803, arXiv: 2104.05730.

[205] A. Crivellin and M. Hoferichter, *$\beta$ Decays as Sensitive Probes of Lepton Flavor Universality*, *Phys. Rev. Lett.* **125** (2020) 111801, arXiv: 2002.07184.

[206] M. Kirk, *Cabibbo anomaly versus electroweak precision tests: An exploration of extensions of the Standard Model*, *Phys. Rev. D* **103** (2021) 035004, arXiv: 2008.03261.

[207] J. Kumar, D. London and R. Watanabe, *Combined Explanations of the $b \to s\mu^+\mu^-$ and $b \to c\tau^-\bar{\nu}$ Anomalies: a General Model Analysis*, *Phys. Rev. D* **99** (2019) 015007, arXiv: 1806.07403.

[208] A. Crivellin, D. Müller and L. Schnell, *Combined constraints on first generation leptoquarks*, *Physical Review D* **103** (jun, 2021) .

[209] C. collaboration, T. Aaltonen, S. Amerio, D. Amidei, A. Anastassov, A. Annovi et al., *High-precision measurement of the w boson mass with the cdf ii detector*, *Science* **376** (2022) 170–176, arXiv: https://www.science.org/doi/pdf/10.1126/science.abk1781.

[210] M. Blennow, P. Coloma, E. Fernández-Martínez and M. González-López, *Right-handed neutrinos and the CDF II anomaly*, arXiv: 2204.04559.

[211] L. Calibbi, M. L. López-Ibáñez, A. Melis and O. Vives, *Implications of the Muon g-2 result on the flavour structure of the lepton mass matrix*, *Eur. Phys. J. C* **81** (2021) 929, arXiv: 2104.03296.

[212] Y.-F. Zhou and Y.-L. Wu, *Lepton flavor changing scalar interactions and muon g-2*, *Eur. Phys. J. C* **27** (2003) 577–585, arXiv: hep-ph/0110302.

[213] G. Isidori, J. Pagès and F. Wilsch, *Flavour alignment of New Physics in light of the $(g-2)_\mu$ anomaly*, *JHEP* **03** (2022) 011, arXiv: 2111.13724.

[214] J. Aebischer, J. Kumar, P. Stangl and D. M. Straub, *A global likelihood for precision constraints and flavour anomalies*, *The European Physical Journal C* **79** (jun, 2019) .

[215] P. Stangl, *smelli – the SMEFT Likelihood*, *PoS* **TOOLS2020** (2021) 035, arXiv: 2012.12211.

[216] H. Dembinski and P. O. et al., *scikit-hep/iminuit*, .

[217] M. Chala and A. Titov, *One-loop matching in the SMEFT extended with a sterile neutrino*, *JHEP* **05** (2020) 139, arXiv: 2001.07732.